

**DRY REFORMING OF WASTE PLASTICS FOR
SYNTHESIS GAS PRODUCTION**

Juniza Md Saad

Submitted in accordance with the requirements for the degree of
Doctor of Philosophy

The University of Leeds
School of Chemical and Process Engineering

July 2016

The candidate confirms that the work submitted is her own, except where work which has formed part of jointly-authored publications has been included. The contribution of the candidate and the other authors to this work has been explicitly indicated below. The candidate confirms that appropriate credit has been given within the thesis where reference has been made to the work of others.

This copy has been supplied on the understanding that it is copyright material and that no quotation from the thesis may be published without proper acknowledgement.

Journal Papers

Investigation of process conditions during the thermal processing of waste high density polyethylene and various nickel-based catalyst for dry reforming process in CHAPTER 5 was based on the following published papers:

1. Md Saad, J., Nahil, M. A, and Williams, P. T. (2015) Influence of process conditions on syngas production from the thermal processing of waste high density polyethylene, *Journal of Analytical and Applied Pyrolysis* 113, 35-40
2. Md Saad, J., Nahil, M. A, Wu, C. and Williams, P. T. (2015) Influence of nickel-based catalysts on syngas production from carbon dioxide reforming of waste high density polyethylene, *Fuel Processing Technology* 138, 156-163

Investigation of dry reforming of waste plastics in CHAPTER 6 was based on the following published papers:

3. Md Saad, J. and Williams, P. T. (2016) Pyrolysis-catalytic-dry reforming of waste plastics and mixed waste plastics for syngas production, *Energy & Fuel* 30, 3198-3204

The candidate Juniza Md Saad performed the experimental work and analytical work, wrote the initial draft of the papers along with supporting material including

Tables and Figures, and carried out the calculation and summarisation of the results and developed the discussion part.

The co-authors, Prof. P. T. Williams, M. A. Nahil and C. Wu, supervised the work and made suggestion and corrections to the draft papers.

The right of Juniza Md Saad to be identified as Author of this work has been asserted by her in accordance with the Copyright, Designs and Patents Act 1988.

© 2016 The University of Leeds and Juniza Md Saad

Acknowledgements

Foremost, I praise Allah, the almighty for granting me the strengths, capabilities, determination and His blessing to proceed successfully. I would like to express my deepest gratitude to my supervisor, Professor Paul T. Williams, for the guidance, persistent support, caring and encouragement. His academic expertise, as well as his unfaltering optimism has been invaluable to me at every stage. I simply could not wish for a better supervisor.

I want to thank the support from Majlis Amanah Rakyat (MARA), Malaysia for the scholarships and Universiti Tenaga Nasional (UNITEN), Malaysia for giving me the opportunity further my PhD journey. Thanks to Professor Peter Jimack and Mr. James Mc Kay for helping me through the university admission process. Also I would like to acknowledge the EU-RISE FLEXI-PYROCAT grant to carry out experiments in Huazhong University of Science and Technology, China.

Special thanks to Dr. Mohamad Anas Nahil and Dr. Chunfei Wu for their involvement with this research. Thanks to Mr. Ed Woodhouse for his technical support. I also want to thank to my colleagues in my research group; Amal, Jonathan, Jude, Paula, Chidi, Ramzi, Eyup, Chika, Qari, Ibrahim, Yeshui, Tomi, Andrew, Peace, Devy, Saba and visiting researchers; Shogo, Jon, Hui, and Maite, for your help and friendship. Also thanks to many colleagues: in Leeds and in Malaysia who supported me on this journey and for the friendship.

Above all, I am sincerely grateful to my beloved family: Ibu, Ayah, Mama, Ayah Wahid, Kakngah, Kacik, Adik, Abang Azri, Itho, Ira, Epit, DikAm, Kak Nita and Kamarol. This work is also part of your untiring love and support. Enormous gratitude to my beloved husband, Sayang for his patience, unconditional love, support, for the laughs, believing in me,... endless list. Thanks for always be there for me. To my grandmothers, uncles, aunties, cousins, nephews, nieces, thanks for always waiting and praying for me. Also thanks to many friends: wherever you are, for your support and friendship.

Abstract

Thermal processing is an effective technique for recycling waste plastics in a sustainable way. The pyrolysis of waste plastics, followed by reforming reactions of the pyrolysis products generates syngas (hydrogen and carbon monoxide) that has a vast array of applications. To date, the steam reforming process has been the most researched technology for syngas production from waste plastics. However, this process produces a large amount of carbon dioxide. Due to the concern related to global warming associated with the emissions of carbon dioxide into the atmosphere, the recycling of carbon dioxide through the pyrolysis-reforming of waste plastic, (dry reforming) is environmentally attractive. The dry reforming process was the focus of this research.

A preliminary thermogravimetric and kinetic analysis was conducted in order to have a general understanding on the effect of CO₂ in a waste plastics pyrolysis. The results show that most plastics required lower activation energy with the presence of CO₂ in the pyrolysis atmosphere (N₂:CO₂ ratio of 7:3). A two-stage pyrolysis-catalytic dry reforming reactor was used to investigate various process conditions and types of catalyst to maximise syngas production. The two-stage fixed bed reaction systems increased the H₂ in both a N₂ or CO₂ atmosphere. Ni/Al₂O₃ based catalysts with different metal promoters (Mg, Cu and Co) were selected for the investigation of pyrolysis-dry reforming of waste plastics. Among the catalysts tested, the Ni-Co/Al₂O₃ catalyst presented the highest catalyst activity resulting in a syngas production of 149.42 mmol_{syngas} g⁻¹_{plastic} with 58% carbon dioxide conversion, also no detectable carbon formation on the catalyst surface was observed. The dry reforming reaction was also favoured with the Ni-Co/Al₂O₃ catalyst with high cobalt content. Various process parameters such as catalyst preparation method, reforming temperature, CO₂ feed input rate and catalyst to plastic ratio were tested. It was found that the addition of steam in the catalytic-dry reforming process manipulated the H₂/CO molar ratio, based on the type of catalyst used and the CO₂/steam feed ratio. Better catalyst activity in relation to H₂ production was observed for the Ni-Mg/Al₂O₃ catalyst and Ni-Co/Al₂O₃ catalyst favoured CO production. Different types of plastics; individual and mixed plastics from different waste treatment plants were also processed through the catalytic-dry reforming process to determine the syngas production and catalyst activity of Ni-Co/Al₂O₃ catalyst. This research has suggested that the use of carbon dioxide as the reforming agent in the dry reforming process of waste plastics was comparable to the current reforming technology with an optimum syngas production of 148.6 mmol g⁻¹_{SWP}.

Table of Contents

Acknowledgements	iv
Abstract	v
Table of Contents	vi
List of Tables	xi
List of Figures	xv
Abbreviations	xx
Chapter 1 INTRODUCTION	1
1.1 Climate Change	1
1.1.1 Greenhouse gases and CO ₂ emission	2
1.2 Waste and Energy Recovery	3
1.2.1 Municipal solid waste generation	3
1.2.2 Plastics production	7
1.2.3 Energy recovery from waste plastics	11
1.3 Research Objectives	13
References	15
Chapter 2 LITERATURE REVIEW	18
2.1 Reforming Processes of Waste Plastics for Synthesis Gas Production	18
2.1.1 Pyrolysis.....	19
2.1.1.1 Product yield distribution from pyrolysis of waste plastics	22
2.1.2 Gasification	27
2.1.3 Pyrolysis-gasification of waste plastics	32
2.1.3.1 Effect of steam injection on the pyrolysis- gasification system: steam reforming process.....	32
2.2 Synthesis Gas Production (H ₂ and CO) from Reforming of Waste Plastics	34
2.2.1 Influence of temperature	34
Figure 2.7 Gas composition for the pyrolysis-gasification of plastics at a gasification temperature of 800 °C [42]	36
2.2.2 Influence of catalysts	37

2.3 Dry Reforming Technology	42
2.3.1 Thermodynamic reactions of methane dry reforming	42
2.3.2 Syngas production from dry reforming process	43
2.3.3 The use of catalyst for syngas production from dry reforming process	46
2.4 Summary	53
References	54
Chapter 3 EXPERIMENTAL METHODOLOGY	67
3.1 Introduction.....	67
3.2 Materials.....	67
3.2.1 Individual plastics composition of municipal solid waste.....	67
3.2.2 Mixed waste plastics from various waste treatment plants	69
3.2.3 Catalyst development	71
3.2.3.2 Ni-Co/Al ₂ O ₃ catalyst prepared by impregnation method.....	71
3.2.3.3 Ni-Co/Al ₂ O ₃ catalyst by different Co metal loading	71
3.3 Experimental Reaction System	72
3.3.1 Operation description of fixed bed pyrolysis reactor	72
3.3.2 Operation description of two-stage pyrolysis/ catalytic- reforming fixed bed reactor	74
3.3.3 Carbon dioxide feed composition for reforming process	76
3.3.4 Start up and validation	78
3.4 Analytical Techniques	83
3.4.1 Material analysis.....	83
3.4.1.1 Proximate and ultimate analysis	83
3.4.1.2 Thermogravimetric analysis (TGA)	88
3.4.1.3 Kinetic analysis calculation.....	88
3.4.2 Catalyst analysis (fresh/ reacted)	92
3.4.2.1 Temperature programmed reduction (TPR)	92
3.4.2.2 Brunauer, Emmet and Teller (BET) surface area analysis	92
3.4.2.3 X-ray diffraction (XRD).....	94
3.4.2.4 Scanning electron microscopy (SEM).....	95
3.4.2.5 Temperature programmed oxidation (TGA-TPO).....	97

3.4.3 Calculation and analysis of product yields	99
3.4.3.1 Gas chromatography (GC).....	100
3.4.3.2 Gas concentration calculation	101
References	105
Chapter 4 THERMOGRAVIMETRIC ANALYSIS OF WASTE PLASTICS	107
4.1 Influence of Nitrogen or Carbon Dioxide Atmosphere in Pyrolysis of Individual Component of Waste Plastics.....	108
4.1.1 Thermogravimetric characteristics.....	108
4.1.2 Kinetic parameters	112
4.2 Influence of Nitrogen and Carbon Dioxide Mixture in Pyrolysis of Waste Plastics	115
4.2.1 Thermogravimetric characteristics and kinetic analysis for high density polyethylene at different N ₂ /CO ₂ ratio.....	115
4.2.1.1 Thermogravimetric characteristics	115
4.2.1.2 Kinetic parameters	117
4.2.2 Thermogravimetric characteristics and kinetic analysis for individual plastics and mixed plastics at N ₂ /CO ₂ ratio of 1:0 and 7:3	119
4.2.2.1 Thermogravimetric characteristics	119
4.2.2.2 Kinetic analysis	121
4.3 Comparison of Analysis Data from Different Experimental Systems...	124
4.4 Summary	125
References	126
Chapter 5 THERMAL PROCESSING OF WASTE HIGH DENSITY POLYETHYLENE FOR SYNGAS PRODUCTION: INFLUENCE OF PROCESS CONDITION AND VARIOUS NICKEL-BASED CATALYSTS.....	128
5.1 Influence of Nitrogen or Carbon Dioxide Atmosphere in Pyrolysis of Waste Plastics using a Fixed Bed Reactor	129
5.1.1 Influence of carbon dioxide flow rate on pyrolysis of polystyrene.....	132
5.2 The Introduction of Gasification Stage into the System using a Two-stage Fixed Bed Reactor.....	134
5.3 Influence of Steam and Carbon Dioxide on the Non-catalytic Pyrolysis-gasification of High Density Polyethylene	137

5.4	Influence of Nickel-Based Catalysts on Syngas Production from Carbon Dioxide Reforming of Waste High Density Polyethylene.....	143
5.4.1	Fresh catalyst characterizations	144
5.4.2	Pyrolysis-catalytic CO ₂ reforming over Ni/Al ₂ O ₃ catalyst	149
5.4.3	Pyrolysis-catalytic CO ₂ reforming over Ni-Cu/Al ₂ O ₃ , Ni-Mg/Al ₂ O ₃ and Ni-Co/Al ₂ O ₃ catalyst.....	151
5.4.4	Ni-Co/Al ₂ O ₃ catalysts with different molar ratios	159
5.4.5	H ₂ :CO molar ratio from catalytic-dry reforming of high density polyethylene	162
5.5	Summary	163
	References	165
	Chapter 6 PYROLYSIS-DRY REFORMING OF VARIOUS PLASTICS FOR SYNGAS PRODUCTION.....	170
6.1	Non-catalytic CO ₂ Dry Reforming of Various Plastics	170
6.2	Ni-Co/Al ₂ O ₃ Catalytic CO ₂ Dry Reforming of Various Plastics.....	178
6.3	Catalytic CO ₂ Dry Reforming of Mixed Waste Plastics	179
6.4	Characterization of the Coked Catalyst	181
6.5	Summary	184
	References	185
	Chapter 7 INFLUENCE OF PROCESS PARAMETERS ON SYNGAS PRODUCTION FROM CATALYTIC-DRY REFORMING OF SIMULATED MIXED WASTE PLASTICS	187
7.1	Different Catalyst Preparation Methods.....	187
7.2	Influence of Catalyst Reforming Temperature	190
7.3	Influence of CO ₂ Inlet Flow Rate	193
7.4	Influence of Catalyst to Plastic Ratio.....	196
7.5	Manipulating H ₂ /CO ratio by the Addition of Steam.....	198
7.5.1	Gas composition	200
7.5.2	Syngas production and H ₂ /CO molar ratio	202
7.5.3	Catalyst coke formation	204
7.6	Summary	208

References	210
Chapter 8 CATALYTIC-DRY REFORMING OF WASTE PLASTICS FROM DIFFERENT WASTE TREATMENT PLANTS FOR PRODUCTION OF SYNGAS	212
8.1 Product Yields Distribution from Dry Reforming of Waste Plastics ...	213
8.2 Gas Composition and Syngas Production from Dry Reforming of Waste Plastics	216
8.3 Coke Formation on the Catalyst from Dry Reforming of Wastes	220
8.4 Summary	226
References	227
Chapter 9 CONCLUSIONS AND SUGGESTIONS FOR FUTURE WORK.....	229
9.1 General Conclusions.....	229
9.1.1 Effect of different pyrolysis atmospheres on thermogravimetric and kinetic study of various plastics	230
9.1.2 Analysis of process conditions on synthesis gas production from pyrolysis and gasification of high density polyethylene.....	231
9.1.3 Characterisation and assessment of Ni/Al ₂ O ₃ catalysts promoted with Cu, Mg and Co.....	231
9.1.4 Investigation of catalytic-dry reforming of various plastics for syngas production.....	232
9.1.5 Influence of catalyst preparation methods, catalyst temperature, CO ₂ input rate, catalyst:plastic ratio.....	233
9.1.6 Effect of the addition of steam on catalytic-dry reforming process towards H ₂ :CO ratio	233
9.1.7 Investigation of catalytic-dry reforming of mixed plastics from various waste treatment plants for syngas production	234
9.2 Recommendations for future work	235
9.2.1 Analysis of plastic/CO ₂ reaction kinetics and mechanism	235
9.2.2 Investigation on catalyst characterisation and activity	235
9.2.3 Application of dry reforming process for syngas production from plastics	236

List of Tables

Table 1.1 The comparison between recent composition of the atmosphere as in 2016 and global-scale trace-gas concentrations from prior to 1750 [8]	3
Table 1.2 Carbon impact of Local Authority waste management in England in the year of 2011/12 [13]	6
Table 2.1 Thermal decomposition products from pyrolysis of polymers [24].....	20
Table 2.2 Chlorine in the pyrolysis fractions (wt.%) from step-pyrolysis [8]	22
Table 2.3(a) Product yield distribution from pyrolysis of waste plastics	25
Table 2.3(b) Product yield distribution from pyrolysis of waste plastics (... continued from previous page)	26
Table 2.4 Effect of temperature on hydrogen and carbon monoxide production from steam gasification of plastic waste (PE) in bench scale fixed bed reactor with a heating rate of 10 °C min ⁻¹	35
Table 2.5 Unit operations in catalyst preparation [60]	37
Table 2.6 Gas composition in the product gases (nitrogen free, vol%) [64].....	39
Table 2.7 Carbon morphology [104]	47
Table 2.8(a) Research on product yield distributions from dry reforming process over Ni-based catalysts	49
Table 2.8(b) Research on product yield distributions from dry reforming process over Ni-based catalysts (... continued from previous page)	50
Table 2.9 Catalytic properties of Ni catalysts in reforming of methane with CO ₂ at 90 min (T=923K; m=0.5g; CH ₄ /CO ₂ =1) [115].....	51
Table 3.1 Composition of plastics according to plastics fraction in the residual municipal solid waste and simulated samples [1]	68
Table 3.4 Pyrolysis experimental parameter set up	74
Table 3.5 General process condition of dry reforming of waste plastics	77
Table 3.8 Initial experiments with the one stage fixed bed reactor (LDPE).....	81
Table 3.9 Validation of the two-stage fixed bed reactor (HDPE)	82
Table 3.10 (a) Ultimate analysis of each raw materials analysed at University of Leeds laboratory, United Kingdom (CE Instrument Wigan, UK, FLASH EA2000CHNS-O analyser).....	85
Table 3.10 (b) Ultimate analysis of each raw materials analysed at Huazhong University of Science and Technology laboratory, China	86
Table 3.11 Proximate analysis of each raw material analysed at Huazhong University of Science and Technology laboratory, China	87

Table 3.12 Concentration of standard permanent and hydrocarbon gases	102
Table 3.13 Example of standard gases GC response peak area and repeatability	102
Table 3.14 Example of gas composition identification and repeatability	104
Table 4.1 Characteristic data of each individual plastic in N ₂ and CO ₂ atmospheres	111
Table 4.2 Comparison table of residue left after the experiment between N ₂ and CO ₂ atmosphere	111
Table 4.3 Kinetic parameters of individual plastic sample from Arrhenius model; activation energy (E), pre-exponential factor (A) and correlation coefficients (R ²).....	113
Table 4.4 Summary of kinetic values using various analytical methods in N ₂ atmosphere	114
Table 4.5 Characteristic data of HDPE in different mixtures of N ₂ and CO ₂	116
Table 4.6 Kinetic parameters of high density polyethylene at different N ₂ /CO ₂ ratios from Arrhenius model; activation energy (E), pre-exponential factor (A) and correlation coefficients (R ²).....	118
Table 4.7 Characteristic data of raw materials in N ₂ /CO ₂ ratio of 1:0 and 7:3...	119
Table 4.8 Kinetic parameters of individual plastics and mixed plastics at N ₂ /CO ₂ ratio of 1:0 and 7:3 from Arrhenius model; activation energy (E), pre-exponential factor (A) and correlation coefficients (R ²).....	122
Table 4.9 Comparison table of thermal degradation data of each individual plastic under N ₂ atmosphere obtained from different experimental setup	124
Table 5.1 Mass balances of the results from pyrolysis of plastic samples	131
Table 5.2 Mass balance for different carbon dioxide flow rate in the pyrolysis of polystyrene	133
Table 5.3 Gas yields comparison between pyrolysis and pyrolysis-gasification of waste high density polyethylene.....	136
Table 5.4 Influence of the reaction atmosphere on the pyrolysis-gasification of waste high density polyethylene using the two-stage fixed bed reactor with sand in the second stage at 800 °C.....	138
Table 5.5 Gas compositions from pyrolysis-gasification high density polyethylene	141
Table 5.6 Comparison table of calculation data and experimental results from pyrolysis-dry reforming of waste high density polyethylene.....	143
Table 5.7 BET surface area of the prepared catalysts.	144

Table 5.8 Pyrolysis-dry reforming of high density polyethylene with different catalysts.....	154
Table 5.9 Pyrolysis-dry reforming of high density polyethylene over different molar ratios of Ni-Co/Al ₂ O ₃ catalyst	160
Table 6.1 Two-stage pyrolysis of different plastics with no catalyst and no carbon dioxide (quartz sand in the 2nd stage at a temperature of 800 °C)	172
Table 6.2 Pyrolysis-catalysis of different plastics in the presence of carbon dioxide and no catalyst (quartz sand in the 2nd stage at a temperature of 800 °C).....	172
Table 6.3 Pyrolysis-dry reforming of different plastics in the presence of Ni-Co/Al ₂ O ₃ catalyst and carbon dioxide (catalyst temperature 800 °C and CO ₂ flow rate of 6.0 gh ⁻¹).....	178
Table 6.4 Pyrolysis-CO ₂ dry reforming of simulated mixture of different plastics in the presence of sand or Ni-Co/Al ₂ O ₃ catalyst and carbon dioxide (2nd stage reactor temperature, 800 °C and CO ₂ flow rate of 6.0 gh ⁻¹)	180
Table 7.1 Product yields and gas composition from the catalytic dry reforming of a simulated mixture of waste plastics (SWP) with different types of Ni-Co/Al ₂ O ₃ catalyst preparation methods.	188
Table 7.2 Product yields, syngas yield, H ₂ :CO molar ratio and CO ₂ conversion from the catalytic dry reforming of a simulated mixture of waste plastics (SWP) in relation to catalyst temperature	191
Table 7.3 Product yields, syngas yield, H ₂ :CO molar ratio and CO ₂ conversion from the catalytic dry reforming of a simulated mixture of waste plastics (SWP) at different inlet CO ₂ flow rates	195
Table 7.4 Product yields and gas composition from the catalytic dry reforming of a simulated mixture of waste plastics (SWP) at different catalyst:plastic ratios	197
Table 7.5 Product yield distribution from catalytic-dry/steam reforming of simulated waste plastic over Ni-Co/Al ₂ O ₃ catalyst at the gasification temperature of 800 °C.....	199
Table 7.6 Product yield distribution from catalytic-dry/steam reforming of simulated waste plastic over Ni-Mg/Al ₂ O ₃ catalyst at the gasification temperature of 800 °C.....	200
Table 8.1 Gas compositions, syngas yield and CO ₂ conversion from dry reforming of waste samples with Ni/Al ₂ O ₃ catalyst at 800 °C gasification temperature.	217

Table 8.2 Gas compositions, syngas yield and CO₂ conversion from dry reforming of waste samples with Ni-Co/Al₂O₃ catalyst at 800 °C gasification temperature.218

List of Figures

Figure 1.1 Changes in ① global mean sea level (teal line: Jevrejeva et al.), ② summer Arctic sea-ice area (yellow line: Walsh & Chapman), ③ 0-700-m ocean heat content (orange line; Levitus et al.), ④ sea-surface temperature (brown line; Rayner et al), ⑤ mean ocean-surface pH (blue line; Natl. Res. Counc) and ⑥ atmosphere ρCO_2 (red line; Petit et al.) [3]	2
Figure 1.2 Waste generation split by nomenclature of economic activities (NACE), 2012 United Kingdom [11]	4
Figure 1.3 Waste generation split by waste material, 2012 United Kingdom [11]	5
Figure 1.4 Management of all Local Authority collected waste and recycling rates in England, 2000/01-2014/15 [12]	5
Figure 1.5 World plastic production [15]	8
Figure 1.6 European plastic demand by applications and polymer type 2014 [15]	8
Figure 1.7 The structure of individual plastics	10
Figure 1.8 Total plastic waste recycling and recovery 2006-2010 [23]	11
Figure 2.1 Schematic diagram of fluidized bed gasification reactor [39]	30
Figure 2.2 Moving-grate gasification and utilization system [40]	30
Figure 2.3 Basic principle of the dual fluidized bed gasification technology [41]	31
Figure 2.4 Distribution of carbon in the dual fluidised bed reactor for pure substances and mixtures [41]	31
Figure 2.5 Gas composition and hydrogen production for different water injection rate [46]	33
Figure 2.6 Evolution of hydrogen production with pyrolysis temperature [27] ...	35
Figure 2.8 Concentration of product gases at different calcination temperature and CeO ₂ content [61]	38
Figure 2.9 Potential H ₂ production from pyrolysis-gasification of polypropylene with different catalyst (a) Ni-Al (1:4); (b) Ni-Al (1:2); (c) Ni-Al (1:1); (d) Ni-Mg-Al (1:1:4); (e) Ni-Mg-Al (1:1:2); (f) Ni-Mg-Al (1:1:1); (g) Ni-Cu-Al (1:1:2) and (h) Ni-Cu-Mg-Al (1:1:1:3); ((a)-(h) are calcined at 750 °C) [65]	39

Figure 2.10 Gas composition in steam gasification and pyrolysis for non-catalytic and catalytic process [44]	40
Figure 2.11 CH ₄ conversion and H ₂ production of steam reforming of methane at 800°C [66].....	41
Figure 2.12 Multi-step chemical vapor deposition and hydrogen inhibition of pyrocarbon from methane (τ the residence time, ρ the pressure, T the temperature, S_v the volume-related surface area) [98]	46
Figure 2.13 CO ₂ reforming of polyethylene with Pd/Al ₂ O ₃ catalyst [106].....	48
Figure 2.14 CH ₄ effect of catalyst prepared by ultrasound irradiation (U) compared to impregnation method (I) on product yield produced at different temperatures [87]	53
Figure 3.1 Photograph of pelletized plastic samples	68
Figure 3.2 Schematic diagram of one-stage fixed bed reactor for preliminary investigation	73
Figure 3.3 Schematic diagram of the two-stage fixed bed reactor.....	75
Figure 3.4 Photograph of the two-stage fixed bed reactor	76
Figure 3.5 Photograph of Nova 2200e surface area and pore analyser	93
Figure 3.6 Multi-point BET plot for fresh Ni-Al catalyst	94
Figure 3.7 Example of diffraction pattern from XRD analysis on fresh Ni-Al catalyst.....	95
Figure 3.8 SEM-EDXS of fresh Ni-Mg-Al catalyst	96
Figure 3.9 Photograph of Hitachi SU8230 SEM equipment.....	96
Figure 3.10 SEM morphologies of coked Ni-Mg/Al ₂ O ₃ catalyst in different magnifications from pyrolysis-gasification process of waste high density polyethylene without CO ₂ addition at gasification temperature of 800 °C	97
Figure 3.11 DTG-TPO results for the reacted Ni-Mg/Al ₂ O ₃ catalyst after pyrolysis-reforming of waste high density polyethylene with and without the addition of carbon dioxide	98
Figure 3.12 Photograph of TGA-50 Shimadzu analyser.....	98
Figure 3.13 Photograph and principal schematic diagram of gas chromatography analyser	101
Figure 4.1 Weight loss profile of individual plastic over N ₂ or CO ₂ atmosphere	109
Figure 4.2 TGA and DTG plot of LDPE, HDPE, PP, PS and PET over N ₂ or CO ₂ atmosphere	109

Figure 4.3 TGA and DTG thermographs of HDPE in different N ₂ /CO ₂ ratio; 100% N ₂ (1:0), 70% N ₂ /30% CO ₂ (7:3), 50% N ₂ /50% CO ₂ (1:1), 30%N ₂ /70% CO ₂ (3:7) and 100% CO ₂ (0:1).....	117
Figure 4.4 Plot of $\ln[-\ln(1-\alpha)]/T^2$ versus 1/T of HDPE in different N ₂ /CO ₂ ratio; 100% N ₂ (1:0), 70% N ₂ /30% CO ₂ (7:3), 50% N ₂ /50% CO ₂ (1:1), 30%N ₂ /70% CO ₂ (3:7) and 100% CO ₂ (0:1).....	118
Figure 4.5 TGA weight loss thermographs of each individual plastic in N ₂ /CO ₂ ratio of 1:0 and 7:3.....	120
Figure 4.6 TGA and DTG thermographs of mixed plastics from different waste treatment plants in N ₂ /CO ₂ ratio of 1:0 and 7:3.....	121
Figure 4.7 Plot of $\ln[-\ln(1-\alpha)]/T^2$ versus 1/T of individual plastics and mixed plastics at N ₂ /CO ₂ ratio of 1:0 and 7:3.....	123
Figure 5.1 Gas composition from pyrolysis of waste plastics under nitrogen or carbon dioxide atmosphere.....	132
Figure 5.2 Comparison in gas concentration on pyrolysis of waste polystyrene in carbon dioxide atmosphere.....	134
Figure 5.3 Comparison on product yield compositions between pyrolysis and pyrolysis-gasification of high density polyethylene under nitrogen atmosphere.....	135
Figure 5.4 Hydrogen, carbon monoxide and carbon deposition production relationship from pyrolysis-gasification of waste high density polyethylene with the addition of carbon dioxide and/or steam.....	140
Figure 5.5 XRD spectra of the fresh catalysts: (a) Ni/Al ₂ O ₃ (1:1) catalyst; (b) Ni-Cu/ Al ₂ O ₃ (1:1:1) catalyst; (c) Ni-Mg/ Al ₂ O ₃ (1:1:1) catalyst; (d) Ni-Co/ Al ₂ O ₃ (1:1:1) catalyst.....	146
Figure 5.6 XRD spectra of the fresh Ni-Co/Al ₂ O ₃ catalysts: (a) 1:0.5:1; (b) 1:1:1; (c) 1:2:1.....	147
Figure 5.7 Temperature programmed reduction (H ₂ -TPR) of the fresh catalysts.....	148
Figure 5.8 Gas compositions for the pyrolysis-dry reforming of high density polyethylene with different type of catalyst at a catalyst temperature of 800 °C.....	155
Figure 5.9 Relationship between carbon deposition and CO ₂ conversion derived from pyrolysis-dry reforming of high density polyethylene over different catalysts.....	156
Figure 5.10 DTG-TPO thermograph of different type of coked catalysts after pyrolysis-dry reforming of high density polyethylene.....	157

Figure 5.11 SEM results of different type of coked catalysts from pyrolysis-gasification/reforming of HDPE, calcined at 750 °C (scale bar represent 1µm and all SEM micrographs are at the same magnification) ..	158
Figure 5.12 DTG-TPO thermograph of different ratio of Ni-Co/Al ₂ O ₃ coked catalysts after pyrolysis-dry reforming of high density polyethylene	161
Figure 5.13 SEM results of different ratio of Ni-Co/Al ₂ O ₃ coked catalysts from pyrolysis-gasification/reforming of HDPE, calcined at 750 °C (all SEM micrographs are at the same magnification)	162
Figure 6.1 Gas compositions for the pyrolysis-dry reforming of the different plastics and the simulated mixture of plastics under various process conditions	176
Figure 6.2 Syngas (hydrogen and carbon monoxide) production and carbon dioxide conversion from pyrolysis-dry reforming of various types of plastics	177
Figure 6.3 SEM tomographic images for the reacted Ni-Co/Al ₂ O ₃ catalyst surface from catalytic-dry reforming of individual plastic (all SEM micrographs are at the same magnification)	182
Figure 6.4 TPO results for the reacted Ni-Co/Al ₂ O ₃ catalyst after catalytic-dry reforming of waste plastics; (a) TGA-TPO, (b) DTG-TPO	183
Figure 7.1 TGA and TGA-DTG thermographs of the reacted catalysts from the dry reforming of the simulated mixture of waste plastics (SWP) with catalyst prepared by the rising-pH technique and the impregnation method	189
Figure 7.2 SEM micrographs of the reacted catalysts from the simulated mixture of waste plastics (SWP) with catalyst prepared by the rising-pH technique and the impregnation method.....	190
Figure 7.3 Gas compositions produced from the catalytic dry reforming of reforming of the simulated mixture of waste plastics (SWP) at different catalytic dry reforming temperatures.	191
Figure 7.4 Gas compositions produced from the catalytic dry reforming of the simulated mixture of waste plastics (SWP) at different CO ₂ flow rates	196
Figure 7.5 Gas compositions produced from the catalytic dry reforming of the simulated mixture of waste plastics (SWP) at different catalyst:plastic ratios	198
Figure 7.6 Gas composition for the catalytic-dry/steam reforming of simulated waste plastic with different CO ₂ /steam ratio over Ni-Co/Al ₂ O ₃ and Ni-Mg/Al ₂ O ₃ catalysts	201

Figure 7.7 Syngas yield, H ₂ /CO molar ratio, reacted water and CO ₂ conversion derived from dry/steam reforming process over Ni-Co/Al ₂ O ₃ catalyst	203
Figure 7.8 Syngas yield, H ₂ /CO molar ratio, reacted water and CO ₂ conversion derived from dry/steam reforming process over Ni-Mg/Al ₂ O ₃ catalyst	204
Figure 7.9 TGA-TPO and DTG-TPO analysis of different type of coked catalysts after pyrolysis-dry/steam reforming of simulated waste plastics over Ni-Co/Al ₂ O ₃ catalyst.	205
Figure 7.10 TGA-TPO and DTG-TPO analysis of different type of coked catalysts after pyrolysis-dry/steam reforming of simulated waste plastics over Ni-Mg/Al ₂ O ₃ catalyst.	206
Figure 7.11 SEM results of different type of coked Ni-Co/Al ₂ O ₃ catalysts from catalytic-dry/steam reforming of simulated waste plastic (all SEM micrographs are at the same magnification)	207
Figure 7.12 SEM results of different type of coked Ni-Mg/Al ₂ O ₃ catalysts from catalytic-dry/steam reforming of simulated waste plastic (all SEM micrographs are at the same magnification)	208
Figure 8.1 Product yields from catalytic-dry reforming of different waste samples under Ni/Al ₂ O ₃ and Ni-Co/Al ₂ O ₃	215
Figure 8.2 TGA-TPO weight loss thermographs of coked Ni/Al ₂ O ₃ and Ni-Co/Al ₂ O ₃ catalysts after dry reforming of different type of waste samples.	221
Figure 8.3 DTG-TPO thermographs of coked Ni/Al ₂ O ₃ and Ni-Co/Al ₂ O ₃ catalysts after dry reforming of different type of waste samples.	222
Figure 8.4 SEM morphologies of coked Ni/Al ₂ O ₃ catalysts after dry reforming of different type of waste samples (all SEM micrographs are at the same magnification)	224
Figure 8.5 SEM morphologies of coked Ni-Co/Al ₂ O ₃ catalysts after dry reforming of different type of waste samples (all SEM micrographs are at the same magnification)	225

Abbreviations

ABS	Acrylonitrile-butadiene-styrene
BET	Brunauer-Emmet-Teller surface area analysis
CCl ₄	Carbon tetrachloride
CFCs	Chlorofluorocarbons
CH ₄	Methane
CO ₂	Carbon dioxide
CO ₂ :CH ₄	Carbon dioxide to methane molar ratio
CO ₂ :plastics	Carbon dioxide to plastics ratio
DAEM	Discrete distributed activation energy method for kinetic analysis
DRM	Dry reforming of methane
DTG	Differential thermogravimetry
EDXS	Energy dispersive X-ray spectrometer
GC	Gas chromatography
HCFCs	Hydrochlorofluorocarbons
HDPE	High density polyethylene
HfC	Hafnium carbide
HHV	Higher heating value
HIPS	High impact polystyrene
LACW	Local Authority collected waste
LDPE	Low density polyethylene
LHV	Lower heating value
MP _{AGR}	Mixed plastics from waste agricultural
MP _{BC}	Mixed plastics from waste building construction

MP _{CRT}	Mixed plastics from cathode ray tube collected from waste old style television sets and monitors
MP _F	Mixed plastics from waste refrigerator and freezer equipment
MP _{HP}	Mixed plastics from waste household packaging
MP _{WEEE}	Mixed plastics from waste electrical and electronics equipment
N ₂ O	Nitrous oxide
O ₃	Tropospheric ozone
PP	Polypropylene
PS	Polystyrene
PVC	Polyvinyl chloride
RDF	Refuse derived fuel containing waste plastics and other waste materials
RSTDV	Relative standard deviation
SEM	Scanning electron microscopy
SF ₆	Sulfur hexafluoride
SO ₂	Silicon oxide
STDV	Standard deviation
SWP	Simulated mixture of waste plastic; consist of LDPE, HDPE, PS, PET and PP
Syngas	Mixture of permanent and hydrocarbon gases in different concentrations. Mainly composed by H ₂ and CO
TGA	Thermogravimetric analysis
TPO	Temperature programmed oxidation
TPR	Temperature programmed reduction
XRD	X-ray diffraction analysis

Chapter 1

INTRODUCTION

1.1 Climate Change

The climate of the earth is generally dependent on the temperature from solar energy. Seinfeld and Pandis [1] described the influence of the gases in the atmosphere and cloud cover in relation to the earth's climate. The white cloud cools the Earth by reflecting solar energy back into space and warms the earth by trapping energy near the surface. In addition, the non-reflecting energy from solar energy is absorbed by the earth surface's and atmosphere. The atmosphere also emits energy from the energy radiated by the earth's surface. The atmosphere's energy is absorbed by greenhouse gases. This concept is known as the greenhouse effect. Over time, the change in global heat of the earth in related to the human activities has intensified climate change, hence affecting this cycle.

Climate change has increased the global average of surface temperature, global air temperature, ocean temperature and the change in snow or ice extent and sea level [2,3]. For example, Doney et al. [3] cites several research papers on the effect of rising temperature towards marine ecosystems over time as illustrated in Figure 1.1. The trend of the changes over the years has suggested that due to climate change, there has been an increase of sea level, rise in ocean stratification, a decrease of sea-ice extent, and altered patterns of ocean circulation, precipitation, and freshwater input. Poloczanska et al. [4] reported that a rise in ocean temperature also influenced the marine biological species life including fish, seabirds, plankton and others. Warming of the climate system has also caused climate disasters in many parts of the world such as floods, storms, and tropical cyclones.

Issues affecting climate change are becoming increasingly important. There is widespread debate on the potential to reduce climate change impact on the environment; forest, wildlife, polar region and water [5-7]. For example, the use of natural gas, hybrid and electric for automobile instead of gasoline, addition of

rooftop solar panels for generating energy and even as simple as carpooling help on improving better air quality [6].

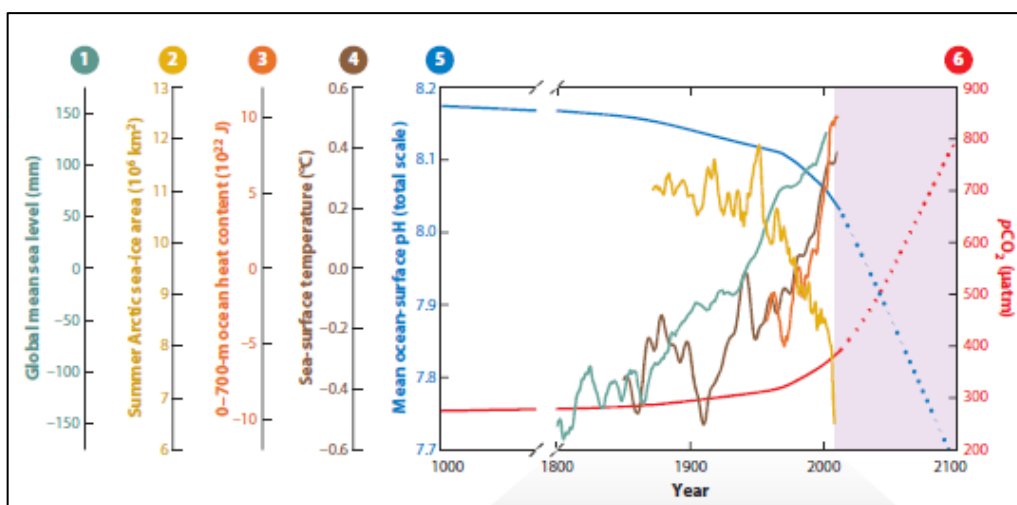


Figure 1.1 Changes in ① global mean sea level (teal line: Jevrejeva et al.), ② summer Arctic sea-ice area (yellow line: Walsh & Chapman), ③ 0-700-m ocean heat content (orange line; Levitus et al.), ④ sea-surface temperature (brown line; Rayner et al), ⑤ mean ocean-surface pH (blue line; Natl. Res. Counc) and ⑥ atmosphere ρCO_2 (red line; Petit et al.) [3]

1.1.1 Greenhouse gases and CO₂ emission

Table 1.1 summarizes the details of the atmosphere's composition including the main constituents and the greenhouse gases [8]. The data obtained excluded the amount of water vapour in the atmospheres due to inconsistency of data that depended on location and season. Overall, the atmosphere's composition has significantly changed compared to the concentration from pre-1750 that is assumed to be unaffected by human activities. It can be said that the rising level of greenhouse gases particularly, ozone, carbon dioxide, methane, chlorofluorocarbons (CFCs) and nitrous oxide are related to human activities such as farming, combustion of fossil fuels and deforestation. These gases also contribute to the increase in global warming temperature. An increase concentration of carbon dioxide may be due to the combustion of fossil fuels while agricultural and waste management activities may contribute to the high amount of methane. The emission from oil and natural gas also influenced methane concentration in the atmosphere. In addition, the use of fossil fuels in the industrial and automotive sectors plays an important role in CO₂ emissions to the atmosphere.

Table 1.1 The comparison between recent composition of the atmosphere as in 2016 and global-scale trace-gas concentrations from prior to 1750 [8]

Gas	Pre-1750 tropospheric concentration	Recent tropospheric concentration
	<u>in parts per million (ppm)</u>	
Carbon dioxide (CO ₂)	~280	399.5
	<u>in parts per billion (ppb)</u>	
Methane (CH ₄)	722	1834
Nitrous oxide (N ₂ O)	270	328
Tropospheric ozone (O ₃)	237	337
	<u>in parts per trillion (ppt)</u>	
Chlorofluorocarbons (CFCs)	zero	820
Hydrochlorofluorocarbons (HCFCs)	zero	279
Halons	zero	6.9
Hafnium carbide (HFC)	zero	84
Carbon tetrachloride (CCl ₄)	zero	82
Sulfur hexafluoride (SF ₆)	zero	8.6

The mitigation strategies to reduce CO₂ include carbon capture. High volumes of carbon dioxide are predicted to be produced from future carbon capture processes because of the concern over climate change. In addition, the high amount of CO₂ capture opens opportunities for CO₂ utilisation.

1.2 Waste and Energy Recovery

1.2.1 Municipal solid waste generation

There has been a significant increase in waste generation as a result of population rise and increased economic growth. Therefore, waste management is a critical issue in many countries due to the increasing impact on the environment.

The municipal solid waste can be classified into three different groups; inert waste, hazardous waste and non-hazardous waste. Inert waste does not consist of hazardous materials and does not undergo any significant physical, chemical or biological transformations when disposed of. The hazardous waste is the waste that

is ignitable, corrosive, reactive and contains certain amounts of toxic chemicals [9]. In contrast, non-hazardous waste is not inert which means it can be transformed physically, chemically or biologically when disposed. Most of the non-hazardous waste comes from municipal solid waste [10].

The waste generation distribution in the United Kingdom is shown in Figure 1.2 [11]. In 2012, United Kingdom has generated approximately 200.0 million tonnes of total waste. The Construction sector has shown to contribute half amount of total waste followed by Commercial & Industrial sector, 100,230 and 47,567 thousand tonnes respectively. The economic activity “Other” consist of waste from “Agriculture, forestry and fishing” and waste from “Mining and quarrying” activities. Figure 1.3 show that the major contribution of waste generated in United Kingdom are mineral wastes (mostly from Construction and Mining & Quarrying) and Soils [11].

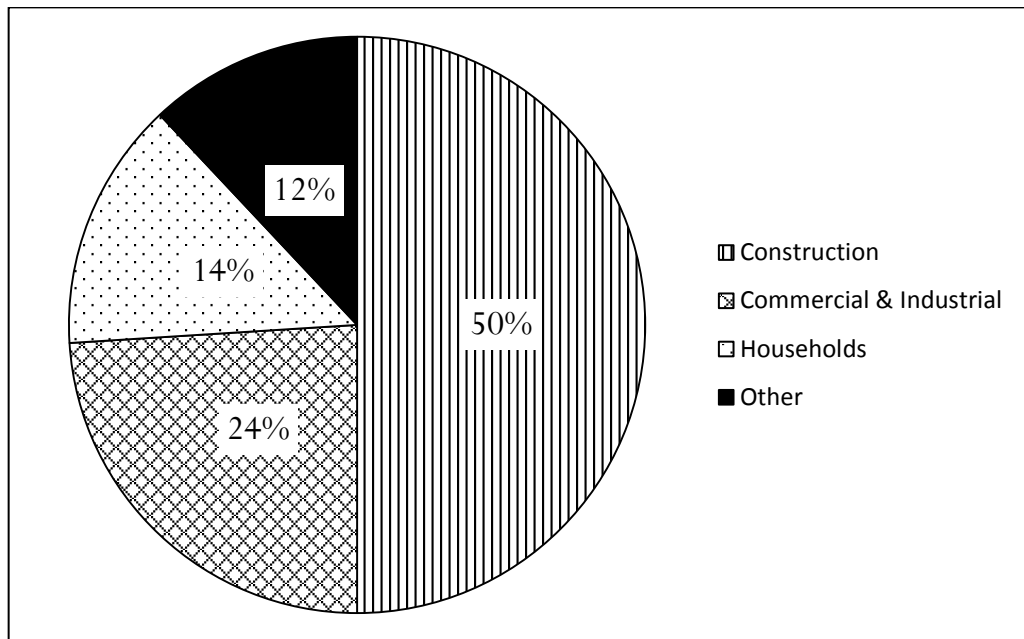


Figure 1.2 Waste generation split by nomenclature of economic activities (NACE), 2012 United Kingdom [11]

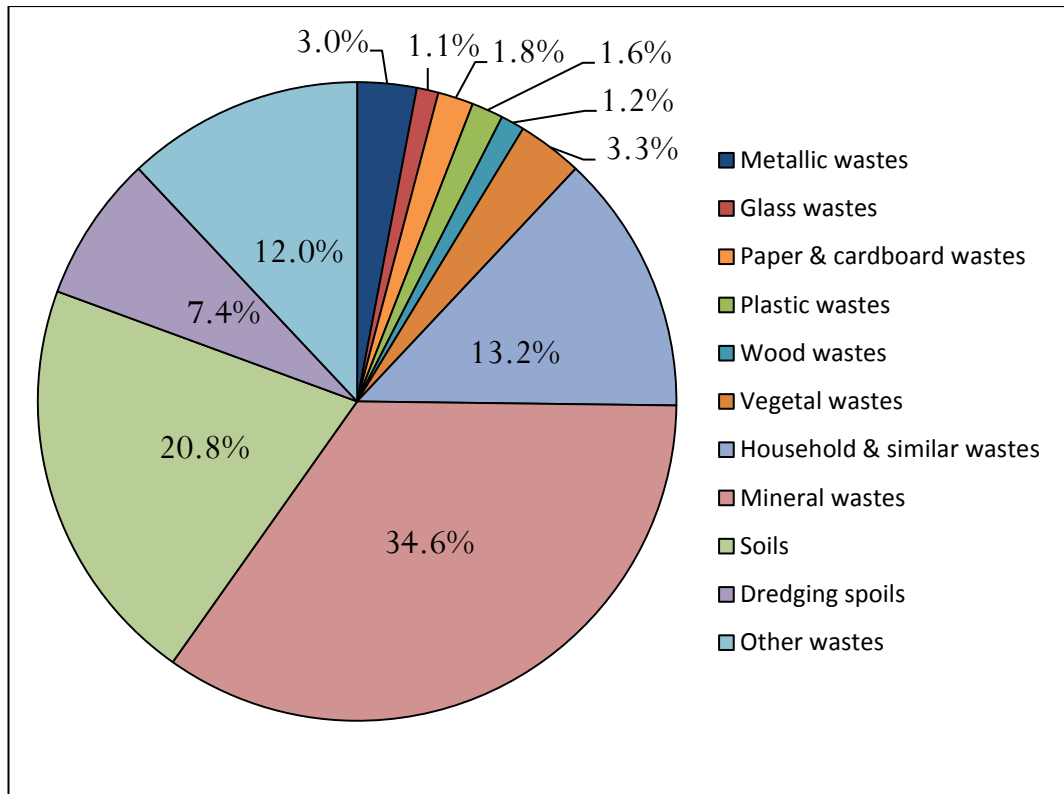


Figure 1.3 Waste generation split by waste material, 2012 United Kingdom [11]

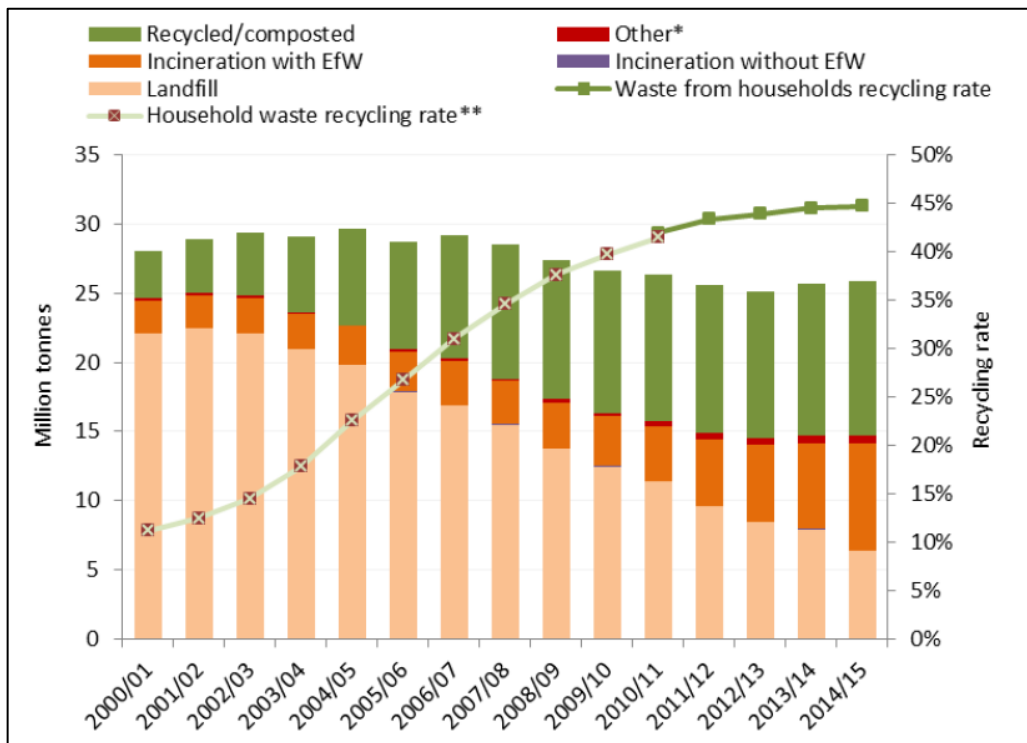


Figure 1.4 Management of all Local Authority collected waste and recycling rates in England, 2000/01-2014/15 [12]

The management of waste in England for Local Authority collected waste is shown in Figure 1.4 [12]. Local Authority collected waste (LACW) is defined as all type of waste including municipal waste such as household waste and business waste which is similar in nature and composition, as well as non-municipal fractions such as construction and demolition waste where collected by the local authority. There is an increasing trend from the recycled/composted method and the amount of waste landfilled has decreased rapidly since 2003/04. In 2014/15, the local authorities recycled almost 43 % of all waste collected. There was a small increase in incineration which might be due to a change from landfill. In recent years, it is shown from the figure that the interest on generating energy from waste (incineration) is increasing than landfilling.

Table 1.2 Carbon impact of Local Authority waste management in England in the year of 2011/12 [13]

Material managed	Treatment method (tonnes waste)			Total CO ₂ save/emitted
	Recycling/ reuse/ composting	Energy recovery	Landfill	Tonnes CO ₂ eq. (positive values are savings)
Glass	1, 139,677			298, 022
Paper & card	2, 587, 653			2, 201, 092
Metal	581, 143			1, 655, 256
Plastics	354, 276			420, 445
Organic	4, 108, 255			1, 011, 261
Wood	661, 725			759, 612
WEEE	257, 596			207, 222
Batteries	8, 003			4, 505
Tyres	9, 378			18, 057
Furniture	22, 719			20, 925
Rubble	1, 433, 511			13, 008
Soil	35, 437			10
Plasterboard	49, 885			6,695
Oil	6, 372			4, 147
Other	126, 364			0
Composite	12, 767			-8, 757
Paint	2, 091			5, 498
Textile	113, 739			302, 173
Residual	0	4, 876, 253	9, 804, 127	-2, 660, 937
Total waste treated	11, 510 592	4, 876, 253	9, 804, 127	4, 258, 233

Table 1.2 [13] shows the carbon impact of Local Authority waste management in England in 2011/12, in CO₂ equivalent terms. Taken as a whole, the management of waste by Local Authorities saved 4.3 million tonnes of CO₂ equivalent in emissions. Recycling, reusing or composting materials instead of landfilling them prevented an estimated 6.9 million tonnes CO₂ equivalent. Incineration and landfill of residual ('black bag') waste produced an estimated 2.7 million tonnes of emissions in CO₂ equivalent.

1.2.2 Plastics production

The plastic fraction of waste represents a considerable proportion of the total waste stream. Plastics produce products for a wide range of applications and will eventually end up as waste. Therefore, plastics consumption is one of the contributors towards the increasing amount of waste. The reason for this is based on high demands for plastics production by the consumer [14]. Moreover, plastics can produce lightweight objects with varieties of shape due to their low density and easy moulded properties. Plastics are also a good insulator as a result of their low thermal and electric conductivity.

Figure 1.5 [15] describes the plastics demand in the world that has gradually risen since 2004 (225 Mtonnes) to 311 Mtonnes in 2014. However, the demand for plastics in Europe was quite stable from within these ten years. The major plastics demand in Europe comes from Germany with 25%, followed by Italy (14%), France (10%), United Kingdom (8%) and Spain (7%). Plastics are also widely needed for the packaging market as well as for the building & construction sector in the European countries.

There are two main groups of plastic; thermosets and thermoplastics. The three-dimensional structures of thermosets are thermally decomposed while heating. Thermosets are generally used in the automobile, furniture and coatings industries. In comparison to thermosets, there is no or very little bonding between individual molecular chain in thermoplastics so they soften when heated and harden again when cooled. Examples of thermoplastics are high and low density polyethylene (HDPE and LDPE), polystyrene (PS), polypropylene (PP) and polyvinyl chloride (PVC). They are typically used in containers, packaging and trash bags production.

Therefore, thermoplastics are generally found in the mix of municipal solid waste of plastic in Europe rather than thermosets [16].

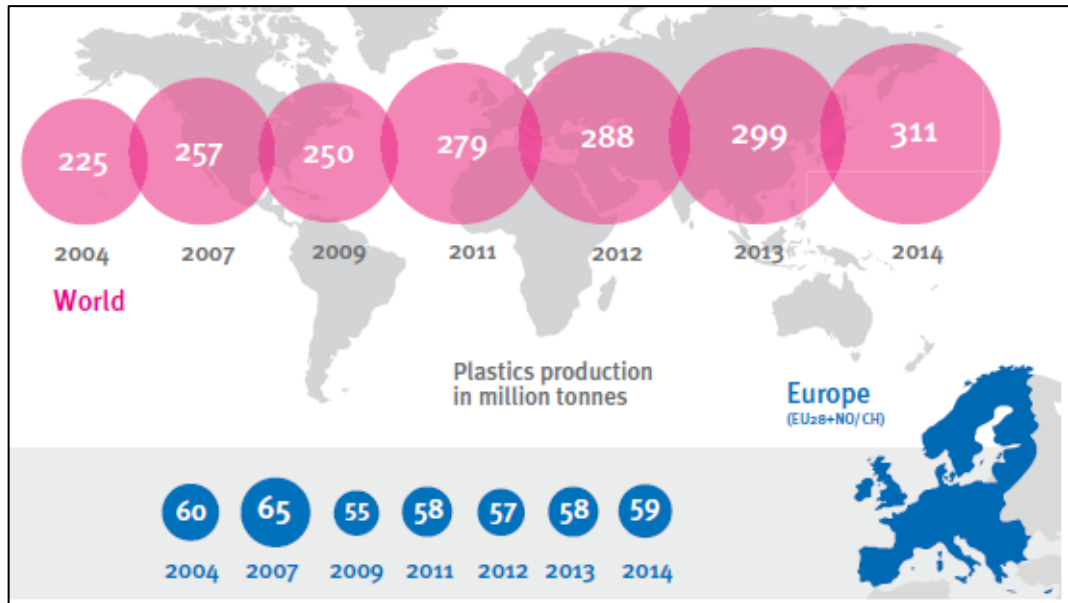


Figure 1.5 World plastic production [15]

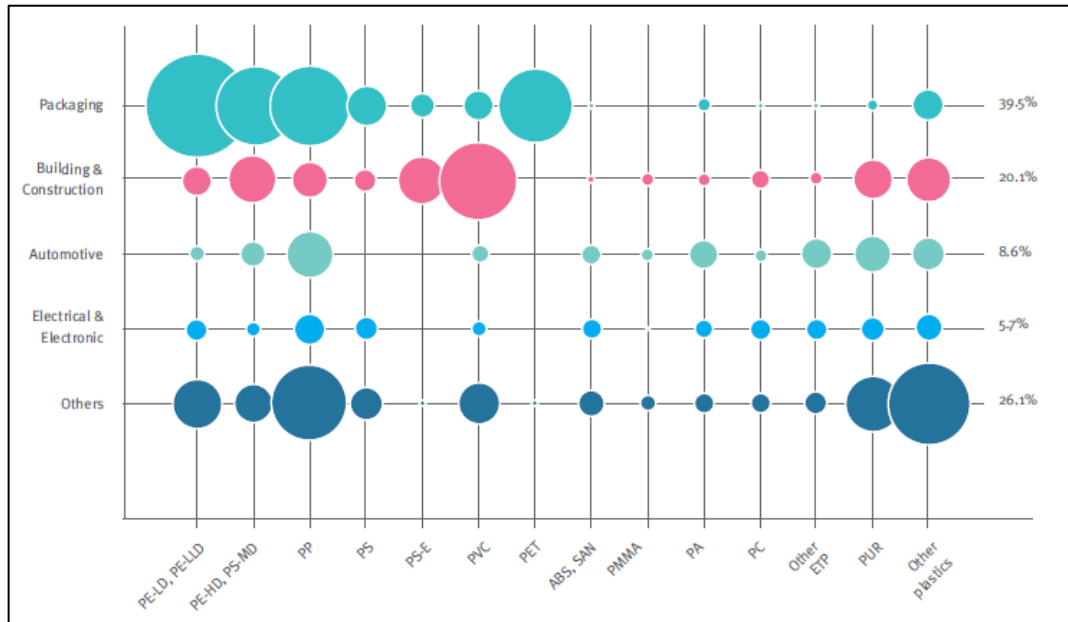


Figure 1.6 European plastic demand by applications and polymer type 2014 [15]

Global plastics usage continues to increase due to high industrial and consumer demand [17]. In 2012, 65.41 million tonnes of polyethylene (PE), 52.75 million tonnes of polypropylene (PP), 37.98 million tonnes of polyvinyl chloride (PVC), 19.8 million tonnes of polyethylene terephthalate (PET), and 10.55 million tonnes of polystyrene (PS) were produced worldwide [18]. The dominant plastics produced worldwide are reported as polyethylene (29.6%), polypropylene (18.9 %), polyvinyl chloride (10.4%), polystyrene (7.1%), polyethylene terephthalate (6.9%), polyurethane (7.4%) and many other types of plastic which represent about 19.7% of the plastics produced [19].

Figure 1.6 [15] indicates the plastics production in Europe by application sectors and type of plastics used. The highest contributor is the packaging sector (40%) represented by polyethylene, polypropylene and polyethylene terephthalate usage. Polyvinyl chloride usages in the building and construction sector also contribute largely to the type of plastic demanded in the Europe. It can be concluded that the highest type of plastic used in Europe are polyethylene which include high, low and linear low density (29%), polypropylene (19%) and polyvinyl chloride (12%) which comprise more than half of the total production demand. The structure of individual plastics that are typically found in municipal solid waste is shown in Figure 1.7.

<u>Plastic structure</u>	<u>Formula</u>
<p>High density polyethylene/ HDPE</p> $\sim\text{CH}_2-\text{CH}_2-\left[\text{CH}_2-\text{CH}_2\right]-\text{CH}_2\sim$	$(\text{C}_2\text{H}_4)_n$
<p>Low density polyethylene/ LDPE</p> $\sim\text{CH}_2-\text{CH}\left(\begin{array}{c} \text{CH}_3 \\ \\ \text{CH}_2 \\ \\ \text{CH}-\text{CH}_2\sim \\ \\ \text{CH}_2 \\ \\ \text{CH}_2 \\ \\ \text{CH}_3 \end{array}\right)-\left[\text{CH}_2-\text{CH}_2\right]-\text{CH}-\text{CH}_2\sim$	$(\text{C}_2\text{H}_4)_n$
<p>Polypropylene/ PP</p> $\left[\begin{array}{c} \text{CH}_3 \\ \\ \text{---} \text{C} \text{---} \\ \\ \text{---} \end{array}\right]_n$	$(\text{C}_3\text{H}_6)_n$
<p>Polyethylene terephthalate/ PET</p> $\left[\begin{array}{c} \text{O} \\ // \\ \text{---} \text{C} \text{---} \\ / \quad \backslash \\ \text{O} \quad \text{O} \end{array} \text{---} \text{C}_6\text{H}_4 \text{---} \begin{array}{c} \text{O} \\ // \\ \text{---} \text{C} \text{---} \\ \backslash \quad / \\ \text{O} \quad \text{O} \end{array} \text{---} \text{O} \text{---} \right]_n$	$(\text{C}_{10}\text{H}_8\text{O}_4)_n$
<p>Polystyrene/ PS</p> $\left[\begin{array}{c} \text{C}_6\text{H}_5 \\ \\ \text{---} \text{C} \text{---} \\ \\ \text{H} \end{array} \text{---} \begin{array}{c} \text{H} \\ \\ \text{---} \text{C} \text{---} \\ \\ \text{H} \end{array} \right]_n$	$(\text{C}_8\text{H}_8)_n$

Figure 1.7 The structure of individual plastics

1.2.3 Energy recovery from waste plastics

The European Union's approach to waste management is based on three principles, waste prevention, recycling and reuse as well as improving final disposal and monitoring [20]. The general management of waste is either by landfilling, incineration and recycling or composting. Each of these management methods has their own advantages and disadvantages. For instance, the only energy recovery collected from landfilling is the landfill gas. The landfill gas mainly consists of CH₄ and CO₂, therefore can contribute to climate change unless properly controlled [21]. Incineration also releases CO₂ to the atmosphere and both landfilling and incineration attract public concern especially on the greenhouse gases, dioxins and fly ashes matters. Landfilling requires more land space and in the United Kingdom the cost is normally high considering the gate fees to the owner of the land as well as the government landfill tax [22].

In Europe, 33.6% of total plastic waste generation was recovered as energy in 2011 as depicted in Figure 1.8 [23]. It is believed that the growing use of post-consumer plastic waste as a complementary fuel in power plants and cement kilns is the reason for the amount of plastic waste used in energy recovery. The waste to energy conversion from waste plastic are not only beneficial to the minimization of landfill utilization but also significantly improving the energy saving.

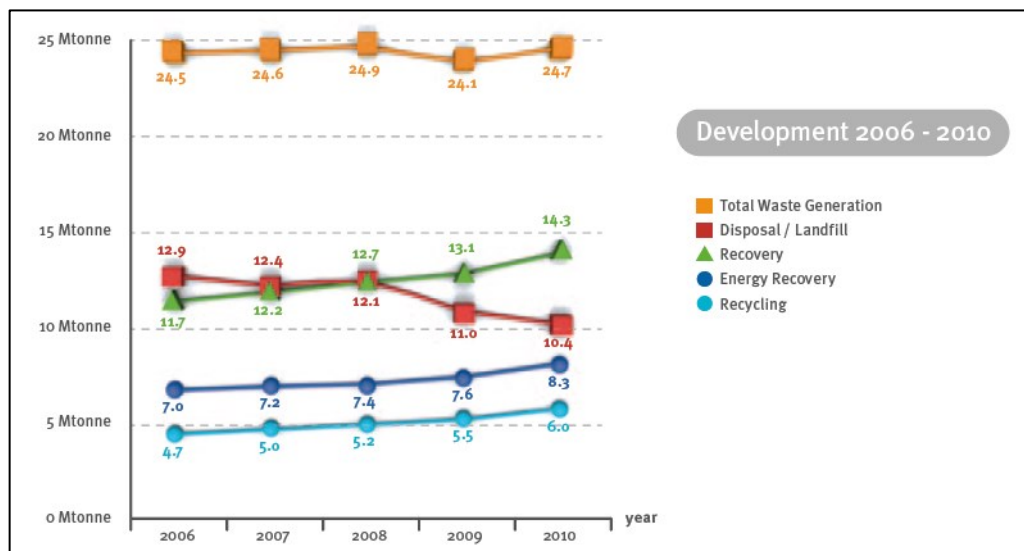


Figure 1.8 Total plastic waste recycling and recovery 2006-2010 [23]

Waste plastic is also considered as a hazardous waste for the environment. The additives in the plastics used for improving and modifying the plastic properties can in some cases generate harm to the environment. Thus according to Tamaddon and Hogland [24], cadmium pigments have been used in plastic all over the world and it is determined that the most cadmium in municipal solid waste is from the waste plastic. Although there has been reduction of cadmium usage in plastic, the impact is still of concern. In addition, the slow degradation of waste plastic causes it to be less suitable for landfilling hence affecting the landfill capacity.

Waste plastics can be recovered from the waste stream and processed, for example, through mechanical recycling to produce new plastic products, used for energy recovery via incineration, pyrolyzed to produce oils, gasified to syngas, or landfilled [25,26]. According to Plastics Europe, the leading European trade association for the plastics industry in Europe, 25.2 million tonnes of waste plastic are generated annually, of which ~26% is recycled [19]. The vast majority of the recycling of the waste plastics is through mechanical processes, however, there is growing interest in thermal recycling [14,27].

Energy conversion from waste generation by thermal recycling is considered as one of the most beneficial processes. The waste can be treated and recycled to produce energy sources. Waste plastic is well known as a potential fuel replacement as its chemical composition contains high calorific value. The calorific value of most plastics is higher compared to some coals and is equivalent to fuel oils [14]. Pyrolysis process can be applied to recycle the waste plastics thermally, in which plastic is heated in an inert atmosphere to produce oil, gas and char [28, 29]. The oil produced from pyrolysis of plastic is fuel-like with the calorific value similar to fuel oil and applicable in petrochemical industries [30]. Catalytic steam reforming of waste plastics is another promising way for energy recovery for the production of hydrogen, carbon monoxide and other useful products [31]. Various types of catalysts such as nickel based catalyst [32], have been extensively studied for plastic catalytic steam reforming.

1.3 Research Objectives

This research concerns the processing of waste plastics through advanced thermal treatment technologies via pyrolysis and gasification/reforming for synthesis gas (syngas) production. Syngas can be produced commercially by the reformation of methane by carbon dioxide also referred to dry reforming of methane (DRM). Since plastics are rich in hydrocarbons, it is interesting to pyrolyse the plastics to produce a suite of hydrocarbons which can then be directly catalytically reformed using carbon dioxide. This process would represent a novel option for the management of waste plastics, but also provide a route for the utilisation of carbon dioxide. Compared with steam reforming, studies on carbon dioxide reforming on wastes are limited especially on waste plastics.

In this work, the following objectives are to be carried out in relation to syngas production from dry reforming of waste plastics:

1. Investigation of the thermogravimetric characteristics and kinetic pyrolysis of waste plastics using thermogravimetric analysis in regards to the influence of carbon dioxide. The degradation temperature of each sample, the rate of weight loss of the sample with temperature and the kinetic analysis under both nitrogen and carbon dioxide are to be determined. These parameters would give an indication for their influence on the pyrolysis process in each type of waste plastics. This objective is discussed in Chapter 4 of this thesis.
2. Investigation of the influence of reaction atmospheres on the non-catalytic pyrolysis of waste plastics. The effects of reactor type between one-stage pyrolysis and two-stage pyrolysis gasification of waste plastics are also to be investigated. The gasification stage at higher temperature will further reform the pyrolyzed products from the pyrolysis furnace, hence the amount of hydrogen and carbon monoxide in the syngas is assumed to be increased. Discussion in achieving this objective is presented in Chapter 5.
3. Investigation of the influence of catalyst type for the dry reforming of waste plastics possessing with the aim of producing catalysts with high catalytic activity and stability in relation to syngas production and reduced carbon formation. The catalyst activity of Ni-based catalysts with different metal promoters is compared to maximise hydrogen and carbon monoxide production. In addition, different catalyst molar ratios are also discussed. The details of this objective are described in Chapter 5 of this thesis.

4. Investigation on the dependence of the type of plastics for syngas production. Different types of individual plastics may behave differently during the process depending on their structure. The discussion of this objective is presented in Chapter 6.
5. Investigation of the optimum process parameters to maximise hydrogen and carbon monoxide in the syngas production from the dry reforming process including gasification temperature, catalyst preparation method, catalyst ratio and CO₂ input rate. This objective is investigated and discussed in Chapter 7.
6. Investigate the influence of inputting steam to improve syngas quality in regards to H₂/CO molar ratio for the reforming process. Discussion of this objective is also presented in Chapter 7.
7. Investigation of real-world waste plastics to determine the influence of different real-world waste plastics obtained from different waste treatment plants for syngas production. Different waste streams will have different types of plastics and different plastics compositions; hence this study would investigate the behaviour of each type of real-world waste plastic during the process. This objective is studied and explained in Chapter 8 of this thesis.

References

1. Seinfeld, J.H. and Pandis, S.N. Atmospheric Chemistry and Physics: From Air Pollution to Climate Change. Wiley, 2012.
2. Bellard, C., Bertelsmeier, C., Leadley, P., Thuiller, W. and Courchamp, F. Impacts of climate change on the future of biodiversity. *Ecology Letters*. 2012, 15(4), pp.365-377.
3. Doney, S.C., Ruckelshaus, M., Duffy, J.E., Barry, J.P., Chan, F., English, C.A., Galindo, H.M., Grebmeier, J.M., Hollowed, A.B., Knowlton, N., Polovina, J., Rabalais, N.N., Sydeman, W.J. and Talley, L.D. Climate Change Impacts on Marine Ecosystems. *Annual Review of Marine Science*. 2012, 4(1), pp.11-37.
4. Poloczanska, E.S., Brown, C.J., Sydeman, W.J., Kiessling, W., Schoeman, D.S., Moore, P.J., Brander, K., Bruno, J.F., Buckley, L.B., Burrows, M.T., Duarte, C.M., Halpern, B.S., Holding, J., Kappel, C.V., O'Connor, M.I., Pandolfi, J.M., Parmesan, C., Schwing, F., Thompson, S.A. and Richardson, A.J. Global imprint of climate change on marine life. *Nature Clim. Change*. 2013, 3(10), pp.919-925.
5. Stephens, P.A., Mason, L.R., Green, R.E., Gregory, R.D., Sauer, J.R., Alison, J., Aunins, A., Brotons, L., Butchart, S.H.M., Campedelli, T., Chodkiewicz, T., Chylarecki, P., Crowe, O., Elts, J., Escandell, V., Foppen, R.P.B., Heldbjerg, H., Herrando, S., Husby, M., Jiguet, F., Lehikoinen, A., Lindström, Å., Noble, D.G., Paquet, J.-Y., Reif, J., Sattler, T., Szép, T., Teufelbauer, N., Trautmann, S., van Strien, A.J., van Turnhout, C.A.M., Vorisek, P. and Willis, S.G. Consistent response of bird populations to climate change on two continents. *Science*. 2016, 352(6281), pp.84-87.
6. Joy, E.A., Horne, B.D. and Bergstrom, S. Addressing Air Quality and Health as a Strategy to Combat Climate Change. *Annals of Internal Medicine*. 2016, 164(9), pp.626-627.
7. McCright, A.M., Dunlap, R.E. and Marquart-Pyatt, S.T. Political ideology and views about climate change in the European Union. *Environmental Politics*. 2016, 25(2), pp.338-358.
8. Blasing, T.J. Recent Greenhouse Gas Concentrations. Carbon Dioxide Information Analysis Center, 2016.
9. U.S Environmental Protection Agency. Solid Waste and Hazardous Waste. Washington, D.C, 2013. Available from: <http://www.epa.gov/>
10. Environment Agency. The State of Our Environment: Waste and Resource Management. Rotherham, 2010. Available from: <http://www.environment-agency.gov.uk/>
11. DEFRA. UK statistic on waste. Department of Environment Food & Rural Affairs, 2015.

12. DEFRA. Statistics on waste managed by local authorities in England in 2014-2015. Department for Environment and Rural Affairs, 2015.
13. DEFRA. Statistic on waste managed by local authorities in England in 2012/13. Department for Environment Food & Rural Affairs, 2012/13.
14. Aguado, J. and Serrano., D.P. Feedstock recycling of plastic wastes Cambridge, United Kingdom: The Royal Society of Chemistry, 1999.
15. PlasticsEurope. Plastics-the Facts 2015: An analysis of European plastics production, demand and waste data. 2015.
16. Scheirs, J. and Kaminsky, W. eds. Feedstock recycling and pyrolysis of waste plastic: Converting waste plastics into diesel and other fuels. United Kingdom: Wiley, 2006.
17. Thompson, R.C., Swan, S.H., Moore, C.J. and vom Saal, F.S. Our plastic age. *Philosophical Transactions of the Royal Society of London B: Biological Sciences*. 2009, 364(1526), pp.1973-1976.
18. Sagel, E. Polyethylene global overview. Ciudad de Mexico, 2012.
19. PlasticsEurope. Plastics the facts 2014/2015. Plastics Europe, Brussels. 2015.
20. Being wise with waste: the EU's approach to waste management. [Leaflet]. Luxembourg: European Union, 2010.
21. U.S. Environmental Protection Agency. Overview of Greenhouse Gases. Washington, D.C, 2013. Available from: <http://www.epa.gov/>
22. Williams, P.T. Waste Treatment and Disposal. Second ed. West Sussex, England: John Wiley & Sons, 2005.
23. PlasticsEurope. Plastic - The Facts 2011 An analysis of European plastics production, demand and recovery for 2010. PlasticsEurope Association of Plastics Manufactures, Brussels. 2011.
24. Tamaddon, F. and Hogland, W. Review Of Cadmium In Plastic Waste In Sweden. *Waste Management & Research*. 1993, 11(4), pp.287-295.
25. Wang, C.-q., Wang, H., Fu, J.-g. and Liu, Y.-n. Flotation separation of waste plastics for recycling—A review. *Waste Management*. 2015, 41, pp.28-38.
26. Al-Salem, S.M., Lettieri, P. and Baeyens, J. Recycling and recovery routes of plastic solid waste (PSW): A review. *Waste Management*. 2009, 29(10), pp.2625-2643.
27. Eriksson, O. and Finnveden, G. Plastic waste as a fuel - CO₂-neutral or not? *Energy & Environmental Science*. 2009, 2(9), pp.907-914.
28. López, A., de Marco, I., Caballero, B.M., Laresgoiti, M.F. and Adrados, A. Influence of time and temperature on pyrolysis of plastic wastes in a semi-batch reactor. *Chemical Engineering Journal*. 2011, 173(1), pp.62-71.
29. Williams, P.T. and Williams, E.A. Interaction of Plastics in Mixed-Plastics Pyrolysis. *Energy & Fuels*. 1999, 13(1), pp.188-196.
30. Demirbas, A. Pyrolysis of municipal plastic wastes for recovery of gasoline-range hydrocarbons. *Journal of Analytical and Applied Pyrolysis*. 2004, 72(1), pp.97-102.
31. Namioka, T., Saito, A., Inoue, Y., Park, Y., Min, T.-j., Roh, S.-a. and Yoshikawa, K. Hydrogen-rich gas production from waste plastics by

pyrolysis and low-temperature steam reforming over a ruthenium catalyst. *Applied Energy*. 2011, 88(6), pp.2019-2026.

32. Luo, S., Zhou, Y. and Yi, C. Syngas production by catalytic steam gasification of municipal solid waste in fixed-bed reactor. *Energy*. 2012, 44(1), pp.391-395.

Chapter 2

LITERATURE REVIEW

2.1 Reforming Processes of Waste Plastics for Synthesis Gas Production

Depending on the end-use of the plastic product at some stage during the lifetime of the plastic, the plastic will end up as waste in various, commercial, industrial and household waste sectors [1]. Waste plastics may be separated from the various waste streams for subsequent recycling, recovery and re-processing. The vast majority of plastic recycling is through mechanical recycling. However, alternative methods for producing fuels and petrochemical feedstocks from waste plastics are being investigated [1].

Anticipating growing interest in alternative methods of obtaining syngas from waste materials and in particular from waste plastics [2-6], the thermal treatment technologies have become more popular. The most well-known technologies including conventional combustion technologies, waste gasification, plasma arc and pyrolysis technologies, thermal cracking, thermal oxidation and waste-to-fuel technology have been reported [7].

Since plastics are mainly composed of hydrocarbons, thermal recycling of waste plastics to reform plastics into chemical products, monomer or synthesis gases which are mainly composed of a mixture of hydrogen and carbon monoxide. The reforming of plastics into new materials is another alternative method for the synthesis gas production and represents a low cost feedstock. There have been many reports into the production of hydrogen and synthesis gases from waste plastics by pyrolysis and gasification process [8-11]. The addition of steam, catalyst and partial oxidation enhancing the production of gases through a catalytic steam reforming type process [12-17].

2.1.1 Pyrolysis

Pyrolysis, also known as thermolysis is the chemical and thermal degradation of waste material in an inert atmosphere. In this scenario, the process takes place with an absence of oxygen. In pyrolysis, the organic waste material decomposes into synthesis gas, liquid as well as solid product yields, and are often endothermic which requires a heat supply. The product yields are dependent on the experimental parameters; the temperature, reaction times, pressures, the presence or absence of reactive gases, liquids or catalyst.

Pyrolysis of plastic waste is normally conducted at low (<400 °C) medium (400-600 °C) and high temperature (>600 °C). Various researches on pyrolysis of single plastic and mixed waste plastic have been carried out to understand the characteristics of the process along with the yields produced.

Pyrolysis is proven as one of the environmentally sustainable methods of managing the plastic waste as compared to landfilling or waste sent to incinerators. Several researches have described the applicability of pyrolysis as a thermochemical technique for managing waste plastic either individually, mixed plastics or real-world plastic waste [18-23].

Table 2.1 [24] shows the thermal decomposition products of waste plastics which are converted into gases, a liquid hydrocarbon fraction (the pyrolytic oil) and a solid residue (char). The absence of oxygen during the process affects the molecular weight and boiling fraction. Normally, high molecular weight and high boiling fractions are obtained, and are then processed and refined to produce petrochemical feedstock such as naphtha.

Table 2.1 Thermal decomposition products from pyrolysis of polymers [24]

Resin	Low-temperature products	High-temperature products
Polyethylene/PE	Waxes, paraffins, oil, α -olefins	Gases, light oils
Polypropylene/PP	Vaseline, olefins	Gases, light oils
Polyvinyl chloride/PVC	HCl, benzene	Toluene
Polystyrene/PS	Styrene	Styrene
Polymethyl methacrylate/PMMA	Methyl Methacrylate(MMA)	
Polytetrafluoroethylene/PTFE	Monomer	Tetrafluoroethylene (TFE)
Polyethylene terephthalate/PET	Benzoic acid, vinyl terephthalate	
Polycaprolactam/PA-6	Caprolactam	

Adrados et al. [9] have compared the pyrolysis of plastics from material recovery facilities and simulated plastic waste using a non-stirred semi batch reactor. The pyrolysis of real-world plastic waste produced higher solid and gas yields and lower liquid yields compared to the simulated municipal solid waste mixture. However, the gases appeared to have a lower HHV (higher heating value) levels as compared to the simulated sample due to their higher carbon dioxide content, which was derived from the cellulose materials (e.g., paper and wood) of the real sample. The high amount of inorganics material in the real sample also affected the solid yields production as a result of unable to fractionate the solids into gaseous or liquids.

A study on pyrolysis of waste low-density polyethylene has been made by Park et al. [25] and also by Bagri and Williams [26] to recover oil. In terms of oil production, they were both agreed that at 500 °C with the absence of catalyst, pyrolysis of LDPE produced about 95 wt.% oil. Park et al. showed that when using 10% NiO/Silica-alumina catalyst, the amount of light oil (below C₁₁) increased when the flow rate of thermally decomposed gas was decreased. Bagri and Williams investigated the reaction of LDPE with Y-zeolite and ZSM-5 catalyst, found that using both types of catalyst the oil production decreased while the gas production increased due to the conversion of liquid hydrocarbon to the gas. The ZSM-5 catalyst gave a higher concentration of gases than the Y-zeolite but Y-zeolite catalyst was proved to produce much higher concentration of aromatic compounds in the derived oil.

Other than normal or conventional pyrolysis, stepwise pyrolysis has also been investigated by Lopez-Urionabarrenechea et al. [8] to reduce the chlorine content in the product oil from packaging plastic waste. In stepwise pyrolysis, the first step is to decompose the low temperature material (dechlorination step) which in this case is PVC (between 250 and 320 °C) within the prescribed time then continuing with conventional pyrolysis by raising the temperature to further complete the pyrolysis process. The study proved that by introducing the dechlorination step, there was a 75% reduction (1.2 to 0.3 wt.%) of chlorine content of the liquids with respect to the conventional catalytic pyrolysis liquids as shown in Table 2.2 [8].

Table 2.2 Chlorine in the pyrolysis fractions (wt.%) from step-pyrolysis [8]

Method	Cl in liquids	Cl in gases ^a	Cl in solids
Conventional thermal pyrolysis	0.2	5.3	<0.1
Conventional catalytic pyrolysis	1.2	1.0	0.4
Catalytic stepwise pyrolysis	0.3	3.0	0.4
Non-catalytic dechlorination step + catalytic process	0.3	2.2	0.4

^aCalculated by difference taking into account that there is 1.1 wt.% chlorine in the original sample

2.1.1.1 Product yield distribution from pyrolysis of waste plastics

The product yield distribution from pyrolysis of waste plastic is normally affected by the pyrolysis operating conditions such as the type of plastic used, operating temperature, heating rate, pressure, type of reactor and the use of catalyst. The product yield from pyrolysis of waste plastic can be classified into solid which contains char, carbon deposition or residue, liquid which are oil or water and pyrolysis gases which are mainly composed of hydrogen, carbon monoxide, carbon dioxide, oxygen, methane, and other hydrocarbons. Table 2.3 summarises the product yield distribution from pyrolysis of waste plastic from several researchers.

The influences of temperature on the product yield distribution from the pyrolysis of high density polyethylene (HDPE) and low density polyethylene (LDPE) were studied by Mastral et al. [27] and Onwudili et al. [28] while Lopez et al. [29] investigated the influence of temperature on pyrolysis of plastic mixtures. In general, it has been demonstrated by several authors that the temperature has a significant effect on the production of liquid and gases. Low temperature produced a liquid with high content of long hydrocarbon chains while with the increase of temperature, the hydrocarbons cracked to form gases.

Mastral et al.[27] reported that at high temperature, the gas production for HDPE was steadily increased with the increasing of temperature from 650 °C up to 780 °C, whereas above 780 °C, the gas production decreased rapidly to 65.1 wt.% from the maximum value of 86.4 wt.%. The changes occurred due to the

cyclisation reactions that form aromatic hydrocarbons. The increased amount of gas production has been reported for the pyrolysis of LDPE at a temperature of 425 °C and 450 °C, whereas the gas yield increased from 10 wt.% to 25 wt.% [28]. Char present at 450 °C was believed to form as a secondary reaction product of the oil vapours. The significant increases in gas production suggest that by increasing the temperature results in cracking of the wax to oil, and to gas at higher temperature. Methane and ethylene were found as the highest volume concentration in the gas production. On the other hand, Lopez et al.[29] suggested that the optimum temperature for high yield of the liquid is at 500 °C from pyrolysis of plastics mixture that contain 40 wt.% of polyethylene (PE), 35 wt.% of polypropylene (PP), 18 wt.% of polystyrene (PS), 4 wt.% polyethylene terephthalate (PET) and 3 wt.% of polyvinyl chloride (PVC), while an extremely viscous liquid was produced at more lower temperature.

Pyrolysis of LDPE, HDPE and PP at 450 °C with the help of an acid fluid catalytic cracking (FCC) catalyst by Achilias et al. [30] proved that different types of plastic waste gave different yields of solid, liquid and gas. LDPE produced more liquid, HDPE more solid and PP more gas. The authors found that the oil and gaseous fractions recovered were mainly aliphatic in composition consisting of a series of alkanes and alkenes of different carbon number with great potential to be recycled back into the petrochemical industry as a feedstock for the production of new plastics or refined fuels. It was also found that the pyrolysis of plastic bags made from LDPE, where the liquid fraction consisted of hydrocarbons in the range of commercial gasoline.

The effects of pyrolysing different types of plastic waste were also shown by Encinar and González [31]. Each type of plastic produced different product yields. At 500 °C and catalyst, LDPE and PP produced nearly no solid and more gas compared to the experiment by Achilias et al. [30]. PET produced more gas that mostly consisted of carbon dioxide and carbon monoxide due to its chemical structure that contain oxygen. It can be concluded that even though each plastic has a different behaviour, the larger fraction was composed of liquid/wax (95–30%) and secondly were the gases (65–3%). However a significant yield of solid may occur depending on the use or no use of catalyst.

Another interesting factor on the pyrolysis process is the type of reactor chosen for the reforming activities. Summarized in Table 2.3, the vacuum type reactor

produced the lowest gas yield from the pyrolysis of HDPE and PP at 500 °C and most of the liquid produced was mainly wax [32].

The product yield distribution from pyrolysis of waste plastics was also shown to be influenced by the type of catalyst used during the process. Seo et al. [33] reported that the use of ZSM-5 catalyst in a stirred reactor produced high gas yield compared to experiments without a catalyst (thermal cracking) and even with Y-zeolite catalyst. They suggested that ZSM-5 catalyst promoted the cracking of liquid with higher hydrocarbons of n -C₅ to n -C₂₂ to the lighter hydrocarbons of C₄ to C₁₀, therefore reducing the liquid yield.

A detailed investigation on the effect of PET present in a real-world municipal waste plastics and PP/PE/PS/PVC mixture towards the quality of liquid yields was investigated by Sakata et al. [34]. They concluded that the addition of PET reduced the production of liquid while increasing the production of gases and char. The liquid yields from pyrolysis of the plastics mixture with the addition of PET contained more chlorinated hydrocarbons (addition of chlorine containing esters of benzoic acid, chloroalkyl esters) but less inorganic chlorine content. In their subsequent studies on pyrolysis of PP/PE/PS/PVC/HIPS-Br plastics mixed with PET, the yield of chlorinated branched alkenes is also increased in the presence of PET [35]. Kulesza and German [36] reported that the additional chlorinated hydrocarbons were formed due to the reaction between HCL (evolved from PVC) and PET before its degradation since PVC was degraded about 100 °C lower than in the case of PET.

Table 2.3(a) Product yield distribution from pyrolysis of waste plastics

Reactor	Feedstock	Temperature (°C)	Heating rate (°C/min)	Solid (wt.%)	Liquid (wt.%)	Gas (wt.%)	Reference
Fluidised bed	HDPE	650	Not stated	0.0	68.5	31.5	[27]
		685		0.0	39.6	59.9	
		730		0.0	13.5	76.1	
		780		0.0	13.4	86.4	
		850		0.0	15.4	65.1	
Batch reactor	LDPE	425	10	-	89.5	10	[28]
		450	10	1.75	72.4	25	
Fixed bed (with acid FCC catalyst)	LDPE	450	Not stated	19.4	72.1	8.5	[30]
	HDPE	450		52.5	44.2	3.3	
	PP	450		20.0	64.7	15.3	
Fixed bed	LDPE	500	20	0	61.24	38.76	[31]
	PP			0.1	68.06	31.84	
	PET			5.63	29.16	65.21	
	PS			1.04	92.65	6.31	
Vacuum	HDPE	500	10	0.80	97.7	0.95	[32]
	PP	500		0.01	95.0	3.5	

Table 2.3 continued on next page ...

Table 2.3(b) Product yield distribution from pyrolysis of waste plastics (... continued from previous page)

Reactor	Feedstock	Temperature (°C)	Heating rate (°C/min)	Solid (wt.%)	Liquid (wt.%)	Gas (wt.%)	Reference
Semi-batch reactor	<u>Plastic mixture</u> (40wt%PE/35wt%PP/18wt%PS/ 4wt%PET/ 3wt%PVC)	460	20	1.1	72.0	26.9	[29]
		500		0.8	65.2	34.0	
		600		0.9	42.9	56.2	
Stirred reactor	HDPE Thermal ZSM-5 catalyst Y-Zeolite catalyst	450	8	3	84	13	[33]
				1.5	35.0	63.5	
				1.5	71.5	27.0	
Glass reactor	<u>Plastic mixture (model)</u> (30%PP/ 30%PE/30%PS/10%PVC) <u>Plastic mixture (model)</u> (27.3%PP/ 27.3%PE/ 27.3%PS/ 9.1%PVC/ 9.1%PET) <u>Municipal waste plastics from treatment plant</u> (24.1%PS/5.1%PVC/1.7%PVCD/ 8.9%PET/ 0.3%ABS/ 42.2%PE/ 17.6%PP)	430	15	5	70	25	[34]
				13	53	34	
				16	59	25	

2.1.2 Gasification

Gasification or partial oxidation was originally developed to transform coal into usable products. However, gasification of polymeric waste can be considered as an efficient technique to degrade and convert the waste. It has been reported that the pyrolysis process of waste plastics produces a low yield of hydrogen [37], hence the gasification process, particularly gasification of waste plastics may improve gas production.

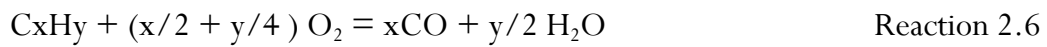
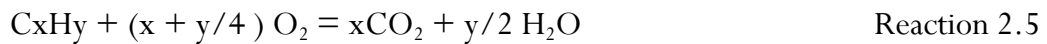
The gasification process may also involve the addition of oxygen or steam into the system at 700-1600 °C temperature range to react and oxidise the hydrocarbon feedstock in a controlled manner. This process yields hydrogen and carbon monoxide known as synthesis gas (syngas) which can be used as a fuel or feedstock for the chemical industry.

In addition, there are several other reactions that may occur during the gasification of a carbonaceous material, including waste plastics, in the presence of oxygen and/or steam as discussed by Aguado and Serrano [38]. Thermal decomposition of the raw material might occur prior to the oxygen, carbon dioxide or steam involvement through reaction 2.1. Reactions 2.2 to reaction 2.6 occur through exothermic transformations which releases heat from the system while reactions 2.7 to 2.11 occur through endothermic transformations. Reaction 2.8 is known as the water gas shift reaction that allows the control of the H₂/CO ratio. The Boudouard reaction occurs between carbon and carbon dioxide to increase the yield of carbon monoxide as shown in reaction 2.10. The methanation reactions by hydrogenation of carbon oxide in reaction 2.12 and 2.13 may lead to a significant decrease in the H₂ concentration of the final synthesis gas. The appropriate combination of exothermic and endothermic reaction results in the balance of the overall energy requirement of gasification, mainly by adjusting the O₂/H₂O ratio in the reaction medium. The gasifier temperature between 1300 and 1500 °C is needed to process these equilibrium reactions. Equilibrium can be approached at the temperature below 900 °C with the presence of catalysts or with longer residence time. The list of possible reaction discussed above are as follows [38]:

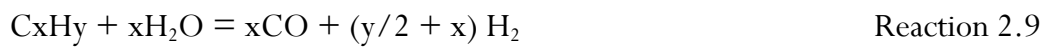
Raw material decomposition



Reactions with oxygen



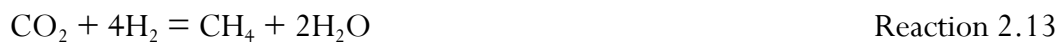
Reactions with water



Reactions with carbon dioxide



Methanation reactions



The gasification process applied to low density polyethylene using a fluidized bed reactor was reported by Zheng Jiao and Yong [39]. Figure 2.1 shows schematic diagram used for their experimental studies. They reported that there were significant improvements in the syngas production with the increasing of temperature, increasing from 73.75 wt.% syngas yield from the experiment at 550 °C to 93.30 wt.% syngas yield produced during the experiment at 750 °C.

They also suggested that the higher heating rate, the long residence time and the effect of oxygen are the possible reasons for influencing decomposition.

The combination of an integrated pilot-scale moving-grate gasification and power generation process by Lee et al. [40], showed significant improvement in the hydrogen production from refused plastic waste (RPW) feedstock. A high percentage of hydrogen and methane in the reformed gas was obtained, resulting in a higher caloric value of clean producer gas which mainly consisted of hydrogen, carbon monoxide, carbon dioxide and methane. They also tested the performance of syngas produced from the experiment using a 30 kWe gas engine to generate power. Approximately 22% efficiency of power generation and more than 20 kWe output power generation were achieved during the field test. Figure 2.2 illustrates the moving-grate gasification and utilization system.

Gasification experiments have been conducted using a dual fluidised bed steam gasifier pilot plant [41]. The feedstock inserted into the reactor was gasified to produce four possible products; tars, product gas, fly char or char. The basic principle of this gasification technology is shown in Figure 2.3. Research by Wilk and Hofbauer [41] using the improved reactor producing different carbon distribution percentage in the different polymer feedstocks as depicted in Figure 2.4. In terms of gas concentration, it was found that the concentration of methane and ethene increased with an increasing proportion of PE. The hydrogen and carbon monoxide was higher for PE+PP and PE+PS. The addition of PET produced more carbon dioxide (28 %) due to high oxygen composition in the material.

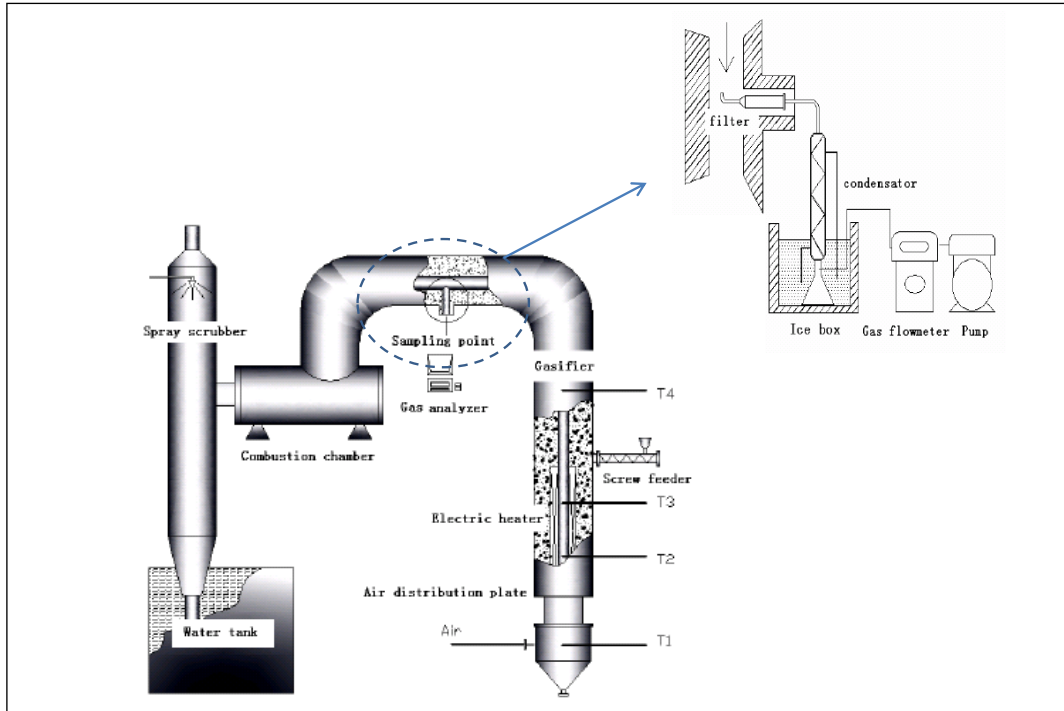


Figure 2.1 Schematic diagram of fluidized bed gasification reactor [39]

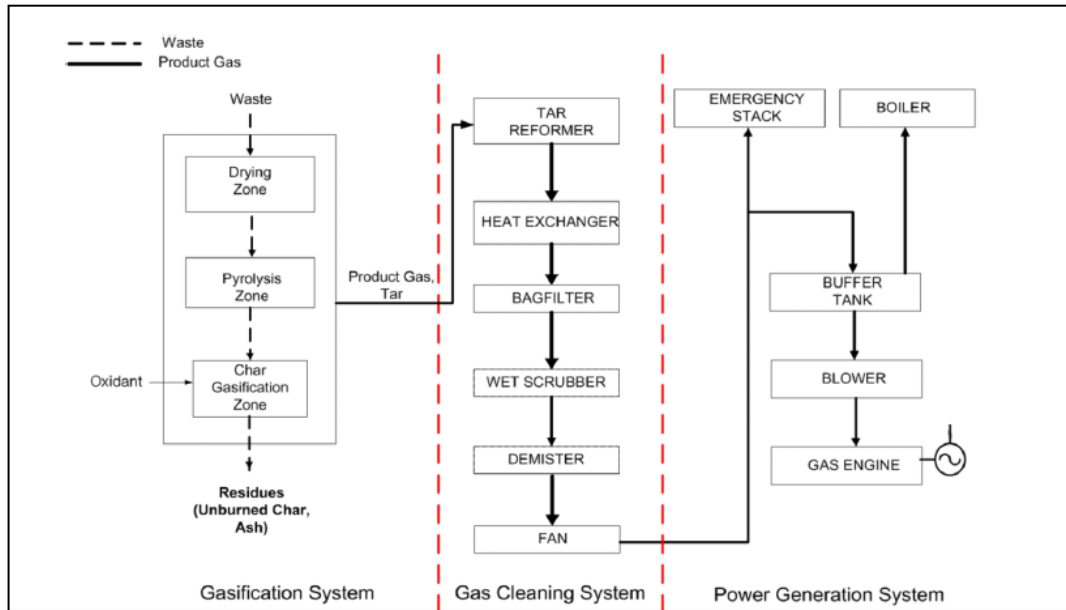


Figure 2.2 Moving-grate gasification and utilization system [40]

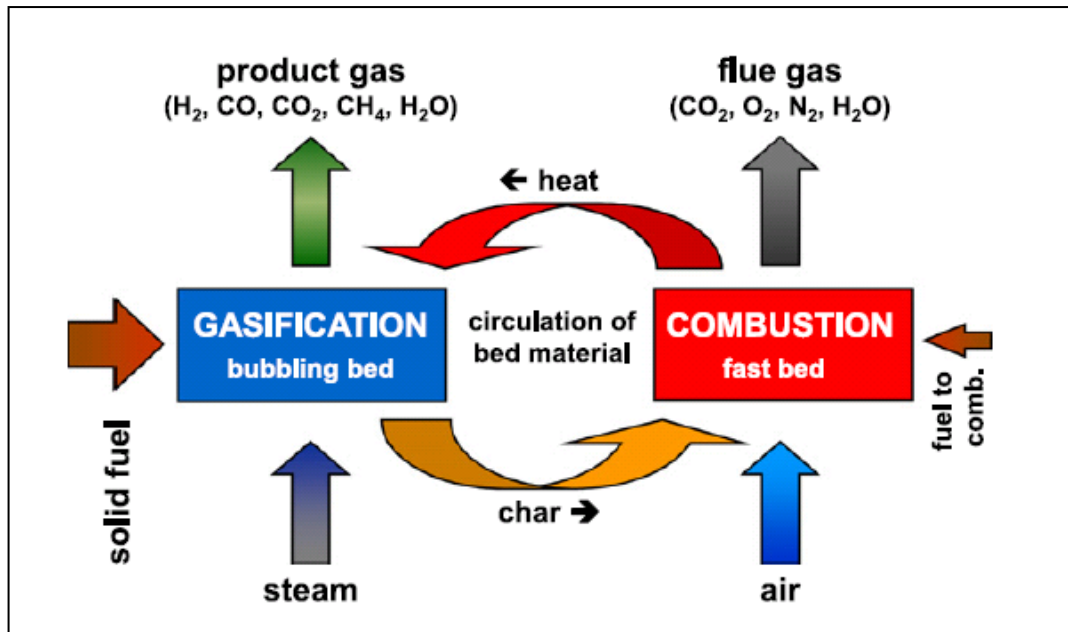


Figure 2.3 Basic principle of the dual fluidized bed gasification technology [41]

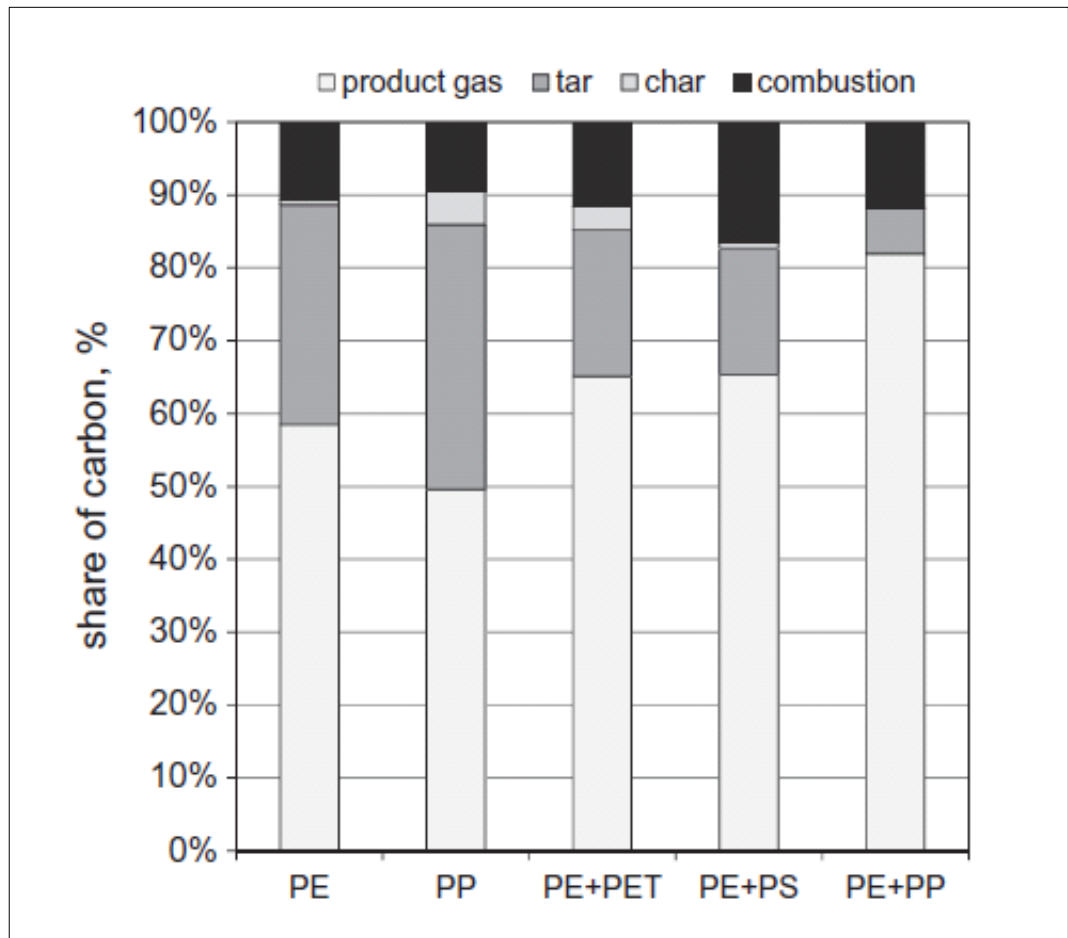


Figure 2.4 Distribution of carbon in the dual fluidised bed reactor for pure substances and mixtures [41]

2.1.3 Pyrolysis-gasification of waste plastics

The combined pyrolysis and gasification process is an alternative for thermal treatment for the decomposition of waste plastics. Pyrolysis and gasification of waste plastics is a promising route to produce high yields of a hydrogen-rich syngas. The process involves combining the thermal degradation of waste plastics in the first stage pyrolysis step followed by gasification/ reforming in a second stage, usually in the presence of catalysts which has the potential to generate high yields of hydrogen [42-44]. The gasification process produces reactions of the volatile products that are released from the pyrolysis process and recombines them to produce synthesis gas.

Toshiro Tsuji et al. [45] stated that the concept of two stage pyrolysis-gasification started with the conversion of plastic into liquid products at moderately low temperature in the first stage. The hydrocarbon liquid is then gasified at high temperature in the second stage. Based on their study of polyethylene, polystyrene and polypropylene feedstock using a quartz tube reactor heated by an electric heater, the coke formation was reduced as compared to the single-stage concept. It also produced high calorific value gas products which were mainly comprised of methane and gaseous alkenes such as ethene and propene. However, the gas yield for the polystyrene feedstock showed lower gas yield value compared to others.

2.1.3.1 Effect of steam injection on the pyrolysis-gasification system: steam reforming process

Introduction of water or steam into the pyrolysis-gasification of waste plastic is recognised to be effective for hydrogen production through promotion of the water gas shift reaction [46]. However this will depend on other factors such as the gasification temperature, steam injection rate and use of catalyst.

Thermal decomposition of waste plastics using a microscale pyrolysis/reforming reactor with molecular beam mass spectrometer (MBMS) by Czernik et al. [47] showed that many common plastics could be efficiently converted to hydrogen and carbon oxides by a pyrolysis and catalytic steam reforming process. It was found that polyethylene was completely converted to gas yielding hydrogen at 80% of the stoichiometric theoretical potential.

The different amount of steam injection rate into the system also affects the product yields. Wu and Williams [46] investigated four different steam injection rate namely 1.90, 4.74, 9.49 and 14.20 g h⁻¹ with waste plastic with 0.5 g of a Ni-Mg-Al catalyst at 800 °C gasification temperature. The gas composition produces are as illustrated in Figure 2.5. It was shown that the hydrogen concentration was stable; however there were large differences in the total hydrogen production as well as the carbon monoxide concentration when the steam injection was increased. The coke formation was also reduced with the addition of steam injection to the system due to the steam reaction with the carbon deposition (carbon gasification).

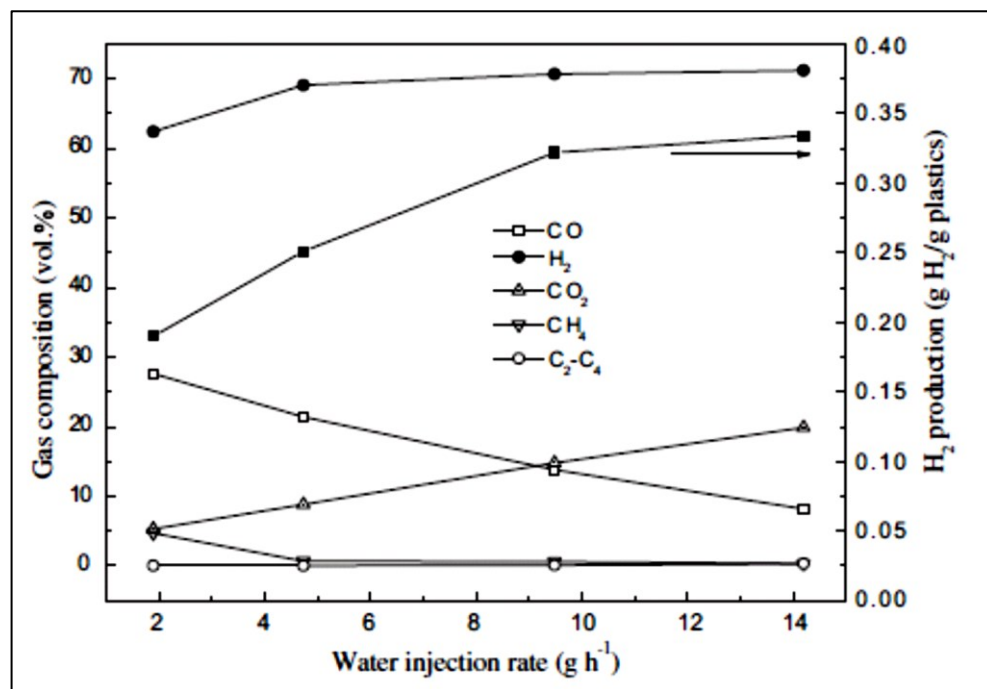


Figure 2.5 Gas composition and hydrogen production for different water injection rate [46]

2.2 Synthesis Gas Production (H₂ and CO) from Reforming of Waste Plastics

Synthesis gas (syngas) mainly consisting of hydrogen and carbon monoxide is viewed as one of the major alternative energy sources. The uses of syngas are including producing methanol, ammonia and synthetic fuel through Fischer-Tropsch synthesis. The H₂/CO molar ratio selection is considered critical to complement with the end-use product processing requirements [48-51]. Waste plastics are among the potential sources for synthesis gas production due to their high hydrocarbon content [52-54]. Many researchers have reported on the thermal and catalytic cracking of waste plastics for H₂ as well as synthesis gas production [55-58].

2.2.1 Influence of temperature

Hydrogen production from the thermal treatment of waste plastic is normally depending on the treatment type such as the reactor used, temperature, heating rate and the process involved. In the case of pyrolysis of high density polyethylene, an experiment using a fluidised bed reactor was performed by Ahmed and Gupta [59]. The results showed that the hydrogen production increased as the pyrolysis temperature increased as shown in Figure 2.6. The difference characteristics between pyrolysis and steam gasification of PS in a semi-batch reactor at three different temperatures; 700°C, 800°C and 900°C was investigated. At both 700°C and 800°C, the hydrogen yield was low as compared to the pyrolysis process due to the competing reaction of polystyrene with steam that forms condensable hydrocarbons (liquid and suspended wax). It was suggested that the gasification temperature of more than 800°C is required in order to get higher hydrogen production as well as better energy yield from the polystyrene feedstock.

The influence of temperature on the steam gasification of polystyrene in a bench-scale down-stream fixed bed reactor was investigated by He et al. [44]. Based on the H₂ and CO results presented in Table 2.4, it was shown that the hydrogen and carbon monoxide was increased with the increase in the temperature. The H₂/CO molar ratio of 0.83-1.35 was achieved in their investigation and this value was considered ideal for Fischer-Tropsch synthesis.

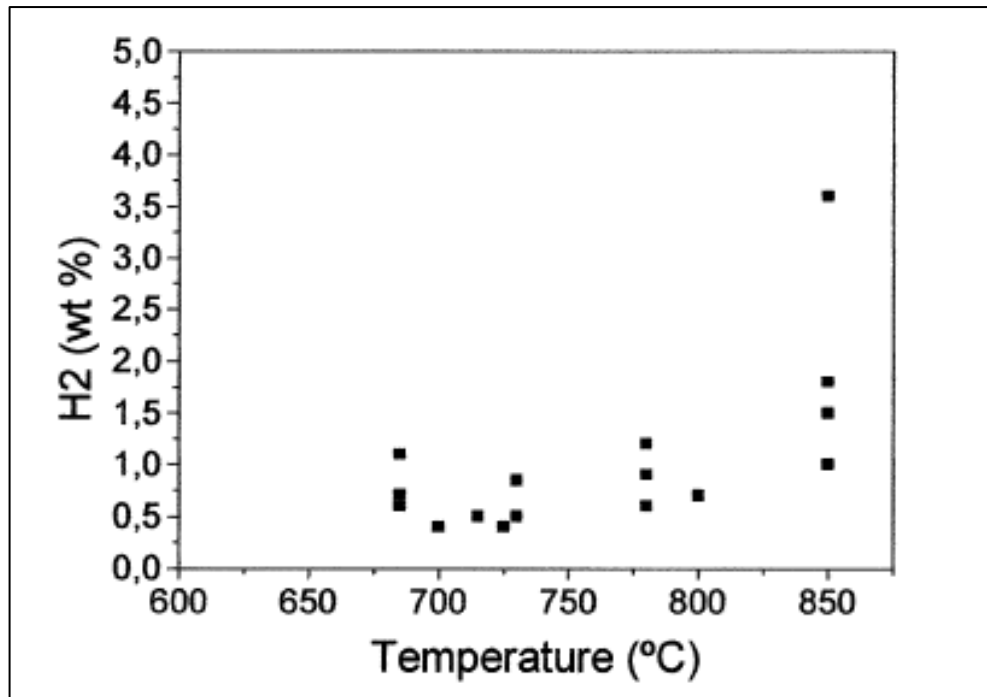


Figure 2.6 Evolution of hydrogen production with pyrolysis temperature [27]

Table 2.4 Effect of temperature on hydrogen and carbon monoxide production from steam gasification of plastic waste (PE) in bench scale fixed bed reactor with a heating rate of 10 °C min⁻¹

Temperature (°C)	H ₂ (mol%)	CO (mol%)
700	16.92	20.33
750	21.31	21.53
800	28.94	22.83
850	34.96	25.87
900	36.98	27.37

Wu and Williams [42] presented results from the pyrolysis-gasification of waste plastics in a two-stage fixed bed reactor with the help of catalyst addition to the system. The addition of steam in the system lowered the hydrogen yield due to the carbonization reactions which were limited by the introduction of steam and generated more C₁-C₄ gases, CO and CO₂. Addition of a Ni-Mg-Al catalyst has proved to enhance the hydrogen production as shown in Figure 2.7. It was suggested that reduction of hydrocarbon gases (C₁-C₄) was due to their reaction with the Ni-Mg-Al catalyst hence decomposed to hydrogen.

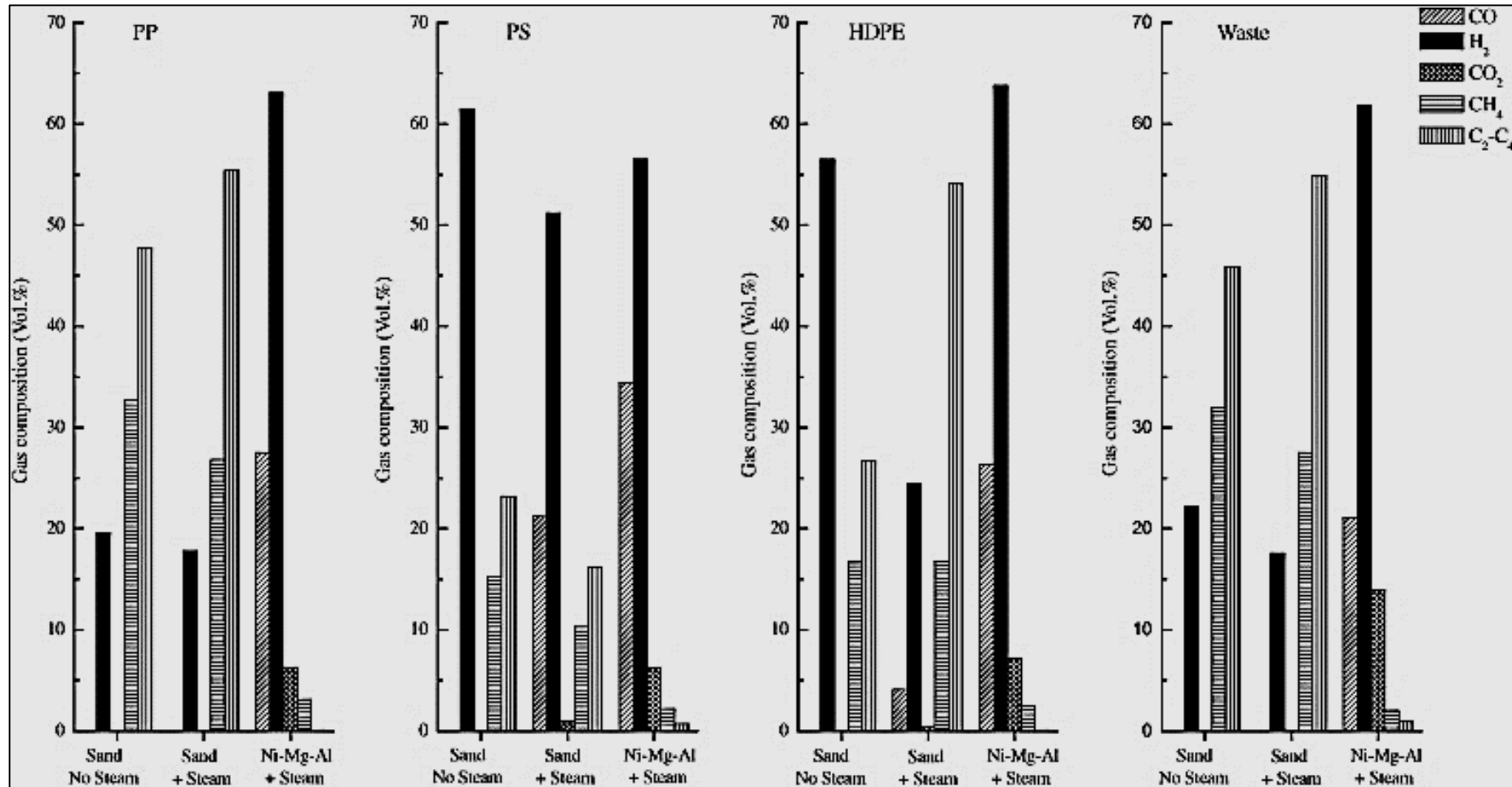


Figure 2.7 Gas composition for the pyrolysis-gasification of plastics at a gasification temperature of 800 °C [42]

2.2.2 Influence of catalysts

Perego and Villa [60] have classified catalyst types depending on the preparation method; bulk catalysts and supports which mainly consist of an active substance, mixed-agglomerated catalysts and impregnated catalysts from the preformed support. There are twelve unit operations that can be chosen for catalyst preparation as shown in Table 2.5. For supported catalysts, the selection is made based on the inertness, desirable mechanical properties, stability under reaction and regeneration conditions, surface area porosity and the cost. Normally, for supported catalysts the preparation method chosen is precipitation or impregnation depending on the product of catalyst that want to be achieved.

It has been shown that the preparation method does influence the yield production. Ni/CeO₂/ZSM-5 catalyst with Ni loading of 10 wt.% and CeO₂ loading of 5 wt.% were used in the pyrolysis-gasification of polypropylene using a two-stage fixed bed reactor [61]. Two different calcination temperatures were used, namely 500°C and 750°C. Overall, the potential hydrogen production concentration were decreased when the temperature was increased from 500 °C to 750 °C as shown in Figure 2.8. Larger metal particle sizes were also found by SEM-EDXS analysis of the reacted Ni/CeO₂/ZSM-5 catalyst with ratio of 10-5-750 reported to be probably caused by more serious sintering for the catalyst prepared in 750 °C. It was proposed that the activity of the Ni/CeO₂/ZSM-5 catalyst was reduced at high calcination temperature and high CeO₂ content.

Table 2.5 Unit operations in catalyst preparation [60]

1. Precipitation	7. Calcination
2. Gelation	8. Forming operation
3. Hydrothermal transformation	9. Impregnation
4. Decantation, filtration, centrifugation	10. Crushing and grinding
5. Washing	11. Mixing
6. Drying	12. Activation

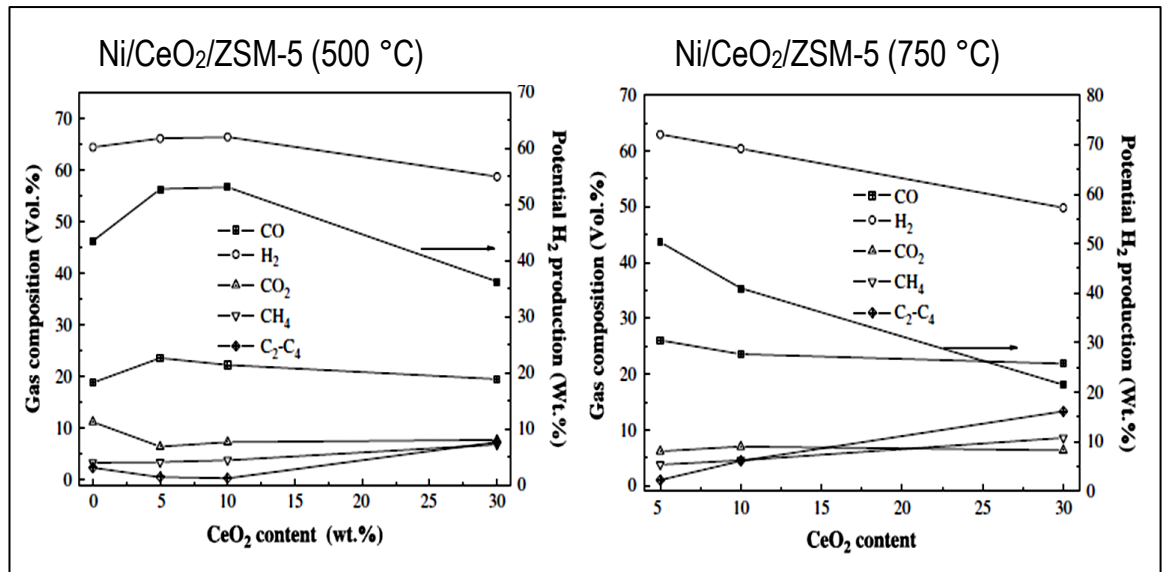


Figure 2.8 Concentration of product gases at different calcination temperature and CeO₂ content [61]

Nickel-based catalysts are well-known catalysts for hydrogen production and are cost effective as compared to other metal-based catalysts. Researches on Ni-based catalysts has suggested that various compositions of metal combinations as well as preparation technique and different gasification temperature can affect the performance of each catalyst in term of catalytic efficiency and deactivation [42, 62-64]. For example, the addition of Mg into a Ni-Al based catalyst has increased the reducible NiO phases and the strength of catalyst thus enhancing the hydrogen production.

Hydrogen production is also affected by the catalyst type as presented in Table 2.6 [64]. Based on the results shown, the lowest H₂/CO ratio is Ni-Mg-Al with 2.15 and the highest is Ni/CeO₂ with 12.17. It has been shown that Ni/Al and Ni/Mg/Al catalysts contain high catalytic activity for hydrogen production for polypropylene feedstock (potential: 53.1 and 51.7 wt.%) as well as producing considerably low coke formation [64]. By adding Mg into the Ni-Al catalyst structure, the filamentous carbon disappeared in the scanning electron microscopy (SEM) results. In term of catalyst preparation techniques, such as incipient wetness, co-impregnation and co-precipitation the preparation method can influence hydrogen yield.

Table 2.6 Gas composition in the product gases (nitrogen free, vol%) [64]

Catalyst	Gas					LHV (MJ m ⁻³)
	H ₂	CO	CO ₂	CH ₄	C ₂ -C ₄	
Sand (Without water)	67.3	0.0	0.0	22.1	10.6	16.1
Sand	25.8	6.7	0.2	22.0	45.3	17.5
Ni/CeO ₂ /Al ₂ O ₃	63.8	22.9	8.1	3.6	1.6	11.5
Ni/ZSM-5	63.6	20.3	11.8	2.8	1.5	10.9
Ni/Al ₂ O ₃	56.3	20.0	9.3	6.1	8.3	13.1
Ni/CeO ₂	75.5	6.2	7.5	5.5	5.3	11.9
Ni/MgO	32.6	7.9	0.8	20.6	38.1	16.8
Ni-Al	64.0	25.7	6.4	3.3	0.6	11.5
Ni-Mg-Al	61.8	28.7	6.5	2.2	0.8	11.4

The addition of Cu into the Ni-Al catalyst structure for hydrogen production of polypropylene using two-stage fixed bed reactor has been reported [65]. The addition of Cu into Ni-Al catalyst structure yields lower hydrogen production as illustrated in Figure 2.9. It may be due to the low reported BET surface area for the catalyst and it has been suggested that Cu is not suitable to be the active metal site during the gasification process. The different metal ratio on each catalyst also gave different results for the potential hydrogen production. It was concluded that the use of Cu in Ni-Al catalyst structure might not be suitable to improve the hydrogen production from the pyrolysis-gasification of polypropylene.

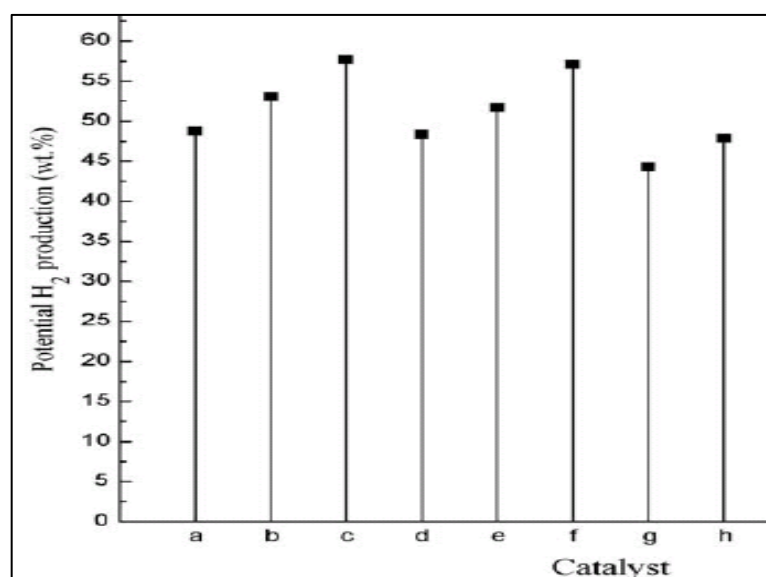


Figure 2.9 Potential H₂ production from pyrolysis-gasification of polypropylene with different catalyst (a) Ni-Al (1:4); (b) Ni-Al (1:2); (c) Ni-Al (1:1); (d) Ni-Mg-Al (1:1:4); (e) Ni-Mg-Al (1:1:2); (f) Ni-Mg-Al (1:1:1); (g) Ni-Cu-Al (1:1:2) and (h) Ni-Cu-Mg-Al (1:1:1:3);((a)-(h) are calcined at 750 °C) [65]

Research on NiO/ γ -Al₂O₃ as catalyst for steam gasification of waste polyethylene in bench scale fixed bed reactor was examined by He et al. (2009) [44]. Hydrogen production from the catalytic gasification showed high improvement as illustrated in Figure 2.10. Although the carbon dioxide production was also increased, in the presence of steam, the NiO/ γ -Al₂O₃ catalyst enriched the quality of the gas yield due to the steam reforming hydrocarbon reactions as well as the water gas shift reaction. At the temperature of 900°C and with the help of steam, carbon deposited on the catalyst was easily removed by the steam reaction and prevented the fast deactivation by carbon deposition. Therefore, nearly no deactivation occurred on the catalyst and proved the good catalytic performance of the NiO/ γ -Al₂O₃ catalyst.

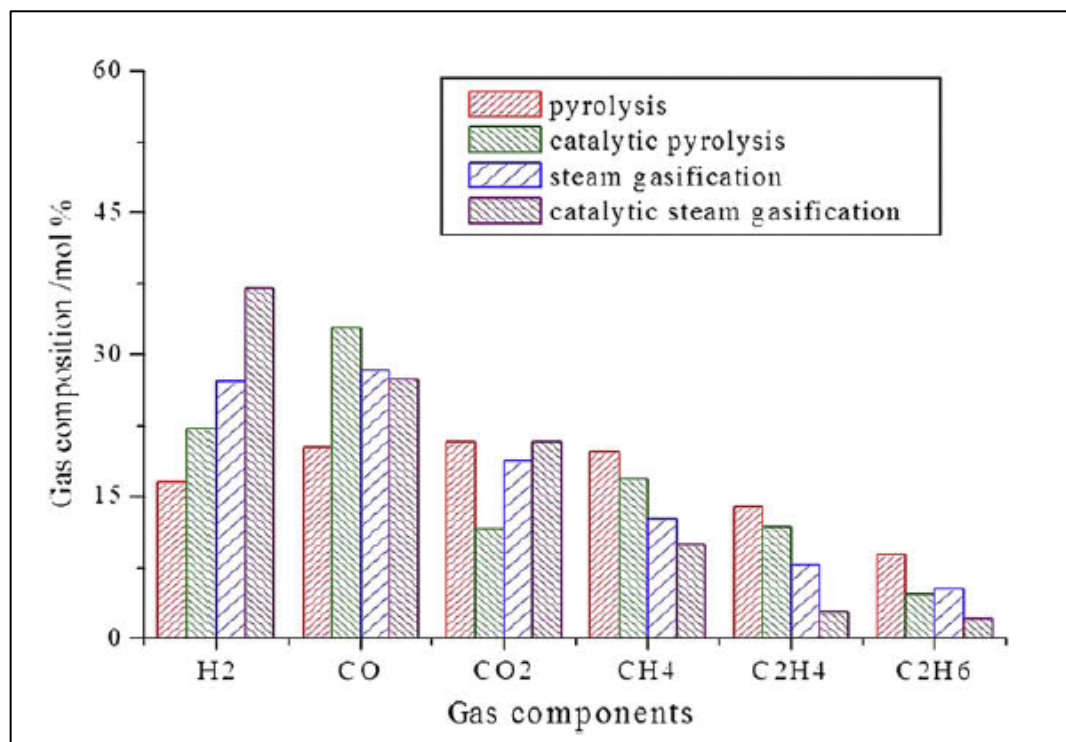


Figure 2.10 Gas composition in steam gasification and pyrolysis for non-catalytic and catalytic process [44]

The effect of γ -Al₂O₃ as well as MgO and CaO catalyst supports together with Ni and Ce loading has been investigated for the steam reforming of methane [66]. Based on the data shown in Figure 2-11, γ -Al₂O₃ support contributed remarkably higher hydrogen production due to higher methane conversion. It was confirmed that the fresh 5Ni/3CeO/Al₂O₃ catalyst displayed higher crystallinity and a high proportion of NiO phase, increasing the ratio of Ni in the catalyst that produced an increase in hydrogen production compared to others. Although MgO and CaO had

a larger surface area compared to γ -Al₂O₃, CaO tended to be influenced by moisture and high temperature catalyst deteriorations therefore it was proposed that CaO is not appropriate as a catalyst support for methane steam reforming.

Park et al. [67] has investigated hydrogen production from the reaction of ruthenium (Ru) catalyst with polypropylene in a 60 gh⁻¹ scale continuous experimental apparatus that consisted of a tank reactor for pyrolysis and a packed-bed catalytic reactor for steam reforming. It was reported that Ru catalyst has higher activity and lower coke formation than Ni-based catalyst. However due to their higher cost, they are less popular to be used as a catalyst for the steam reforming process. The experimental results with 0.5 wt.% of Ru content showed slightly lower hydrogen production than with 5.0 wt.% of Ru content, 66.6 vol.% and 70.6 vol.% respectively. It was also determined that the optimum temperature for pyrolyzer was 673K and optimum temperature for steam reformer was 903K to achieve lower coke formation with sufficient carbon conversion to gaseous products.

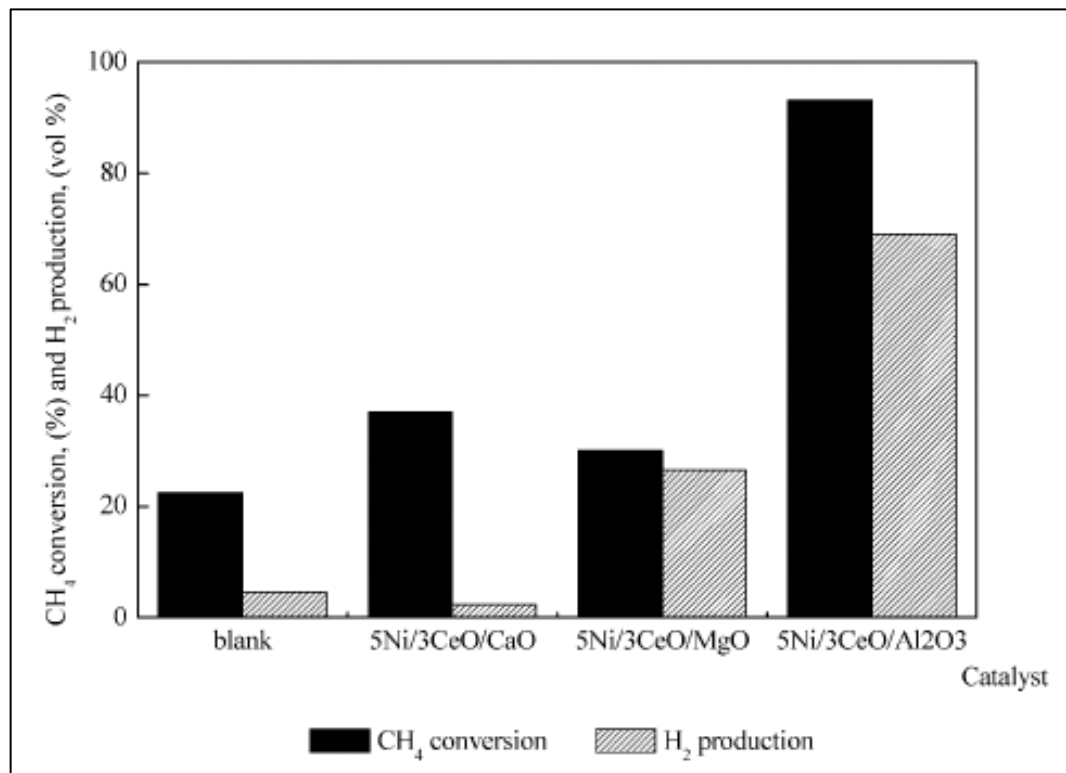


Figure 2.11 CH₄ conversion and H₂ production of steam reforming of methane at 800°C [66]

2.3 Dry Reforming Technology

Recently, many efforts have been made to reduce carbon dioxide emissions to the atmosphere because of the projected high environmental impact related to climate change. In addition, the concerns around the increasing levels of carbon dioxide in the atmosphere particularly arising from anthropogenic activities has resulted in research into carbon capture schemes and storage process which are likely to generate large quantities of carbon dioxide which has the potential for use, rather than sequestration [68]. The prediction of the expansion of such carbon capture processes are expected to mitigate against climate change.

Therefore the use of carbon dioxide for hydrocarbon reformation would be of economic and environmental benefit because carbon dioxide is known to be a cost effective, recyclable and a toxic-free carbon source. One such process is dry reforming, where the utilisation of carbon dioxide instead of steam or air is applied for the catalytic reforming of high molecular weight hydrocarbons for the production of synthesis gases (syngas). Even though the dry reforming still requires optimization of the process technique, this process is particularly suitable for oilfield gas which contains high concentrations of carbon dioxide gas that could be simply converted to synthesis gas without the requirement of CO₂ separation [69].

The most well-known feedstock used for studies on the dry reforming process is methane [70-72]. However there is increasing recent interest for the dry reforming process with other feedstocks such as biogas, ethanol and glycerol [73-75].

2.3.1 Thermodynamic reactions of methane dry reforming

Methane dry reforming is thermodynamically favourable when Gibbs free energy is less than zero ($\Delta G < 0$). Gibbs free energy minimization technique was normally applied during thermodynamic analysis [76]. Methane reforming is thermodynamically favoured above 913K as was first studied by Fischer and Tropsch in 1928. Dry methane reforming of methane is an endothermic process because both the carbon dioxide and hydrocarbon is a stable compound with low potential energy, therefore high temperatures are required.

The primary chemical reaction during the dry reforming of methane is the reaction between methane and carbon dioxide to produce syngas; hydrogen and carbon monoxide as shown in Reaction 2.14. The dry reforming reaction is favoured by low pressure but requires high temperature. Bulushev [77] also suggested that the dry reforming process has to be performed at high temperature and low pressure to achieve maximum conversion because of the highly endothermic nature of the reaction.

Furthermore due to the high temperature, other side reactions apart from the dry reforming reaction can occur, especially those that could increase the carbon coke formation on the catalyst such as methane cracking (Reaction 2.15), Boudouard reaction (Reaction 2.16) and reverse water gas shift reaction (Reaction 2.17). The methane decomposition (Reaction 2.15) is an important source of carbon deposition and is reduced with increasing temperature making this reaction thermodynamically more complimentary. The increased in temperature also affected the reverse water gas shift reaction (Reaction 2.17), when less H₂O is produced when the temperatures increased. In opposite, the Boudouard Reaction (Reaction 2.16) is favorable with temperature increase.



In general, the thermodynamic reaction of the dry reforming process is affected by temperature, pressure and reactant ratio. Tsang et al. [78] reported that the dry reforming of methane is more endothermic than steam reforming because it is thermodynamically favoured above 913 K.

2.3.2 Syngas production from dry reforming process

Widespread studies have been made specifically on methane reforming to synthesis gas. The reforming of methane with CO₂ (dry reforming) involves cracking of the methane molecule for the production of H₂ and CO rich syngas and has been reported to be promising by some researchers [79,80]. One of the reasons for such

interest is because methane reforming with carbon dioxide produces synthesis gas with a ratio close to unity, i.e. $H_2/CO = 1$ which has been suggested to be beneficial for the production of Fischer–Tropsch liquid hydrocarbon and oxygenate [81-83].

A recent review [84] concluded that dry reforming of methane was reliable for hydrogen production due to the carbon dioxide consumption during the process thereby encouraging the reduction of greenhouse gases emissions. However, due to its highly endothermic characteristic, the high energy consumption in order to complete the process needs to be taken into consideration. Nevertheless, this high temperature condition will help in the reduction of carbon formation while avoiding the catalyst deactivation, resulting in higher reactant conversion and high product yield.

The syngas production from the dry reforming process is affected by temperature, CH_4/CO_2 input ratio, mass to flow ratio, catalyst selection and reaction mixtures. Serrano-Lotina et al. [85] investigated the influence of temperature in the dry reforming of methane using a tubular fixed bed reactor. They reported that, the CO_2 and CH_4 conversion was increased with the increase in temperature from 450 °C to 800 °C. This result is in agreement with the perspective from thermodynamic analysis which stated that reaction of carbon dioxide reforming is endothermic. The increase in temperature also showing an improvement in the syngas, H_2 and CO production. Fakeeha et al. [86] and Adollahifaret al. [87] also supported that the increase in temperature produced greater H_2 yields.

Zanganeh et al. [88] studied the effect of feed ratio (CO_2/CH_4) on CH_4 and CO_2 conversion as well as H_2/CO molar ratio over $Ni_{0.10}Mg_{0.90}O$ catalyst in a fixed bed quartz reactor at 700 °C. They found that with the increase in CO_2/CH_4 feed ratio from 1:1 to 4:1, the CO_2 conversion and H_2/CO molar ratio decreased while CH_4 conversion was increased. They have suggested that these phenomena occurred due to the water gas shift reaction that was carried out simultaneously in the reformer.

In addition, the effect of increasing the CO_2 flowrate in dry reforming process was studied by Wang et al [89]. In their study, they reported that the Boudouard reaction is more favoured with the increase in CO_2 flow rate into the system. Apart

from that, the syngas with a lower heating value is also produced with the increasing of CO₂ flow rate.

Several studies on dry reforming of methane suggested that the additions of steam and/or oxygen were helpful in controlling the H₂/CO molar ratio [90-94]. The combination of steam reforming with dry reforming of methane reduced the carbon dioxide emission compared to the reference steam reforming process. Hydrogen production from this combination also increased as compared to only dry reforming due to the reaction with steam. Lim et al. [95] showed that less amount of raw material was needed if more carbon dioxide was fed into the system. They also concluded that the reasons for the decrease in net emission of carbon dioxide in the combined process were as follows:

- 1) In the dry methane reformer, CO₂ is also consumed by the reverse water-gas shift reaction which has a lower heat of reaction.
- 2) Dry methane reforming requires relatively lower heat to produce carbon monoxide compared with steam reforming. Therefore, dry methane reforming produces less indirect CO₂ emissions from a heating source than steam reforming does.
- 3) The reduced amount of CO₂ before CO₂ capture process by dry methane reforming can also abate the required regeneration energy required in the CO₂ capture process.

In the dry reforming process, carbon dioxide also reacts with coal/char via the Boudouard reaction and produces carbon monoxide that can enhance the total of syngas yield. However, in the pyrolysis of lignite by Reuther and Jenkins [96] it has been shown that the Bourdourd reaction is unimportant in rapid pyrolysis. The presence of carbon dioxide hypothetically stabilized the reactive site of the char surface which in turn prevents cracking of volatiles, and/or to cap reactive volatile species much as hydrogen is believed to do during hydrolysis.

Jianguo et al. [97] discussed in detail the carbon formation during the methane dry reforming process that may deactivate the catalyst, hence reducing the amount of

syngas produced from the reforming process. They suggested that the carbon formation occurs when the formation rate of carbon species is higher than its removal rate through reforming reaction; either the reaction 2.18 is more rapid than reaction 2.19 or/and reaction 2.20 is retarded. M is the active metal site on the catalyst while S is the surface of the catalyst support. They also discussed the two types of carbon formed on the catalyst during the dry reforming process. The filamentous type carbon (whisker like) is formed by the adsorbed carbon atom derived mainly from methane decomposition while encapsulated hydrocarbon films type carbon is formed by the polymerization process [97]. Figure 2.12 shows the proposed principal reaction pathway of the carbon deposition from methane reforming [98].

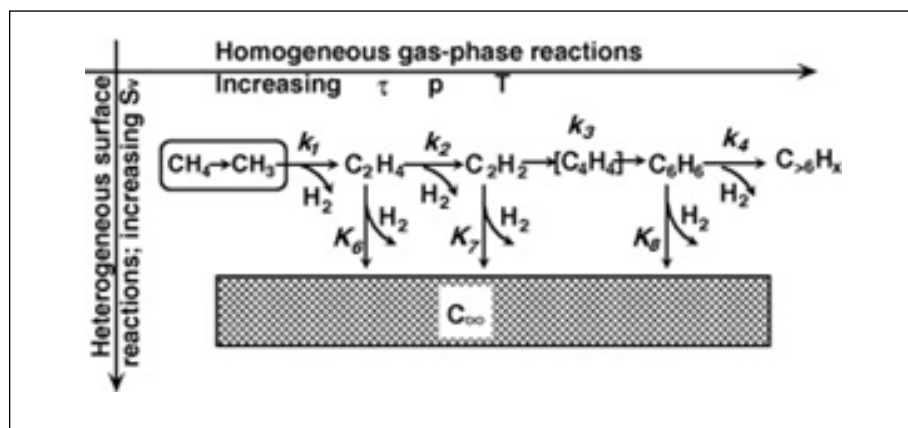


Figure 2.12 Multi-step chemical vapor deposition and hydrogen inhibition of pyrocarbon from methane (τ the residence time, ρ the pressure, T the temperature, S_v the volume-related surface area) [98]

2.3.3 The use of catalyst for syngas production from dry reforming process

Studies on the catalytic reaction of hydrocarbons with carbon dioxide are focused on increasing the potential of catalyst activity and ability to resist catalyst deactivation due to coke formation during the dry reforming process. Furthermore, the addition of catalysts in the reforming process has a beneficial influence on

syngas production. It is known that the use of suitable catalysts further enhances the reforming process and might also improve the coke resistance ability [99-102]. Tsang et al. [78] reviewed the conversion of methane to synthesis gas by methane reforming reactions and also suggested that the different catalysts used in the dry reforming process affected the yield results.

The type of metal catalyst also impacts the selectivity of CO₂ or CH₄ conversion. Studies of dry reforming of methane over a 20%Co/ 80%La₂O₃ catalyst which were seen to be more active towards the conversion of CO₂ than CH₄ due to side reactions such as water gas shift reaction which is more prone to the production of CO from partly consumed H₂ [103].

Noble metals group based catalysts have showed high catalyst activity towards carbon resistance as reported by Rostrup-Nielsen et al. [104]. The carbon morphology of each catalyst used are presented in Table 2.7 [104]. They reported that less carbon formation and no carbon whiskers were observed on the noble metals particularly for ruthenium (Ru), rhodium (Rh) and irridium (Ir). They have also suggested that ruthenium as a suitable applicant for the carbon dioxide reforming process is due to its lower cost compared to rhodium. The order of reactivity of catalysts for dry reforming of methane over transition metal catalysts was concluded as Ru>Rh>Ni≈Ir>Pt>Pd.

Table 2.7 Carbon morphology [104]

Catalyst	Temp. (°C)	Carbon (wt.%)	Metal crystal size (nm)	Whisker diameter (nm)	Metal in whisker
Ni-1	500	3.5	5-20	5-20	Ni
	650	2.0	5-20	5-20	Ni
Ru	500	0.3	1.5-7	No whisker	
	650	1.8	1.5-7	No whisker	
Rh	500	1.1	1-10	No whisker	
	650	2.5	3-100	10-30	Fe/Rh
Pd	500	0			
	650	2.8	10-25	10-25	Pd
Ir	500	0.5	<4	No whisker	
	650	2.3	<4	No whisker	
Pt	500	0.2	<3-4	10-15	Fe
	650	2.6	<3-4	10-15	Fe

In contrast, Sakai et al. [105] suggested that Rh with the addition of Al_2O_3 support gave a better catalyst performance than Ru. They showed that a Rh (1 wt.%) / Al_2O_3 catalyst was suitable for reactions of carbon dioxide with various hydrocarbons such as toluene, heptane, cyclohexane, methyl cyclohexane and methane. Based on their findings, methane was noticeably high in reactivity compared to others. They have ranked the noble metal catalyst activity based on their studies was decreased in the order of $\text{Rh} > \text{Pd} > \text{Pt} > \text{Ru}$.

Yamada et al. [106] investigated the carbon dioxide reforming of polyethylene with a $\text{Pd}/\text{Al}_2\text{O}_3$ catalyst. Figure 2.13 shows the results of carbon dioxide reforming of polyethylene with catalyst, nitrogen and carbon dioxide. It was concluded that polyethylene was completely reformed to synthesis gas at the catalyst temperature of 1120K. High polyethylene reaction temperature resulted in a high thermal decomposition rate and catalyst could not reform all reactants to CO and H_2 , while low polyethylene temperature slowed the thermal degradation rate and completely reformed the polyethylene to hydrogen and carbon monoxide. However, the reaction time was found to be longer in order to consume all the polyethylene.

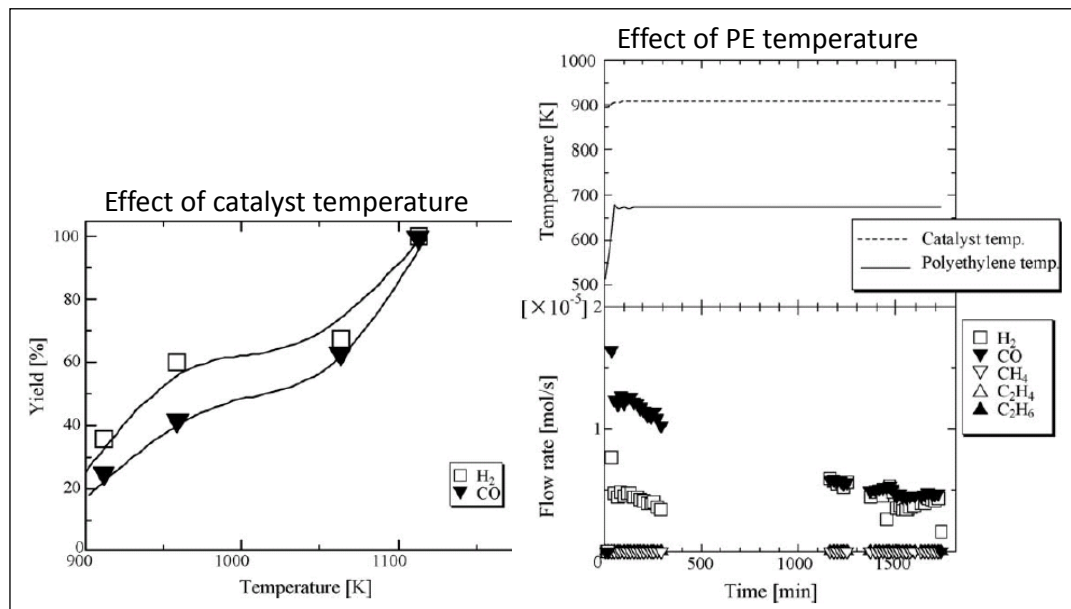


Figure 2.13 CO_2 reforming of polyethylene with $\text{Pd}/\text{Al}_2\text{O}_3$ catalyst [106]

Apart from noble metals catalysts, the most widely used catalysts tend to be nickel-based and have been used to enhance steam reforming, partial oxidation, hydrogenation and dry reforming. Recent reviews on the use of catalysts in dry

reforming suggest that Ni-based catalysts are the most suitable option due to their low cost and relatively high catalytic activity compared to noble metal catalysts are the reasons that they are preferred for the reforming process [99, 107]. However, nickel catalysts are known to be prone to deactivation due to coke formation on the catalyst and nickel sintering [104, 108, 109]. Studies have reported that the addition of a metal promoter, adjusting the support and suitable catalyst preparation methods for Ni-based catalysts can further improve the production of syngas from the dry reforming process by improving the structure and uniformity of the catalyst particles, resulting in better metal dispersion [110-113]. Table 2.8 is a summary of the product yield distribution from various researchers for the dry reforming process.

Lv et al. [114] investigated the pre-treatment of a silica supported nickel catalyst with ethylene glycol for the dry reforming of CH₄. They reported that the ethylene glycol pre-treatment modified the surface properties of the silica support, resulting in lower deposition of carbon on the catalyst and a lower degree of sintering. Furthermore, a study on dry reforming of methane over a Ni/γ-Al₂O₃ catalyst in a fixed bed continuous flow quartz reactor and direct current corona discharge found an increase in selectivity for CO and decreased carbon formation on the catalyst surface [121].

Table 2.8(a) Research on product yield distributions from dry reforming process over Ni-based catalysts

Catalyst	H ₂ yield (%)	CO yield (%)	CO ₂ conv. (%)	CH ₄ conv. (%)	H ₂ /CO	Carbon formation (%)	Ref.
Ni/SiO ₂			49	33	0.79		[114]
Ni/SiO ₂ -EG			83	72	0.82		
Ni/Al	41.3	58.5	76.5	67.5	0.7	12.6	[115]
Ni/SiAl	29.5	48.9	67.0	51.8	0.6	18.3	
Ni/MgAl	46.5	66.3	81.2	75.3	0.7	Nd ^a	
Ni/ZrAl	42.6	59.3	78.7	66.8	0.7	5.1	

^aNd = not detected

Table 2.8 continued on next page ...

Table 2.8(b) Research on product yield distributions from dry reforming process over Ni-based catalysts (... continued from previous page)

Catalyst	H ₂ yield (%)	CO yield (%)	CO ₂ conv. (%)	CH ₄ conv. (%)	H ₂ /CO	Carbon formation (%)	Ref.
Co/SiO ₂			51.5	47.8	Nd ^a	Nd ^a	[116]
Ni/SiO ₂			6.37	7.74	1.07	6.18	
Ni-Co/SiO ₂			6.95	3.95	0.99	0.39	
Co (7.6%)			82	72		0.53	[117]
Co (4.3%)			52	40		<0.01	
Co (2.0%)			43	30		<0.01	
Co (1%)			0	0		<0.01	
Ni (7.7%)			66	54		0.10	
Ni (4.4%)			52	40		<0.01	
Ni (2.5%)			50	38		<0.01	
Ni (1.3%)			40	29		<0.01	
NA (650°C)	28	42	50	48			[118]
NCuA (650°C)	26	42	48	48			
NCoA (650°C)	34	48	58	52			
NA (750°C)	62	77	79	78			
NCuA (750°C)	60	80	80	79			
NCoA (750°C)	68	82	82	81			
NA(850°C)	84	98	95	96			
NCuA (850°C)	82	97	95	95			
NCoA(850°C)	90	100	97	98			
7Ni3Co/LaAl	94.9 ^b	97.8 ^b	94.0	93.7	0.97	0.0946 ^c	[119]
Ni-Cu				<16	0.96	0.00222 ^d	[120]
Ni-Fe				(stable)	0.90	0.02104 ^d	
Ni-Mn				53-18	0.94	0.00543 ^d	
Ni-Co				85-63	0.98	0.00204 ^d	
Ni-Co (L)*			87.0- 87.1	91.4 (stable) 83.8- 83.9		Nd ^a	
Co/CeO ₂			94	90	0.98	6	[82]
Ni/CeO ₂			89	90	1.0	25	
Co-Ni/CeO ₂			90	97	1.03	6	

^aNd = not detected, ^bselectivity, ^cunit in mg g_{cat}⁻¹ h⁻¹, ^dunit in g_c/g_{cat}-h, *Lower Ni-Co content

The addition of metal promoters in Ni-based catalysts has shown to produce catalysts which inhibit carbon deposition and show high catalyst activity towards

syngas production from the dry reforming of methane. However, it is uncertain whether such metal promoted catalysts would be effective for the dry reforming of the wide range of hydrocarbons derived from the pyrolysis of waste plastics.

Different nickel catalysts supported on various supports (δ,θ -Al₂O₃, MgAl₂O₄, SiO₂-Al₂O₃ and ZrO₂-Al₂O₃) were also investigated by Damyanova et al. for inhibition of carbon formation for dry reforming of CH₄ [115]. They found that there was a strong interaction between nickel oxide species and MgAl₂O₄ which retarded the sintering of the nickel and also reduced the formation of coke. Ni/MgAl yielded a maximum value of hydrogen production (46.5%) due to high methane and carbon dioxide conversion as shown in Table 2.9 [115]. In contrast, Ni/SiAl catalyst resulted in a lower hydrogen yield. In terms of the coke formation, it was suggested that Ni catalyst supported on MgAl₂O₄ have very strong interaction that affected the smaller size of Ni particles hence influenced carbon deposition. The absence of filamentous carbon was reported for the Ni catalyst supported on MgAl₂O₄.

Table 2.9 Catalytic properties of Ni catalysts in reforming of methane with CO₂ at 90 min (T=923K; m=0.5g; CH₄/CO₂=1) [115]

Sample	CH ₄ conv. (%)	CO ₂ conv. (%)	H ₂ yield (%)	CO yield (%)	H ₂ /CO
Ni/Al	67.5	76.5	41.3	58.5	0.7
Ni/SiAl	51.8	67.0	29.5	48.9	0.6
Ni/MgAl	75.3	81.2	46.5	66.3	0.7
Ni/ZrAl	66.8	78.7	42.6	59.3	0.7

A good catalytic activity according to long term experiments was reported for bimetallic Ni-Pt/Al₂O₃ during a 6500 min reaction time for the dry reforming of methane; since lesser carbon deposition and high stability of catalyst was observed compared with the use of monometallic Pt/Al₂O₃ and Ni/Al₂O₃, suggested to be caused by the homogenous surface distribution of nickel particles in the close proximity of Pt [122].

Most studies recently have concentrated on the addition of a cobalt (Co) promoter on Ni-based catalysts for the dry reforming process due to their promising results of enhancing catalyst activity and at the same time suppressing carbon formation [118]. It is believed that Co metal has the ability to control the size of active sites

[118]. Xu et al. [119] and Zhang et al. [120] have also suggested that the high catalytic activity and excellent carbon resistance of Ni-Co catalysts was due to the synergetic effect between Co and Ni metal; i.e. high dispersion of metals, high metallic surface, strong metal-support interaction (SMSI) and uniform distribution of pore diameter. The metal content influenced the stability of Ni-Co bimetallic catalysts has also been investigated by Zhang et al. [123]. The catalyst with lower Ni-Co content showed higher and stable catalytic activity than catalyst with higher Ni-Co content as a result of large surface area, smaller metal particle and better metal dispersion on the lower Ni-Co content catalyst.

Adollahifar et al. [87] also investigated the effect of metal content over bimetallic Ni-Co/Al₂O₃-MgO nanocatalyst towards hydrogen production from CO₂ reforming of methane. They have reported that with the addition of more cobalt content, the surface area of the catalyst was reduced which was related to the pore filling of the support. In term of syngas production, the increase in cobalt content up to 3 wt.% was shown to increase the syngas yield, but was reduced afterwards due to the low active surface area.

Apart from the type of catalyst chosen for the reforming process, the catalyst preparation method has also been showed to influence the performance of the catalyst. For example, a study on dry reforming of methane over ceria nanopowders prepared by a microwave-assisted hydrothermal method suggested an improvement in the catalyst resistance towards thermal sintering compared to the catalyst without microwave irradiation [124].

In addition, Adollahifar et al. [87] investigated the effect of ultrasound irradiation at different temperatures over bimetallic Ni-Co/Al₂O₃-MgO nanocatalyst from the CO₂ reforming of methane. They reported that the catalyst prepared by ultrasound irradiation increased the surface area of the catalyst and consequently the number of active sites per unit mass compared to the impregnation method, hence increasing the conversion of methane to form syngas, hydrogen and carbon monoxide, as shown in Figure 2.14.

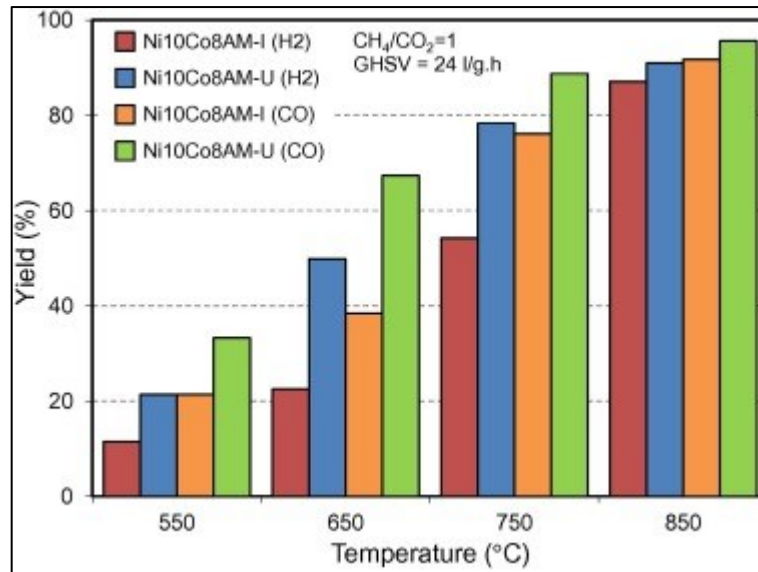


Figure 2.14 CH₄ effect of catalyst prepared by ultrasound irradiation (U) compared to impregnation method (I) on product yield produced at different temperatures [87]

2.4 Summary

From the review of the literature discussed in this chapter, methane dry reforming has shown promising results for producing synthesis gases. The use of carbon dioxide in the process uses a process gas that is problematic as a green-house gas in the atmosphere. Reducing the level of carbon dioxide emission in the atmosphere has become a concern and methods are being developed to capture carbon dioxide from various industrial processes. Using carbon dioxide may therefore create a useful product, i.e. syngas, whilst also contributing towards mitigation against climate change. . In addition, waste plastics could be a potential source of methane and other hydrocarbons required in the reforming process. This research is an attempt to fill that gap by introducing carbon dioxide as the reforming agent in the gasification stage of pyrolysis-gasification/reforming of waste plastics. The research will be focused on producing optimum synthesis gas yield and composition from the dry reforming process of waste plastics. Various parameters are to be investigated such as reactor configuration and experimental process conditions. Based on Ni/Al₂O₃ catalysts for steam reforming of waste plastics and dry reforming of methane, copper, cobalt and magnesium metal are worth considering for further research due to their high catalytic activity reported in the process.

References

1. Shonfield, D.P. LCA of Management Options for Mixed Waste Plastics. Waste & Resource Action Programme, Banbury, Oxon. 2008.
2. Garcia, L., Benedicto, A., Romeo, E., Salvador, M.L., Arauzo, J. and Bilbao, R. Hydrogen production by steam gasification of biomass using Ni-Al coprecipitated catalysts promoted with magnesium. *Energy & Fuels*. 2002, 16(5), pp.1222-1230.
3. Namioka, T., Saito, A., Inoue, Y., Park, Y., Min, T.-j., Roh, S.-a. and Yoshikawa, K. Hydrogen-rich gas production from waste plastics by pyrolysis and low-temperature steam reforming over a ruthenium catalyst. *Applied Energy*. 2011, 88(6), pp.2019-2026.
4. Efika, C.E., Wu, C. and Williams, P.T. Syngas production from pyrolysis–catalytic steam reforming of waste biomass in a continuous screw kiln reactor. *Journal of Analytical and Applied Pyrolysis*. 2012, 95(0), pp.87-94.
5. Luo, S., Zhou, Y. and Yi, C. Syngas production by catalytic steam gasification of municipal solid waste in fixed-bed reactor. *Energy*. 2012, 44(1), pp.391-395.
6. Martínez-Lera, S., Torrico, J., Pallarés, J. and Gil, A. Design and first experimental results of a bubbling fluidized bed for air gasification of plastic waste. *Journal of Material Cycles and Waste Management*. 2013, 15(3), pp.370-380.
7. Environmental Protection Division, Waste to energy: A technical review of municipal solid waste thermal treatment practices. Victoria, BC. 2011.
8. Lopez-Urionabarrenechea, A., de Marco, I., Caballero, B.M., Laresgoiti, M.F. and Adrados, A. Catalytic stepwise pyrolysis of packaging plastic waste. *Journal of Analytical and Applied Pyrolysis*. 2012, 96, pp.54-62.
9. Adrados, A., de Marco, I., Caballero, B.M., Lopez, A., Laresgoiti, M.F. and Torres, A. Pyrolysis of plastic packaging waste: A comparison of plastic residuals from material recovery facilities with simulated plastic waste. *Waste Management*. 2012, 32(5), pp.826-832.

10. Straka, P. and Bičáková, O. Hydrogen-rich gas as a product of two-stage co-gasification of lignite/waste plastics mixtures. *International Journal of Hydrogen Energy*. 2014, 39(21), pp.10987-10995.
11. Yang, X., Sun, L., Xiang, J., Hu, S. and Su, S. Pyrolysis and dehalogenation of plastics from waste electrical and electronic equipment (WEEE): A review. *Waste Management*. 2013, 33(2), pp.462-473.
12. Bustamante, f., Enick, R., Rothenberger, K., Howard, B., Cugini, A., Ciocco, M. and Morreale, B. Kinetic Study of the Reverse Water Gas Shift Reaction in High Temperature, High Pressure Homogeneous Systems. *Fuel Chemistry Division Preprints*. 2002, 47(2), p.663.
13. Zhang, H., Xiao, R., Nie, J., Jin, B., Shao, S. and Xiao, G. Catalytic pyrolysis of black-liquor lignin by co-feeding with different plastics in a fluidized bed reactor. *Bioresource Technology*. 2015, 192, pp.68-74.
14. Chattopadhyay, J., Pathak, T.S., Srivastava, R. and Singh, A.C. Catalytic co-pyrolysis of paper biomass and plastic mixtures (HDPE (high density polyethylene), PP (polypropylene) and PET (polyethylene terephthalate)) and product analysis. *Energy*. 2016, 103, pp.513-521.
15. Narobe, M., Golob, J., Klinar, D., Francetič, V. and Likozar, B. Co-gasification of biomass and plastics: Pyrolysis kinetics studies, experiments on 100 kW dual fluidized bed pilot plant and development of thermodynamic equilibrium model and balances. *Bioresource Technology*. 2014, 162, pp.21-29.
16. Dou, B., Wang, K., Jiang, B., Song, Y., Zhang, C., Chen, H. and Xu, Y. Fluidized-bed gasification combined continuous sorption-enhanced steam reforming system to continuous hydrogen production from waste plastic. *International Journal of Hydrogen Energy*. 2016, 41(6), pp.3803-3810.
17. Kumagai, S., Hasegawa, I., Grause, G., Kameda, T. and Yoshioka, T. Thermal decomposition of individual and mixed plastics in the presence of CaO or Ca(OH)₂. *Journal of Analytical and Applied Pyrolysis*. 2015, 113, pp.584-590.
18. Scheirs, J. and Kaminsky, W. eds. Feedstock recycling and pyrolysis of waste plastic: Converting waste plastics into diesel and other fuels. United Kingdom: Wiley, 2006.
19. de Marco, I., Caballero, B.M., López, A., Laresgoiti, M.F., Torres, A. and Chomón, M.J. Pyrolysis of the rejects of a waste packaging separation and

- classification plant. *Journal of Analytical and Applied Pyrolysis*. 2009, 85(1–2), pp.384-391.
20. L.D, M., Caballero, B.M., Torres, A., Laresgoiti, M.F., M.J, C. and M.A, C. Recycling polymeric wastes by means of pyrolysis. *Journal of Chemical Technology & Biotechnology*. 2002, 77(7), pp.817-824.
 21. Vasile, C., Pakdel, H., Mihai, B., Onu, P., Darie, H. and Ciocâlțeu, S. Thermal and catalytic decomposition of mixed plastics. *Journal of Analytical and Applied Pyrolysis*. 2001, 57(2), pp.287-303.
 22. Kiran, N., Ekinçi, E. and Snape, C.E. Recycling of plastic wastes via pyrolysis. *Resources, Conservation and Recycling*. 2000, 29(4), pp.273-283.
 23. Williams, P.T. and Bagri, R. Hydrocarbon gases and oils from the recycling of polystyrene waste by catalytic pyrolysis. *International Journal of Energy Research*. 2004, 28(1), pp.31-44.
 24. Brems, A., Baeyens, J. and Dewil, R. Recycling and recovery of post-consumer plastic solid waste in a European context. *Thermal Science*. 2012, 16(3), pp.669-685.
 25. Park, J.A., Park, K., Park, J.W. and Kim, D.C. Characteristics of LDPE pyrolysis. *Korean Journal of Chemical Engineering*. 2002, 19(4), pp.658-662.
 26. Bagri, R. and Williams, P.T. Catalytic pyrolysis of polyethylene. *Journal of Analytical and Applied Pyrolysis*. 2002, 63(1), pp.29-41.
 27. Mastral, F.J., Esperanza, E., Garcí a, P. and Juste, M. Pyrolysis of high-density polyethylene in a fluidised bed reactor. Influence of the temperature and residence time. *Journal of Analytical and Applied Pyrolysis*. 2002, 63(1), pp.1-15.
 28. Onwudili, J.A., Insura, N. and Williams, P.T. Composition of products from the pyrolysis of polyethylene and polystyrene in a closed batch reactor: Effects of temperature and residence time. *Journal of Analytical and Applied Pyrolysis*. 2009, 86(2), pp.293-303.
 29. López, A., de Marco, I., Caballero, B.M., Laresgoiti, M.F. and Adrados, A. Influence of time and temperature on pyrolysis of plastic wastes in a semi-batch reactor. *Chemical Engineering Journal*. 2011, 173(1), pp.62-71.
 30. Achilias, D.S., Roupakias, C., Megalokonomos, P., Lappas, A.A. and Antonakou, E.V. Chemical recycling of plastic wastes made from

- polyethylene (LDPE and HDPE) and polypropylene (PP). *Journal of Hazardous Materials*. 2007, 149(3), pp.536-542.
31. Encinar, J.M. and González, J.F. Pyrolysis of synthetic polymers and plastic wastes. Kinetic study. *Fuel Processing Technology*. 2008, 89(7), pp.678-686.
 32. Miranda, R., Pakdel, H., Roy, C. and Vasile, C. Vacuum pyrolysis of commingled plastics containing PVC II. Product analysis. *Polymer degradation and stability*. 2001, 73(1), pp.47-67.
 33. Seo, Y.-H., Lee, K.-H. and Shin, D.-H. Investigation of catalytic degradation of high-density polyethylene by hydrocarbon group type analysis. *Journal of Analytical and Applied Pyrolysis*. 2003, 70(2), pp.383-398.
 34. Sakata, Y., Bhaskar, T., Kaneki, J., Hamano, K., Kusaba, T. and Muto, A. Comparison of thermal degradation products from real municipal waste plastics and model mixed plastics. *Journal of Analytical and Applied Pyrolysis*. 2003, 70, pp.579-587.
 35. Bhaskar, T., Kaneko, J., Muto, A., Sakata, Y., Jakab, E., Matsui, T. and Uddin, M.A. Pyrolysis studies of PP/PE/PS/PVC/HIPS-Br plastics mixed with PET and dehalogenation (Br, Cl) of the liquid products. *Journal of Analytical and Applied Pyrolysis*. 2004, 72(1), pp.27-33.
 36. Kulesza, K. and German, K. Chlorinated pyrolysis products of co-pyrolysis of poly(vinyl chloride) and poly(ethylene terephthalate). *Journal of Analytical and Applied Pyrolysis*. 2003, 67(1), pp.123-134.
 37. Williams, P.T. and Williams, E.A. Interaction of Plastics in Mixed-Plastics Pyrolysis. *Energy & Fuels*. 1999, 13(1), pp.188-196.
 38. Aguado, J. and Serrano., D.P. Feedstock recycling of plastic wastes Cambridge, United Kingdom: The Royal Society of Chemistry, 1999.
 39. Zheng Jiao and Yong, C. Characteristics of the pyrolysis and gasification of low-density polyethylene (LDPE). In: *International Symposium on Feedstock Recycling of Polymeric Materials*, Chengdu (China). 2009, pp.134-139.
 40. Lee, J.W., Yu, T.U., Moon, J.H., Jeong, H.J., Park, S.S., Yang, W. and Do Lee, U. Gasification of Mixed Plastic Wastes in a Moving-Grate Gasifier and Application of the Producer Gas to a Power Generation Engine. *Energy & Fuels*. 2013, 27(4), pp.2092-2098.

41. Wilk, V. and Hofbauer, H. Conversion of mixed plastic wastes in a dual fluidized bed steam gasifier. *Fuel*. 2013, 107(0), pp.787-799.
42. Wu, C. and Williams, P.T. Pyrolysis-gasification of plastics, mixed plastics and real-world plastic waste with and without Ni-Mg-Al catalyst. *Fuel*. 2010, 89(10), pp.3022-3032.
43. Tsuji, T., Tanaka, Y. and Itoh, H. Two-stage thermal gasification of polyolefins. *Journal of Material Cycles and Waste Management*. 2001, 3(1), pp.2-7.
44. He, M., Xiao, B., Hu, Z., Liu, S., Guo, X. and Luo, S. Syngas production from catalytic gasification of waste polyethylene: Influence of temperature on gas yield and composition. *International Journal of Hydrogen Energy*. 2009, 34(3), pp.1342-1348.
45. Toshiro Tsuji, Yoshiki Tanaka, Toshiharu Shibata, Osamu Uemaki and Itoh, H. Two-stage Thermal Gasification of Plastics. In: *International Symposium on Feedstock Recycling of Plastic*, Japan. Tohoku University Press, 1999, pp.211-214.
46. Wu, C. and Williams, P.T. Pyrolysis-gasification of post-consumer municipal solid plastic waste for hydrogen production. *International Journal of Hydrogen Energy*. 2010, 35(3), pp.949-957.
47. Czernik, S. and French, R.J. Production of Hydrogen from Plastics by Pyrolysis and Catalytic Steam Reform. *Energy & Fuels*. 2006, 20(2), pp.754-758.
48. Wu, J., Fang, Y., Wang, Y. and Zhang, D.-k. Combined Coal Gasification and Methane Reforming for Production of Syngas in a Fluidized-Bed Reactor. *Energy & Fuels*. 2005, 19(2), pp.512-516.
49. Ravaghi-Ardebili Z., M.F., Pirola C., Soares F., Corbetta M., Pierucci S., Ranzi E. Influence of the effective parameters on H₂:CO ratio of syngas at low-temperature gasification. *Chemical Engineering Transactions*. 2014, 37, pp.253-258.
50. Sahoo, B.B., Sahoo, N. and Saha, U.K. Effect of H₂:CO ratio in syngas on the performance of a dual fuel diesel engine operation. *Applied Thermal Engineering*. 2012, 49, pp.139-146.
51. Cao, Y., Gao, Z., Jin, J., Zhou, H., Cohron, M., Zhao, H., Liu, H. and Pan, W. Synthesis Gas Production with an Adjustable H₂/CO Ratio through the Coal Gasification Process: Effects of Coal Ranks And Methane Addition. *Energy & Fuels*. 2008, 22(3), pp.1720-1730.

52. Wong, S.L., Ngadi, N., Abdullah, T.A.T. and Inuwa, I.M. Current state and future prospects of plastic waste as source of fuel: A review. *Renewable and Sustainable Energy Reviews*. 2015, 50, pp.1167-1180.
53. Buekens, A.G. and Huang, H. Catalytic plastics cracking for recovery of gasoline-range hydrocarbons from municipal plastic wastes. *Resources, Conservation and Recycling*. 1998, 23(3), pp.163-181.
54. Miskolczi, N., Bartha, L. and Angyal, A. High Energy Containing Fractions from Plastic Wastes by Their Chemical Recycling. *Macromolecular Symposia*. 2006, 245-246(1), pp.599-606.
55. Namioka, T., Saito, A., Inoue, Y., Park, Y., Min, T.J., Roh, S.A. and Yoshikawa, K. Hydrogen-rich gas production from waste plastics by pyrolysis and low-temperature steam reforming over a ruthenium catalyst. *Applied Energy*. 2011, 88(6), pp.2019-2026.
56. Mastellone, M.L. and Zaccariello, L. Metals flow analysis applied to the hydrogen production by catalytic gasification of plastics. *International Journal of Hydrogen Energy*. 2013, 38(9), pp.3621-3629.
57. Ishii, A., Amagai, K., Furuhata, T. and Arai, M. Thermal gasification behavior of plastics with flame retardant. *Fuel*. 2007, 86(15), pp.2475-2484.
58. Okajima, I. and Sako, T. Chapter 13 - Energy Conversion of Biomass and Recycling of Waste Plastics Using Supercritical Fluid, Subcritical Fluid and High-Pressure Superheated Steam. In: Fan, V.A. ed. *Supercritical Fluid Technology for Energy and Environmental Applications*. Boston: Elsevier, 2014, pp.249-267.
59. Ahmed, I.I. and Gupta, A.K. Hydrogen production from polystyrene pyrolysis and gasification: Characteristics and kinetics. *International Journal of Hydrogen Energy*. 2009, 34(15), pp.6253-6264.
60. Perego, C. and Villa, P. Catalyst preparation methods. *Catalysis Today*. 1997, 34(3-4), pp.281-305.
61. Wu, C. and Williams, P.T. Ni/CeO₂/ZSM-5 catalysts for the production of hydrogen from the pyrolysis–gasification of polypropylene. *International Journal of Hydrogen Energy*. 2009, 34(15), pp.6242-6252.
62. Wu, C. and Williams, P.T. Investigation of coke formation on Ni-Mg-Al catalyst for hydrogen production from the catalytic steam pyrolysis-gasification of polypropylene. *Applied Catalysis B: Environmental*. 2010, 96(1–2), pp.198-207.

63. Wu, C. and Williams, P.T. A novel Ni–Mg–Al–CaO catalyst with the dual functions of catalysis and CO₂ sorption for H₂ production from the pyrolysis–gasification of polypropylene. *Fuel*. 2010, 89(7), pp.1435-1441.
64. Wu, C. and Williams, P.T. Hydrogen production by steam gasification of polypropylene with various nickel catalysts. *Applied Catalysis B: Environmental*. 2009, 87(3–4), pp.152-161.
65. Wu, C. and Williams, P.T. Investigation of Ni-Al, Ni-Mg-Al and Ni-Cu-Al catalyst for hydrogen production from pyrolysis–gasification of polypropylene. *Applied Catalysis B: Environmental*. 2009, 90(1–2), pp.147-156.
66. Isha, R. and Williams, P.T. Hydrogen production from catalytic steam reforming of methane: influence of catalyst composition. *Journal of the Energy Institute*. 2012, 85(1), pp.29-37.
67. Park, Y., Namioka, T., Sakamoto, S., Min, T.J., Roh, S.A. and Yoshikawa, K. Optimum operating conditions for a two-stage gasification process fueled by polypropylene by means of continuous reactor over ruthenium catalyst. *Fuel Processing Technology*. 2010, 91(8), pp.951-957.
68. Treacy, D. and Ross, J.R.H. The potential of the CO₂ reforming of CH₄ as a method of CO₂ mitigation. A thermodynamic study. In: *American Chemical Society Energy and Fuels Symposia Spring (Anaheim), Anaheim*. American Chemical Society, 2004, pp.126-127.
69. Ibrahim, A.A., Fakeeha, A.H. and Al-Fatesh, A.S. Enhancing hydrogen production by dry reforming process with strontium promoter. *International Journal of Hydrogen Energy*. 2014, 39(4), pp.1680-1687.
70. Pakhare, D. and Spivey, J. A review of dry (CO₂) reforming of methane over noble metal catalysts. *Chemical Society Reviews*. 2014, 43(22), pp.7813-7837.
71. Fidalgo, B. and Menendez, J.A. Carbon Materials as Catalysts for Decomposition and CO₂ Reforming of Methane: A Review. *Chinese Journal of Catalysis*. 2011, 32(2), pp.207 - 216.
72. Zhang, X., Yang, C., Zhang, Y., Xu, Y., Shang, S. and Yin, Y. Ni–Co catalyst derived from layered double hydroxides for dry reforming of methane. *International Journal of Hydrogen Energy*. 2015, 40(46), pp.16115-16126.

73. Al-Doghachi, F.J., Zainal, Z., Saiman, M.I., Embong, Z. and Taufiq-Yap, Y.H. Hydrogen Production from Dry-Reforming of Biogas over Pt/Mg_{1-x}Ni_xO Catalysts. *Energy Procedia*. 2015, 79, pp.18-25.
74. Hou, T., Lei, Y., Zhang, S., Zhang, J. and Cai, W. Ethanol dry reforming for syngas production over Ir/CeO₂ catalyst. *Journal of Rare Earths*. 2015, 33(1), pp.42-45.
75. Siew, K.W., Lee, H.C., Gim bun, J., Chin, S.Y., Khan, M.R., Taufiq-Yap, Y.H. and Cheng, C.K. Syngas production from glycerol-dry(CO₂) reforming over La-promoted Ni/Al₂O₃ catalyst. *Renewable Energy*. 2015, 74, pp.441-447.
76. Özkara-Aydinoğlu, Ş. Thermodynamic equilibrium analysis of combined carbon dioxide reforming with steam reforming of methane to synthesis gas. *International Journal of Hydrogen Energy*. 2010, 35(23), pp.12821-12828.
77. Bulushev, D.D. Dry Reforming of Methane to Syn-Gas. [Online]. 2009. [Accessed 29 July 2013]. Available from: <http://www.carbolea.ul.ie/project.php?methane>
78. Tsang, S.C., Claridge, J.B. and Green, M.L.H. Recent advances in the conversion of methane to synthesis gas. *Catalysis Today*. 1995, 23(1), pp.3-15.
79. Albarazi, A., Beaunier, P. and Da Costa, P. Hydrogen and syngas production by methane dry reforming on SBA-15 supported nickel catalysts: On the effect of promotion by Ce_{0.75}Zr_{0.25}O₂ mixed oxide. *International Journal of Hydrogen Energy*. 2013, 38(1), pp.127-139.
80. Asencios, Y.J.O. and Assaf, E.M. Combination of dry reforming and partial oxidation of methane on NiO–MgO–ZrO₂ catalyst: Effect of nickel content. *Fuel Processing Technology*. 2013, 106(0), pp.247-252.
81. Z. Jiang, T.X., V. L. Kuznetsov and P. P. Edwards. Turning Carbon Dioxide into Fuel. *Philosophical Transactions of The Royal Society A*. 2010, 368, pp.3343-3364.
82. Luisetto, I., Tuti, S. and Di Bartolomeo, E. Co and Ni supported on CeO₂ as selective bimetallic catalyst for dry reforming of methane. *International Journal of Hydrogen Energy*. 2012, 37(21), pp.15992-15999.
83. Tomishige, K. and Fujimoto, K. Ultra-stable Ni catalysts for methane reforming by carbon dioxide. *Catalysis Surveys from Asia*. 1998, 2(1), pp.3-15.

84. Er-rbib, H., Bouallou, C. and Werkoff, F. Dry reforming of methane - Review of feasibility study. *Chemical Engineering Transactions*. 2012, 29, pp.163-168.
85. Serrano-Lotina, A. and Daza, L. Influence of the operating parameters over dry reforming of methane to syngas. *International Journal of Hydrogen Energy*. 2014, 39(8), pp.4089-4094.
86. Fakeeha, A.H., Khan, W.U., Al-Fatesh, A.S., Abasaheed, A.E. and Naeem, M.A. Production of hydrogen and carbon nanofibers from methane over Ni-Co-Al catalysts. *International Journal of Hydrogen Energy*. 2015, 40(4), pp.1774-1781.
87. Abdollahifar, M., Haghghi, M., Babaluo, A.A. and Talkhonchek, S.K. Sono-synthesis and characterization of bimetallic Ni-Co/Al₂O₃-MgO nanocatalyst: Effects of metal content on catalytic properties and activity for hydrogen production via CO₂ reforming of CH₄. *Ultrasonics Sonochemistry*. 2016, 31, pp.173-183.
88. Zanganeh, R., Rezaei, M. and Zamaniyan, A. Dry reforming of methane to synthesis gas on NiO-MgO nanocrystalline solid solution catalysts. *International Journal of Hydrogen Energy*. 2013, 38(7), pp.3012-3018.
89. Wang, S., Lu, G.Q. and Millar, G.J. Carbon Dioxide Reforming of Methane To Produce Synthesis Gas over Metal-Supported Catalysts: State of the Art. *Energy & Fuels*. 1996, 10(4), pp.896-904.
90. Choudhary, V.R. and Mondal, K.C. CO₂ reforming of methane combined with steam reforming or partial oxidation of methane to syngas over NdCoO₃ perovskite-type mixed metal-oxide catalyst. *Applied Energy*. 2006, 83(9), pp.1024-1032.
91. Luyben, W.L. Control of parallel dry methane and steam methane reforming processes for Fischer-Tropsch syngas. *Journal of Process Control*. 2016, 39, pp.77-87.
92. Kahle, L.C.S., Roussière, T., Maier, L., Herrera Delgado, K., Wasserschaff, G., Schunk, S.A. and Deutschmann, O. Methane Dry Reforming at High Temperature and Elevated Pressure: Impact of Gas-Phase Reactions. *Industrial & Engineering Chemistry Research*. 2013, 52(34), pp.11920-11930.
93. Rieks, M., Bellinghausen, R., Kockmann, N. and Mleczko, L. Experimental study of methane dry reforming in an electrically heated reactor. *International Journal of Hydrogen Energy*. 2015, 40(46), pp.15940-15951.

94. Song, C. and Pan, W. Tri-reforming of methane: a novel concept for catalytic production of industrially useful synthesis gas with desired H₂/CO ratios. *Catalysis Today*. 2004, 98(4), pp.463-484.
95. Lim, Y., Lee, C.J., Jeong, Y.S., Song, I.H. and Han, C. Optimal Design and Decision for Combined Steam Reforming Process with Dry Methane Reforming to Reuse CO₂ as a Raw Material. *Industrial & Engineering Chemistry Research*. 2012, 51(13), pp.4982-4989.
96. Reuther, R.B. and Jenkins, R.G. The effects of carbon dioxide and cation content on the rapid pyrolysis of lignite. In: *American Chemical Society Energy and Fuels Symposia Fall (Miami Beach)*, Miami Beach. American Chemical Society, 1989, pp.1124-1136.
97. Zhang, J., Wang, H. and Dalai, A.K. Effects of metal content on activity and stability of Ni-Co bimetallic catalysts for CO₂ reforming of CH₄. *Applied Catalysis A: General*. 2008, 339(2), pp.121-129.
98. Li, A., Norinaga, K., Zhang, W. and Deutschmann, O. Modeling and simulation of materials synthesis: Chemical vapor deposition and infiltration of pyrolytic carbon. *Composites Science and Technology*. 2008, 68(5), pp.1097-1104.
99. Theofanidis, S.A., Batchu, R., Galvita, V.V., Poelman, H. and Marin, G.B. Carbon gasification from Fe–Ni catalysts after methane dry reforming. *Applied Catalysis B: Environmental*. 2016, 185, pp.42-55.
100. Baktash, E., Littlewood, P., Schomäcker, R., Thomas, A. and Stair, P.C. Alumina coated nickel nanoparticles as a highly active catalyst for dry reforming of methane. *Applied Catalysis B: Environmental*. 2015, 179, pp.122-127.
101. Makri, M.M., Vasiliades, M.A., Petalidou, K.C. and Efstathiou, A.M. Effect of support composition on the origin and reactivity of carbon formed during dry reforming of methane over 5 wt% Ni/Ce_{1-x}M_xO_{2-δ} (M = Zr⁴⁺, Pr³⁺) catalysts. *Catalysis Today*. 2016, 259, Part 1, pp.150-164.
102. Ay, H. and Üner, D. Dry reforming of methane over CeO₂ supported Ni, Co and Ni–Co catalysts. *Applied Catalysis B: Environmental*. 2015, 179, pp.128-138.
103. Ayodele, B.V., Khan, M.R., Lam, S.S. and Cheng, C.K. Production of CO-rich hydrogen from methane dry reforming over lanthania-supported cobalt catalyst: Kinetic and mechanistic studies. *International Journal of Hydrogen Energy*. 2016, 41(8), pp.4603-4615.

104. Rostrupnielsen, J.R. and Hansen, J.H.B. CO₂-Reforming of Methane over Transition Metals. *Journal of Catalysis*. 1993, 144(1), pp.38-49.
105. Sakai, Y., Saito, H., Sodesawa, T. and Nozaki, F. Catalytic Reactions of Hydrocarbon with Carbon-dioxide over Metallic Catalysts. *Reaction Kinetics and Catalysis Letters*. 1984, 24(3-4), pp.253-257.
106. Yamada, H., Mori, H. and Tagawa, T. CO₂ reforming of waste plastics. *Journal of Industrial and Engineering Chemistry*. 2010, 16(1), pp.7-9.
107. Zagaynov, I.V., Loktev, A.S., Arashanova, A.L., Ivanov, V.K., Dedov, A.G. and Moiseev, I.I. Ni(Co)-Gd_{0.1}Ti_{0.1}Zr_{0.1}Ce_{0.7}O₂ mesoporous materials in partial oxidation and dry reforming of methane into synthesis gas. *Chemical Engineering Journal*. 2016, 290, pp.193-200.
108. Bradford, M.C.J. and Vannice, M.A. Catalytic reforming of methane with carbon dioxide over nickel catalysts I. Catalyst characterization and activity. *Applied Catalysis A: General*. 1996, 142(1), pp.73-96.
109. Barroso-Quiroga, M.M. and Castro-Luna, A.E. Catalytic activity and effect of modifiers on Ni-based catalysts for the dry reforming of methane. *International Journal of Hydrogen Energy*. 2010, 35(11), pp.6052-6056.
110. Galetti, A.E., Gomez, M.F., Arrúa, L.A. and Abello, M.C. Ni catalysts supported on modified ZnAl₂O₄ for ethanol steam reforming. *Applied Catalysis A: General*. 2010, 380(1-2), pp.40-47.
111. Du, X., Zhang, D., Gao, R., Huang, L., Shi, L. and Zhang, J. Design of modular catalysts derived from NiMgAl-LDH@m-SiO₂ with dual confinement effects for dry reforming of methane. *Chemical Communications*. 2013, 49(60), pp.6770-6772.
112. Castro Luna, A.E. and Iriarte, M.E. Carbon dioxide reforming of methane over a metal modified Ni-Al₂O₃ catalyst. *Applied Catalysis A: General*. 2008, 343(1-2), pp.10-15.
113. A.Shamsi. Methane Dry Reforming: Effects of Pressure and Promoters on Carbon Formation. In: *American Chemical Society Energy and Fuels Symposia Fall*, Washington DC. American Chemical Society, 2000, pp.690-693.
114. Lv, X., Chen, J.-F., Tan, Y. and Zhang, Y. A highly dispersed nickel supported catalyst for dry reforming of methane. *Catalysis Communications*. 2012, 20(0), pp.6-11.

115. Damyanova, S., Pawelec, B., Arishtirova, K. and Fierro, J.L.G. Ni-based catalysts for reforming of methane with CO₂. *International Journal of Hydrogen Energy*. 2012, 37(21), pp.15966-15975.
116. Huang, C.J., Zheng, X.M., Mo, L.Y. and Fei, J.H. A novel catalyst for CO₂ reforming of CH₄. *Chinese Chemical Letters*. 2001, 12(3), pp.249-232.
117. San José-Alonso, D., Illán-Gómez, M.J. and Román-Martínez, M.C. Low metal content Co and Ni alumina supported catalysts for the CO₂ reforming of methane. *International Journal of Hydrogen Energy*. 2013, 38(5), pp.2230-2239.
118. Rahemi, N., Haghighi, M., Babaluo, A.A., Jafari, M.F. and Khorram, S. Non-thermal plasma assisted synthesis and physicochemical characterizations of Co and Cu doped Ni/Al₂O₃ nanocatalysts used for dry reforming of methane. *International Journal of Hydrogen Energy*. 2013, 38(36), pp.16048-16061.
119. Xu, J., Zhou, W., Li, Z., Wang, J. and Ma, J. Biogas reforming for hydrogen production over nickel and cobalt bimetallic catalysts. *International Journal of Hydrogen Energy*. 2009, 34(16), pp.6646-6654.
120. Zhang, J., Wang, H. and Dalai, A.K. Development of stable bimetallic catalysts for carbon dioxide reforming of methane. *Journal of Catalysis*. 2007, 249(2), pp.300-310.
121. Aziznia, A., Bozorgzadeh, H.R., Seyed-Matin, N., Baghalha, M. and Mohamadizadeh, A. Comparison of dry reforming of methane in low temperature hybrid plasma-catalytic corona with thermal catalytic reactor over Ni/γ-Al₂O₃. *Journal of Natural Gas Chemistry*. 2012, 21(4), pp.466-475.
122. de Miguel, S.R., Vilella, I.M.J., Maina, S.P., San José-Alonso, D., Román-Martínez, M.C. and Illán-Gómez, M.J. Influence of Pt addition to Ni catalysts on the catalytic performance for long term dry reforming of methane. *Applied Catalysis A: General*. 2012, 435–436(0), pp.10-18.
123. Xu, G., Shi, K., Gao, Y., Xu, H. and Wei, Y. Studies of reforming natural gas with carbon dioxide to produce synthesis gas: X. The role of CeO₂ and MgO promoters. *Journal of Molecular Catalysis A: Chemical*. 1999, 147(1–2), pp.47-54.
124. Matei-Rutkovska, F., Postole, G., Rotaru, C.G., Florea, M., Pârvulescu, V.I. and Gelin, P. Synthesis of ceria nanopowders by microwave-assisted

hydrothermal method for dry reforming of methane. *International Journal of Hydrogen Energy*. 2016, 41(4), pp.2512-2525.

Chapter 3

EXPERIMENTAL METHODOLOGY

3.1 Introduction

This chapter describes in detail the experimental methodology that is used for the entire research. The first section describes the type of raw materials and catalysts prepared in the studies. The experimental reactor systems are also discussed including the reproducibility of the systems. The characterization of chosen materials, fresh and coked catalysts are been analysed thoroughly. The activation energy calculation of the thermal decomposition of waste plastics is also discussed in detail. Finally, the mass balance calculation for determining product yields from the pyrolysis/reforming process are presented.

3.2 Materials

In this section, the types of raw feedstock used in the research, together with the metals used in catalyst development are discussed.

3.2.1 Individual plastics composition of municipal solid waste

Individual plastics compositions from municipal solid waste were used as raw material for pyrolysis-reforming process. As mentioned in Chapter 2, plastics from municipal solid waste mainly consists of high density polyethylene (HDPE), low density polyethylene (LDPE), polystyrene (PS), polypropylene (PP) and polyethylene terephthalate (PET). Therefore, these five individual plastics were chosen in this research.

The HDPE, PS and PP were obtained as 2 mm waste polymer pellets provided by Regain Polymers Ltd, United Kingdom. The PET and LDPE were obtained as 2 mm virgin polymer pellets provided by Sigma-Aldrich Company Ltd, United Kingdom. Figure 3.1 shows the pelletized plastic samples that were used for the experiments.



Figure 3.1 Photograph of pelletized plastic samples

A mixture of LDPE, HDPE, PS, PET and PP was also prepared to simulate the real plastic wastes generated by countless areas of human activities. The composition of the simulated mixture of waste plastics sample is based on a report by Delgado et al. [1], which mostly plastics used for packaging, for diverse houseware and disposable items and cases of electronics. As shown in Table 3.1, the composition of plastics used in this study is quite similar to those of the real plastics found in the municipal solid waste. The plastics mixture has been investigated in Chapter 6, 7 and 8 and is known as simulated waste plastic (SWP).

Table 3.1 Composition of plastics according to plastics fraction in the residual municipal solid waste and simulated samples [1]

Material	Real plastics mixture/ wt.%	Simulated sample (SWP)/ wt.%
Low density polyethylene/ LDPE	43-38	42
High density polyethylene/ HDPE	20-15	20
Polystyrene/ PS	17-12	16
Polyethylene terephthalate/ PET	12-7	12
Polypropylene/ PP	10-5	10

3.2.2 Mixed waste plastics from various waste treatment plants

The real-world and post-consumer waste plastics used in Chapter 8 were collected from several municipal waste treatment plants. The plastic waste samples included; mixed plastics from household waste packaging (MP_{HP}), mixed plastics from a building construction site waste (MP_{BC}), mixed plastics from agricultural waste (MP_{AGR}), mixed plastics from electrical and electronic equipment (refrigerator and freezer (MP_F), old style television sets and monitors (MP_{CRT}) and mixture plastics (MP_{WEEE}) and refuse derive fuel containing waste plastics and other waste materials (RDF). These selections of mixed plastics were chosen in this research as they were normally found in municipal waste treatment plants as well as industrial waste treatment plants. The list of mixed waste plastics from various waste treatment plants used in this research is shown in Table 3.2.

Table 3.2 List of mixed waste plastics from various waste treatment plants

No	Mixed plastic sample
1	Mixed plastics from household waste packaging/ MP_{HP}
2	Mixed plastics from building construction site waste/ MP_{BC}
3	Mixed plastics from agricultural waste/ MP_{AGR}
4	Mixed plastics from electrical and electronic equipment/ MP_{WEEE}
5	Mixed plastics from old style television sets and monitors/ MP_{CRT}
6	Mixed plastics from refrigerators and freezers/ MP_F
7	Refuse derived fuel/ RDF
8	Virgin acrylonitrile-butadiene-styrene/ ABS
9	Virgin high impact polystyrene/ HIPS

The mixed plastics from household packaging (MP_{HP}) was obtained from Fost Plus in Belgium and mainly consist of HDPE and PET. 5.0 mm sized flakes of MP_{HP} was obtained from a low density fraction through the air separation process.

Both real mixed plastic from building construction (MP_{BC}) and real mixed plastic from agriculture (MP_{AGR}) were supplied from University of Pannonia, Hungary.

The agricultural foils (MP_{AGR}) consist of high/low density polyethylene and polypropylene, while mixed plastic waste from building construction (MP_{BC}) contains mainly polystyrene, polyurethane, polyethylene and polypropylene.

Plastics from electrical and electronic equipment were recycled from a commercial waste treatment plant that specifically recovered the plastics from this type of waste. Three different types of plastic waste were collected from this treatment plant; plastics from waste refrigerator and freezer equipment (MP_F), waste from cathode ray tube casings from old style television sets and computer monitors (MP_{CRT}) and a mixture of general electrical and electronic equipment plastic wastes (MP_{WEEE}). MP_F was obtained by shredding the refrigerator and freezer equipment. The compressor of the equipment was removed prior to the shredding process. Air blowing was used to separate the foam insulation from the equipment, while electromagnets were used to trap the ferrous metals. Finally, cyclones were used to separate the non-ferrous metal as well as plastics. Though all processes were carried out, some of the non-ferrous metal pieces still remained in the MP_F . MP_{CRT} was obtained by grinding the plastic fractions into 10-20 mm sized pieces. The circuit board, plastic outer casing and the glass monitor of the equipment were removed before the grinding process. MP_{WEEE} samples were carefully taken from a large mixed batch of waste plastics of electrical and electronic equipment. Multiple grab procedure was used in order to ensure the mixture of the sample was a representative of the waste plastics of electrical and electronic equipment.

In addition, virgin acrylonitrile-butadiene-styrene (ABS) and virgin high impact polystyrene (HIPS) were also investigated as representing major components of waste from electrical and electronic equipment. Both ABS and HIPS were obtained from Vamptech and Atofina UK respectively. The product yields from these two feedstocks may perhaps be compared with the results obtained from the real plastic waste from the electrical and electronic equipment recycling plant.

Furthermore, refused derived fuel (RDF) was also been investigated simulating the municipal solid waste that contains mixtures of plastics and other waste materials. RDF was mainly composed of plastics, paper, board, wood and other textile materials. The RDF sample was collected in pellet shape form from a commercial municipal solid waste treatment in United Kingdom. The RDF sample was further shredded and ground to a particle sized of about 1.0 mm.

3.2.3 Catalyst development

Several Ni-based alumina catalysts; Ni/Al₂O₃, Ni-Mg/Al₂O₃, Ni-Cu/Al₂O₃ and Ni-Co/Al₂O₃, were used in this study. The catalysts were prepared by the rising-pH technique according to the method reported by Garcia et al (2002) [2]. Mg(NO₃)₂.6H₂O, Cu(NO₃)₂.2.5H₂O or Co(NO₃)₂.6H₂O was added to Ni(NO₃)₂.6H₂O and Al(NO₃)₃.9H₂O and dissolved in 200 ml deionised water with moderate stirring at 40 °C. 1 M ammonium solution, as the precipitant was then added to the aqueous solutions until the PH value of 8.3 was reached. The precipitates were filtered, dried overnight at 105 °C and calcined at a temperature of 750 °C with a heating rate of 10 °C min⁻¹ and held at 750 °C for 3 hours. The molar ratios of 1:1 were prepared for Ni/Al₂O₃ and 1:1:1 for the other catalysts. All the catalysts were crushed using a mortar and pestle and finally sieved using a 50-212 µm particle sieve. In this research, the Ni-based catalysts were not reduced prior to the experiment.

3.2.3.2 Ni-Co/Al₂O₃ catalyst prepared by impregnation method

For the impregnation method, Ni(NO₃)₂.6H₂O was first stirred in deionised water at 80 °C until dissolved. Then Co(NO₃)₂.6H₂O was added with continued stirring for another 30 minutes. Lastly, γ-Al₂O₃ was added to the aqueous solution and left to mix until it formed a slurry. The precipitates were filtered, dried overnight at 105 °C and calcined at a temperature of 750 °C with a heating rate of 10 °C min⁻¹ and held at 750 °C for 3 hours. The molar ratio for Ni-Co-Al is 1:1:1. The catalysts were crushed using a mortar and pestle and finally sieved using a 50-212 µm particle sieve. In this research, the Ni-Co/Al₂O₃ catalysts were not reduced prior to the experiment.

3.2.3.3 Ni-Co/Al₂O₃ catalyst by different Co metal loading

Three different cobalt metal loadings for Ni-Co/Al₂O₃ catalysts were prepared. The catalysts were prepared by using the rising-pH technique as mentioned in 3.2.3.1. The ratios of the catalysts were namely 1:0.5:1, 1:1:1 and 1:2:1. In this research, the catalysts were not reduced prior to the experiment.

List of catalysts used in this research are shown in Table 3.3.

Table 3.3 List of catalysts

Catalyst	Molar ratio
<u>Catalyst prepared by rising-pH technique</u>	
Ni-Al ₂ O ₃	1:1
Ni-Mg/ Al ₂ O ₃	1:1:1
Ni-Cu/ Al ₂ O ₃	1:1:1
Ni-Co/ Al ₂ O ₃	1:1:1
Ni-Co/ Al ₂ O ₃	1:0.5:1
Ni-Co/ Al ₂ O ₃	1:2:1
<u>Catalyst prepared by impregnation method</u>	
Ni-Co/ Al ₂ O ₃	1:1:1

3.3 Experimental Reaction System

In this section, two types of fixed bed reactors used in this research are discussed. A one-stage fixed bed pyrolysis reactor was used in initial studies to understand the behaviour of the thermal degradation of waste plastics. For the rest of the studies, a two-stage fixed bed pyrolysis-reforming reactor was used. Both reactors were designed by former PhD students of Professor Paul T. Williams.

3.3.1 Operation description of fixed bed pyrolysis reactor

The preliminary investigation in Chapter 5 started with pyrolysis experiments of six individual plastic samples namely HDPE, LDPE, PP, PS, PET and real mixed plastics using a one-stage fixed bed reactor as shown in Figure 3.2.

These sets of experiments were set up to investigate the difference in product yields from the pyrolysis of plastics in nitrogen or carbon dioxide atmosphere without any influence from the second catalytic reforming stage. 2 g of plastic

sample for each type was used. The sample was placed in the sample holder and the reactor was heated by electrical furnace from ambient temperature to 500 °C with heating rate of 10 °C min⁻¹. The pyrolysis temperature was kept at 500 °C for 30 minutes. Nitrogen or carbon dioxide was used as the carrier gas with a flow rate of 200 ml min⁻¹. After the experiment had finished, the oil yields from the three stage condenser were collected and the gases in the sample bag were analysed. The summary of experimental parameter set up is shown in Table 3.4.

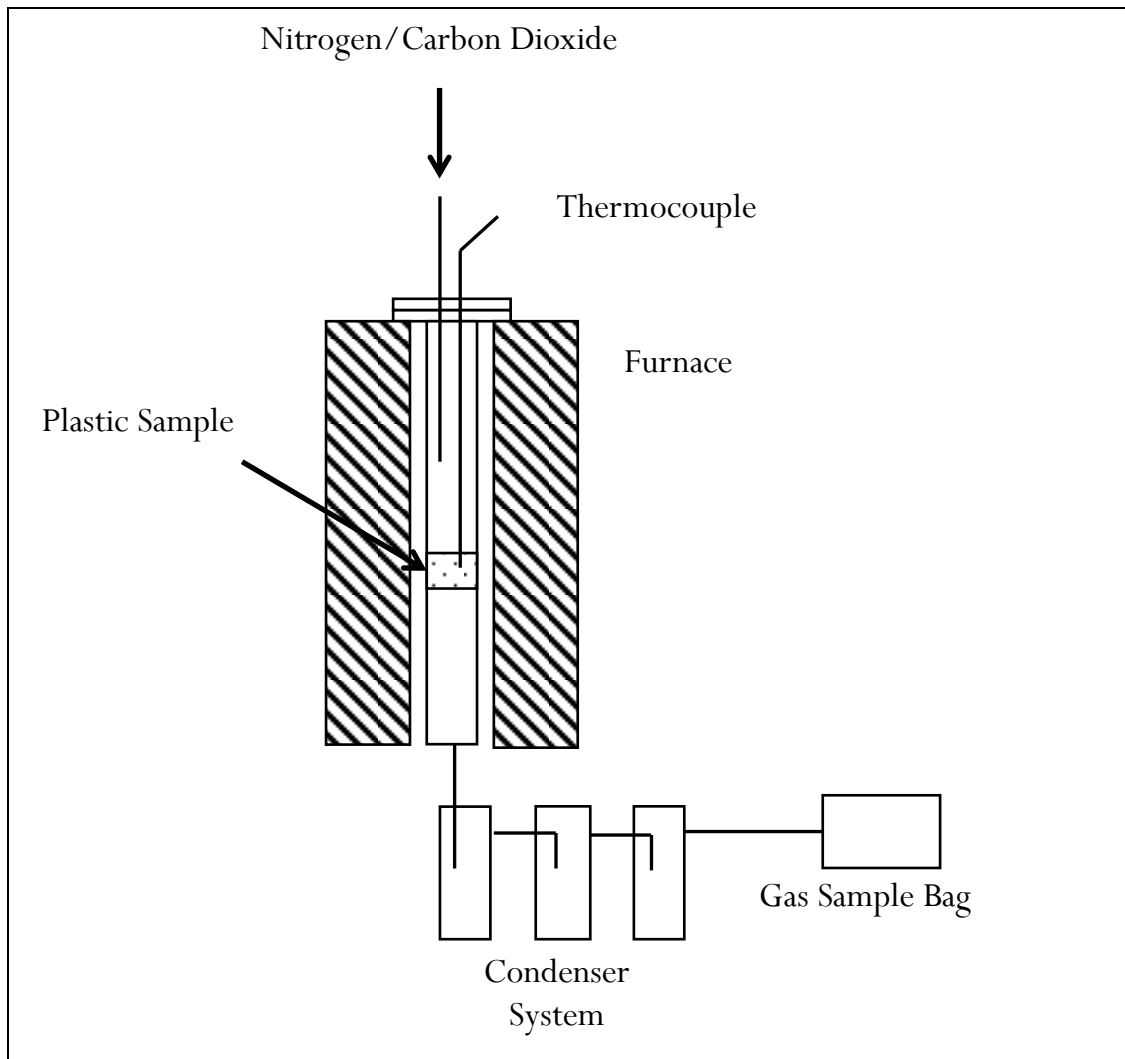


Figure 3.2 Schematic diagram of one-stage fixed bed reactor for preliminary investigation

Table 3.4 Pyrolysis experimental parameter set up

Feedstock / weight	HDPE, LDPE, PP, PS, PET / 2g
Pyrolysis temperature	500 °C
Heating rate	10 °C min ⁻¹
Hold time	30 min
Carrier gas / flow rate	N ₂ , CO ₂ / 200 ml min ⁻¹

3.3.2 Operation description of two-stage pyrolysis/ catalytic-reforming fixed bed reactor

A two-stage pyrolysis-reforming reactor as shown in the schematic diagram in Figure 3.3 and Figure 3.4 was used for further investigation as discussed in Chapter 5, 6, 7 and 8. The size of the reactor was 60 cm in length with 2.5 cm inner diameter and constructed of Inconel. The pyrolysis furnace was placed on top of the second stage reforming furnace and each furnace had its own heating control system and thermocouple to measure the temperature. The feedstocks were pyrolysed in the top furnace under the flow of nitrogen that acts as the carrier gas. The generated gaseous products were then passed through to the second stage reactor. The steam, carbon dioxide or combination of both was introduced into the second reactor to reform the generated gaseous products over the catalyst bed supported by quartz wool. Sand which is mainly composed of silicon oxide (SiO₂) was used as a substitute for the catalyst when the experiment was carried out without the catalyst. It should be noted that sand might contain trace metals, however an experiment was performed to investigate the influence of sand (with or without sand on the catalyst bed). The result (not shown here) proved that sand does not give significant effect towards the product yields. In addition, the early investigation using a two-stage pyrolysis-dry reforming reactor in Chapter 5 (5.2 and 5.3), the CO₂ was introduced into the 1st stage of the reactor system. An experiment with high density polyethylene was conducted to compare between CO₂ introduced into the 1st stage and 2nd stage reactor system (result not shown here). Both of the settings show similar product yields, proved that there were no reaction occurs in the 1st stage furnace due to the dry reforming reaction required high temperature (endothermic).

The gaseous products from the hot reactor zone were swept by the carrier gas into the three stages of the condenser system to collect the liquid products. The first condenser was held at room temperature while the second and third condensers were enclosed and cooled by dry ice. An additional glass wool filled third

condenser was used to further trap any remaining oil particles and prevent them from flowing through into the gas sample bag. The non-condensed gaseous products were then entrapped in the Tedlar gas sample bag to be analysed using gas chromatography. The total reaction time was 80 mins; with an additional of 20 mins collection time after each experiment (system turned off) to ensure all the gases were collected. The two-stage pyrolysis-reforming experiments started with the same investigation as the first set of experimental setup but using the two-stage pyrolysis-reforming reactor. Therefore, the difference was at the reforming stage. The reforming reactor was first heated up to desired reforming temperature at $40\text{ }^{\circ}\text{C min}^{-1}$ heating rate. When the second stage temperature stabilized, the pyrolysis reactor was heated up to $500\text{ }^{\circ}\text{C}$ at $10\text{ }^{\circ}\text{C min}^{-1}$.

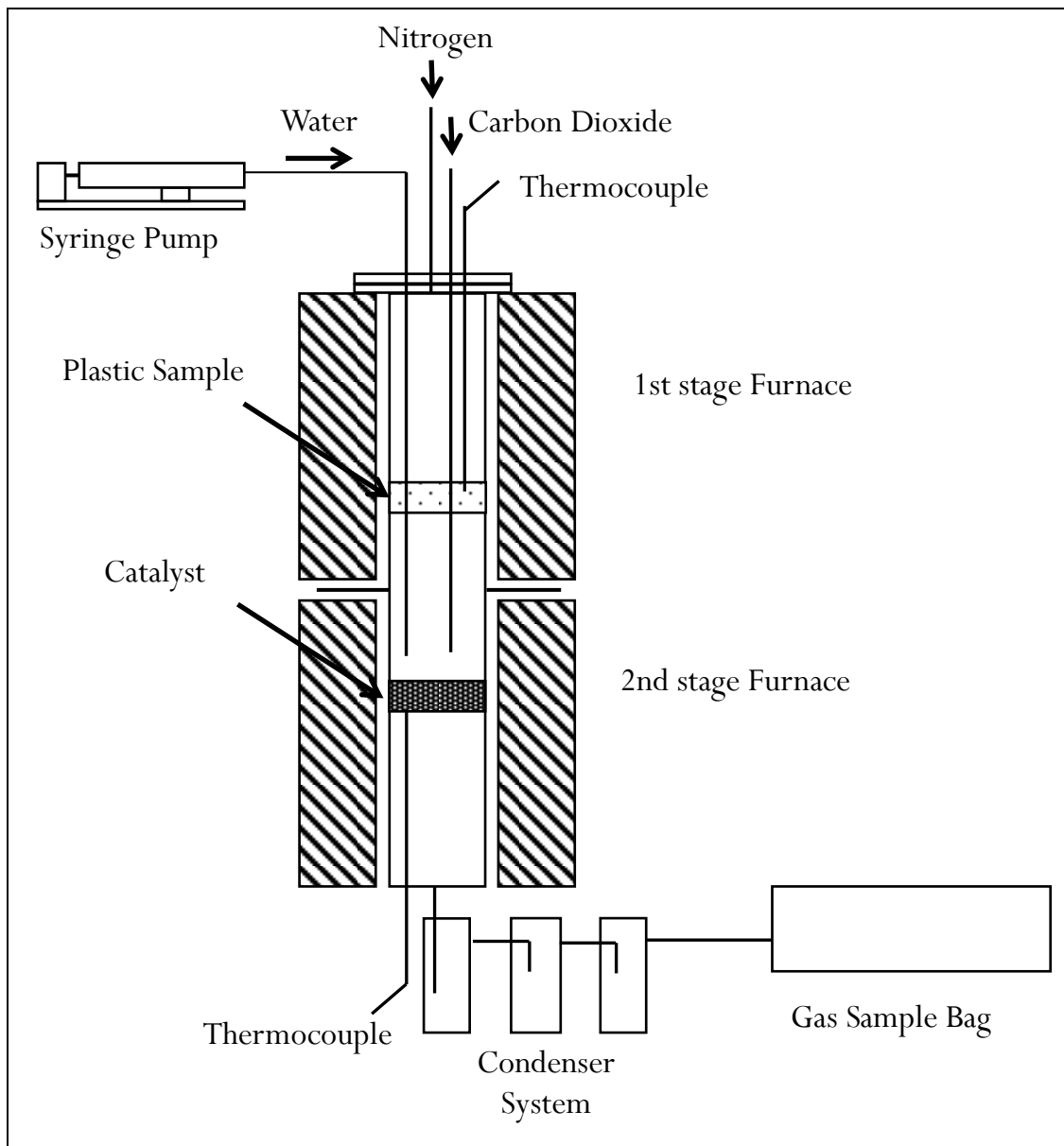


Figure 3.3 Schematic diagram of the two-stage fixed bed reactor

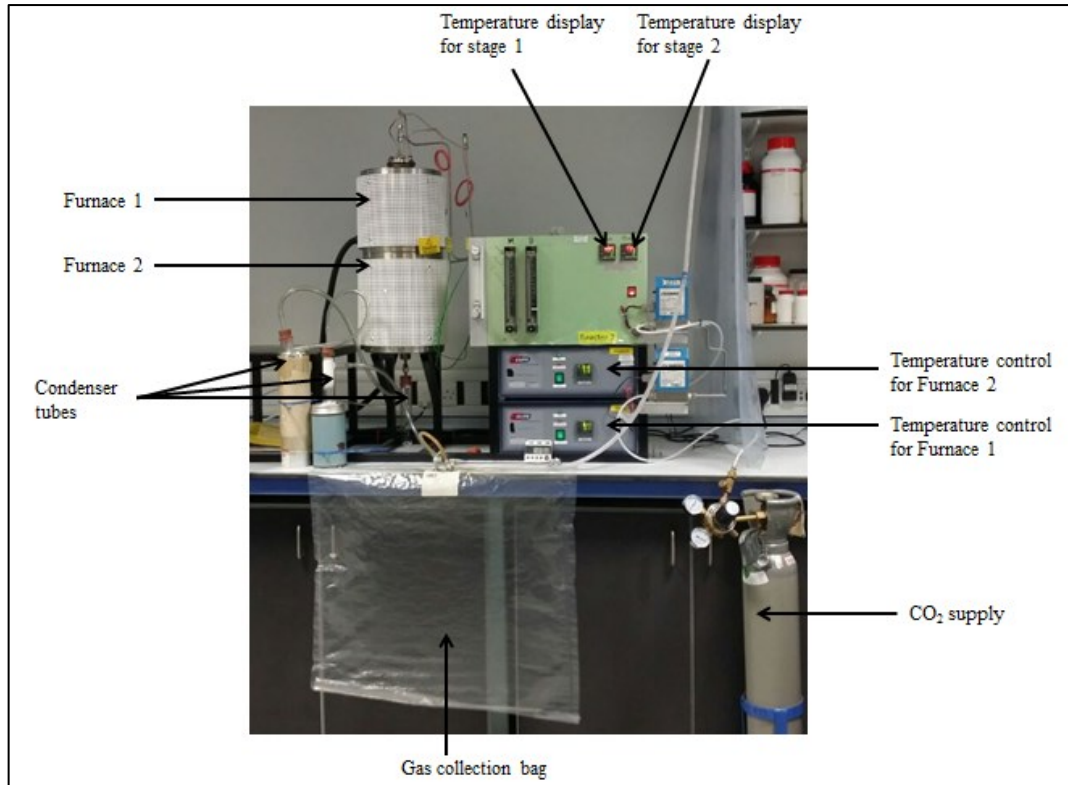


Figure 3.4 Photograph of the two-stage fixed bed reactor

3.3.3 Carbon dioxide feed composition for reforming process

For this study, carbon dioxide was used in the reforming stage of two-stage fixed bed reactor and was purchased from BOC, United Kingdom. The feed gas flow rates were controlled by Omega FMA-A2406-SS mass-flow controllers. In methane dry reforming, the typical feed of carbon dioxide introduced into the system was measured in $\text{CO}_2:\text{CH}_4$ molar ratio [3, 4]. Since the evolution of pyrolysis gases released from the pyrolysis of plastics and their interaction with carbon dioxide are complicated, the carbon dioxide feed was measured in g h^{-1} . For most of the experiments, the ratio of CO_2 :plastics used in this study was 4:1 except in Chapter 6 where the influence of process parameters were discussed. 8 g of carbon dioxide (6 g h^{-1}) with a flow rate of 50.9 ml min^{-1} was injected in the system and 2 g of plastics were placed in the sample holder. The general process condition of dry reforming of waste plastics are presented in Table 3.5. Further discussion on the reaction are discussed in Chapter 5, in which the theoretical calculation of dry reforming reactions, between hydrocarbons and carbon dioxide were compared with the experimental data.

Table 3.5 General process condition of dry reforming of waste plastics

Time collecting gases (min)	100
Plastic sample weight (g)	2
CO ₂ injected (g)	8
CO ₂ injected time (min)	80
CO ₂ flow rate (g h ⁻¹ / ml min ⁻¹)	6/ 50.9
CO ₂ :plastic ratio	4:1
Pyrolysis temperature	500 °C
Gasification/reforming temperature	800 °C

An example of the CO₂ flow rate calculation in ml min⁻¹ used in this study was obtained using the following formula:

$$CO_2 \text{ flow rate} = \text{Total volume of } CO_2 / \text{time}$$

and

$$1 \text{ moles of } CO_2 = 44.0095 \text{ g (mass)} = 22400 \text{ ml (volume)}$$

The mass of CO₂ can be converted to volume as followed:

$$\begin{aligned} 8 \text{ g of } CO_2 &= 8 / 44.0095 \\ &= 0.1818 \text{ moles} \end{aligned}$$

and,

$$\begin{aligned} 0.1818 \text{ moles of } CO_2 &= 0.1818 \times 22400 \\ &= 4072.32 \text{ ml} \end{aligned}$$

Therefore, the flow rate for 8 g of CO₂ at 80 min reaction time is:

$$\begin{aligned} CO_2 \text{ flow rate for } 8 \text{ g of } CO_2 &= 4072.32 \text{ ml} / 80 \text{ min} \\ &= 50.9 \text{ ml min}^{-1} \end{aligned}$$

It should also be noted that the starting temperature of pyrolysis reactor (1st stage furnace) was normally at around 70 °C, due to heat transfer from the gasification/reforming reactor. At this rate, the gasification/reforming reactor (2nd stage furnace) was already heated up to 800 °C. The pyrolysis reactor was then heated up to 500 °C with a heating rate of 10 °C min⁻¹. The decomposition of plastic was normally started to degrade at around 400 °C for individual plastic and

around 250 °C for mixed plastics (as discussed in Chapter 4), in which no reaction of pyrolysis gases with carbon dioxide should happen before reaching this temperature theoretically. Approximately 18 mins is required to reach 250 °C. Therefore, at least 1.8 g of unreacted carbon dioxide was passed to the gas sample bag during the pyrolysis heating-up.

3.3.4 Start up and validation

The reactor system was initially validated and optimized. Several experiments were carried out. During the whole research, several repetitions of most experiments were also made to ensure accuracy of the data.

The temperature for both reactors; one stage and two stage reactor, were monitored by thermocouples as earlier described and shown in Figure 3.2 and Figure 3.3. This arrangement was to control the temperature required for the process, hence to ensure the accuracy of the output products from the reactors. Several experiments were conducted to ensure the stability and reproducibility of both systems and the results are shown in Table 3.6 and 3.7.

For both reactors, the heating rate of the pyrolysis reactor (1st stage furnace in the case of two-stage reactor) was kept at 10 °C min⁻¹. As described earlier the temperature of the 2nd stage furnace for the two-stage reactor was pre-heated prior to the experiment at 800 °C, and the temperature was maintained throughout the experiment (monitored by a separate thermocouple at 2nd furnace). Based on the results, it is shown that the temperature of both reactors were stable for entire experiments, hence reflect the reactor system stability and accuracy.

Table 3.6 Reproducibility of thermocouple temperature for pyrolysis of LDPE at 500 °C using one stage fixed bed reactor

Time (min)	Thermocouple temperature (°C)					*AVG	*STDV	*RSTDV
	#1	#2	#3	#4	#5	(°C)	(°C)	(%)
0	24	23	22	23	24	23.2	0.75	3.23
5	73	72	73	72	75	73.0	1.10	1.50
10	122	125	123	124	122	123.2	1.17	0.95
15	176	177	176	175	175	175.8	0.75	0.43
20	220	222	221	223	222	221.6	1.02	0.46
25	265	266	265	262	264	264.4	1.36	0.51
30	332	331	333	330	332	331.6	1.02	0.31
35	378	380	376	380	377	378.2	1.60	0.42
40	433	435	430	432	434	432.8	1.72	0.40
45	475	478	476	475	476	476.0	1.10	0.23
50	501	500	499	500	501	500.2	0.75	0.15
55	500	500	500	500	500	500.0	0.00	0.00
60	500	500	500	500	500	500.0	0.00	0.00
65	500	500	500	500	500	500.0	0.00	0.00
70	500	500	500	500	500	500.0	0.00	0.00
75	500	500	500	500	500	500.0	0.00	0.00
80	500	500	500	500	500	500.0	0.00	0.00

Table 3.7 Reproducibility of thermocouple temperature at 1st stage furnace for pyrolysis-gasification/reforming of HDPE using two stage fixed bed reactor, 2nd stage furnace was pre-heated at 800 °C.

Time (min)	Thermocouple temperature for 1st stage furnace (°C)					*AVG (°C)	*STDV (°C)	*RSTDV (%)
	#1	#2	#3	#4	#5			
0	54	56	53	52	55	54	1.41	2.62
5	71	70	77	71	76	73	2.90	3.97
10	118	119	105	112	120	114.8	5.64	4.91
15	149	145	140	147	145	145.2	2.99	2.06
20	194	192	191	192	189	191.6	1.62	0.85
25	243	226	232	231	237	233.8	5.78	2.47
30	276	266	270	278	281	274.2	5.46	1.99
35	339	323	324	320	333	327.8	7.08	2.16
40	383	393	386	389	383	386.8	3.82	0.99
45	412	411	416	417	420	415.2	3.31	0.80
50	489	488	485	483	489	486.8	2.40	0.49
55	500	500	500	500	500	500	0.00	0.00
60	500	500	500	500	500	500	0.00	0.00
65	500	500	500	500	500	500	0.00	0.00
70	500	500	500	500	500	500	0.00	0.00
75	500	500	500	500	500	500	0.00	0.00
80	500	500	500	500	500	500	0.00	0.00

Apart from that, the reproducibility of the output products were also observed. The results presented in Table 3.8 showed that the initial set of experiments using a fixed bed pyrolysis reactor is reproducible. The repeatability data from pyrolysis of low-density polyethylene in nitrogen (N₂) atmosphere are presented to show the stability and repeatability of the reactor system as well as the consistency of the results. Based on the results, all five experiments showed consistency of the mass balance result.

Table 3.8 Initial experiments with the one stage fixed bed reactor (LDPE)

	1	2	3	4	5	*AVG	*STDV	*RSTDV (%)
General conditions	2 g of LDPE, 200 ml min ⁻¹ of N ₂							
Gas (wt.%)	13.4	13.5	13.7	13.7	13.6	13.6	0.11	0.79
Liquid (wt.%)	83.5	85.0	82.5	85.5	85.0	84.3	1.12	1.33
Mass balance (wt.%)	96.9	98.5	96.2	98.0	98.6	97.6	0.93	0.95

**AVG = average, *STDV = standard deviation, *RSTDV = relative standard deviation*

The repeatability of the two-stage fixed bed reactor system was also investigated. Table 3.9 shows the repeatability data of the product yields from the catalytic dry reforming of high density polyethylene using the two-stage, pyrolysis-reforming fixed bed reactor.

Table 3.9 Validation of the two-stage fixed bed reactor (HDPE)

	1	2	3	4	5	*AVG	*STDV	*RSTDV (%)
<u>General conditions</u>								
Sample/ weight	HDPE/ 2 g							
Pyrolysis temperature	500 °C							
Reforming temperature	800 °C							
Catalyst	Ni-Co-Al							
Carrier gas/ flow rate	N ₂ / 200 mlmin ⁻¹							
Reformer gas/ flow rate	CO ₂ / 6 g h ⁻¹							
<u>Mass balance</u>								
Sample conversion rate (wt. %)	100.0	99.9	100.0	100.0	99.9	99.96	0.05	0.05
Gas yield (wt. %)	102.4	92.2	94.8	94.8	94.8	95.8	3.44	3.59
Mass balance (%)	102.9	93.9	97.2	97.2	97.3	97.7	2.89	2.96
H ₂ +CO (mmol g ⁻¹)	164.6	144.2	149.1	148.9	149.0	151.1	6.98	4.62
CO ₂ conversion (%)	55.9	58.7	57.6	57.5	57.6	57.5	0.90	1.56

*AVG = average, *STDV = standard deviation, *RSTDV = relative standard deviation

3.4 Analytical Techniques

In this section, the analytical techniques used to determine the characteristics and behaviour of the waste plastics, also the catalysts along with the product yields from pyrolysis and reforming of waste plastics are discussed.

3.4.1 Material analysis

3.4.1.1 Proximate and ultimate analysis

The composition of individual type of waste feedstock contribute substantial role on the syngas (H_2 and CO) production. The ultimate analysis was carried out to obtain the composition of nitrogen (N), carbon (C), hydrogen (H) and sulphur (S) weight fraction in each raw material while the oxygen (O) value was obtained by the difference of the weight fraction. Furthermore, the proximate analysis was carried out to measure the moisture, ash and volatile content of each raw material while the fixed carbon was determined by the different of the weight fraction. The ultimate and proximate analyses of the plastics sample used in this study are shown in Table 3.10 and Table 3.11.

The ultimate analysis of individual plastics; HDPE, LDPE, PP, PS and PET (received basis) was carried out using a CHNS/O elemental analyser (CE Instruments Wigan, UK, FLASH EA2000 CHNS-O analyser). This analysis was performed at Energy Research Institute, University of Leeds.

In addition, the ultimate analysis of HIPS, ABS and different types of waste obtained from several waste treatment plants (MP_{HP} , MP_{AGR} , MP_{BC} , MP_F , MP_{CRT} , MP_{WEEE} , RDF) along with proximate analysis for all raw materials were performed by the thesis author at the laboratory at Huazhong University of Science & Technology, China during a two month research secondment. This analysis was part of the FLEXI-PYROCAT EU-RISE project. The ultimate analysis of waste samples (dry basis) was carried out in two separate machine; a CHNO elemental analyser (Vario Micro cube, Germany) in which the oxygen content was obtained by difference and a specific sulphur analyser (Rapid S Cube Elementar

Analysensysteme GmbH, Germany). The proximate analysis of plastic samples was measured using three different methods. The plastic samples (received basis) which were dried in an oven at 110 °C overnight in order to measure the moisture content. Then, the dried plastic samples (dry basis) were heated in a horizontal tube furnace from room temperature to 900 °C, with a heating rate of 10 °C min⁻¹ and 20 minutes hold time. N₂ was used as a carrier gas with a heating rate of 200 ml min⁻¹. This was to measure the volatile content of the sample. Another horizontal tube furnace was used to measure the ash content of the plastic samples (received basis). The furnace was heated from room temperature to 925 °C with a heating rate of 10 °C min⁻¹, 20 minutes hold time and under air atmosphere. The moisture, volatile and ash content were obtained by difference of sample weight before and after the experiment.

Table 3.10 (a) Ultimate analysis of each raw materials analysed at University of Leeds laboratory, United Kingdom (CE Instrument Wigan, UK, FLASH EA2000CHNS-O analyser)

Sample	N (wt.%)	C (wt.%)	H (wt.%)	O (wt.%)	S (wt.%)	HHV (Kcal/Kg)	LHV (Kcal/Kg)	H/C ratio
High density polyethylene/ HDPE	0.94	80.58	18.48	<i>nd</i> ²	<i>nd</i> ²	12401.99	11393.80	0.23
Low density polyethylene/ LDPE	0.94	81.01	18.06	<i>nd</i> ²	<i>nd</i> ²	12415.75	11421.97	0.22
Polypropylene/ PP	0.95	80.58	10.42	8.89	<i>nd</i> ²	11900.33	10954.18	0.13
Polystyrene/ PS	0.86	86.19	12.43	0.52	<i>nd</i> ²	10797.32	10132.75	0.14
Polyethylene terephthalate/ PET	0.57	61.0	11.30	27.13	<i>nd</i> ²	8392.52	7788.34	0.19

¹received basis, ²*nd* = not detected, ³dry basis

Table 3.10 (b) Ultimate analysis of each raw materials analysed at Huazhong University of Science and Technology laboratory, China

Sample	N (wt.%)	C (wt.%)	H (wt.%)	O (wt.%)	S (wt.%)	H/C ratio
Mixed plastic from household packaging/ MP _{HP}	0.16	82.90	13.37	3.57	0.23	0.161
Mixed plastics from agricultural/ MP _{AGR}	0.89	79.08	12.91	7.12	0.26	0.163
Mixed plastics from building construction/ MP _{BC}	0.14	80.91	12.22	6.74	0.22	0.151
Mixed plastics from cathode ray tube/ MP _{CRT}	4.82	85.10	7.80	2.29	0.26	0.092
High impact polystyrene/ HIPS	0.03	80.76	7.31	11.89	0.16	0.091
Acrylonitrile-butadiene-styrene/ ABS	3.42	72.89	6.77	16.91	0.23	0.093
Mixed plastics from freezer and refrigerator equipment/MP _F	1.15	71.95	6.86	20.05	0.22	0.095
Mixed plastics from electrical and electronic equipment/ MP _{WEEE}	0.70	75.17	5.87	18.26	0.22	0.078
Refuse derived fuel/ RDF	0.58	44.78	6.23	48.41	0.29	0.139

¹received basis, ²nd = not detected, ³dry basis

Table 3.11 Proximate analysis of each raw material analysed at Huazhong University of Science and Technology laboratory, China

Sample	Ash ¹ (wt.%)	Volatile ² (wt.%)	Moisture ¹ (wt.%)	Fixed carbon ¹ (wt.%)
High density polyethylene/ HDPE	0.38	99.27	0.72	nd ³
Low density polyethylene/ LDPE	0.08	99.95	0.01	nd ³
Polypropylene/ PP	0.39	95.00	5.68	nd ³
Polystyrene/ PS	5.23	98.25	1.72	nd ³
Polyethylene terephthalate/ PET	1.20	85.64	0.06	13.10
Mixed plastic from household packaging/ MP _{HP}	1.74	99.15	0.90	nd ³
Mixed plastics from agricultural waste/ MP _{AGR}	0.99	99.06	1.26	nd ³
Mixed plastics from building construction waste/ MP _{BC}	0.81	99.02	0.49	nd ³
Mixed plastics from cathode ray tube/ MP _{CRT}	3.71	93.88	1.40	1.02
High impact polystyrene/ HIPS	2.48	95.71	0.08	1.73
Acrylonitrile-butadiene-styrene/ ABS	7.93	89.81	0.85	1.41
Mixed plastics from freezer and refrigerator equipment/ MP _F	0.80	81.99	20.10	nd ³
Mixed plastics from electrical and electronic equipment/ MP _{WEEE}	0.28	81.04	2.89	15.79
Refuse derived fuel/ RDF	4.47	70.74	11.32	13.48

¹received basis, ²dry basis, ³nd = not detected

3.4.1.2 Thermogravimetric analysis (TGA)

The thermogravimetric analysis was carried out as discussed in Chapter 4 in order to generate the weight loss profile of raw materials in relation to temperature.

The first study is to investigate the influence of nitrogen or carbon dioxide atmosphere in pyrolysis of individual component of waste plastics; HDPE, LDPE, PS, PP and PET. Two different analysers were used in this study; a TGA-50 Shimadzu and a TGH-1000 analyser. Approximately 8-9 mg of each raw material in a flake size approximately 1 mm, was placed in the alumina pan. The sample was kept at 500 °C for 30 min with heating rate of 10 °C min⁻¹. The nitrogen or carbon dioxide flow rate used was 50 ml min⁻¹. This study was carried out in University of Leeds laboratory, United Kingdom.

The second study was carried out to investigate the influence of nitrogen and carbon dioxide mixture in the pyrolysis process. The non-isothermal degradation of each raw material was performed in a thermogravimetric analyser (STA449F3, NETZSCH). Approximately 4-6 mg of sample in powder form was placed in an alumina sample pan, and heated from room temperature to 900 °C at 10 °C min⁻¹. Three different flow gases were used, either with 100% of N₂, 100% of CO₂ or ratio of N₂/CO₂ (70/30%, 50/50% or 30/70%) for HDPE (N₂/CO₂ ratio of 1:0, 0:1, 7:3, 1:1 and 3:7). While for the rest of the plastic samples, only two different flow gases were used, 100 % of N₂ and 70/30% N₂/CO₂ (N₂/CO₂ ratio of 1:0 and 7:3). The total flow rate of gas for each analysis was 100 ml min⁻¹. This analysis was part of the FLEXI-PYROCAT EU-RISE project and the work was carried out by the thesis author at Huazhong University of Science & Technology laboratory, China during a two month research secondment.

3.4.1.3 Kinetic analysis calculation

A modified Coats-Redfern technique [5] was used to obtain the values of activation energy of decomposition of each plastic samples. The technique has been reported and discussed by many researchers [6-9]. All kinetic studies presented here utilized the basic rate equation of conversion α for the thermal degradation under a nitrogen or carbon dioxide atmosphere and are presented as the following:

The basic decomposition kinetic equation is given by:

$$\frac{d\alpha}{dt} = kf(\alpha) \quad (\text{Equation 3.4})$$

The reaction rate constant, k is given by the Arrhenius equation:

$$k = A e^{\left(\frac{-E}{RT}\right)} \quad (\text{Equation 3.5})$$

where A is pre-exponential factor (min^{-1}); E is apparent activation energy (kJ mol^{-1}); T is reaction temperature (K); R is universal gas constant, it equals to 8.314×10^{-3} ($\text{KJ mol}^{-1} \text{K}^{-1}$).

Both equations are simplified as:

$$\frac{d\alpha}{dt} = A e^{\left(\frac{-E}{RT}\right)} f(\alpha) \quad (\text{Equation 3.6})$$

If $f(\alpha)$ is presented as:

$$f(\alpha) = (1-\alpha)^n \quad (\text{Equation 3.7})$$

where n is the reaction order.

The waste plastics are pyrolyzed with a constant heating rate, β is defined as the following:

$$\beta = \frac{dT}{dt} \quad (\text{Equation 3.8})$$

The time dependency of Equation 3.6 is removed by substituting dt with dT and Equation 3.7 is substituted into the equation:

$$\frac{d\alpha}{dT} = \frac{A}{\beta} e^{\left(\frac{-E}{RT}\right)} (1-\alpha) \quad (\text{Equation 3.9})$$

Rearranging the equation:

$$\frac{1}{(1-\alpha)} d\alpha = \frac{A}{\beta} e^{\left(\frac{-E}{RT}\right)} dT \quad (\text{Equation 3.10})$$

Taking integration on both side of Equation 3.10:

$$\int_0^\alpha \frac{1}{(1-\alpha)} d\alpha = \int_{T_0}^T \frac{A}{\beta} e^{\left(\frac{-E}{RT}\right)} dT \quad (\text{Equation 3.11})$$

The left hand side (LHS) of the Equation 3.11 is solved by integration by substitution method as following:

$$\int_0^\alpha \frac{1}{(1-\alpha)} d\alpha$$

Let $u = (1-\alpha)$ in order to simplify the integrand to $\frac{1}{u}$, and $\int_0^u \frac{1}{u} du$ is the natural logarithm of u , $\ln(u)$.

$$\text{If } du = \frac{du}{d\alpha} d\alpha$$

$$\text{And so with } u = (1-\alpha) \text{ and } \frac{du}{d\alpha} = -1$$

$$\text{It follows that } du = \frac{du}{d\alpha} d\alpha = -1d\alpha$$

The integral become:

$$\int_0^u \frac{1}{u} (-1) du = (-1) \int_0^u \frac{1}{u} du = (-1) [\ln(u)]_0^u = -\ln(1-\alpha)$$

The right hand side (RHS) of the Equation 3.11 is solved by integration by substitution method as following:

$$\frac{A}{\beta} \int_{T_0}^T e^{\left(\frac{-E}{RT}\right)} dT$$

Let $u = \left(-\frac{E}{RT}\right)$ in order to simplify the integrand to e^u , and $\int_0^u e^u du$ is the exponential of u , e^u ,

$$\text{If } du = \frac{du}{dT} dT$$

$$\text{And so with } u = \left(-\frac{E}{RT}\right) \text{ and } \frac{du}{dT} = \frac{E}{RT^2}$$

$$\text{It follows that } du = \frac{du}{dT} dT = \frac{E}{RT^2} dT$$

The integral become

$$\frac{A}{\beta} \int_{u_0}^u e^{-u} \frac{RT^2}{E} du = \frac{ART^2}{\beta E} \int_{u_0}^u e^{-u} du = \frac{ART^2}{\beta E} \left[e^{-u} \right]_{u_0}^u = \frac{ART^2}{\beta E} \left[e^{-\frac{E}{RT}} - e^{-\frac{E}{RT_0}} \right]$$

By approximation of $e^{-\frac{E}{RT_0}} \sim 0$, the combination of left hand side(LHS) and right hand side (RHS) equations can be simplified to:

$$\frac{-\ln(1-\alpha)}{T^2} = \frac{AR}{\beta E} e^{-\frac{E}{RT}} \quad (\text{Equation 3.12})$$

Taking natural logarithm on both side of Equation 3.12, it becomes:

$$\ln \frac{-\ln(1-\alpha)}{T^2} = \ln \left[\frac{AR}{\beta E} e^{-\frac{E}{RT}} \right]$$

$$\text{Since } \ln \left[e^{-\frac{E}{RT}} \right] = -\frac{E}{RT}$$

Therefore, the equation can be reduced to:

$$\ln \frac{-\ln(1-\alpha)}{T^2} = \ln \frac{AR}{\beta E} - \frac{E}{RT} \quad (\text{Equation 3.13})$$

The left side of Equation 3.13 was plotted against 1/T by considering α as the conversion of the waste plastics.

α is defined as the following:

$$\alpha = \frac{m_0 - m}{m_0 - m_f}$$

where m_0 is the initial sample weight, m is the sample weight at time t , and m_f is the final sample weight.

The slope of the resultant straight line from the plotted data represents the activation energy ($-E/R$) of the thermal degradation of the waste plastics. In this work, a reaction order of $n=1.0$ was used to calculate the kinetic parameters.

3.4.2 Catalyst analysis (fresh/ reacted)

3.4.2.1 Temperature programmed reduction (TPR)

Temperature programmed reduction (H₂-TPR) of the prepared catalysts used a Stanton–Redcroft thermogravimetric analyser (TGA). The H₂-TPR was conducted to investigate the adsorption of hydrogen on all active sites of the fresh catalysts, also their reducibility characteristic. During the H₂-TPR analysis, each fresh catalyst sample (20 mg) was first heated from room temperature to 150 °C at 20 °C min⁻¹ and held for 30 minutes to remove the moisture, then heated at 10 °C min⁻¹ to a final temperature of 900 °C. The feed gas used was hydrogen (5% H₂ balanced with N₂).

3.4.2.2 Brunauer, Emmet and Teller (BET) surface area analysis

BET method is one of the commonly used methods for analysing the surface area of the porous solid materials. The general BET equation is shown in Equation 3.1;

$$\frac{1}{W\left(\left(\frac{P_0}{P}\right)-1\right)} = \frac{1}{W_m C} + \frac{C-1}{W_m C} \left(\frac{P}{P_0}\right) \quad (\text{Equation 3.1})$$

where W is the weight of gas adsorbed at a relative pressure, P/P_0 and W_m is the weight of adsorbate constituting a monolayer of surface coverage. C constant is related to the energy adsorption in the first adsorbed layer and consequently its value is an indication of the magnitude of the adsorbent/adsorbate interaction. The linear graph of the left side of the Equation 3.2 is plotted against P/P_0 by using the point-by-point adsorption data from the multipoint analysis. The slope s and intercept i can be obtained from the BET plot, where $s=((C-1)/W_m C)$ and $i=(1/W_m C)$, thus weight of the monolayer; $W_m=1/(s+i)$. The total surface area St of the sample can be expressed as:

$$St = \frac{W_m N A_{cs}}{M} \quad (\text{Equation 3-2})$$

where N is Avogadro's number (6.02×10^{23} molecules/mol), M is the molecular weight of the adsorbate and the cross-sectional area of nitrogen, A_{cs} is 16.2 \AA^2 [10].

A Nova 2200e surface area and pore analyser as shown in Figure 3.5 was used to obtain the Brunauer, Emmet and Teller (BET) surface area of each catalyst using the nitrogen adsorption technique. NovaWin software was used to gather data information from the analyser. Powdered catalyst samples were placed in the sample holder. Prior to the analysis, the samples were outgassed for 5 hours at 110 °C. About 100 mg of sample is used for every run. Figure 3.6 showed an example of the plotted multi-point linear graph and the BET surface area of fresh Ni-Al catalyst generated by the NovaWin software.



Figure 3.5 Photograph of Nova 2200e surface area and pore analyser

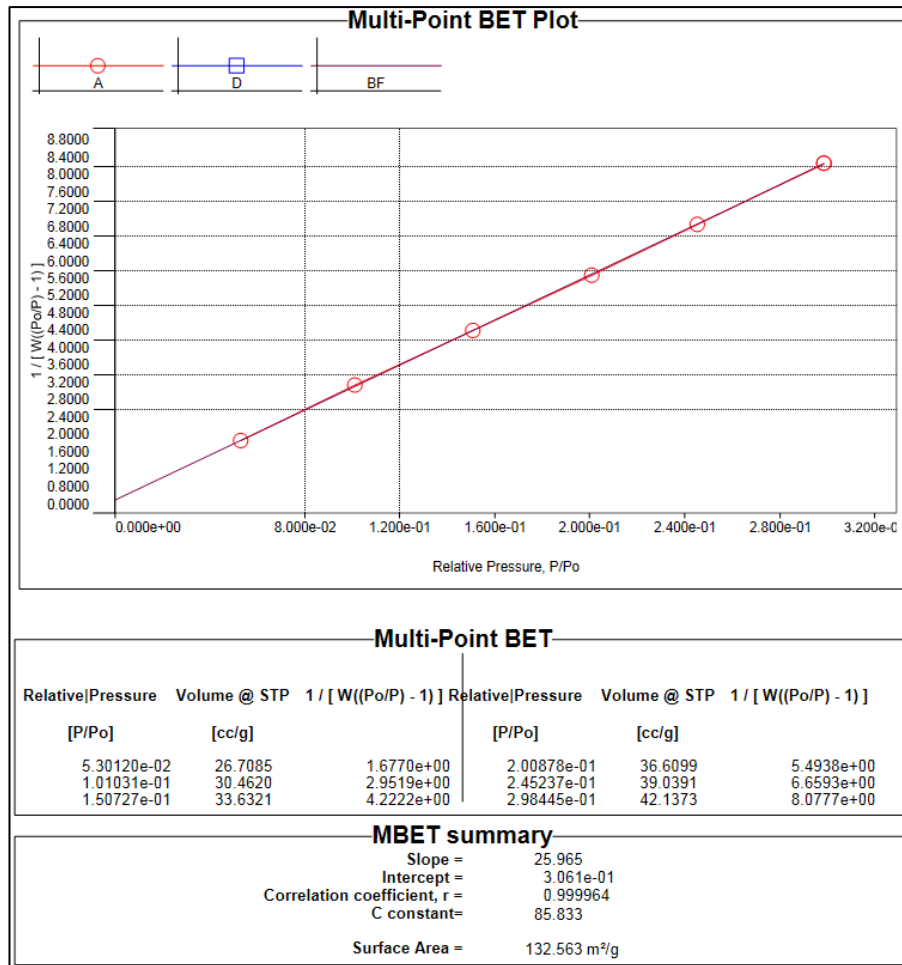


Figure 3.6 Multi-point BET plot for fresh Ni-Al catalyst

3.4.2.3 X-ray diffraction (XRD)

A Bruker D-8 diffractometer was used to record the X-ray diffraction (XRD) patterns of the fresh and coked catalysts using a Cu-K α radiation X-ray source with a Vantec position sensitive detector. The range was 10 $^{\circ}$ –70 $^{\circ}$ with a scanning step of 0.05 $^{\circ}$. The data was recorder by DIFFRACplus software and the pattern identification was obtained using HighScore Plus software. The crystallographic structure/phase of the fresh/coked catalyst powders could be obtained through XRD analysis by comparing diffraction data with a standard database. XRD analysis can also be used to determine the main chemical compound of catalyst particle.

The principle of XRD analysis is based on the Bragg's Law principle as shown in the following equation:

$$\lambda = 2d \sin \theta \quad (\text{Equation 3.3})$$

The plotted peak was matched up with the software library database to identify the crystalline phases. This is because the X-ray diffraction pattern corresponded solely for each crystalline solid. An example of an XRD pattern generated by the software is shown in Figure 3.7. The raw generated pattern is including the noise and background signal.

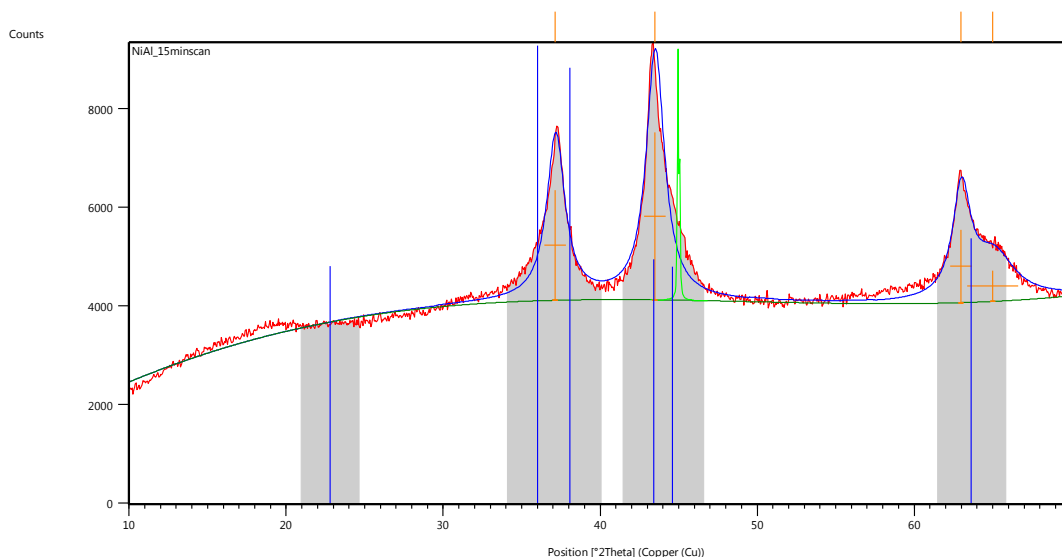


Figure 3.7 Example of diffraction pattern from XRD analysis on fresh Ni-Al catalyst

3.4.2.4 Scanning electron microscopy (SEM)

The fresh catalysts were analysed using a high resolution scanning electron microscope (LEO 1530) coupled to an energy dispersive X-ray spectrometer (EDXS). The image of the fresh/coked catalyst surface is obtained by scanning the surface sample using the high energy beam of electrons. The morphology of the catalyst surface images before and after experiment, together with other information from different characterisation technique are used to give better understanding on the coke formation on the catalyst surface. Example of a SEM-EDXS image captured by the microscope is presented in Figure 3.8.

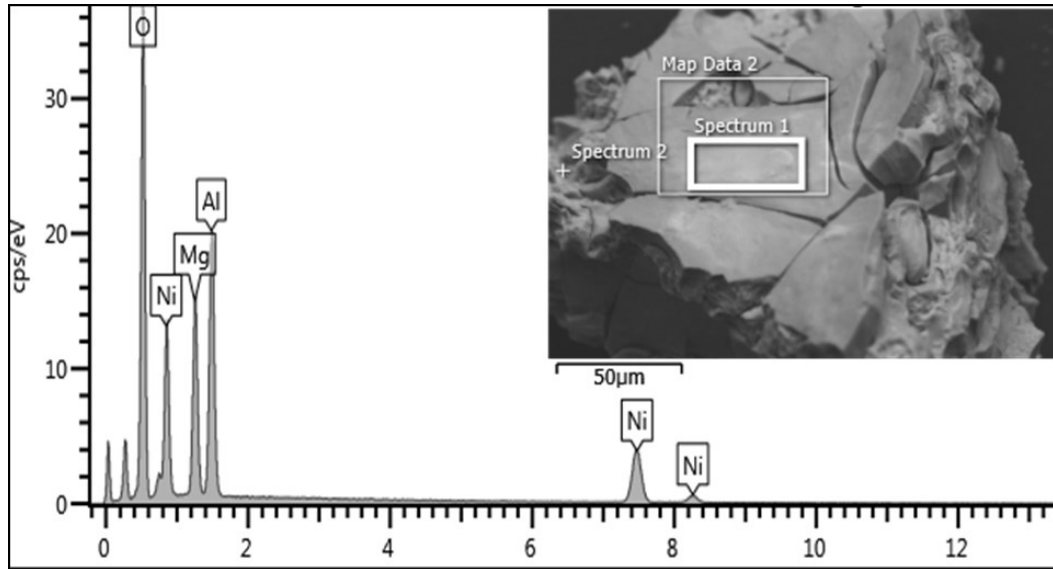


Figure 3.8 SEM-EDXS of fresh Ni-Mg-Al catalyst

In addition, the coked/reacted catalysts from the pyrolysis–reforming of waste plastics were analysed using a Hitachi SU8230 SEM high performance cold field emission, CFE as shown in Figure 3.9.

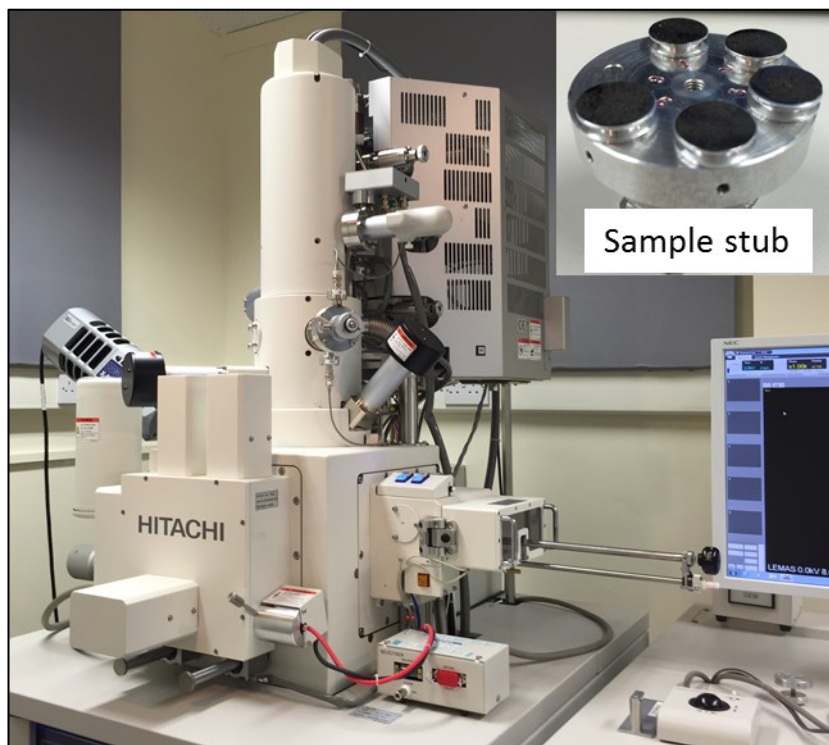


Figure 3.9 Photograph of Hitachi SU8230 SEM equipment

Small amounts of the coked catalysts were placed on a sample stub. An air stream was blown to remove any excess carbon and the stub was placed in the SEM. The characteristics of carbon deposited on the reacted catalysts was examined and analyzed. Figure 3.10 shows an example of SEM morphology of a coked catalyst sample captured by the SEM at different magnifications.

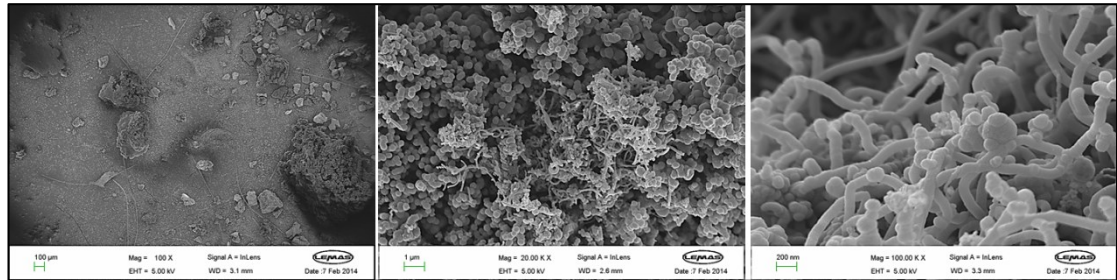


Figure 3.10 SEM morphologies of coked Ni-Mg/Al₂O₃ catalyst in different magnifications from pyrolysis-gasification process of waste high density polyethylene without CO₂ addition at gasification temperature of 800 °C

3.4.2.5 Temperature programmed oxidation (TGA-TPO)

The temperature programmed oxidation (TGA-TPO) is a common technique used to determine the characteristics of carbon deposited on the reacted catalyst surface [11-14]. Normally, three different weight loss peaks of coked catalyst could be identified representing three different stages of decomposition. The water vaporization is identified at low temperature around 100 °C while at temperatures around 350 °C, metal oxidation occurred. Carbon combustion of the deposited carbon on the catalyst might be identified at the temperatures above 400 °C. Figure 3.11 shows an example of a DTG-TPO thermogram of coked Ni-Mg/Al₂O₃ catalyst.

Temperature programmed oxidation (TGA-TPO) experiments were carried out using a thermogravimetric analyser (TGA-50 Shimadzu) as shown in Figure 3.12. About 8mg of reacted catalyst was heated in an atmosphere of air with a heating rate of 15 °C min⁻¹ from ambient temperature to a final temperature of 800 °C.

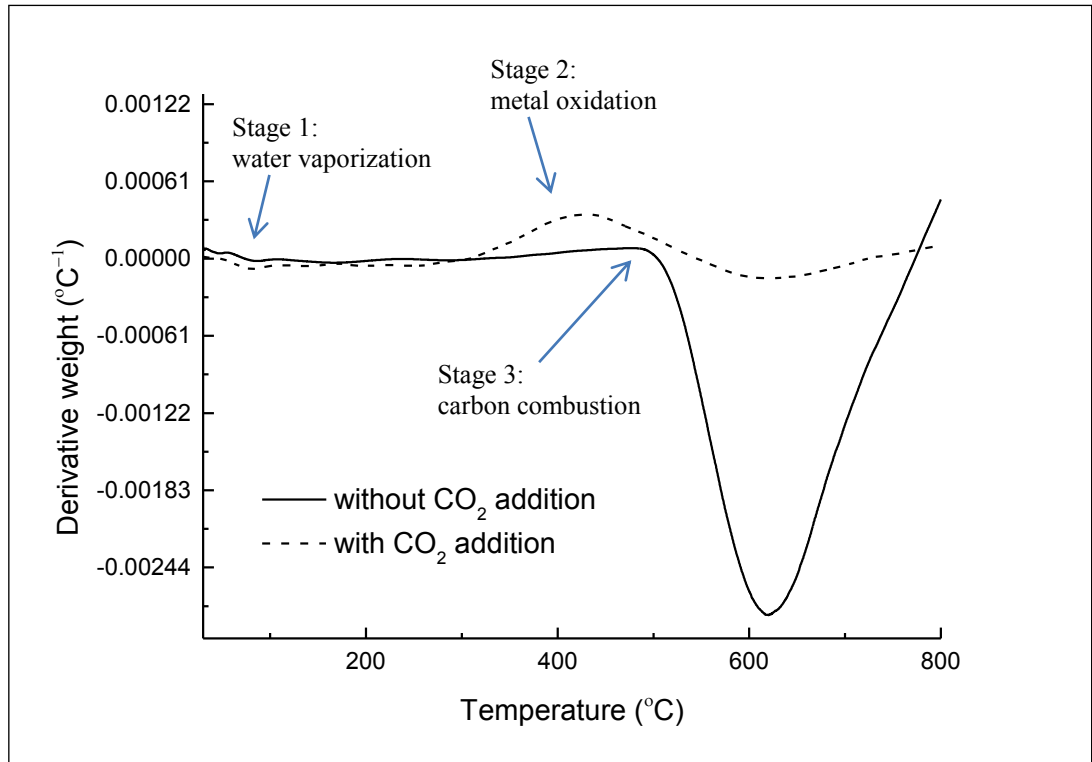


Figure 3.11 DTG-TPO results for the reacted Ni-Mg/Al₂O₃ catalyst after pyrolysis-reforming of waste high density polyethylene with and without the addition of carbon dioxide

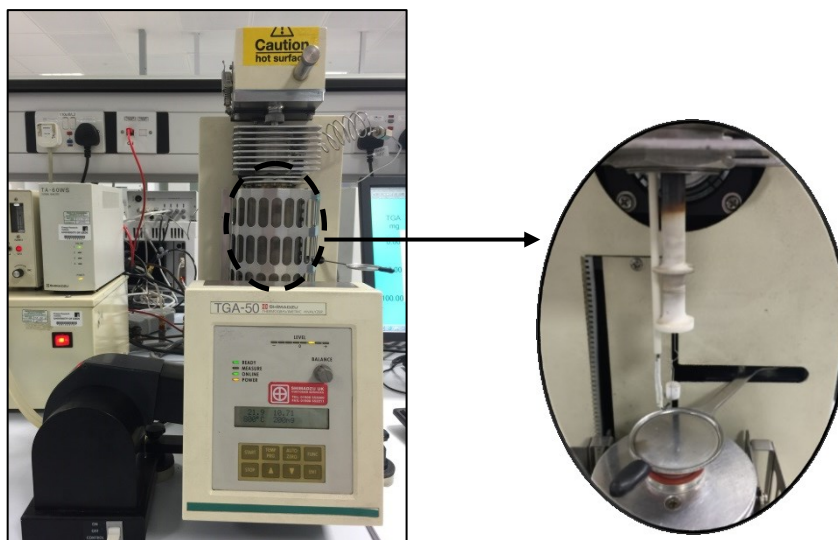


Figure 3.12 Photograph of TGA-50 Shimadzu analyser

3.4.3 Calculation and analysis of product yields

The product distributions from the thermal treatment of waste plastics are namely gas, liquid, char and carbon deposition. The gas yields are collected gaseous product in the gas sample bag, including unreacted CO₂ gases. Each gas composition was measured by the gas chromatography analyser (GC). Detailed explanation on the gas yield calculation will be discussed in Section 3.4.3.2 below. The liquid yield is defined as the liquid collected in the three stage condenser system. Char is the pyrolysis residue remaining in the sample holder located in the 1st stage furnace after the experiment. Carbon deposition is the carbon deposited on the catalyst surface after the experiment. Liquid, char and carbon deposition were calculated by difference, weight of condensers, weight of sample holder and weight of reactor tube (together with catalyst) respectively; before and after the experiment. The product yield calculations can be expressed by the following formulas:

$$\text{Gas yield, } Y_G (\%) = \frac{W_{GA}}{W_S + W_R} \times 100$$

$$\text{Liquid yield, } Y_L (\%) = \frac{W_{CA} - W_{CB}}{W_S + W_R} \times 100$$

$$\text{Char yield } (\%), Y_C = \frac{W_{HA} - W_{HB}}{W_S + W_R} \times 100$$

$$\text{Carbon deposition yield, } Y_{CD} (\%) = \frac{W_{RTA} - W_{RTB}}{W_S + W_R} \times 100$$

$$\text{Mass balance } (\%) = Y_G + Y_L + Y_C + Y_{CD}$$

where W_G is weight of gas produced from the experiment, W_C is weight of the three-stage condenser system, W_H is the weight of sample holder and W_{RT} is the weight of reactor tube. The annotation *A* representing the measurement taken after the experiment while annotation *B* is the measurement taken before the experiment began. W_S is the weight of plastic samples and W_R is the weight of reformers used in

the system. Reformer used in the experiment were either steam, carbon dioxide or the combination of both. All measurements were in gram.

In this research, the carbon dioxide conversion (as percentage) was calculated according to the formula reported by several researchers; Albarazi et al., Asencios et al. and Oyama et al. [15-17]. The CO₂ conversion is used to monitor how much carbon dioxide was consumed during the experiment. The measurement was calculated by the difference of the weight of CO₂ gases injected to the reactor system and the weight after the experiment finished (measured by the GC analyser). Apart from that, carbon dioxide conversion in g_{CO₂} g⁻¹_{plastic} was also used.

$$XCO_2 (\%) = \frac{[molsCO_2]in - [molsCO_2]out}{[molsCO_2]in} \times 100$$

$$XCO_2 (g_{CO_2} g_{plastic}^{-1}) = \frac{[massCO_2]in - [massCO_2]out}{[mass plastic]in}$$

3.4.3.1 Gas chromatography (GC)

The gas chromatography (GC) analyser was used to analyse the gasses collected in the gas sample bag as shown in Figure 3.13. There were three different categories of analyser set up for the analysis. A Varian 3380 gas chromatography with a flame ionisation detector, 80-100 mesh HayeSep column and nitrogen carrier gas was used to analyse hydrocarbon (C₁-C₄). A Varian 3380 gas chromatography with two separate columns which were 2m long and 2mm diameter each were used to analyse the permanent gases (H₂, CO, O₂, N₂ and CO₂), both in argon carrier gas. Hydrogen, carbon monoxide, oxygen and nitrogen were analysed on a 60-80 mesh molecular sieve column while carbon dioxide was analysed on a HayeSep 80-100 mesh column.

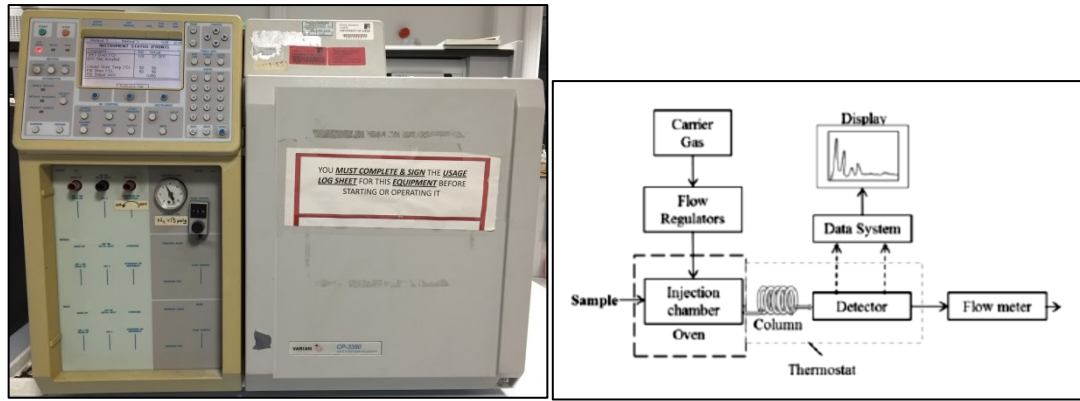


Figure 3.13 Photograph and principal schematic diagram of gas chromatography analyser

3.4.3.2 Gas concentration calculation

The gas concentration calculation is dependent on the standard permanent and hydrocarbon gases, both of which were obtained from Scientific & Technical Gases Ltd. A typical concentration of the standard permanent and hydrocarbon gases in the cylinder used for analysis are as listed in Table 3.12.

The concentration of each gas was used as the benchmark for the calculations was obtained from the injection of 1 ml standard gas from the standard permanent and hydrocarbon cylinder to each GC analyser. The GC analytical software then calculated the response peak area of each gas in which the values were equivalent to the concentration of the standard gases. The gases collected in the sample gas bag from the experiment were analysed in the same procedure as for the standard gases. 1 ml of gas from the sample gas bag was injected to each GC analyser. The GC peak area corresponds to the concentration of the standard gases. An example of the GC results obtained is shown in Table 3.13 and the injection was made several times in order to ensure the repeatability and accuracy of the data. The standard gases were also injected regularly to ensure the accuracy of the data and calculations made. From the data, it can be shown that the results are reproducible.

Table 3.12 Concentration of standard permanent and hydrocarbon gases

	Concentration (vol.%)
<u>Permanent gases</u>	
Carbon Monoxide (CO)	0.999
Carbon Dioxide (CO ₂)	0.992
Hydrogen (H ₂)	0.994
Oxygen (O ₂)	1.0
Nitrogen (N ₂)	96.015
<u>Alkane hydrocarbon gases</u>	
Methane (CH ₄)	0.998
Ethane (C ₂ H ₆)	1.010
Propane (C ₃ H ₈)	1.0
Butane (C ₄ H ₁₀)	1.0
<u>Alkene hydrocarbon gases</u>	
Ethene (C ₂ H ₄)	0.991
Propene (C ₃ H ₆)	0.985
Butene & Butadiene (C ₄ H ₈)	2.0

Table 3.13 Example of standard gases GC response peak area and repeatability

Gas	Peak area (injection 1)	Peak area (injection 2)
CO	0	0
H ₂	55234	52343
O ₂	0	0
N ₂	3400902	3383379
CO ₂	0	0
CH ₄	80135	78261
C ₂ H ₄	223122	217692
C ₂ H ₆	162258	158436
C ₃ H ₆	310876	303157
C ₃ H ₈	111608	109350
C ₄ H ₈	165345	184322
C ₄ H ₁₀	126407	138370

The concentration for each gas was obtained using Equation 3.14;

$$C_S = \frac{PA_S}{PA_r} \times C_r \quad \text{(Equation 3.14)}$$

where C_s is the sample gas concentration, PA_s is the peak area of the sample, PA_r is the peak area from the standard gas and C_r is the concentration value from the standard gas. The analysis of sample gases were repeated in the GC analysers and calculated to obtain the average values and thereby the gas concentration.

The mole value for each gas was then calculated using Equation 3.15 and Equation 3.16 based on the assumption that the nitrogen flow rate was constant throughout the experiment.

$$\mathbf{Total\ Volume} = \frac{100}{CN_2} \times \frac{N_2\ Flow\ Rate \times Gas\ Collection\ Time}{1000} \quad (\text{Equation 0.15})$$

$$\mathbf{Moles\ of\ Gas} = \frac{Percent\ of\ Gas}{100} \times \frac{Total\ Volume}{22.4} \quad (\text{Equation 0.26})$$

where the total volume of gases are in litres, CN_2 is the concentration value of nitrogen and gas collection time is in minutes. Another parameter used in the calculation was that one mole of gas occupies 22.4 litres at standard temperature and pressure.

The mass value of each gas in gram was determined based on the molecular weight and number of moles for each gas as shown in Equation 3.17.

$$\mathbf{Mass\ of\ Gas} = \mathbf{No.\ of\ Moles} \times \mathbf{Molecular\ Weight} \quad (\text{Equation 3.17})$$

The calculations were determined using a designed Microsoft Excel spread sheet to avoid any errors during the repetition as well as to maintain their consistency for each experimental result. An example of the gas calculations and their repeatability for each gas is shown in Table 3.14.

Table 3.14 Example of gas composition identification and repeatability

Gas	Gas data from standard curve:			Gas data from GC analysis:						
	Real con. (Vol%)	Peak Area	Rf	Sample 1	Con. (Vol%)	Sample 2	Con. (Vol%)	STDV	*RSTDV (%)	
CO	0.999	48877	48926	684332	13.99	686457	14.03	0.02	0.155	
H ₂	0.994	595080	598672	4513992	7.54	4518495	7.55	0	0.05	
O ₂	1	94350	94350	0	0	0	0	0	0	
N ₂	96.015	4654272	48474	3360939	69.33	3379563	69.72	0.19	0.276	
CO ₂	0.992	12075	12172	93588	7.69	94186	7.74	0.02	0.318	
CH ₄	0.998	736836	738313	564117	0.76	554374	0.75	0.01	0.871	
C ₂ H ₄	0.991	1401037	1413761	56478	0.04	55917	0.04	0	0.499	
C ₂ H ₆	1.01	1387131	1373397	82980	0.06	82047	0.06	0	0.565	
C ₃ H ₆	0.985	2025483	2056328	0	0	0	0	0	0	
C ₃ H ₈	1	2053669	2053669	5685	0	5649	0	0	0.318	
C ₄ H ₈	2	5210197	2605099	0	0	0	0	0	0	
C ₄ H ₁₀	1	2725382	2725382	0	0	0	0	0	0	
					99.42			99.89		

*RSTDV = Relative standard deviation

References

1. Clara Delgado, Leire Barruetabeña, Salas, O. and Wolf, O. Assessment of the Environmental Advantages and Drawbacks of Existing and Emerging Polymers Recovery Processes JRC37456. Brussels: European Joint Research Centre, 2007.
2. Garcia, L., Benedicto, A., Romeo, E., Salvador, M.L., Arauzo, J. and Bilbao, R. Hydrogen production by steam gasification of biomass using Ni-Al coprecipitated catalysts promoted with magnesium. *Energy & Fuels*. 2002, 16(5), pp.1222-1230.
3. Al-Fatesh, A. Suppression of carbon formation in CH₄-CO₂ reforming by addition of Sr into bimetallic Ni-Co/ γ -Al₂O₃ catalyst *Journal of King Saud University - Engineering Sciences*. 2015, 27(1), pp.101-107.
4. Ay, H. and Üner, D. Dry reforming of methane over CeO₂ supported Ni, Co and Ni-Co catalysts. *Applied Catalysis B: Environmental*. 2015, 179, pp.128-138.
5. Coats, A.W. and Redfern, J.P. Kinetic Parameters from Thermogravimetric Data. *Nature*. 1964, 201(4914), pp.68-69.
6. Singh, S., Wu, C. and Williams, P.T. Pyrolysis of waste materials using TGA-MS and TGA-FTIR as complementary characterisation techniques. *Journal of Analytical and Applied Pyrolysis*. 2012, 94(0), pp.99-107.
7. Oyedun, A.O., Tee, C.Z., Hanson, S. and Hui, C.W. Thermogravimetric analysis of the pyrolysis characteristics and kinetics of plastics and biomass blends. *Fuel Processing Technology*. 2014, 128, pp.471-481.
8. Chen, J., Fan, X., Jiang, B., Mu, L., Yao, P., Yin, H. and Song, X. Pyrolysis of oil-plant wastes in a TGA and a fixed-bed reactor: Thermochemical behaviors, kinetics, and products characterization. *Bioresource Technology*. 2015, 192, pp.592-602.
9. Arenales Rivera, J., Pérez López, V., Ramos Casado, R. and Sánchez Hervás, J.-M. Thermal degradation of paper industry wastes from a recovered paper mill using TGA. Characterization and gasification test. *Waste Management*. 2016, 47, Part B, pp.225-235.
10. Characterizing Porous Materials and Powders, NOVA-e Series Models 25 and 26, NovaWin/NovaWin-CFR, Gas Sorption System Operating Manual, Instruments, Q., Version 11.01-11.03 ed. [Exhibition catalogue]. 2008-2013.
11. Querini, C.A. and Fung, S.C. Temperature-programmed oxidation technique: kinetics of coke-O₂ reaction on supported metal catalysts. *Applied Catalysis A: General*. 1994, 117(1), pp.53-74.
12. Kauppi, E.I., Kaila, R.K., Linnekoski, J.A., Krause, A.O.I. and Veringa Niemelä, M.K. Temperature-programmed oxidation of coked noble metal

- catalysts after autothermal reforming of n-hexadecane. *International Journal of Hydrogen Energy*. 2010, 35(15), pp.7759-7767.
13. Querini, C.A. and Fung, S.C. Coke characterization by temperature programmed techniques. *Catalysis Today*. 1997, 37(3), pp.277-283.
 14. Sánchez, B., Gross, M.S., Costa, B.D. and Querini, C.A. Coke analysis by temperature-programmed oxidation: Morphology characterization. *Applied Catalysis A: General*. 2009, 364(1–2), pp.35-41.
 15. Albarazi, A., Beaunier, P. and Da Costa, P. Hydrogen and syngas production by methane dry reforming on SBA-15 supported nickel catalysts: On the effect of promotion by $\text{Ce}_{0.75}\text{Zr}_{0.25}\text{O}_2$ mixed oxide. *International Journal of Hydrogen Energy*. 2013, 38(1), pp.127-139.
 16. Asencios, Y.J.O. and Assaf, E.M. Combination of dry reforming and partial oxidation of methane on NiO–MgO–ZrO₂ catalyst: Effect of nickel content. *Fuel Processing Technology*. 2013, 106(0), pp.247-252.
 17. Oyama, S.T., Hacırlıoğlu, P., Gu, Y. and Lee, D. Dry reforming of methane has no future for hydrogen production: Comparison with steam reforming at high pressure in standard and membrane reactors. *International Journal of Hydrogen Energy*. 2012, 37(13), pp.10444-10450.

Chapter 4

THERMOGRAVIMETRIC ANALYSIS OF WASTE PLASTICS

Thermogravimetric analysis (TGA) was implemented to determine the thermal degradation characteristics of waste plastics as presented in Research Objective 1. The weight loss profile would give an indication of the degradation temperature of pyrolysis of the waste plastics in their subsequent investigation using the fixed bed reactor. The TGA was also able to identify the moisture content of each individual waste plastic. The moisture content can be calculated by difference of the mass of waste plastic from the temperature of 0 °C up to 100 °C [1]. However, in this study all samples have been dried prior to the analysis, hence no detectable moisture content in the TGA plots was detected on the waste materials between the temperature of 0 °C to 100 °C. In addition, a kinetic analysis was carried out mainly to determine the activation energy of the raw materials in relation to pyrolysis atmosphere. The activation energy is the energy required for the reaction to begin. Higher activation energy value means that larger amount of energy are required to initiate the reaction [2].

The chapter presents thermogravimetric analysis and kinetic-pyrolysis of each individual plastic normally found in the municipal waste treatment plant; high and low density polyethylene (HDPE and LDPE), polystyrene (PS), polypropylene (PP) and polyethylene terephthalate (PET) in two different sets of experiment. The first set of experiment was to investigate the effect of nitrogen or carbon dioxide as a carrier gas in the pyrolysis process; from ambient temperature up to 500 °C. The investigation continued with a set of experiments at higher temperature, from ambient temperature to 900 °C. This set of experiments was to investigate the effect of mixtures of nitrogen and carbon dioxide; between 100% N₂ and 70%/30% of N₂/CO₂ mixture (N₂/CO₂ ratio of 1:0 and 7:3) on the thermal degradation of the plastics. Mixed plastics from household packaging, building construction and agricultural waste treatment plant (MP_{HP}, MP_{BC} and MP_{AGR}) were also analysed in this set of experiments to investigate the thermal degradation characteristics of real-world waste plastics.

4.1 Influence of Nitrogen or Carbon Dioxide Atmosphere in Pyrolysis of Individual Component of Waste Plastics

4.1.1 Thermogravimetric characteristics

Figure 4.1 and Figure 4.2 show the weight loss profile and decomposition rate of five different individual plastics; high density and low density polyethylene (HDPE and LDPE), polypropylene (PP), polystyrene (PS) and polyethylene terephthalate (PET) with N₂ or CO₂ atmospheres using the TGA-50 Shimadzu analyser. The plastic samples were prepared as ~1 mm flake size and approximately 8-9 mg used in each experiment. The sample was heated to 500 °C at a heating rate of 10 °C min⁻¹, and then held at the final temperature for 30 mins. The nitrogen or carbon dioxide flow rate used was 50 ml min⁻¹. The TGA curves represent the weight loss while the dTG curves illustrate the rate of decomposition reaction and temperature of maximum decomposition. Both of the curves were plotted with respect to the temperature.

From the plotted graphs, the overall shapes of the weight loss and degradation graph profiles were similar for each type of plastic. It can be observed that there was only one degradation peak for each individual plastic, which started at temperatures higher than 300 °C. The pyrolysis degradation of polystyrene, polypropylene and polyethylene terephthalate in either N₂ or CO₂ atmospheres occurred with a gentler slope while the pyrolysis degradation of both low and high density polyethylene took place more rapidly. Ahmad et al. [3] suggested that, heating rate is an important parameter affecting the degradation of samples. They have reported that two degradation peaks were observed for the pyrolysis of polystyrene under N₂ atmosphere with a heating rate lower than 10 °C min⁻¹, and only one degradation peak temperature was found at higher heating rate. They have concluded that, there are certain limitations on the degradation of product, in which at some point, the product may not get sufficient time to condense with each other. The starting degradation temperature of pure polystyrene in their studies was observed between 300 °C and 400 °C. They have also cited other researchers which suggested that the degradation of polystyrene producing mainly styrene monomer, benzene, toluene, some dimers and trimers as volatile products and cross-linked residue above 400 °C.

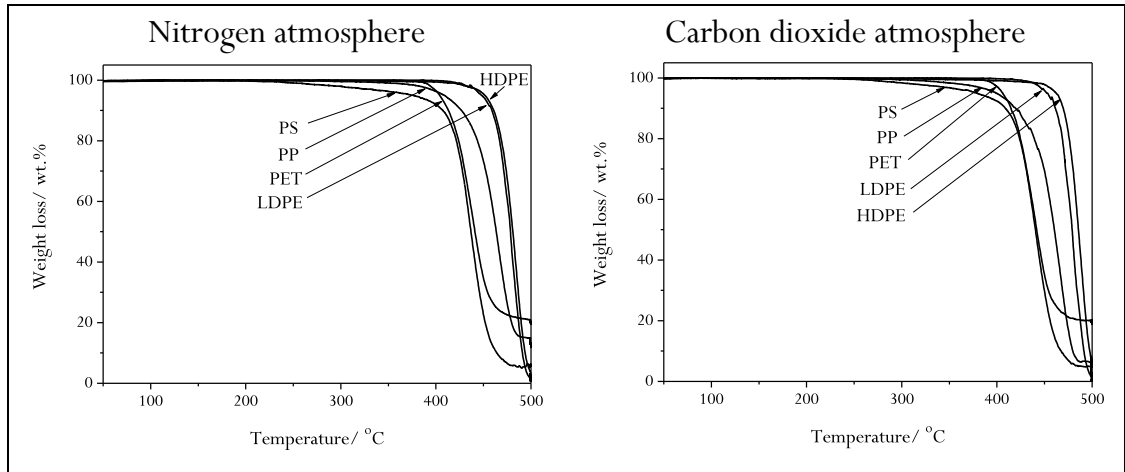


Figure 4.1 Weight loss profile of individual plastic over N₂ or CO₂ atmosphere

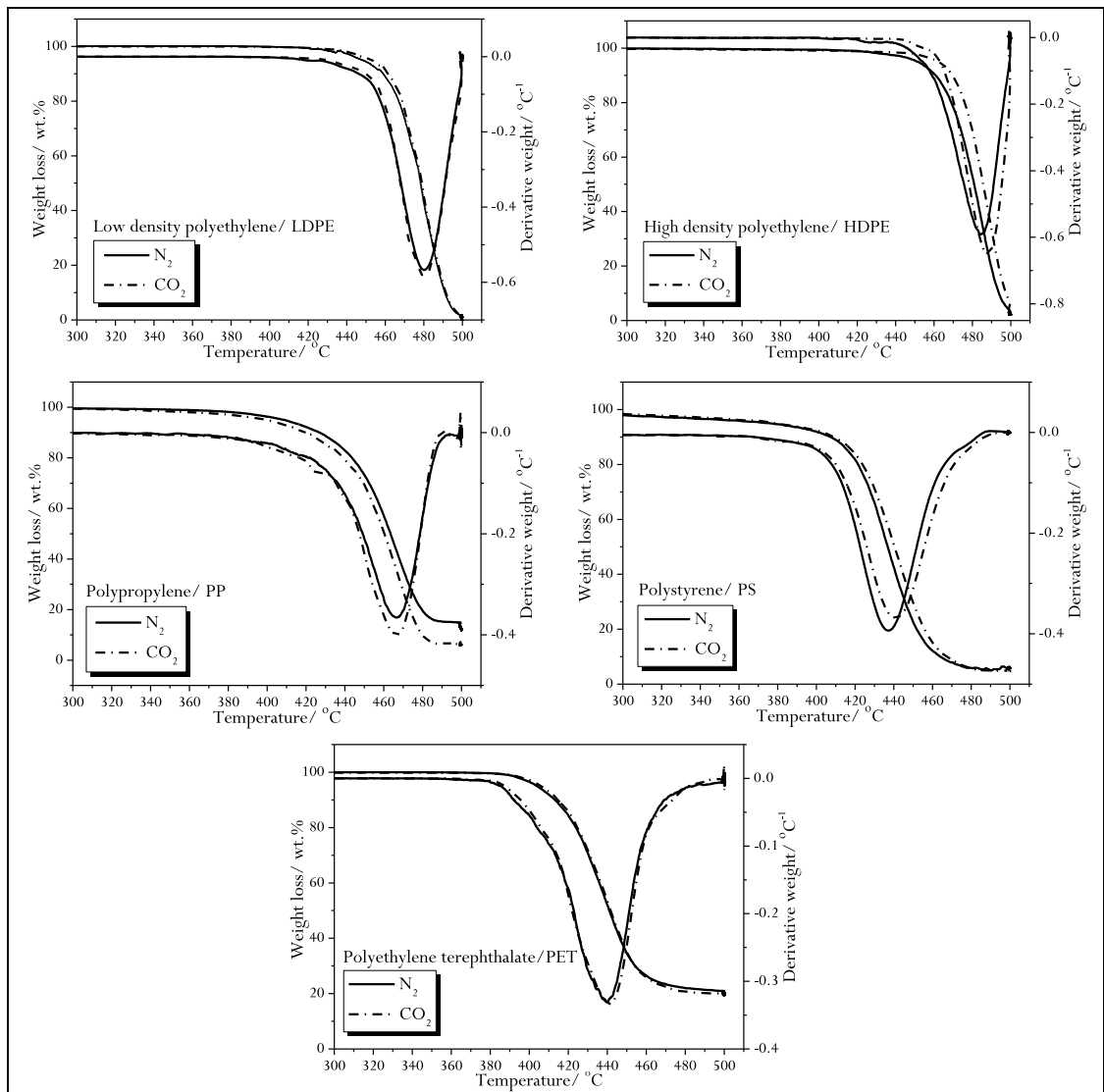


Figure 4.2 TGA and DTG plot of LDPE, HDPE, PP, PS and PET over N₂ or CO₂ atmosphere

The characteristics of the thermal decomposition of the plastic materials should be known in order to describe the possible reaction kinetics of pyrolysis. Characteristic data of each raw material is shown in Table 4.1. The initial temperature (T_i) is defined as the temperature where the plastic started to degrade, while the end temperature (T_f) represents the final degradation temperature. The peak temperature (T_m) is related to the chemical structure of the material. Although there were only small differences in the range of decomposition temperatures of the plastics in relation to either nitrogen or carbon dioxide purge gas, these differences were significant. Experiments using the TGA system were very reproducible, and any changes in decomposition temperature were attributed to the change in the TGA purge gas.

There is only a slight difference on the degradation temperature range (T_i - T_f) for both N_2 and CO_2 atmospheres for each plastics type. The decomposition of polypropylene, polystyrene and polyethylene terephthalate started at lower temperature in both N_2 and CO_2 atmospheres as compared to both low and high density polyethylene. The lowest initial degradation temperature was observed at polyethylene terephthalate in N_2 atmosphere while in CO_2 atmosphere, polystyrene started to degrade earlier than other plastics. The highest initial degradation temperature was observed at high density polyethylene in both atmospheres. According to Hujuri et al. [4] the linear polymers (high and low density polyethylene) decompose at higher temperatures in N_2 atmosphere than substituted/branched polymers such as polypropylene or polyethylene terephthalate. These show that polypropylene, polystyrene and polyethylene terephthalate were easily degraded into oil product. In comparison, high density polyethylene in CO_2 atmosphere required the highest temperature to start the degradation process. Albeit the decomposition temperature difference between each individual plastic was not substantial, it can be summarized that the degradation of plastics started earlier in N_2 atmosphere for high density polyethylene, polyethylene terephthalate and low density polyethylene while in CO_2 atmosphere, polypropylene and polystyrene started to decomposed a bit earlier than in N_2 atmosphere. The degradation of individual plastics reach their maximum peaks slightly higher in CO_2 atmosphere for high density polyethylene, polystyrene and polyethylene terephthalate. In contrast, the temperature at peak maximum was decreased slightly for low density polyethylene and was remained the same for polypropylene in CO_2 atmosphere compared to N_2 atmosphere. In summary, based on the degradation peak temperature, the decomposition rate of

each plastic was in the order of: PET<PS<PP<LDPE<HDPE in both N₂ and CO₂ atmospheres.

A study by Chen et al. [5] of pyrolysis and gasification of 8 different combustible solid wastes, including polystyrene (PS) and polyethylene (PE) summarized that degradation of both plastics reached their maximum peak value at 477 and 417 °C respectively in a N₂ atmosphere, while in a CO₂ atmosphere, the maximum degradation temperature decreased slightly to 473 and 413 °C respectively. They have also reported that the starting and finishing degradation temperature of polyethylene was higher than that in polystyrene similarly as reported in this study.

Table 4.1 Characteristic data of each individual plastic in N₂ and CO₂ atmospheres

Plastic samples	T _i (°C)		T _f (°C)		T _m (°C)	
	N ₂	CO ₂	N ₂	CO ₂	N ₂	CO ₂
HDPE	464	465	497	500	487	490
PP	441	435	483	481	466	466
PS	420	417	452	462	435	440
PET	414	418	456	453	436	441
LDPE	457	462	495	497	480	474

T_i=initial temperature, *T_f*=final temperature, *T_m*=temperature at peak maximum

Table 4.2 presents the residue obtained after the TGA experiments. It can be observed that the residue of each individual waste plastic was higher in the N₂ than in the CO₂ atmosphere. As discussed by Irfan [6] for coal pyrolysis-gasification in N₂/O₂/CO₂ atmospheres, these differences may be explained due to the density difference and transport properties of these two gases in which the mass of the CO₂ molecule is different from that of N₂. Overall, both low and high density polyethylene was nearly fully decomposed at 500 °C, hence producing a low mass of residue. In contrast, polyethylene terephthalate produced a high residue value as compared to other plastics in both N₂ and CO₂ atmospheres.

Table 4.2 Comparison table of residue left after the experiment between N₂ and CO₂ atmosphere

Atmosphere	Residue (wt.%)				
	LDPE	HDPE	PP	PS	PET
N ₂	1.25	2.16	11.91	5.91	19.66
CO ₂	<i>nd*</i>	1.86	5.89	4.78	18.97

**nd* = not detected

4.1.2 Kinetic parameters

The activation energies, overall rate constants and other kinetic reaction parameters of material degradation were obtained based on the weight loss decomposition curves from thermogravimetric analysis. In this study, the kinetic calculation was focused on a first order parallel reaction due to the fact that only one degradation peak was observed in all plastics as mentioned above. The kinetic analysis was based on the modified Coats-Redfern technique [7], as discussed in Chapter 3. The activation energy and the pre-exponential constant are determined from the logarithmic form of the Arrhenius equation:

$$\frac{d\alpha}{dt} = A e^{\left(\frac{-E}{RT}\right)} (1-\alpha) \quad (\text{Equation 4.1})$$

Where t is the time of pyrolysis, E is the activation energy degradation, A is the pre-exponential constant, T is temperature and α is the conversion or weight loss fraction. Table 4.3 summarizes the resultant activation energy, pre-exponential factor and correlation coefficient using the modified Coats-Redfern method for the purpose of comparison the results between N_2 and CO_2 atmospheres.

From the kinetics consideration, it was found that slightly higher activation energy was required for thermal decomposition of the plastics in a CO_2 atmosphere rather than a N_2 atmosphere for high and low density polyethylene and polyethylene terephthalate. In contrast, polystyrene and polypropylene showed marginally higher activation energy in the experiments with a N_2 atmosphere compared to a CO_2 atmosphere. Chen et al. [5] also observed a slight decrease in the activation energy of polystyrene under CO_2 atmosphere compared to N_2 atmosphere by using the discrete distributed activation energy method (DAEM) kinetic analysis. To further confirm the results, an experiment with polystyrene using a TGH-1000 TGA analyser has been carried out (result not shown here). Both of the analysers show that higher activation energy required for polystyrene in the N_2 atmosphere.

Table 4.3 Kinetic parameters of individual plastic sample from Arrhenius model; activation energy (E), pre-exponential factor (A) and correlation coefficients (R^2)

Sample type	Condition	Temperature (°C)	E (kJ mol ⁻¹)	A (min ⁻¹)	R ²
HDPE	N ₂	467-494	445.9	5.27x10 ³⁰	0.99
	CO ₂	468-497	472.1	2.40x10 ³³	0.99
LDPE	N ₂	460-492	446.7	7.61x10 ³⁰	0.99
	CO ₂	465-494	467.0	1.83x10 ³²	0.99
PP	N ₂	444-480	274.2	1.47x10 ¹⁹	0.99
	CO ₂	438-478	264.8	3.44x10 ¹⁸	0.99
PET	N ₂	417-453	273.2	5.84x10 ¹⁹	0.99
	CO ₂	421-450	281.2	2.20x10 ²⁰	0.99
PS	N ₂	423-449	283.4	3.47x10 ²⁰	0.99
	CO ₂	420-459	260.3	5.03x10 ¹⁸	0.99

Wang et al. [8] described in details on the morphological characteristic of polyethylene and polypropylene pyrolysis process in N₂ atmosphere. They have discovered that the decomposition process of polypropylene was started and completed earlier than polyethylene. This result is in agreement with results from our studies, which also observed from the activation energy value that polyethylene required more energy to initiate the reaction than polypropylene; 446 and 274 kJ mol⁻¹ respectively.

The relationship between activation energy and initial degradation temperature between N₂ and CO₂ atmosphere can be concluded as a lower initial degradation temperature of waste plastics resulted in lower activation energy and vice versa. The activation energy of each individual waste plastic increases in the following order LDPE>HDPE>PS>PP>PET in N₂ atmosphere and HDPE>LDPE>PET>PP>PS in CO₂ atmosphere.

Table 4.4 Summary of kinetic values using various analytical methods in N₂ atmosphere

Sample type	Method	Temp. / °C	Heating rate / °C min ⁻¹	N ₂ Flow rate/ ml min ⁻¹	E/ kJ mol ⁻¹	Others	Ref.
HDPE/ 15.5 mg	Coast- Redfern	590	20	50	263.4	A=5.36x10 ¹⁷ min ⁻¹	[9]
HDPE/ 13-14.3 mg	Horowitz -Metzger	600	10	50	329.1	NR	[10]
PP/ 13-14.3 mg					338.5	NR	
HDPE/ 22-25 mg	Dynamic	~577	20	50	337.6	n=0.98	[11]
LDPE/ 22-25 mg					196.4	n=0.64	
MSW Plastic/ 15-20 mg (mainly HDPE & PET)	Modified Coast- Redfern	410- 500	25	NR	277.9	r=0.990	[12]

NR, not reported

Table 4.4 shows the activation energy and other parameters obtained by other researchers. It can be concluded that, the calculated kinetic parameters depended on the mathematical approach of the analysis as well as the various parameters such as heating rate in the TGA experiments. For example, the activation energy of high density polyethylene compared between the Coats Redfern method [9] and Dynamic method [11] at a similar heating rate of 20 °C min⁻¹ was 263.4 and 337.6 kJ mol⁻¹ respectively. Kim and Oh [10] reported in detail on the activation energy of waste polypropylene, waste high density polyethylene and a waste blend obtained from different kinetic models. They suggested that the best method for their study was the Dynamic and Friedman method due to the capability to give the activation energies upon the conversion of waste at any time.

4.2 Influence of Nitrogen and Carbon Dioxide Mixture in Pyrolysis of Waste Plastics

This study was carried out using a different thermogravimetric analyser (STA449F3, NETZSCH) by the thesis author at the laboratory at Huazhong University of Science & Technology, China during a two month research secondment. The plastic samples were in powdered form, approximately 4-6 mg, and heated from room temperature to 900 °C at 10 °C min⁻¹, with 100 ml min⁻¹ total gas flow rate.

4.2.1 Thermogravimetric characteristics and kinetic analysis for high density polyethylene at different N₂/CO₂ ratio

4.2.1.1 Thermogravimetric characteristics

The weight loss and rate of degradation curves of high density polyethylene (HDPE) over five different N₂/CO₂ ratios; 1:0, 7:3, 1:1, 3:7 and 0:1 were carried out and the results are presented in Table 4.5 and Figure 4.3. A N₂/CO₂ ratio of 1:1 showed the highest initial degradation temperature and final degradation temperature, starting at 407 °C to 501 °C. Furthermore, only one peak temperature of plastic degradation was observed in all given ratios as shown in Figure 4.3, and the maximum peak degradation temperature was observed at N₂/CO₂ ratio of 3:7, 480 °C.

The mass decomposition curves for all N₂/CO₂ ratios showed a similar degradation rate, however, there were slight differences in terms of the residual mass. The addition of CO₂ increased the residual mass with the highest at the N₂/CO₂ ratio of 1:1 at 8.9 wt.%. This result was in disagreement with results reported by Lai et al. [13], which observed a decrease of residual mass with the increase in CO₂ addition for the thermal decomposition of municipal solid waste (MSW) due to the char gasification at high temperature. However, the mass loss percentage from the residue at 500 °C to 900 °C shown in Table 4.5 confirmed that char gasification was occurred since the residual mass was further reduced at high temperature. In the case of the study here, the non-stable residual mass losses in regards to the

increase of N₂/CO₂ ratios were may caused by the characterisation of HDPE decomposition may also affect the residual mass. The CO₂ may react with the surface of the plastics during the pyrolysis heat-up. A principal component analysis (PCA) of waste HDPE plastics reported by Aguado et al. [14] suggested a five lump kinetic scheme for thermal pyrolysis between 550 °C – 650 °C temperature range as follows:

- (i) waxes, C₁₁+; the primary products derived from raw polymer cracking
- (ii) gaseous products, C₁-C₄; the primary or secondary products depending on the reaction
- (iii) non-aromatic C₅-C₉ hydrocarbons; the primary or secondary products
- (iv) aromatic products; the secondary products
- (v) char; the tertiary product derived from polyaromatic products.

In addition, Al-Salem and Lettieri [15] summarized the activation energy of each primary lumped products from the thermal degradation of high density polyethylene as; 26.7, 44.1, 124.3, 98.9 and 282.0 kJ mol⁻¹ for waxes (> C₁₁), char, liquids (non-aromatics C₅-C₁₀), rich gases (C₁-C₄) and aromatics (single ring structures) respectively.

Based on the residual mass observation, the addition of more than 30% of carbon dioxide in the gas mixture may affect the thermal degradation process of high density polyethylene; hence high residual mass was obtained.

Table 4.5 Characteristic data of HDPE in different mixtures of N₂ and CO₂

N ₂ /CO ₂ ratio	T _i (°C)	T _f (°C)	T _m (°C)	Residue at 500 °C (wt.%)	Residue at 900 °C (wt.%)	Weight loss at 900 °C (wt.%)
1:0	397	500	475	5.5	4.4	95.6
7:3	393	500	475	4.9	4.2	95.8
1:1	407	501	476	9.6	8.9	91.1
3:7	402	499	480	7.7	6.8	93.2
0:1	402	495	476	7.6	7.2	92.8

T_i=initial temperature, *T_f*=final temperature, *T_m*=temperature at peak maximum

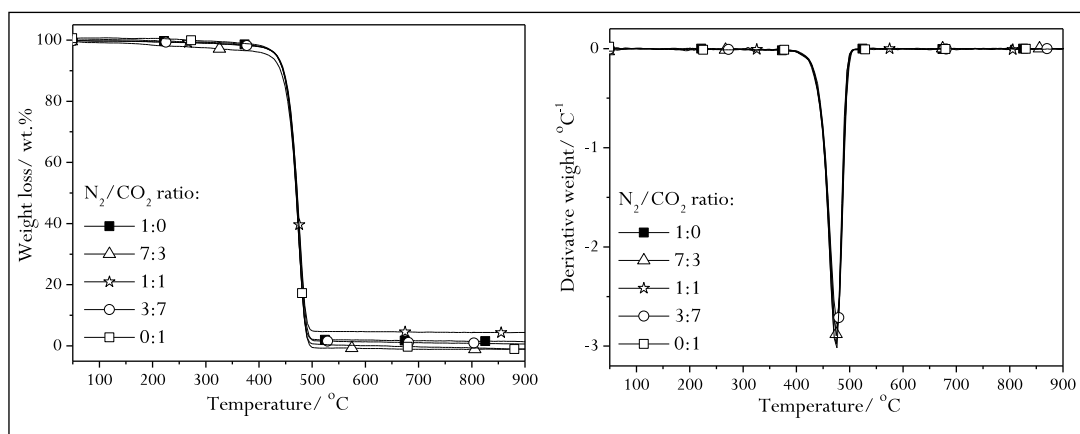


Figure 4.3 TGA and DTG thermographs of HDPE in different N₂/CO₂ ratio; 100% N₂ (1:0), 70% N₂/30% CO₂ (7:3), 50% N₂/50% CO₂ (1:1), 30%N₂/70% CO₂ (3:7) and 100% CO₂ (0:1)

4.2.1.2 Kinetic parameters

Figure 4.4 and Table 4.6 show the kinetic parameters of the thermal degradation of high density polyethylene in five different N₂/CO₂ ratios; 100% N₂ (1:0), 70% N₂/30% CO₂ (7:3), 50% N₂/50% CO₂ (1:1), 30%N₂/70% CO₂ (3:7) and 100% CO₂ (0:1). The data show that the values of activation energy have increased with the increase of N₂/CO₂ ratio, from 317.5 kJ mol⁻¹ at 100% N₂ to 345.9 kJ mol⁻¹ at 100% CO₂.

It can be noted that the addition of carbon dioxide does not produce a significant impact on the degradation peak temperature. Based on the comparison obtained the analysis for HDPE, two different ratios of N₂/CO₂ were chosen for the following study; 1:0 and 7:3 due to its lowest residual mass and lowest activation energy range.

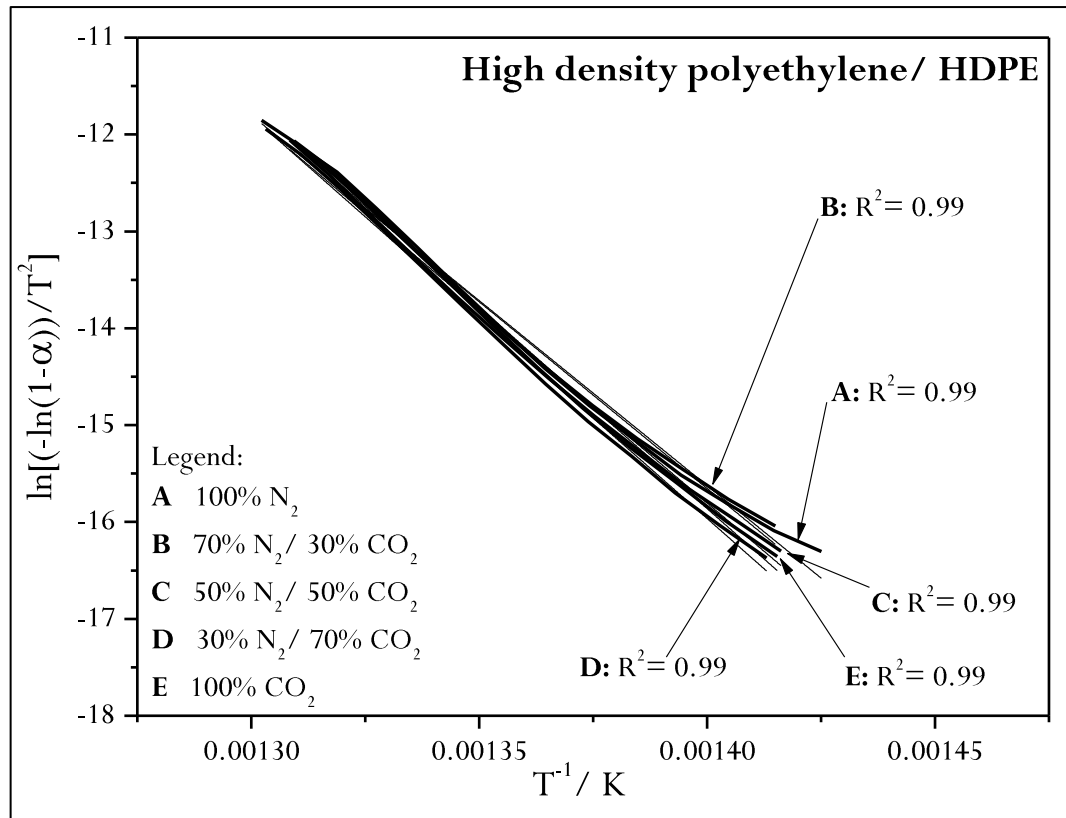


Figure 4.4 Plot of $\ln[(-\ln(1-\alpha))/T^2]$ versus $1/T$ of HDPE in different N₂/CO₂ ratio; 100% N₂ (1:0), 70% N₂/30% CO₂ (7:3), 50% N₂/50% CO₂ (1:1), 30%N₂/70% CO₂ (3:7) and 100% CO₂ (0:1)

Table 4.6 Kinetic parameters of high density polyethylene at different N₂/CO₂ ratios from Arrhenius model; activation energy (E), pre-exponential factor (A) and correlation coefficients (R²)

N ₂ /CO ₂ ratio	Temperature (°C)	E (kJ mol ⁻¹)	A (min ⁻¹)	R ²
1:0	429 – 490	317.5	1.03 x 10 ²²	0.99
7:3	434 – 495	320.4	1.66 x 10 ²²	0.99
1:1	433 – 491	331.5	9.48 x 10 ²²	0.99
3:7	435 – 494	345.2	8.53 x 10 ²³	0.99
0:1	433 – 491	345.9	1.06 x 10 ²⁴	0.99

4.2.2 Thermogravimetric characteristics and kinetic analysis for individual plastics and mixed plastics at N₂/CO₂ ratio of 1:0 and 7:3

4.2.2.1 Thermogravimetric characteristics

The TGA and DTG thermographs of each individual plastic in N₂/CO₂ ratio of 1:0 and 7:3 are shown in Figure 4.5 and the characteristic data of each raw material in both conditions is shown in Table 4.7. In general, the degradation peak of each plastic was higher in the experiments with mixture of N₂ and CO₂ compare to only N₂. The highest increment of degradation peak temperature from the experiment with only N₂ compared to a mixture of N₂ and CO₂ was observed for polyethylene terephthalate with an increase of 1.15%, followed by polystyrene, polypropylene, low density polyethylene and high density polyethylene. The decomposition rate in both conditions showing a degradation peak temperature trend of PS>PET>PP>LDPE>HDPE. Although the experimental temperature was increased to 900 °C, no significant further decomposition of plastics would occur after a temperature of 500 °C.

Table 4.7 Characteristic data of raw materials in N₂/CO₂ ratio of 1:0 and 7:3

Plastic samples	T _i (°C)		T _f (°C)		T _m (°C)		Residue at 900 °C (wt.%)		Weight loss (wt.%)	
	1:0	7:3	1:0	7:3	1:0	7:3	1:0	7:3	1:0	7:3
HDPE	397	393	500	500	475	475	4.4	4.2	95.6	95.8
PP	349	340	488	480	458	460	9.7	6.9	90.3	93.1
PS	273	275	492	479	426	429	7.9	7.3	92.1	92.7
PET	369	367	579	509	436	441	14.7	15.9	85.3	84.1
LDPE	359	378	500	500	480	480	2.2	3.2	97.8	96.8
MP _{HP}	274	263	497	509	479	489	4.8	5.0	95.2	95.0
MP _{BC}	340	330	489	499	469	470	7.3	7.2	92.7	92.8
MP _{AGR}	298	286	499	501	480	481	5.0	3.8	95.0	96.2

T_i=initial temperature, *T_f*=final temperature, *T_m*=temperature at peak maximum

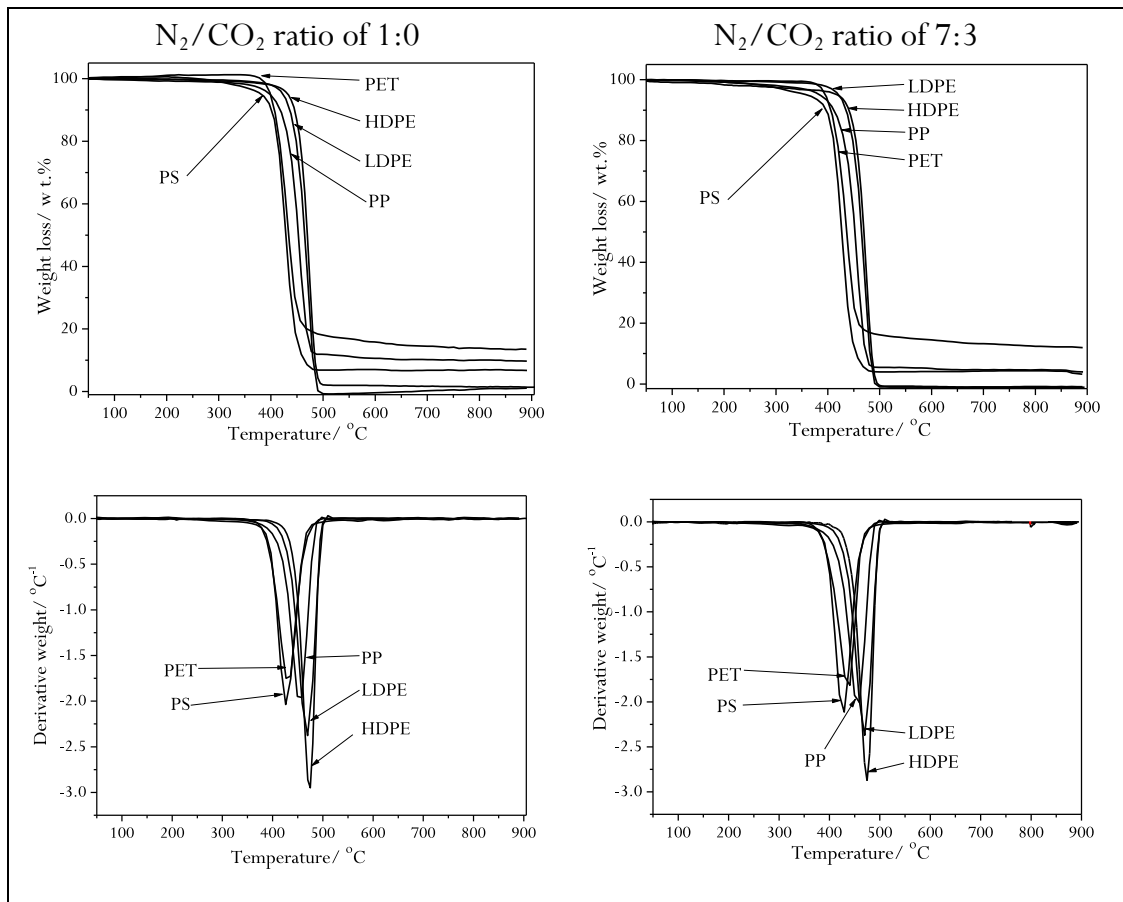


Figure 4.5 TGA weight loss thermographs of each individual plastic in N_2/CO_2 ratio of 1:0 and 7:3

Figure 4.6 presents the weight loss curves and thermal degradation temperature peaks of mixed plastics collected from three different waste treatment plants; household packaging (MP_{HP}), building construction (MP_{BC}) and agricultural (MP_{AGR}) in N_2/CO_2 ratios of 1:0 and 7:3. Only one decomposition peak was observed for each plastic. The weight loss peak of these three different mixed plastics appeared to be more or less in the same temperature range in both conditions. The highest degradation peak temperature in both conditions was obtained from mixed plastic obtained from agricultural waste treatment plant (MP_{AGR}); 479.75 °C and 480.62 °C in N_2/CO_2 ratio of 1:0 and 7:3 respectively. Between both conditions, the degradation peak temperature remain the same for MP_{HP} , but increased for MP_{BC} and MP_{AGR} with 100% N_2 compare to 70% $N_2/30\%$ CO_2 ratio. MP_{BC} showing the highest increment of degradation peak temperature with an increase of 0.25%. From the degradation data for each individual plastic and mixed plastics, it is recommended that the mixed plastics contains mostly HDPE and LDPE. MP_{HP} and MP_{AGR} may as well contain PS since they both started to degrade a bit earlier in both conditions.

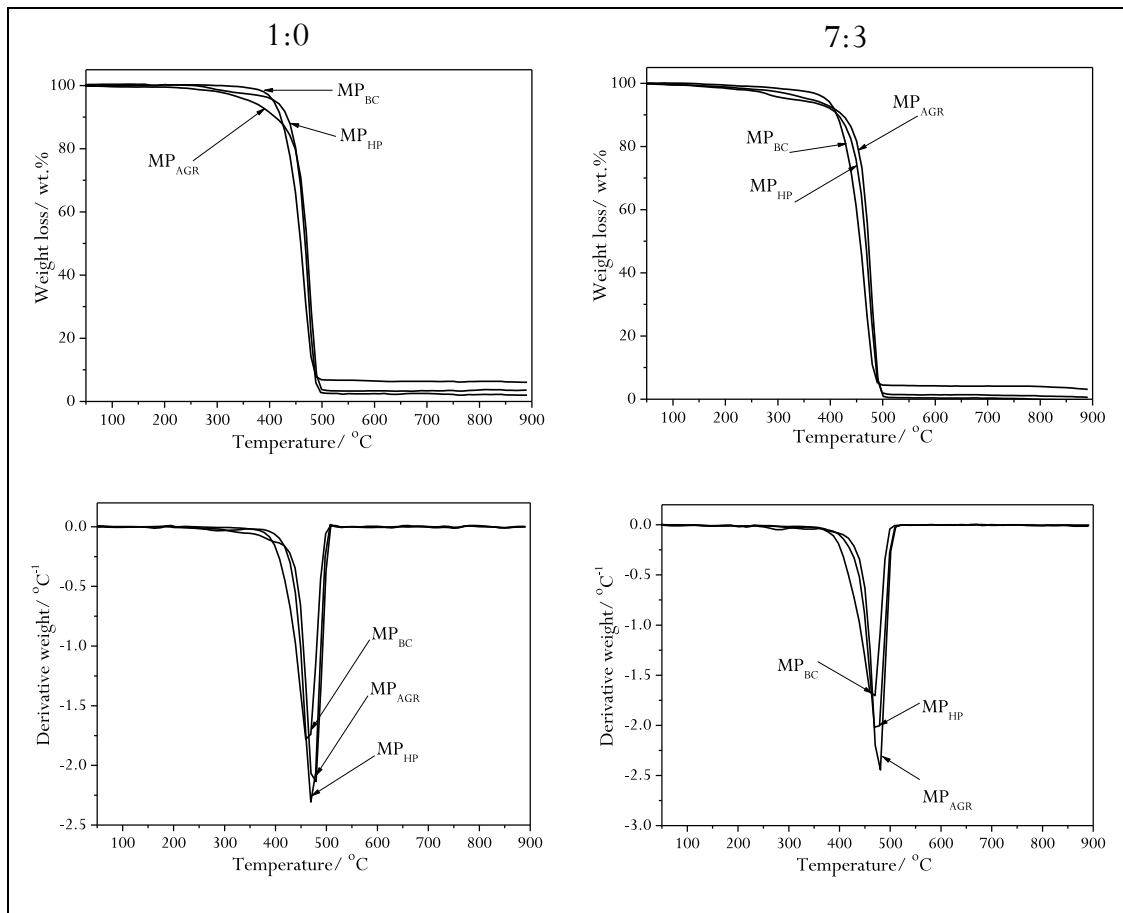


Figure 4.6 TGA and DTG thermographs of mixed plastics from different waste treatment plants in N_2/CO_2 ratio of 1:0 and 7:3

4.2.2.2 Kinetic analysis

The kinetic parameters of each individual plastics and mixed plastics are shown in Table 4.8 and Figure 4.7. In accordance with the aforementioned TGA and DTG thermograph of each individual plastics and mixed plastics, thermal decomposition of all samples could be simulated in a first order parallel reaction. The correlation coefficients of each sample were greater than 0.9 supporting the credibility of the kinetic model.

The results indicated that there were slight influences on the activation energy value of each individual plastic and mixed plastics. The values were decreased in almost all samples at the N_2/CO_2 ratio of 7:3 compared to 1:0 except for high density polyethylene, polystyrene and polyethylene terephthalate which showed very small increments in the activation energy. High density polyethylene required more energy to activate the reaction in both conditions compared to other samples,

317.5 kJ mol⁻¹ at N₂/CO₂ ratio of 1:0 and 320.4 kJ mol⁻¹ at N₂/CO₂ ratio of 7:3. In contrast, polystyrene showed the lowest activation energy at N₂/CO₂ ratio of 1:0 with 203.1 kJ mol⁻¹ while at N₂/CO₂ ratio of 7:3, the lowest activation energy was observed in polypropylene. It should also be noted that the activation energy of mixed plastics, MP_{HP}, MP_{AGR} and MP_{BC} are in between the range of the individual plastics. The variation of mixed plastics composition and characteristic was due to the different thermal stability of each individual plastic in the mixture sample [4]. Silvarrey and Phan [16] also suggested that the Ea and A value of mixed plastics varied depending on the nature of the feedstock, pointing the complexity of mixed plastics pyrolysis.

Table 4.8 Kinetic parameters of individual plastics and mixed plastics at N₂/CO₂ ratio of 1:0 and 7:3 from Arrhenius model; activation energy (E), pre-exponential factor (A) and correlation coefficients (R²)

Sample	N ₂ /CO ₂ ratio	Temperature (°C)	E (kJ mol ⁻¹)	A (min ⁻¹)	R ²
HDPE	1:0	429 – 490	317.5	1.03 x 10 ²²	0.99
	7:3	434 – 495	320.4	1.66 x 10 ²²	0.99
PP	1:0	410 – 468	228.3	1.17 x 10 ¹⁶	0.98
	7:3	408 – 470	155.7	5.38 x 10 ¹⁰	0.94
PS	1:0	397 – 469	203.1	3.99 x 10 ¹⁴	0.97
	7:3	401 – 468	207.1	8.28 x 10 ¹⁴	0.96
PET	1:0	398 – 467	210.2	1.13 x 10 ¹⁶	0.96
	7:3	398 – 460	234.3	7.25 x 10 ¹⁶	0.99
LDPE	1:0	429 – 490	293.4	2.88 x 10 ²⁰	0.99
	7:3	428 – 490	287.9	1.05 x 10 ²⁰	0.99
MP _{HP}	1:0	429 – 488	248.4	1.37 x 10 ¹⁷	0.98
	7:3	418 – 499	200.1	4.43 x 10 ¹³	0.97
MP _{AGR}	1:0	438 – 499	236.6	1.75 x 10 ¹⁶	0.97
	7:3	429 – 491	224.4	1.88 x 10 ¹⁵	0.95
MP _{BC}	1:0	408 – 479	207.4	2.28 x 10 ¹⁴	0.99
	7:3	408 – 480	189.3	1.13 x 10 ¹³	0.99

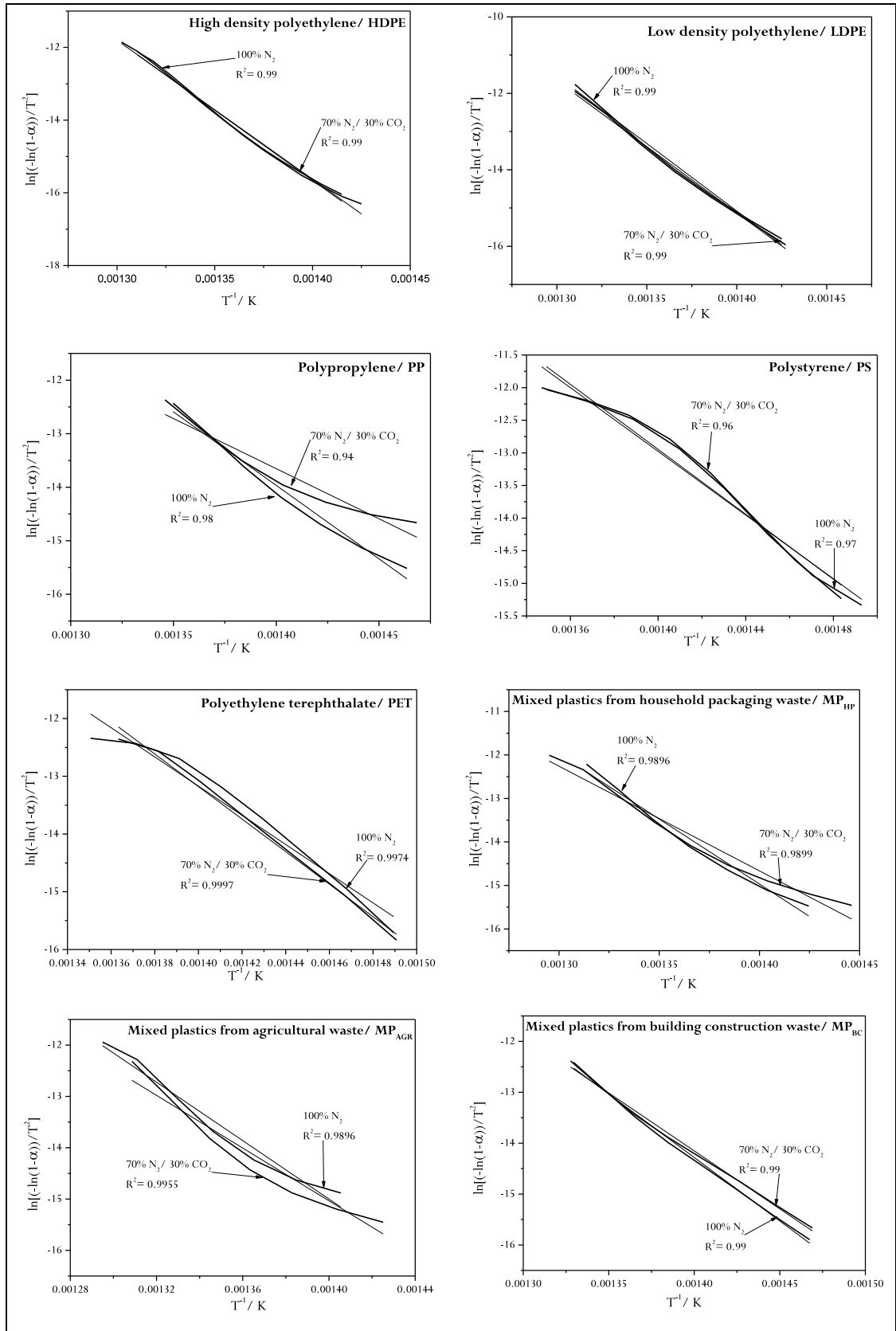


Figure 4.7 Plot of $\ln[(-\ln(1-\alpha))/T^2]$ versus $1/T$ of individual plastics and mixed plastics at N₂/CO₂ ratio of 1:0 and 7:3

Several other studies on the pyrolysis of waste plastics have also been reported in the literature. The activation energy of pyrolysis of polypropylene (PP) at a temperature range between 650 and 800 °C was reported as 264 kJ mol⁻¹ with an exponential factor of 1.1 x 10¹⁵ [17]. The activation energy value of 120.96 kJ mol⁻¹ was reported by Ahmed and Gupta [18] obtained by the Coats and Redfern method from pyrolysis of polystyrene at a heating rate of 10 °C min⁻¹.

4.3 Comparison of Analysis Data from Different Experimental Systems

In this chapter, the kinetic parameters and plastic degradation characteristics have been studied in different experimental setups, one at the laboratory at University of Leeds and another at the laboratory at Huazhong University of Science and Technology, China. Even though similar samples were used in both laboratories by the same operator (thesis author) and similar kinetic models were applied for both sets of data, there were slight differences observed for the kinetic parameters and thermal degradation characteristics, for example in the activation energy values obtained from the kinetic models.

Table 4.9 Comparison table of thermal degradation data of each individual plastic under N₂ atmosphere obtained from different experimental setup

Plastic Sample	Ea/ kJ mol ⁻¹		Residue at 900 °C	
	Lab. 1	Lab. 2	Lab. 1	Lab. 2
HDPE	445.9	317.5	2.2	4.0
PP	274.2	228.3	11.9	9.7
PS	283.4	203.1	5.9	7.9
PET	273.2	210.2	19.7	14.7
LDPE	446.7	293.4	1.3	2.2

Lab.1 at University of Leeds, UK; Lab.2 at Huazhong University of Science and Technology, China

As shown in Table 4.9, the value of activation energy and the residual mass for each sample were different. It should be noted that the experimental setup was similar in both laboratory systems except for the sample mass, 8-9 mg versus 4-6 mg, the sample particle size ~1 mm flake versus powdered and the nitrogen flow rate; 50 ml min⁻¹ versus 100 ml min⁻¹ at the Leeds laboratory and China laboratory respectively. For residual mass of each plastics, it seems that the range of

increments are similar in both laboratories even the values were different; LDPE < HDPE < PS < PP < PET.

This variation was probably due to the above-mentioned differences in the experimental parameters as well as differences in measurement systems such as thermocouple setup and type of instrument [13, 15]. Niksiar et al. also reported that different particle sizes of polyethylene terephthalate in the thermal degradation process gave a very small effect on the activation energy [19]. For the pyrolysis of waste, Singh et al. obtained an activation energy of municipal solid waste plastic (MSWP) at 294.8 kJ mol⁻¹ using a TGA-MS analyser and 277.9 kJ mol⁻¹ using a TGA-FTIR analyser [12].

4.4 Summary

The thermal degradation characteristics and kinetic parameters of individual plastics and mixed plastics from three different waste treatment plants were investigated under N₂, CO₂ and N₂/CO₂ atmospheres in two different thermogravimetric analysers. In all atmospheres, only one degradation peak temperature was observed between 250-510 °C depending on the sample type. The replacement of N₂ by CO₂ showed different effects on the activation energy, which was also influenced by the plastic type. Mixtures of N₂/CO₂ in the pyrolysis atmosphere resulted in lower activation energy for all plastic samples, with the exception of high density polyethylene, polystyrene and polyethylene terephthalate. The lower activation energy suggested that lower energy was required for the degradation process. However, a mixture of more than 30% carbon dioxide may influence the degradation process of plastics due to a higher value of residue obtained after the experiment.

References

1. Schuhmann, R. Metallurgical Engineering Vol. 1 : Engineering Principles. Addison-Wesley Longman, Incorporated, 1952.
2. Carey, F.A. Organic Chemistry. Sixth Edition ed. New York, London: McGraw-Hill, 2005.
3. Ahmad, Z., Al-Sagheer, F. and Al-Awadi, N.A. Pyro-GC/MS and thermal degradation studies in polystyrene–poly(vinyl chloride) blends. *Journal of Analytical and Applied Pyrolysis*. 2010, 87(1), pp.99-107.
4. Hujuri, U., Ghoshal, A.K. and Gumma, S. Modeling pyrolysis kinetics of plastic mixtures. *Polymer degradation and stability*. 2008, 93(10), pp.1832-1837.
5. Chen, S., Meng, A., Long, Y., Zhou, H., Li, Q. and Zhang, Y. TGA pyrolysis and gasification of combustible municipal solid waste. *Journal of the Energy Institute*. 2015, 88(3), pp.332-343.
6. F.Irfan, M. Pulverized Coal Pyrolysis & Gasification in N₂/O₂/CO₂ Mixtures by Thermo-gravimetric Analysis. G-COE Program Kyushu University, NCRS Newsletter. 2010, 2, pp.27-33.
7. Coats, A.W. and Redfern, J.P. Kinetic Parameters from Thermogravimetric Data. *Nature*. 1964, 201(4914), pp.68-69.
8. Wang, H., Chen, D., Yuan, G., Ma, X. and Dai, X. Morphological characteristics of waste polyethylene/polypropylene plastics during pyrolysis and representative morphological signal characterizing pyrolysis stages. *Waste Management*. 2013, 33(2), pp.327-339.
9. Khaghanikavkani, E. and Farid, M.M. Thermal Pyrolysis of Polyethylene: Kinetic Study. *Energy Science and Technology*. 2011, 2(1), pp.1-10.
10. Kim, H.T. and Oh, S.C. Kinetics of Thermal Degradation of Waste Polypropylene and High-Density Polyethylene. *J. Ind. Eng. Chem.* 2005, 11(5), pp.648-656.
11. Woo Park, J., Cheon Oh, S., Pyeong Lee, H., Taik Kim, H. and Ok Yoo, K. A kinetic analysis of thermal degradation of polymers using a dynamic method. *Polymer degradation and stability*. 2000, 67(3), pp.535-540.

12. Singh, S., Wu, C. and Williams, P.T. Pyrolysis of waste materials using TGA-MS and TGA-FTIR as complementary characterisation techniques. *Journal of Analytical and Applied Pyrolysis*. 2012, 94(0), pp.99-107.
13. Lai, Z., Ma, X., Tang, Y. and Lin, H. Thermogravimetric analysis of the thermal decomposition of MSW in N₂, CO₂ and CO₂/N₂ atmospheres. *Fuel Processing Technology*. 2012, 102, pp.18-23.
14. Aguado, R., Elordi, G., Arrizabalaga, A., Artetxe, M., Bilbao, J. and Olazar, M. Principal component analysis for kinetic scheme proposal in the thermal pyrolysis of waste HDPE plastics. *Chemical Engineering Journal*. 2014, 254, pp.357-364.
15. Al-Salem, S.M. and Lettieri, P. Kinetic study of high density polyethylene (HDPE) pyrolysis. *Chemical Engineering Research and Design*. 2010, 88(12), pp.1599-1606.
16. Diaz Silvarrey, L.S. and Phan, A.N. Kinetic study of municipal plastic waste. *International Journal of Hydrogen Energy*.
17. Westerhout, R.W.J., Kuipers, J.A.M. and van Swaaij, W.P.M. Experimental Determination of the Yield of Pyrolysis Products of Polyethene and Polypropene. Influence of Reaction Conditions. *Industrial & Engineering Chemistry Research*. 1998, 37(3), pp.841-847.
18. Ahmed, I.I. and Gupta, A.K. Hydrogen production from polystyrene pyrolysis and gasification: Characteristics and kinetics. *International Journal of Hydrogen Energy*. 2009, 34(15), pp.6253-6264.
19. Niksiar, A., Faramarzi, A.H. and Sohrabi, M. Kinetic study of polyethylene terephthalate (PET) pyrolysis in a spouted bed reactor. *Journal of Analytical and Applied Pyrolysis*. 2015, 113, pp.419-425.

Chapter 5

THERMAL PROCESSING OF WASTE HIGH DENSITY POLYETHYLENE FOR SYNGAS PRODUCTION: INFLUENCE OF PROCESS CONDITION AND VARIOUS NICKEL-BASED CATALYSTS

In this chapter, the influence of process conditions on the yield of syngas, i.e. hydrogen and carbon monoxide from waste high density polyethylene has been investigated as presented in Research Objective 2 and 3. The objective of this chapter is to identify the influence of two type of fixed bed reactor toward the concentration of hydrogen and carbon monoxide in syngas; one-stage which involve the pyrolysis of sample at specific temperature and two-stage where the gasification stage was introduced into the process to gasify the pyrolyzed product. In addition the use of Ni-based catalyst is also proposed in the two-stage fixed bed reactor to improve the production of syngas.

Based on the thermogravimetric analysis discussed in previous chapter, only one degradation peak was observed between 250 - 510 °C depending on the sample type in all atmospheres. Therefore, the pyrolysis temperature of 500 °C was chosen for this set of experiment. The yield of syngas from pyrolysis in nitrogen and carbon dioxide are compared, followed by comparison with two-stage pyrolysis-gasification/reforming. Further investigations on syngas production from carbon dioxide reforming of high-density polyethylene using the two-stage reactor with the addition of steam were also carried out.

The study continued with the investigation on the effect of the addition of different metal promoters in the form of cobalt, magnesium and copper into nickel-alumina based catalysts in relation to the production of product syngas from the carbon dioxide reforming of waste high density polyethylene in a two-stage fixed bed reactor. Carbon dioxide conversion and carbon formation on the catalysts was also investigated. Further investigation into the relation of the different molar ratios of Ni:Co:Al on syngas quality has also been conducted.

5.1 Influence of Nitrogen or Carbon Dioxide Atmosphere in Pyrolysis of Waste Plastics using a Fixed Bed Reactor

The difference in nitrogen and carbon dioxide composition plays a significant role in the pyrolysis of waste plastic [1]. In pyrolysis or gasification processes, nitrogen usually acts as a carrier gas for the pyrolysis products in which non-detectable reactions occur between the nitrogen and the product gases. However in the case of carbon dioxide, there may be some reactions which occur between carbon dioxide and the product gases during the pyrolysis or gasification process. These arguments are in agreement with many researchers [2-6].

In this section, a one-stage fixed bed reactor was used. The reactor was 250 mm in length by 30 mm internal diameter and was externally heated by an electrical tube furnace (1.2 kW) as described in Chapter 3. 2 g of plastics sample was placed in the sample crucible boat. The pyrolysis temperature was increased from ambient to 500 °C at a heating rate of 10 °C min⁻¹ and maintained at 500 °C for 30 min. Nitrogen or carbon dioxide was used as the carrier gas with a flow rate of 200 ml min⁻¹. 200 ml min⁻¹ of CO₂ flow rate was chosen in this study to make comparison between 200 ml min⁻¹ of N₂. The flow rate of 200 ml min⁻¹ of CO₂ was equivalent to 23.6 g h⁻¹.

The mass balance results for the thermal degradation of each plastic sample in the pyrolysis reactor are shown in Table 5.1. For pyrolysis under a nitrogen atmosphere, the data demonstrates that polystyrene has the lowest gas yield (1.2 wt.%) and produces high yield of liquid; which mainly consists of oil and wax (91.0 wt.%) due to its aromatic structure. Apart from that, pyrolysis of polystyrene produces a significant amount of char (4.3 wt.%) compared to low and high-density polyethylene. These results are confirmed by those of others [7] where mainly viscous dark-coloured oil which consisted almost entirely of aromatic compounds from pyrolysis of polystyrene was reported. Using a temperature of 500 °C and a batch pressurized autoclave reactor, the amount of char produced was about twice the amount of char obtained from the low-density polyethylene. It was concluded that this represented the role of aromatic compounds in char formation via condensation of the aromatic ring structure.

In contrast, polyethylene terephthalate shows a high production of gas (27.1 wt.%) but is low in liquid yield (50 wt.%). It also produces the highest amount of char (23 wt.%) compared to the other plastics. Cabaellero et al. [8] suggested that the formation of PET char was caused by the doubly substituted aromatic nucleus of the PET structure and by the presence of the =O of the ester groups of the polymer. This suggestion was further strengthened by the research of Krevelen and Nijenhuis [9] which confirmed that the char is formed in the decomposition of certain polymers and depends on the capability of the chemical structure of the polymer to react with hydrogen atoms of the polymeric structure, such as –OH and =O.

Pyrolysis of waste plastics under the carbon dioxide atmosphere shows the highest gas concentration and char yields for polypropylene at, 9.92 wt.% and 10.5 wt.% respectively. The highest liquid yield was observed for low density polyethylene at 95.3 wt.%. Polystyrene, polypropylene and low density polyethylene showed the lowest yields of gas, liquid and char, at 9.92 wt.%, 82.5 wt.% and 0.5 wt.% respectively. However, in this chapter, the study has mainly focused on low density polyethylene, polystyrene, polypropylene and high density polyethylene.

In terms of the gas composition at 500 °C, it can be observed that there was no carbon monoxide and carbon dioxide detected on the pyrolysis of waste plastics (LDPE, HDPE, PP and PS) in both atmospheres since the carbon dioxide produced from the experiment was the same amount with the carbon dioxide introduced to the system. The carbon monoxide and carbon dioxide produced in nitrogen atmosphere for polypropylene and polystyrene feedstocks are also negligible since the values are very low. However, the methane and other C₂-C₄ hydrocarbons concentrations in carbon dioxide atmosphere showed an increase in amount as compared to nitrogen atmosphere as shown in Figure 5.1 except for C₂-C₄ hydrocarbons for high density polyethylene.

The hydrogen production in mmol per gram of sample was in the order of: LDPE>PP>HDPE>PS in nitrogen atmosphere and LDPE>HDPE>PP>PS in carbon dioxide atmosphere. In both atmospheres, it was shown that the highest hydrogen production was for low density polyethylene and the lowest hydrogen production was for polystyrene. Generally, it is believed that pyrolysis of waste plastic produced more hydrogen in the nitrogen atmosphere compared to the carbon dioxide atmosphere.

Table 5.1 Mass balances of the results from pyrolysis of plastic samples

Feedstock / 2g	LDPE		PS		PP		HDPE		PET	
Atmosphere	N ₂	CO ₂								
Gas/ wt. %	13.5	8.59	1.2	0.65	12.0	9.92	12.6	7.90	27.1	-
Liquid/ wt. %	85.0	95.3	91.0	92.0	68.3	82.5	84.5	90.0	50.0	-
Char/ wt. %	0.00	0.50	4.3	5.50	9.5	10.5	0.0	1.50	23.0	-
Mass balance/ wt. %	98.5	104.3	96.5	98.2	89.8	102.9	97.1	99.4	100.1	-

Reactor type = Fixed bed reactor Feedstock weight / temperature = 2g / 500 °C N₂ or CO₂ flow rate = 200 ml min⁻¹ Heating rate = 10 C min⁻¹ Syngas collection time = 79 min

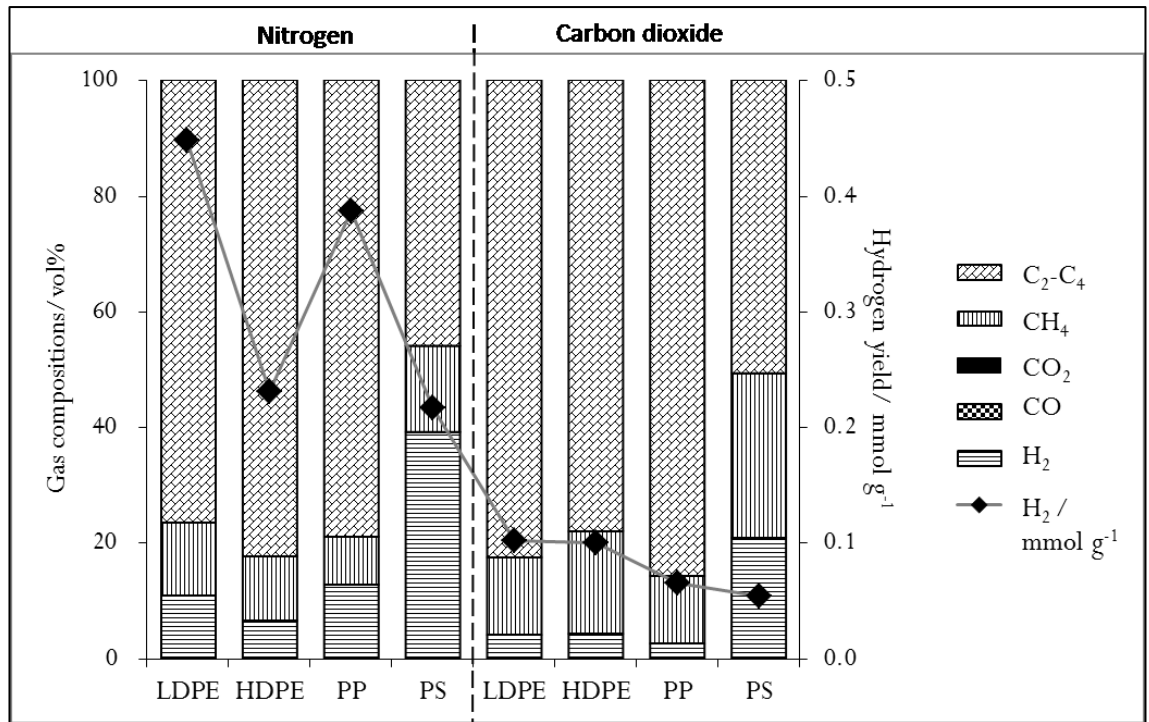


Figure 5.1 Gas composition from pyrolysis of waste plastics under nitrogen or carbon dioxide atmosphere

Overall, the data show that only a small amount of hydrogen was produced during pyrolysis of the waste plastics and the highest yield was for the nitrogen atmosphere compared to carbon dioxide. In addition, the methane concentration was correspondingly decreased in nitrogen compared to the carbon dioxide pyrolysis atmosphere. No carbon monoxide was detected with the nitrogen or carbon dioxide pyrolysis atmospheres. Since the carbon dioxide reaction with hydrocarbons is normally endothermic, it is considered that carbon dioxide will be effective at temperatures higher than 500 °C. In comparison, both atmospheres showed almost similar gas concentrations. Therefore, it can be suggested that the carbon dioxide does not significantly affect the pyrolysis products at 500 °C.

5.1.1 Influence of carbon dioxide flow rate on pyrolysis of polystyrene

The introduction of carbon dioxide in the pyrolysis of waste plastic seems to produce small effects on the product yields. To further confirm the effect of carbon dioxide in the pyrolysis process, an experiment with a lower carbon dioxide concentration was introduced to the system. The carbon dioxide flow rate of

200 ml min⁻¹ and 100 ml min⁻¹ was investigated for hydrogen production from pyrolysis of polystyrene.

The product yield and the gas composition results are shown in Table 5.2. From the table, it is shown that the gas yield corresponding to the polystyrene was increased with the decreasing carbon dioxide flow rate. It is believed that increasing the amount of the syngas production is due to the longer residence time for the gases in the reactor, hence cracking the heavy hydrocarbons into gases. It is supported by the less amount of liquid yield produced by the 100 ml min⁻¹ flow rate of carbon dioxide compared to the 200 ml min⁻¹ flow rate. However, there was no change in the char yield production, which shows that no further reaction occurs with the carbon dioxide even though the flow rate was reduced. It can be suggested that reducing the flow rate of carbon dioxide does not give significant changes on the product yields at the range tested.

In term of the hydrogen production, a lesser amount of hydrogen was produced at 100 ml min⁻¹ injection of carbon dioxide as shown in Figure 5.2. However, the hydrogen production in mmol per gram of sample showed a small increase from 0.054 in 200 ml min⁻¹ injection to 0.07 in 100 ml min⁻¹ injection.

Table 5.2 Mass balance for different carbon dioxide flow rate in the pyrolysis of polystyrene

CO ₂ flow rate /ml min ⁻¹	200	100
CO ₂ flow rate/ g h ⁻¹	23.6	11.8
<i>Product yields/ wt.%</i>		
Gas yield	0.7	1.4
Liquid yield	92.0	91.2
Char yield	5.5	5.5
Mass balance	98.5	98.1

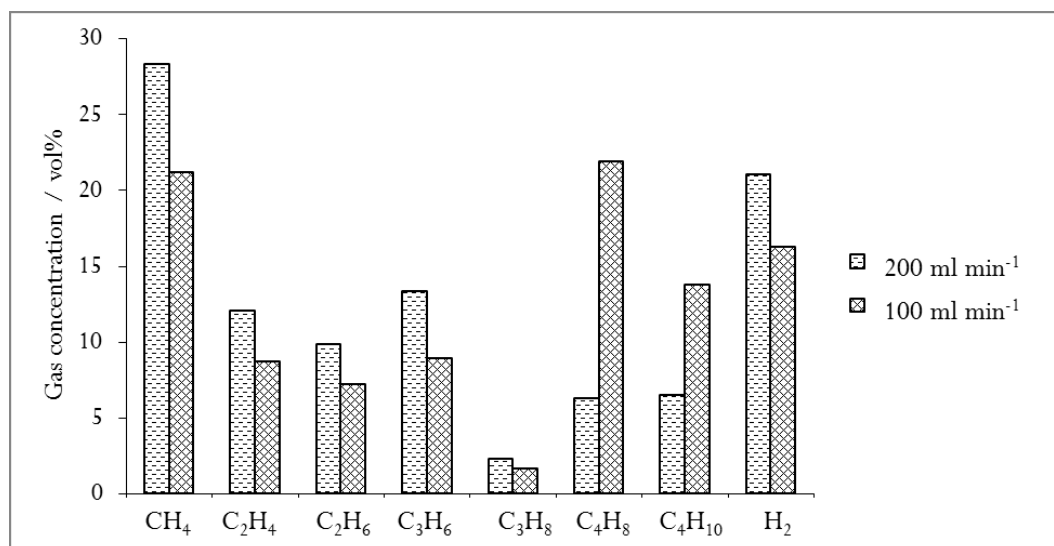


Figure 5.2 Comparison in gas concentration on pyrolysis of waste polystyrene in carbon dioxide atmosphere

5.2 The Introduction of Gasification Stage into the System using a Two-stage Fixed Bed Reactor

In order to improve the hydrogen production, a two-stage pyrolysis gasification system was introduced and several preliminary experiments have been conducted. High density polyethylene has been chosen as the pilot feedstock to investigate whether the addition of the gasification stage at 800 °C to the two-stage pyrolysis gasification reactor will enhance the hydrogen production than that only with one-pyrolysis stage at 500 °C. Nitrogen or carbon dioxide was used in this study with a flow rate of 200 ml min⁻¹. As mentioned in previous section, the CO₂ flow rate of 200 ml min⁻¹ was equivalent to 23.6 g h⁻¹.

In a nitrogen atmosphere, the gas yield showed a high improvement, from 12.75 wt.% to 46.87 wt.% for the pyrolysis-gasification of waste plastic in a nitrogen atmosphere compared to the only pyrolysis experiment as shown in Figure 5.3. During the pyrolysis-gasification, sand was used as the catalyst replacement in the 2nd stage furnace. Therefore, the solid yield was mainly the carbon deposition presence on the sand. There was no pyrolysis char present after the experiment. The amount of liquid produced was also reduced by more than half proving that the significant increase of gas yield in pyrolysis-gasification of waste high density polyethylene was due to the gasification stage at 800 °C that gasified

the heavy hydrocarbons molecules into gases hence reducing the liquid yield from 84.5 wt.% in pyrolysis conditions to 33.5 wt.% in pyrolysis-gasification system.

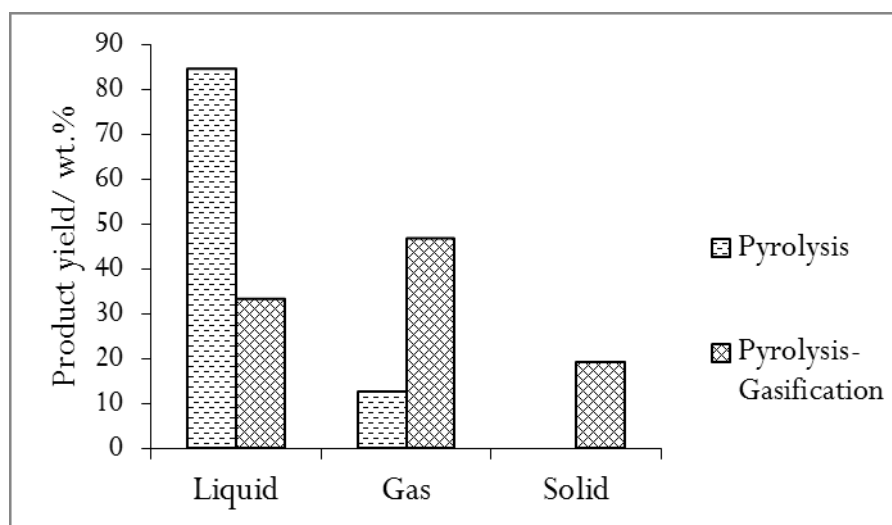


Figure 5.3 Comparison on product yield compositions between pyrolysis and pyrolysis-gasification of high density polyethylene under nitrogen atmosphere

Regardless of the type of atmosphere, the hydrogen yield was significantly increased with the two-stage fixed bed reaction process compared to the one-stage pyrolysis reactor as shown in Table 5.3. It is apparent that there was massive improvement in hydrogen production, which was due to secondary reactions of hydrocarbons in the second reactor, as shown by the reduction of C_2-C_4 hydrocarbon gases concentrations in the two-stage reactor system. The reaction at $800\text{ }^\circ\text{C}$ in the 2nd stage reactor enhanced the carbon dioxide reaction with hydrocarbons, hence raising the volume concentration of hydrogen.

In the presence of the nitrogen atmosphere, the hydrogen production in the two-stage fixed bed reactor increased from $0.23\text{ mmol}_{\text{H}_2}\text{ g}^{-1}_{\text{HDPE}}$ to $20.10\text{ mmol}_{\text{H}_2}\text{ g}^{-1}_{\text{HDPE}}$. While in the carbon dioxide atmosphere, the hydrogen yield increased from 0.1 to $33.58\text{ mmol}_{\text{H}_2}\text{ g}^{-1}_{\text{HDPE}}$. There was also a marked increase in the production of carbon monoxide in the presence of the carbon dioxide atmosphere. This suggests that in the carbon dioxide atmosphere dry reforming reactions (Reaction 2.11) occurred between methane and other hydrocarbons with carbon dioxide in the second stage as compared to the result obtained for the experiment with a nitrogen atmosphere. This was also suggested from the marked decrease in the concentration of methane and other hydrocarbon gases in the experiment using carbon dioxide atmosphere. Several researchers reported that the highly

endothermic characteristic of CO₂/dry reforming requires high temperature for the reaction to occur since both carbon dioxide and methane are stable compounds with low potential energies [10, 11]. Dry reforming has to be performed at high temperature and low pressure to achieve maximum conversion because of the highly endothermic characteristic of the process [12]. Therefore, clear changes in the hydrogen and carbon monoxide concentrations from the experiment with the carbon dioxide atmosphere can be seen when the 800 °C second stage was introduced.

Table 5.3 Gas yields comparison between pyrolysis and pyrolysis-gasification of waste high density polyethylene

	Pyrolysis N ₂	Pyrolysis CO ₂	Pyrolysis- gasification N ₂	Pyrolysis- gasification CO ₂
Mass balance /%	97.25	99.40	99.87	111.45
Hydrogen /mmol g ⁻¹	0.23	0.1	20.1	33.58
Carbon deposition /g g ⁻¹	<i>n/a</i>	<i>n/a</i>	0.20	0.44
<i>Gas concentration /vol.%</i>				
CO	0.0	0.0	0.0	62.89
H ₂	6.59	4.37	45.89	23.82
CH ₄	11.19	17.68	45.03	11.94
C ₂ -C ₄	82.22	77.95	9.08	1.35

n/a; not applicable

The efficiency of the dry reforming process was also compared with the steam reforming process. Wu et al. [13] reported in their studies that steam reforming of 1 g of HDPE with 4.74 g h⁻¹ of steam addition produced 0.023 g g⁻¹_{plastics} of H₂. As equally calculated, dry reforming of 1 g of HDPE with 4.74 g h⁻¹ of carbon dioxide addition produced 0.055 g g⁻¹_{plastics} of H₂, twice the amount of hydrogen produced in the steam reforming process. This finding further strengthens the objective of the dry reforming process on producing high amount of syngas. The summary of comparison is shown below:

Steam reforming of HDPE [13] using a two-stage fixed bed reactor

Sample: 1 g of HDPE, no catalyst (sand)

Reformer agent: 4.74 g h⁻¹ of steam addition

Output: 0.023 g g⁻¹_{plastic} of H₂

Dry reforming of HDPE using a two-stage fixed bed reactor

Sample: 2 g of HDPE, no catalyst (sand)

Reformer agent: 6.0 g h⁻¹ of carbon dioxide addition

Output: 0.07 g g⁻¹_{plastic} of H₂

5.3 Influence of Steam and Carbon Dioxide on the Non-catalytic Pyrolysis-gasification of High Density Polyethylene

Table 5.4 shows the influence of varying the process conditions for the two-stage reactor with 1st stage pyrolysis at 500 °C, followed by reaction in the 2nd stage at 800 °C in the presence of quartz sand. In this series of experiments, the carbon dioxide was mixed with nitrogen at the inlet to the 1st stage. In additional experiments, steam was introduced into the 2nd stage reactor. Instead of using high amounts of carbon dioxide (which acted as the carrier gas as discussed in section 5.3), a small amount of carbon dioxide was added as the reforming agent, as in the case of steam. The carbon dioxide and steam were introduced at different ratios, CO₂:H₂O = 1:0, CO₂:H₂O = 0:1, CO₂:H₂O = 3:1 and CO₂:H₂O = 1:3 to the system. The total amount of carbon dioxide and steam addition was 8 g and the nitrogen flow rate was 200 ml min⁻¹ for all experiments.

The first experiment was with the addition of only carbon dioxide to nitrogen (6 g h⁻¹ of carbon dioxide (8 g in total)) introduced into the 1st stage of the reactor system. The products from the process were mainly gases, however a small amount of water was found in the condenser system. Oyama et al.[14] suggested that the production of water was due to the reverse water gas shift reaction (RWGS). From Table 5.4, the addition of carbon dioxide into the system resulted in an increase in hydrogen production from 20.1 mmolH₂ g⁻¹_{HDPE} (Table 5.3) to 34.2 mmol H₂ g⁻¹_{HDPE} representing a 70% increase in the hydrogen production in mmol per gram. The carbon dioxide conversion was the highest compared to the other plastics with 41% conversion. The presence of carbon monoxide shows that the CO₂ reforming or dry reforming process occurred. During the CO₂/dry reforming process, the hydrocarbons produced from the pyrolysis of the waste high density polyethylene reacted with the carbon dioxide producing more hydrogen as well as carbon monoxide. It is suggested that thermal cracking of heavy

hydrocarbons during the second stage reactor was influenced by the addition of carbon dioxide. This was further supported by the large reduction in methane concentration, from 45.03 vol.% (Table 5.3) to 3.45 vol.% (Table 5.4) and reduction of other hydrocarbons, from 9.08 (Table 5.3) vol.% to 0.22 vol.% (Table 5.4) in the experiment with the addition of carbon dioxide.

Table 5.4 Influence of the reaction atmosphere on the pyrolysis-gasification of waste high density polyethylene using the two-stage fixed bed reactor with sand in the second stage at 800 °C

	N ₂ /CO ₂	N ₂ /H ₂ O	N ₂ /CO ₂ :H ₂ O =3:1	N ₂ /CO ₂ :H ₂ O =1:3
Mass balance/ %	95.64	91.14	99.64	92.17
Hydrogen/ mmol g ⁻¹ _{HDPE}	34.2	78.9	58.39	66.47
Carbon yield/ g g ⁻¹ _{HDPE}	0.14	0.13	0.14	0.11
CO ₂ conversion/ %	40.81	<i>n/a</i>	27.92	7.433
<i>Gas concentration/ vol.%</i>				
CO	43.07	24.9	35.72	26.02
H ₂	20.71	59.1	31.09	49.09
CH ₄	3.45	9.2	6.68	7.62
C ₂ -C ₄	0.22	1.4	0.26	1.65

n/a; not applicable

The addition of 8 gram of steam (4.5 g h⁻¹) into the pyrolysis-gasification of high density polyethylene process produced more hydrogen compared to 8 gram of carbon dioxide (6 g h⁻¹) addition. Hydrogen production was reduced by more than half (steam: 59.1 vol.% to carbon dioxide: 20.7 vol.%), methane production was reduced (steam: 9.2 vol.% to carbon dioxide: 3.4 vol.%) and C₂-C₄ hydrocarbons were also reduced (steam: 1.4 vol.% to carbon dioxide: 0.2 vol.%). However more carbon monoxide was produced (steam: 24.9 vol.% to carbon dioxide: 43.1 vol.%). It could be suggested that the steam addition enhanced the hydrogen production, while the carbon dioxide addition promoted the carbon monoxide production.

The carbon deposition data in the table represents the formation of carbon on the sand in the 2nd stage reactor. The data indicates that with the addition of carbon dioxide or steam, the carbon deposition was reduced from 0.2 g g⁻¹ of sample (Table 5.3) to around 0.13 to 0.14 g g⁻¹ of sample (Table 5.4). Huang et al. [15]

found that carbon dioxide has the ability to reduce carbon by the gasification reaction as shown in Reaction 2.10. Steam also plays a significant role in reducing the carbon deposition (Reaction 2.7). This also contributed towards the amount of carbon monoxide produced from the process. In addition, the water gas shift reaction (Reaction 2.8) might also occur, thereby consuming carbon monoxide and producing carbon dioxide.

Table 5.4 also shows the results from the pyrolysis–gasification of waste high density polyethylene with the addition of steam at a $N_2/CO_2:H_2O$ ratio of 3:1 and 1:3. The results show that the addition of steam into the system markedly increased the amount of hydrogen production. The highest amount of hydrogen produced was $66.47 \text{ mmol H}_2 \text{ g}^{-1}_{\text{HDPE}}$ which was achieved at a $N_2/CO_2:H_2O$ ratio of 1:3. From the table, it appears that more hydrogen yield resulted when more steam was injected into the system. The addition of steam introduced the steam reforming reaction (Reaction 2.9), which contributes towards hydrogen production.

The addition of steam also produced high amounts of methane and other hydrocarbons and increased with a higher level of steam addition. Despite the consumption of methane in the reforming reaction, the increase in methane concentration might be caused by the lower hydrocarbon-cracking efficiency. The addition of steam might affect the reaction conditions inside the reactor and steam may consume some energy in the reactor, hence limiting the cracking of methane and other hydrocarbons. These results are consistent with those obtained by Wu et al. [13] in which the hydrocarbon concentration of non-catalytic steam reforming of high density polyethylene was higher compared to without steam addition. However, with the addition of catalyst in that study, the hydrocarbon-cracking efficiency was greatly improved resulting in higher hydrogen concentration but lower concentrations of methane and other hydrocarbons.

Figure 5.4 shows the relationship between hydrogen and carbon monoxide production in mmol g^{-1} of plastic with the carbon deposition in g g^{-1} of plastic. It appears that more carbon monoxide was produced when less steam was injected to the system. The carbon monoxide yields from the experiment with the addition of steam and carbon dioxide were produced from two different reactions; the steam reforming reaction and dry reforming reaction. Compared to the steam reforming reaction, the dry reforming reaction produces twice the number of moles of carbon monoxide in each reaction. Therefore when the concentration of steam was low in

the system, the carbon monoxide production was higher. Furthermore, due to the high temperature, the reverse water gas shift reaction might also occur, consuming more carbon dioxide and resulting in high carbon monoxide concentration. This is also suggested from the carbon dioxide conversion results, which showed 27.92% carbon dioxide conversion when less steam was injected into the system as compared to 7.4% carbon dioxide conversion at higher steam injection rate.

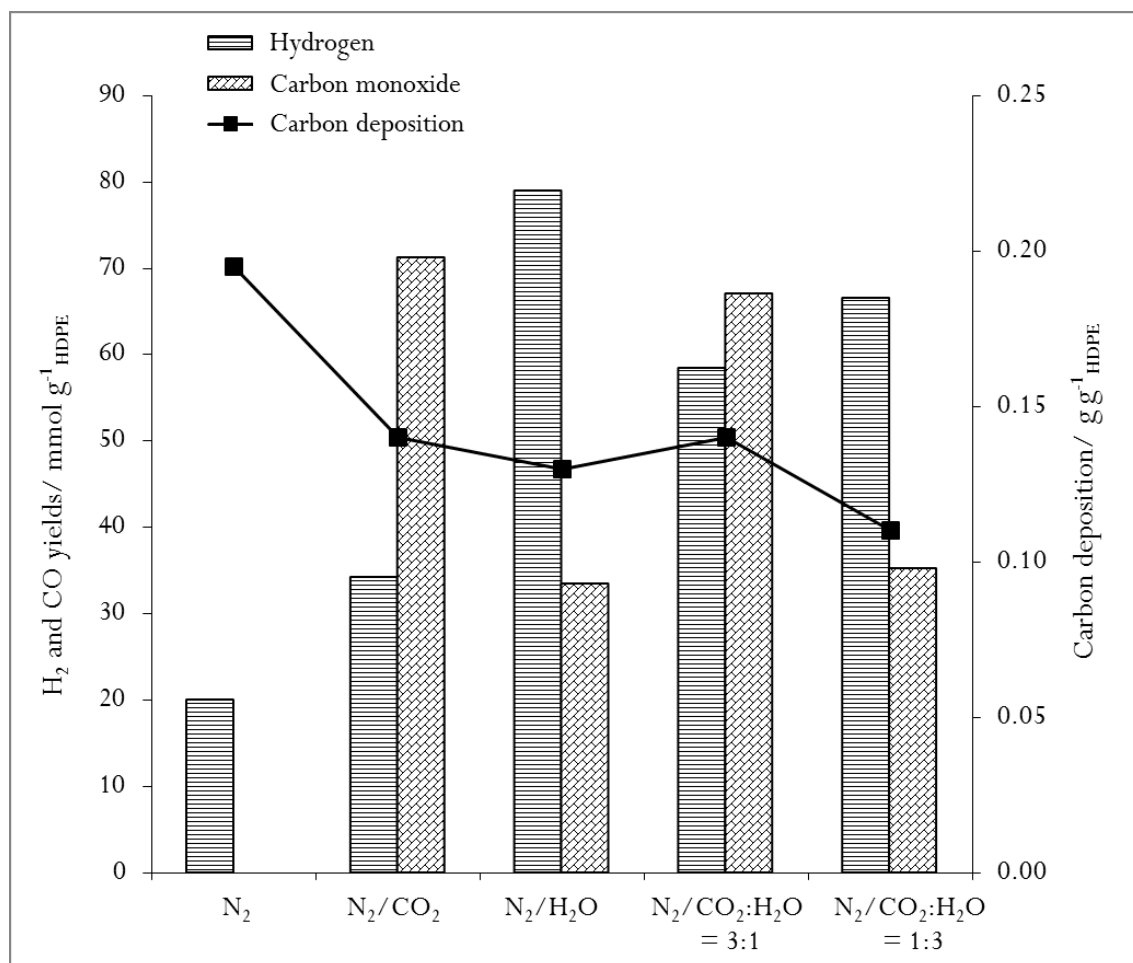


Figure 5.4 Hydrogen, carbon monoxide and carbon deposition production relationship from pyrolysis-gasification of waste high density polyethylene with the addition of carbon dioxide and/or steam.

In terms of the carbon deposition, the lowest carbon deposition was achieved at a CO₂/N₂:H₂O ratio of 1:3. Edwards and Maitra [16] reported that methane dry reforming produced more carbon compared to steam reforming due to the lower H/C ratio in both the feed and product gases. However, with the addition of suitable catalyst [17], the carbon formation in methane dry reforming (without steam) can be reduced and might achieve a carbon-free process.

The theoretical calculations for hydrocarbon conversion in dry reforming were made to further confirm the result. The calculations were based on the data from pyrolysis-gasification with nitrogen and pyrolysis-gasification with nitrogen and 8 g (6 g h⁻¹) of carbon dioxide introduced to the system (dry reforming) as shown in Table 5.5. Based on the carbon dioxide data, since only 5.67 g of carbon dioxide remained after the experiment, it was assumed that 2.329 g of carbon dioxide reacted/ consumed during the gasification/reforming process in the reactor.

Table 5.5 Gas compositions from pyrolysis-gasification high density polyethylene

	Pyrolysis-gasification (N ₂)	Pyrolysis-dry reforming (N ₂ + 8 g of CO ₂)
<i>Gas concentration/ g</i>		
H ₂	0.08	0.13
CO	<i>n/d</i>	3.42
CH ₄	0.63	0.17
C ₂ H ₄	0.2	0.06
C ₂ H ₆	0.02	0.003
C ₃ H ₆	0.004	0.001
C ₃ H ₈	<i>n/d</i>	<i>n/d</i>
C ₄ H ₈	0.01	<i>n/d</i>
C ₄ H ₁₀	<i>n/d</i>	<i>n/d</i>
CO ₂	<i>n/d</i>	5.67

n/d; not detected

Firstly, the hydrocarbon and carbon dioxide reactions were used as mentioned in Reaction 2.11a to Reaction 2.11g. This was based on the basic reaction of carbon dioxide with carbonaceous material (Reaction 2.11).



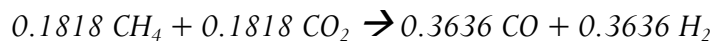


Therefore, theoretically for 8 g of CO_2 , the amount of CO and H_2 produced after the dry reforming reaction with CH_4 is as follow:

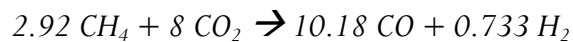
$$8 \text{ g of } \text{CO}_2 = 0.1818 \text{ moles}$$



In moles:



In grams:

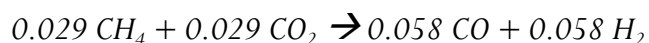


However in pyrolysis-gasification with only nitrogen involved, only 0.63 g of CH_4 was produced and 0.165 g of CH_4 remained in pyrolysis-dry reforming system. Therefore, it is assumed that 0.465 g of methane was reacted with carbon dioxide to produced carbon monoxide and hydrogen.

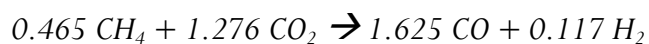
$$0.465 \text{ g of } \text{CH}_4 = 0.029 \text{ moles}$$



In moles:



In grams:



The calculation continues with the other hydrocarbons. Based on the calculations, the total of carbon monoxide and hydrogen productions as well as carbon dioxide consumption was compared with the experimental results as shown in Table 5.6.

Table 5.6 Comparison table of calculation data and experimental results from pyrolysis-dry reforming of waste high density polyethylene

	Total calculation /g	Experimental result /g	Difference /g
CO production	2.28	3.42	+ 1.14
H ₂ production	0.14	0.13	- 0.01
CO ₂ consumption	1.78	2.33	+ 0.55

It can be assumed from the difference that the hydrogen may further react with carbon dioxide to produce carbon monoxide and water based on the reverse water gas shift reaction (RWGS). Furthermore, at temperatures above 720 °C, other side reactions such as the Boudouard reaction may also occur that causes the reaction of the carbon deposition with carbon dioxide to produce carbon monoxide.

5.4 Influence of Nickel-Based Catalysts on Syngas Production from Carbon Dioxide Reforming of Waste High Density Polyethylene

This section describes and compares the influence of nickel-based catalyst on syngas production from carbon dioxide/dry reforming process. Nickel-based catalysts were widely used for hydrogen and syngas production from steam reforming process of waste as well as in dry reforming of methane due to their high stability and catalytic activity, and lower cost compared to noble metal catalysts [18, 19]. However, nickel catalysts are known to be prone to deactivation due to coke formation on the catalyst and nickel sintering [20]. It has been suggested that the addition of Mg, Cu and Co for methane dry reforming could improve catalyst activity and stability towards syngas production and coke formation [21-23].

5.4.1 Fresh catalyst characterizations

Table 5.7 shows the surface area of the freshly prepared nickel based catalysts, Ni/Al₂O₃, Ni-Cu/Al₂O₃, Ni-Mg/Al₂O₃ and Ni-Co/Al₂O₃ and the three different cobalt containing catalyst compositions for the Ni-Co/Al₂O₃ catalyst. The surface area is generally related to the catalytic activity of the catalyst, in which high surface area typically improves the activity of the catalyst [24, 25]. The surface area of the fresh catalyst was in the order, Ni-/Al₂O₃ > Ni-Co/Al₂O₃ (1:0.5:1) > Ni-Cu/Al₂O₃ > Ni-Mg/Al₂O₃ > Ni-Co/Al₂O₃ (1:1:1) > Ni-Co/Al₂O₃ (1:2:1). Addition of the Cu, Mg and Co promoters to the Ni/Al₂O₃ catalyst reduced the surface area of the catalysts. Wu and Williams (2009) also reported a similar effect of the addition of Mg into a Ni-Al catalyst where the surface area of the catalyst was reduced from 155 m² g⁻¹ (Ni-Al (1:2)) to 99m² g⁻¹ (Ni-Mg-Al (1:1:1)) [26].

Table 5.7 BET surface area of the prepared catalysts.

Catalyst	Molar ratio	BET surface area (m ² g ⁻¹)
Ni/Al ₂ O ₃	1:1	133
Ni-Cu/Al ₂ O ₃	1:1:1	73
Ni-Mg/Al ₂ O ₃	1:1:1	66
Ni-Co/Al ₂ O ₃	1:1:1	48
Ni-Co/Al ₂ O ₃	1:0.5:1	81
Ni-Co/Al ₂ O ₃	1:2:1	31

The XRD spectra patterns of the Ni/Al₂O₃, Ni-Cu/Al₂O₃, Ni-Mg/Al₂O₃ and Ni-Co/Al₂O₃ catalysts were obtained from the X-ray diffraction analysis and the results are shown in Figure 5.5. The metal appears to be well distributed throughout the catalysts. All of the catalysts exhibited XRD intensity peaks for the presence of NiO, γ -Al₂O₃ and NiAl₂O₄. In addition, four intensity peaks representative of CuO were observed for the Ni-Cu/Al₂O₃ catalyst [24], two peaks for MgO and a peak of NiMgO for the Ni-Mg/Al₂O₃ catalyst [27] and five peaks of Co₃O₄ for the Ni-Co/Al₂O₃ catalyst [28, 29]. Since the catalyst was not treated or reduced prior to the analysis, the XRD patterns show that all the metal added to the catalysts remains in their oxide forms as expected. The XRD patterns for the different ratios of Ni-Co/Al₂O₃ catalyst are shown in Figure 5.6. The patterns were similar, however small difference can be seen in the diffraction peaks, in which the peaks became more sharper as the amount of cobalt was increased, as the ratio was increased from 1:0.5:1 to 1:2:1.

The H₂-TPR profiles of the fresh catalysts are shown in Figure 5.7. The main reduction peaks of both Ni/Al₂O₃ and Ni-Mg/Al₂O₃ catalyst occur at high temperature at around 750 °C to 850 °C, showing the strong interaction between the metal and the support. In contrast, the Ni-Cu/Al₂O₃ catalyst demonstrated a low intensity peak at a temperature between 230 °C and 260 °C, which may be attributed to the reduction of NiO that was weakly interacted with the support material [30]. The Ni-Co/Al₂O₃ catalysts with increasing cobalt content exhibited similar profiles of two reduction peaks. The first peak was observed at a temperature between 290 and 450 °C and the second reduction peak was detected between 550 and 730 °C. The first peak may be assigned to the reduction of Co₃O₄ and NiO species which occur at the same time and the second peak suggests the reduction of NiCo₂O₄ and/or Co₃O₄; NiO species and metal aluminate spinel species (such as NiAl₂O₄ and CoAl₂O₄) having strong interaction with support. A Similar trend has been reported in studies of Ni-Co-Al catalysts with the addition of Sr [31]. The complete reduction of Ni-Co bimetallic catalysts was reported to involve two or more overlapping reduction peaks due to the simultaneous reduction of Co₃O₄ and NiO species [31].

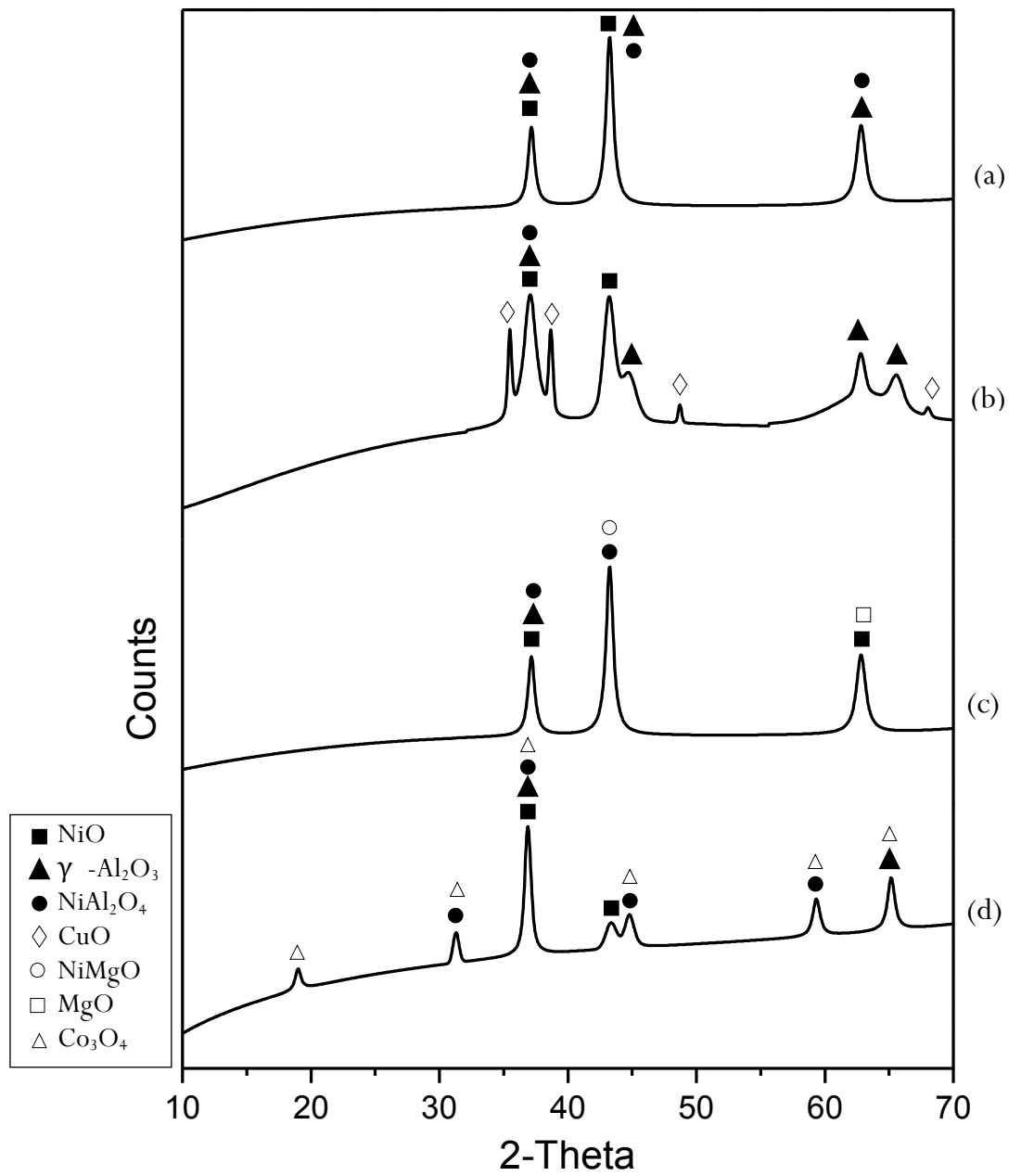


Figure 5.5 XRD spectra of the fresh catalysts: (a) Ni/Al₂O₃ (1:1) catalyst; (b) Ni-Cu/Al₂O₃ (1:1:1) catalyst; (c) Ni-Mg/Al₂O₃ (1:1:1) catalyst; (d) Ni-Co/Al₂O₃ (1:1:1) catalyst

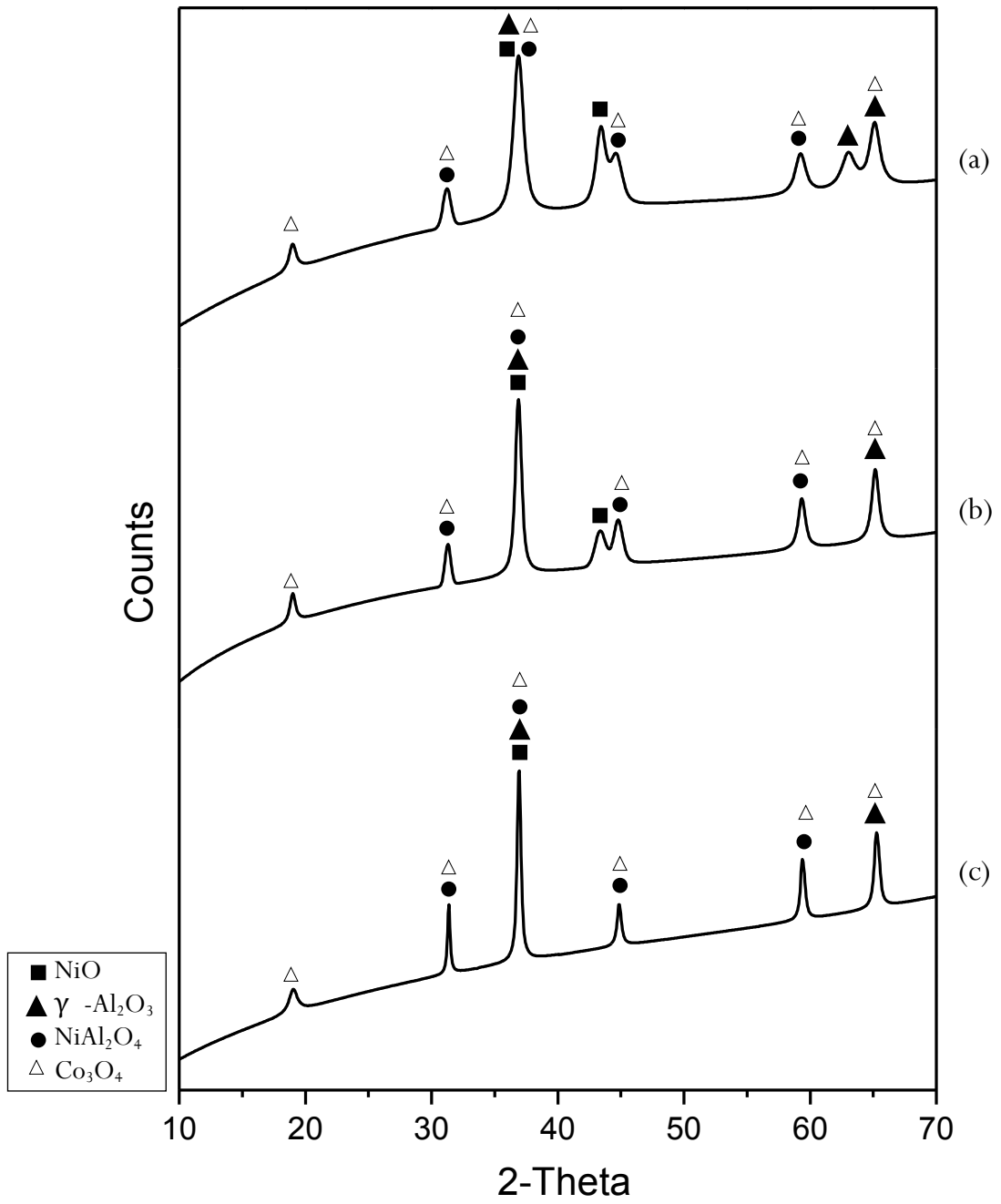


Figure 5.6 XRD spectra of the fresh Ni-Co/Al₂O₃ catalysts: (a) 1:0.5:1; (b) 1:1:1; (c) 1:2:1

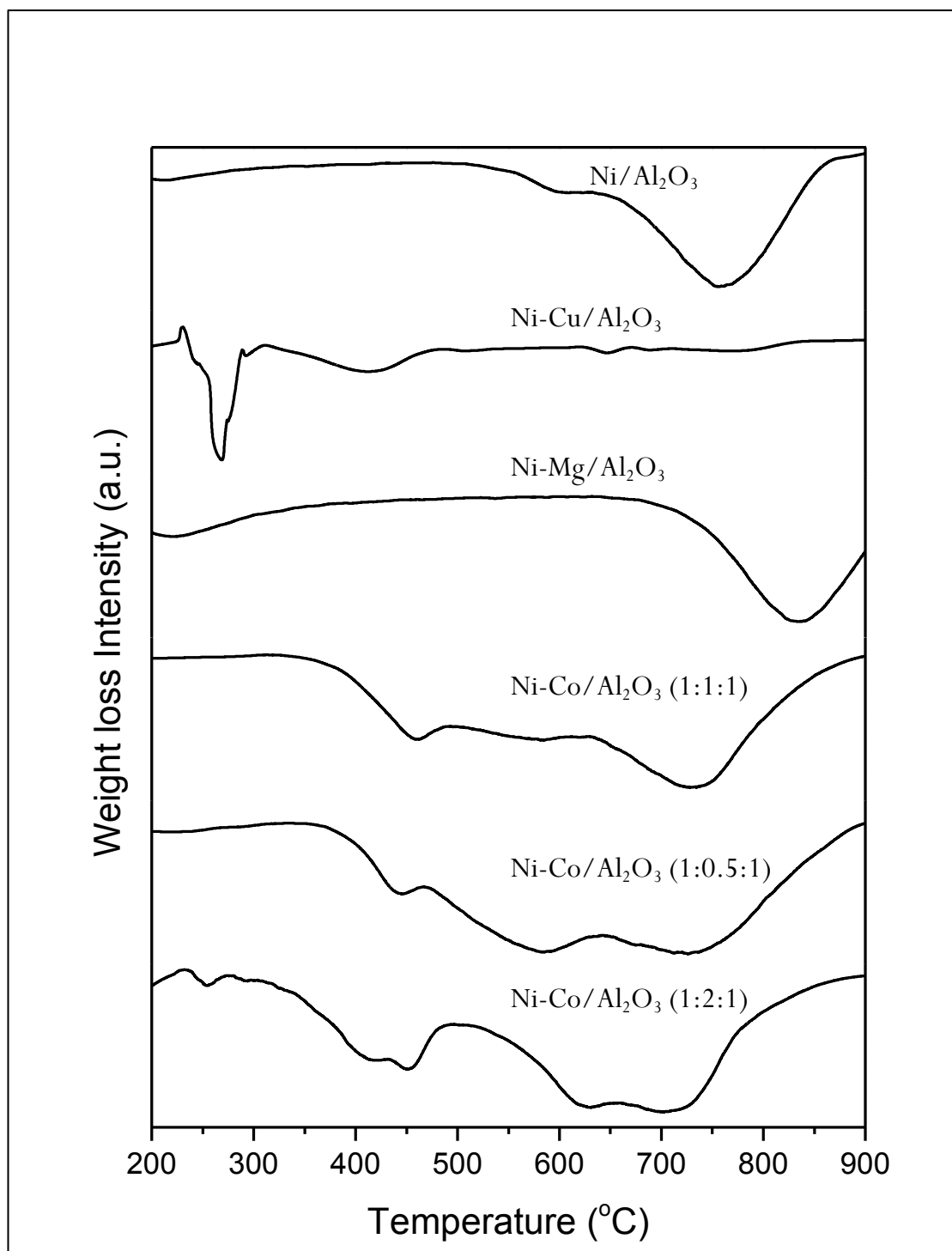


Figure 5.7 Temperature programmed reduction (H₂-TPR) of the fresh catalysts

5.4.2 Pyrolysis-catalytic CO₂ reforming over Ni/Al₂O₃ catalyst

The pyrolysis-catalytic CO₂ reforming of high density polyethylene with the Ni/Al₂O₃ catalyst was carried out at a catalyst temperature of 800 °C. The non-catalytic pyrolysis-CO₂ reforming of high density polyethylene was also carried out where sand was used as the substitute for catalyst. Experiments without any catalyst or sand were also carried out as a baseline experiment for comparison with the results when sand or catalyst was used. The product yields are shown in Table 5.8 and the gas compositions of the experimental results are presented in Figure 5.8. Figure 5.9 shows the carbon deposition and the CO₂ conversion from the pyrolysis-dry reforming of high density polyethylene. The carbon deposition was the carbon deposited on the catalyst/sand after the experiment.

Table 5.8 shows that in the absence of catalyst and with no CO₂ reforming agent, the high density polyethylene was pyrolysed to produce a liquid product (33.5 wt.%), gas (46.9 wt.%) and significant deposition of carbon on the sand surface. The pyrolysis residue from high density polyethylene was negligible. The residue was measured by weighing the sample holder in the 1st stage furnace before and after the experiment. Pyrolysis of high density polyethylene usually produces high yields of oil/wax, typically ~80 wt.% [32]. However, in this work for the uncatalysed experiments, the pyrolysis gases pass through the sand bed at a temperature of 800 °C and are cracked to produce higher gas yield and significant deposits of carbon on the sand. The introduction of CO₂ in the non-catalytic experiment produced a marked increase in gas yield from 46.9 to 90.6 wt.%. It is suggested that the CO₂ was involved in the cracking and reforming of the hydrocarbon oil/wax to produce gases due to the marked reduction of liquid yield from 33.5 to 2.0 wt.%. CO₂ reforming also reduced the carbon deposited on the sand from 19.5 to 2.8 wt.%.

The introduction of the Ni/Al₂O₃ catalyst in the absence of CO₂ produced a slight decrease on the gas yield from 46.9 wt.% (sand) to 33.7 wt.%. This decrease in gas yield corresponded to a high carbon deposition of 56.0 wt.% on the Ni/Al₂O₃ catalyst and reduction of liquid yield to 7.5 wt.%. The introduction of CO₂ to the second reactor to produce dry CO₂ catalytic reforming reactions of the high density polyethylene pyrolysis gases resulted in an improved production of gases to 93.2 wt.% while reducing the carbon deposited on the catalyst to 1.0 wt.%.

Figure 5.8 shows the analysis of the gases produced from the pyrolysis-catalytic CO₂ reforming of high density polyethylene with the Ni/Al₂O₃ catalyst. Compared with the gas produced in the absence of catalyst (sand) and absence of CO₂, where high concentrations of CH₄ and C₂-C₄ were found, the introduction of CO₂ in the absence of the catalyst (sand) produced a syngas with increased concentrations of hydrogen and carbon monoxide.

However, with the introduction of the Ni/Al₂O₃ catalyst to the CO₂ reforming process, the concentration of carbon monoxide markedly increased, with also high concentrations of hydrogen. The syngas (H₂+CO) production was increased from 20.01 mmol_{syngas} g⁻¹_{HDPE} for non-catalytic and no CO₂ experiment to 138.81 mmol_{syngas} g⁻¹_{HDPE} for the CO₂ reforming of high density polyethylene with the Ni/Al₂O₃ catalyst (Table 5.8). The increase of hydrogen and carbon monoxide concentration and the decrease of CH₄ and C₂-C₄ hydrocarbon in the gas yield in CO₂ reforming of high density polyethylene are due to the promotion of CO₂/dry reforming reactions (Reaction 2.11) in the second reactor. This can be supported by the increase in CO₂ conversion from 40.81% for CO₂ reforming of high density polyethylene with sand to 54.46% with the Ni/Al₂O₃ catalyst (Figure 5.9). The increase in hydrogen yield in the presence of catalyst in the CO₂ reforming of polyethylene was similarly reported by Yamada et al. [33], where hydrogen yield was increased from 1.7 % in the absence of catalyst to 35.4 % using a Pd/Al₂O₃ catalyst. The catalyst used was pre-treated with H₂ for 3 h. They also reported that the decomposition of polyethylene into hydrogen and carbon monoxide was completely reformed at the catalyst temperature of 850 °C.

The used Ni/Al₂O₃ catalyst was analysed by temperature programmed oxidation (TPO) and scanning electron microscopy and the DTG-TPO thermographs and SEM micrographs are shown in Figure 5.10 and Figure 5.11 respectively.

The DTG-TPO thermographs of the reacted Ni/Al₂O₃ catalyst with and without CO₂ (Figure 5.10), indicated a mass increase in the DTG-TPO thermographs at around 450 °C which was attributed to the oxidation of the Ni particles during the oxidation process [34]. A large peak of carbonaceous coke oxidation occurred at a temperature of ~650 °C for the Ni/Al₂O₃ catalysts in the absence of CO₂. The oxidation peak at ~650 °C was assigned to the oxidation of graphitic filamentous carbons which are more resistant to oxidation compared to amorphous carbons which are typically oxidised at ~450 °C [35]. Figure 5.11 confirmed the presence

of large quantities of filamentous carbons on the surface of coked Ni/Al₂O₃ in the absence of CO₂. In the presence of CO₂ and the Ni/Al₂O₃ catalyst there was only a small oxidation peak at 650 °C, suggesting low carbon deposition, also confirmed by the carbon deposition shown in Table 5.8 and the SEM micrograph in Figure 5.11. It is suggested that the reduction of carbon deposited on the catalyst might be due to the reaction between carbon and CO₂ (Reaction 2.10). Guzzi, et al. [36] investigated the formation of surface carbon on a Ni/MgAl₂O₄ catalyst for the CO₂ reforming of methane. It was reported that the accumulation of carbon decreased at high temperature and most of the carbonaceous coke was removed by this reverse-Boudouard reaction.

5.4.3 Pyrolysis-catalytic CO₂ reforming over Ni-Cu/Al₂O₃, Ni-Mg/Al₂O₃ and Ni-Co/Al₂O₃ catalyst

Table 5.8 and Figure 5.8 illustrate the effect of Cu, Mg or Co addition to the Ni/Al₂O₃ catalyst on syngas (H₂ and CO) production and gas composition. In the experiments with no CO₂ addition to the second stage reactor, the gas yield for the Ni/Al₂O₃ catalyst was 33.7 wt.%, when Cu was added to the Ni/Al₂O₃ catalyst the syngas yield increase to 52.3 wt.%, and for Mg addition and Co addition, the gas yield showed less of an increase to 39.9 wt.% and 38.6 wt.% respectively (Table 5.8). There was also a small decrease in the amount of carbon deposited on the catalyst when the metal promoter was added, decreasing from 56.0 wt.% for the Ni/Al₂O₃ to 43.5 wt.% for Cu addition, 43.0 wt.% for Mg addition and to 49.5 wt.% for Co addition. Figure 5.8 shows the gas yields for the pyrolysis-catalysis of high density polyethylene with Ni-Cu/Al₂O₃, Ni-Mg/Al₂O₃ and Ni-Co/Al₂O₃ catalysts in the absence of CO₂. The Ni-Cu/Al₂O₃ catalyst showed the highest CH₄ and other hydrocarbons concentrations, resulting in higher gas yield but lower syngas production compared to the Mg and Co nickel based catalysts. The syngas productions for pyrolysis-catalysis of high density polyethylene were similar for all the catalysts in the absence of CO₂ at ~50 mmol_{syngas} g⁻¹ high density polyethylene (Table 5.8).

When carbon dioxide was introduced into the pyrolysis-catalytic CO₂ reforming of high density polyethylene process, the amount of gases produced showed a small increase in the presence of the Ni-Cu/Al₂O₃, Ni-Mg/Al₂O₃ and Ni-Co/Al₂O₃ catalysts compared to the gas yield using Ni/Al₂O₃ with CO₂ (Table 5.8). In addition, the relationship between carbon deposition and CO₂ conversion are

shown in Figure 5.9. The carbon deposited on the catalyst showed only a small influence of the addition of the Cu and Mg promoters where carbon deposition was increased from 1.0 wt.% (Ni/Al₂O₃) to 1.1 wt.% with Cu addition and decreased to 0.7 wt.% with Mg addition. However, there was no coke formation detected on the Ni-Co/Al₂O₃ catalyst. This is also in agreement with the results from DTG-TPO thermographs in Figure 5.10. The carbon deposition results are also reflected in the carbon conversion data with lower coke deposition producing higher CO₂ conversion (Figure 5.9). The carbons formed on the Ni/Al₂O₃ catalyst with the addition of Cu, Mg and Co were also observed from SEM morphology (Figure 5.11). The Ni-Cu/Al₂O₃ and Ni-Mg/Al₂O₃ catalysts showing evidence of the presence of filamentous carbons, but the Ni-Co/Al₂O₃ catalyst showing no filamentous carbons.

Figure 5.8 shows the gas yields for the pyrolysis-catalytic CO₂ reforming of high density polyethylene with the Ni-Cu/Al₂O₃, Ni-Mg/Al₂O₃ and Ni-Co/Al₂O₃ catalysts. The concentrations of gases, as shown in Figure 5.8, indicated that there was little influence of Cu, Mg or Co metal addition to the Ni/Al₂O₃ catalyst in the presence of carbon dioxide. The carbon monoxide yields were influenced by metal addition, with the highest carbon monoxide concentration with Co addition and Cu addition, producing lower carbon monoxide compared to the Ni/Al₂O₃ catalyst. High CH₄ and other hydrocarbon concentrations were found for Cu addition with lower carbon monoxide concentrations.

Table 5.8 shows that the addition of carbon dioxide produces an increase in syngas production (H₂+CO) from 105.41 mmol_{syngas} g⁻¹_{HDPE} in the presence of sand but with no catalyst to 138.81 mmol_{syngas} g⁻¹_{HDPE} for the Ni/Al₂O₃ catalyst. The addition of the Cu metal promoter to the Ni/Al₂O₃ catalyst reduced syngas production to 130.56 mmol_{syngas} g⁻¹_{HDPE}. However, the addition of the Mg and Co metal promoters to the Ni/Al₂O₃ increased syngas production to 146.96 mmol_{syngas} g⁻¹_{HDPE} for the Ni-Mg/Al₂O₃ and 149.42 mmol_{syngas} g⁻¹_{HDPE} for the Ni-Co/Al₂O₃. The syngas (H₂ and CO) production for catalytic – CO₂ reforming of high density polyethylene was therefore in the order: Ni-Co/Al₂O₃ > Ni-Mg/Al₂O₃ > Ni/Al₂O₃ > Ni-Cu/Al₂O₃ (Table 5.8, Figure 5.8). The data shown in Table 5.8 and figures 5.8 and 5.9 show small but significant influences of the metal promoter addition. (Chapter 3 confirmed the reproducibility of the reactor system). Therefore, the addition of the metal promoters, particularly for the Mg and Co promoters showed a significant increase in syngas yield.

For the Ni-Cu/Al₂O₃ catalyst, this was also reflected in the H₂-TPR data (Figure 5.7), where Cu had a very weak metal-support interaction, resulting in low catalytic activity and consequently, the lowest syngas production and highest carbon deposition. The H₂-TPR data for the Ni-Co/Al₂O₃ catalyst suggest the strongest metal-support interaction and with the highest syngas production and lowest carbon formation on the catalyst surface suggesting the highest catalytic activity.

The results suggest that the addition of Co into the Ni/Al₂O₃ catalyst increased the syngas production and CO₂ conversion for the CO₂ reforming of high density polyethylene. The reduction of carbon deposited on the catalyst surface was also observed. Zhang et al. have also reported a high catalytic activity of a Ni-Co catalyst for the CO₂ reforming of methane which was attributed to a strong metal-support interaction [37]. Others have also highlighted the importance of strong metal-support interaction of Ni-Co catalysts to enhance catalytic activity and the low coke formation properties of Ni-Co catalysts [38-40]. Liu et al. have suggested that Cu on the catalyst surface has a very weak interaction with CO₂ compared to other metals based on their density functional theory studies of CO₂ adsorption and decomposition on Fe, Co, Ni and Cu surfaces [41].

Table 5.8 Pyrolysis-dry reforming of high density polyethylene with different catalysts

Catalyst	None	None	Sand	Sand	Ni/ Al ₂ O ₃	Ni/ Al ₂ O ₃	Ni-Cu/ Al ₂ O ₃	Ni-Cu/ Al ₂ O ₃	Ni-Mg/ Al ₂ O ₃	Ni-Mg/ Al ₂ O ₃	Ni-Co/ Al ₂ O ₃	Ni-Co/ Al ₂ O ₃
CO ₂ flow rate (g h ⁻¹)	0	6.0	0	6.0	0	6.0	0	6.0	0	6.0	0	6.0
<i>Product yield (wt. %)</i>												
Gas	38.1	93.9	46.9	90.6	33.7	93.2	52.3	96.2	39.9	97.6	38.6	94.8
Liquid	27.0	1.4	33.5	2.0	7.5	1.2	4.0	2.5	7.5	1.1	6.5	2.4
Residue	0.0	0.3	0.0	0.2	1.0	0.1	0.0	0.1	1.0	0.1	0.0	0.0
Carbon deposition	28.0	3.4	19.5	2.8	56.0	1.0	43.5	1.1	43.0	0.7	49.5	0.0
Mass balance	93.0	99.0	99.9	95.6	98.2	95.5	99.8	99.9	91.4	99.5	94.5	97.2
<i>Syngas yield (mmol_{syngas} g⁻¹_{HDPE})</i>												
H ₂ + CO	25.32	112.35	20.01	105.41	51.90	138.81	47.53	130.56	48.78	146.96	50.83	149.42
H ₂ :CO molar ratio	-	0.49	-	0.48	14.21	0.47	9.52	0.51	10.11	0.49	11.15	0.47

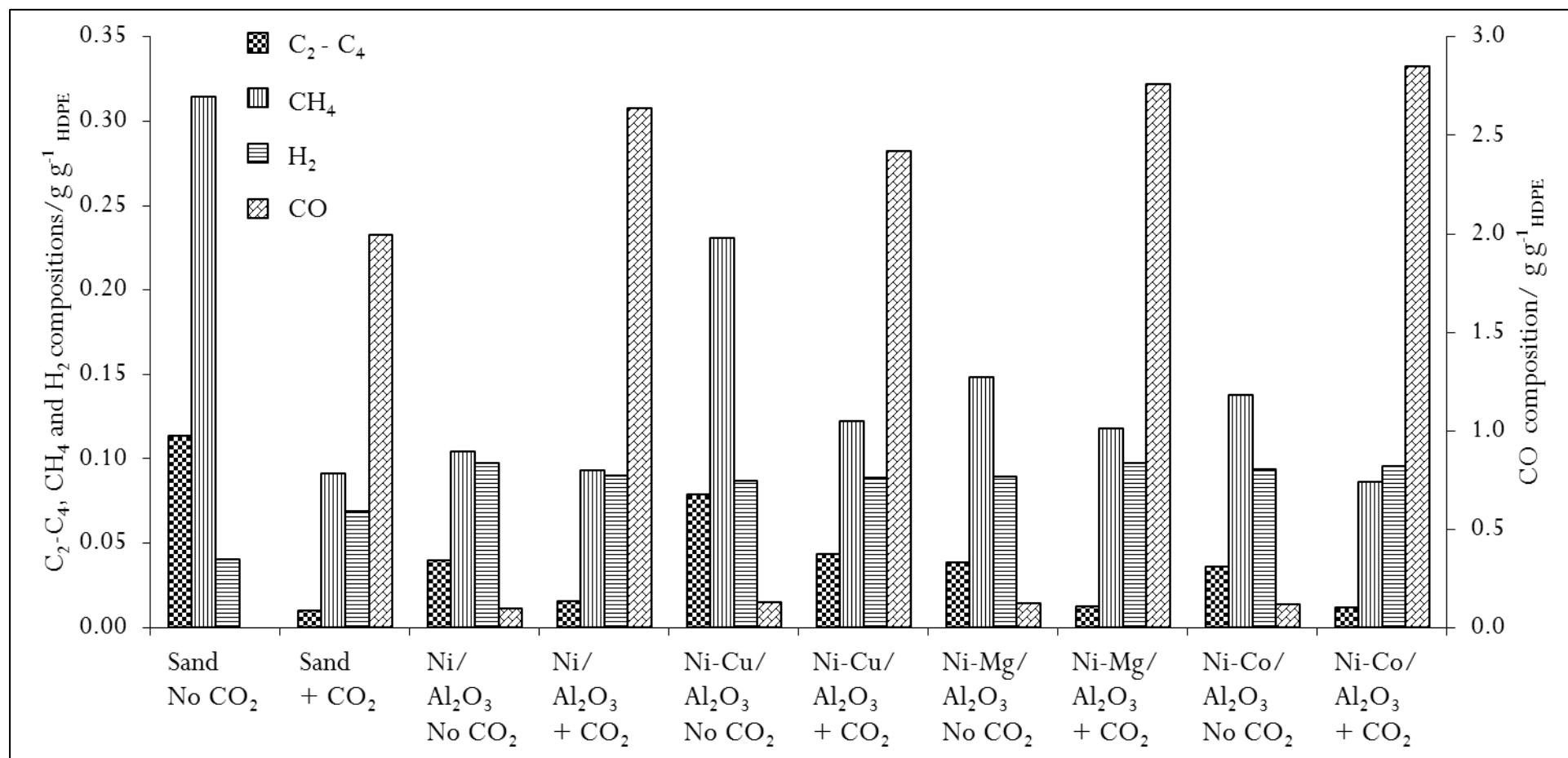


Figure 5.8 Gas compositions for the pyrolysis-dry reforming of high density polyethylene with different type of catalyst at a catalyst temperature of 800 °C.

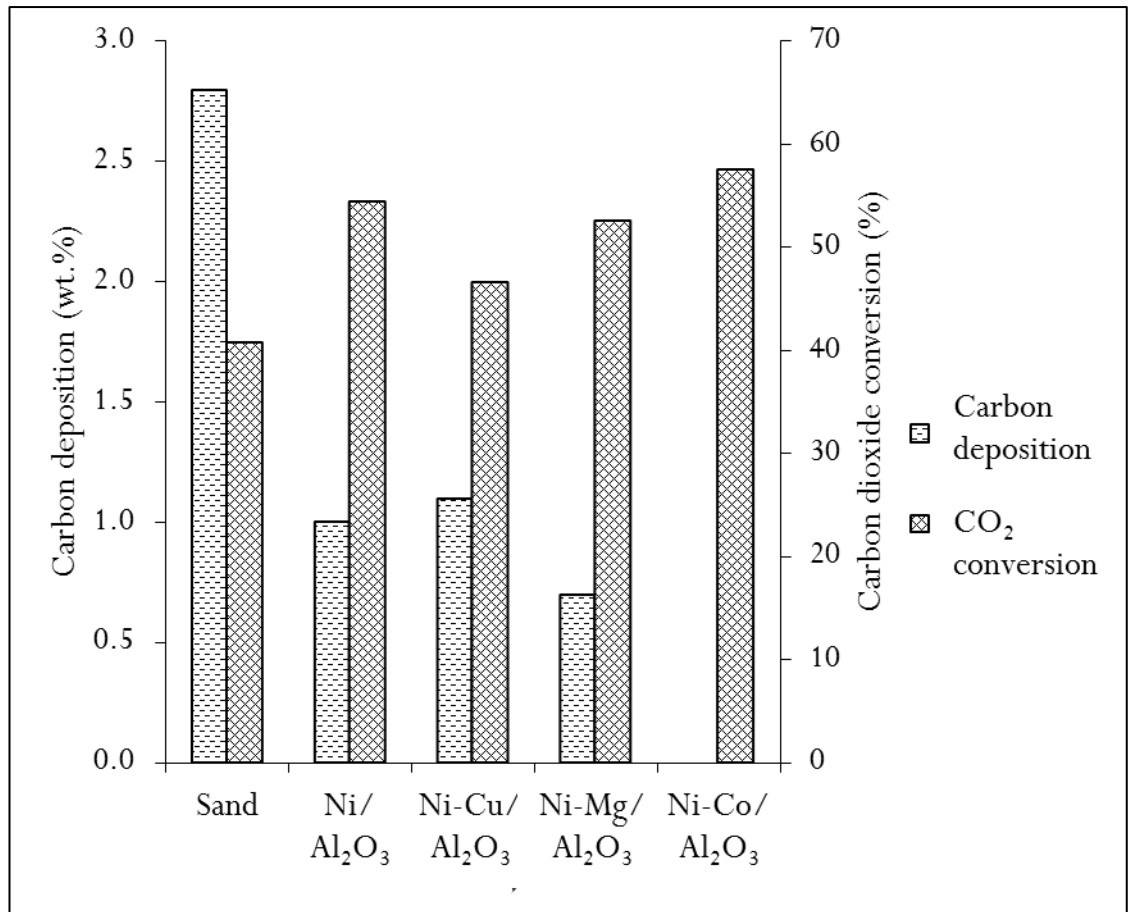


Figure 5.9 Relationship between carbon deposition and CO₂ conversion derived from pyrolysis-dry reforming of high density polyethylene over different catalysts.

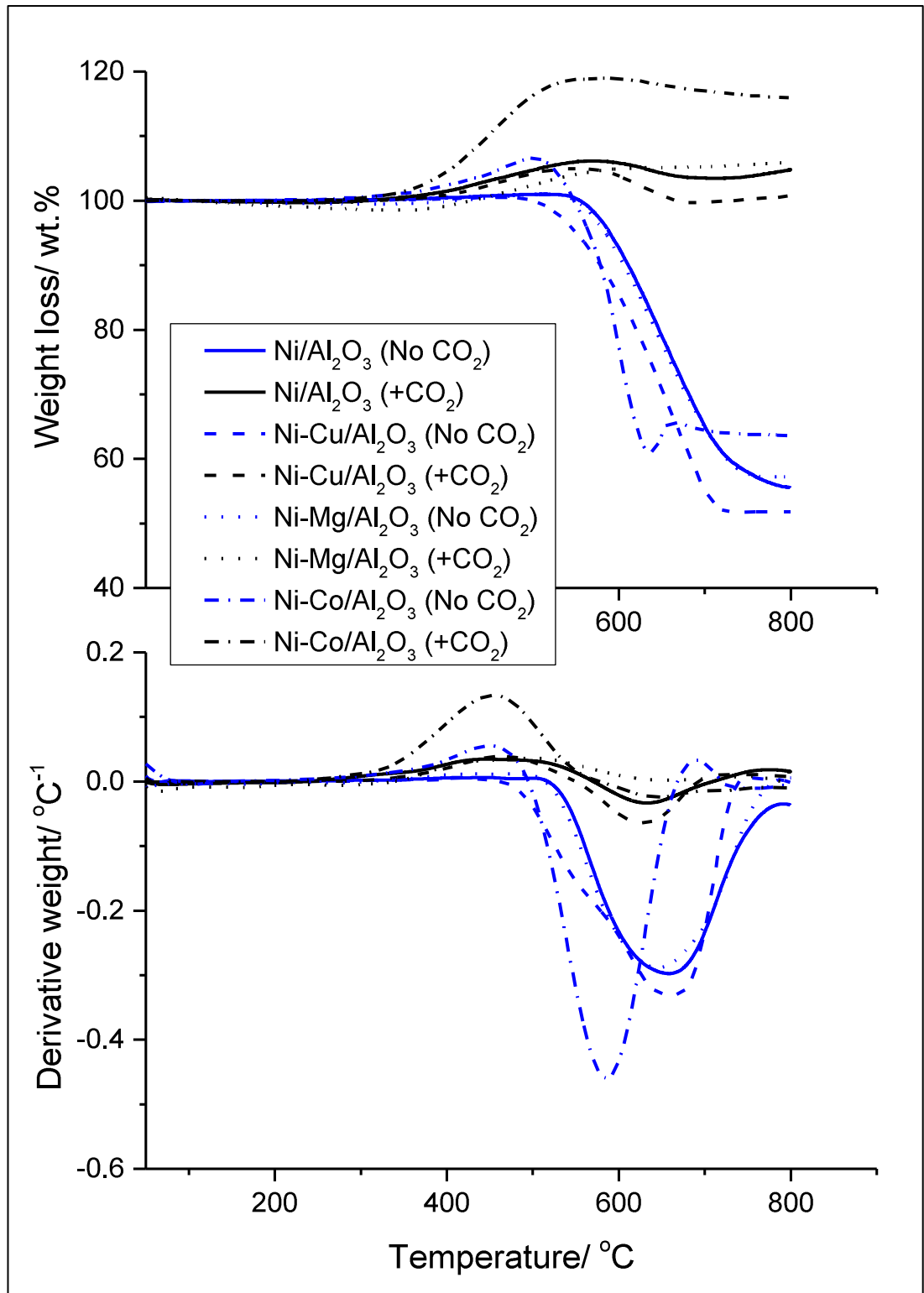


Figure 5.10 DTG-TPO thermograph of different type of coked catalysts after pyrolysis-dry reforming of high density polyethylene

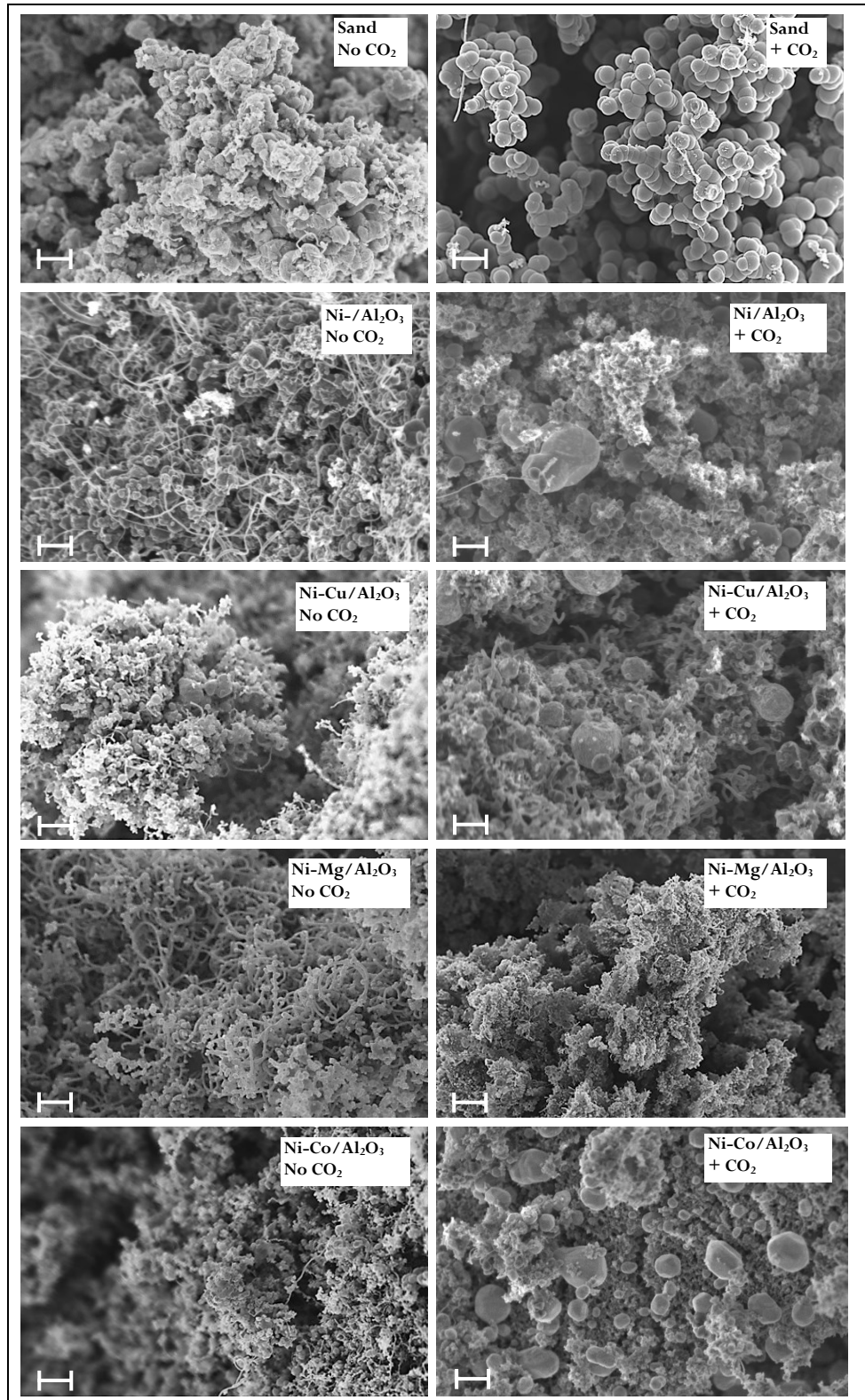


Figure 5.11 SEM results of different type of coked catalysts from pyrolysis-gasification/reforming of HDPE, calcined at 750 °C (scale bar represent 1 μm and all SEM micrographs are at the same magnification)

5.4.4 Ni-Co/Al₂O₃ catalysts with different molar ratios

The Ni-Co/Al₂O₃ catalyst produced the highest syngas (H₂ and CO) yield, a high CO₂ conversion and no detectable carbon formation on the catalyst from the CO₂ reforming of high density polyethylene. Further work was therefore undertaken to determine the influence of cobalt metal content in the Ni/Al₂O₃ catalyst in terms of optimising the syngas production. With high CO₂ conversion and low coke formation. Ni-Co/Al₂O₃ catalysts with molar ratios of 1:0.5:1, 1:1:1 and 1:2:1 was prepared.

Table 5.9 shows the influence of cobalt content on the product yield and gas composition for the CO₂ reforming of high density polyethylene. There was a marginal increase in liquid yield and gas yield with the increase of molar ratio from 1:0.5:1 to 1:2:1. There was 0.9 wt.% of deposited carbon on the Ni-Co/Al₂O₃ catalyst with low cobalt content while no carbon was detected on the Ni-Co/Al₂O₃ catalysts with molar ratios of 1:1:1 and 1:2:1. This result is in agreement with results from DTG-TPO analysis where an intense oxidation peak was found at 600 °C for the Ni-Co/Al₂O₃ catalyst with low cobalt content (Figure 5.12). The SEM morphology of the Ni-Co/Al₂O₃ catalyst shown in Figure 5.13 also suggests that carbons were observed in Ni-Co/Al₂O₃ catalyst with molar ratio of 1:0.5:1 and the amount were reduced at higher cobalt contents. The effects of different Ni-Co [41, 42] content have been investigated before, but there are few studies involving cobalt addition to a nickel-based catalyst. Jose-Alonso et al. [40] studied several different compositions of cobalt or Ni alumina supported catalysts for the CO₂ reforming of methane. They reported that increased metal content enhanced the CO₂ conversion and very low carbon deposits are also expressed, albeit that they used low metal concentrations (<4 wt.%). Zhang et al. [42] also reported that lower Ni-Co content catalysts had lower carbon deposition, but higher Ni-Co content produced significant carbon deposition when the catalyst were used over extended periods (~250 h). For the work reported here, there was no carbon deposition at the higher cobalt content Ni-Co/Al₂O₃ catalyst. However, no extended, time-on-stream experiments were carried out.

Table 5.9 Pyrolysis-dry reforming of high density polyethylene over different molar ratios of Ni-Co/Al₂O₃ catalyst

Ratio	(1:0.5:1)	(1:1:1)	(1:2:1)
<i>Product yield (wt. %)</i>			
Gas	91.3	94.8	95.0
Liquid	2.1	2.4	2.9
Residue	0.1	0.0	0.0
Carbon deposition	0.9	0.0	0.0
Mass balance	94.4	97.2	97.9
<i>Gas composition ($g_{gas} g^{-1}_{HDPE}$)</i>			
H ₂	0.094	0.096	0.099
CO	2.615	2.852	2.965
CH ₄	0.087	0.086	0.079
C ₂ -C ₄	0.016	0.012	0.010
H ₂ + CO production (mmol _{syngas} g ⁻¹ _{HDPE})	139.74	149.42	155.13
CO ₂ conversion (%)	56.11	57.62	60.08
H ₂ :CO molar ratio	0.50	0.47	0.47

The composition of the product gases obtained from the experiments showed that the syngas (H₂ and CO) yield increased with the increase in Ni-Co/Al₂O₃ molar ratio from 139.74 to 155.13 mmol_{syngas} g⁻¹_{HDPE} for the CO₂ reforming of high density polyethylene. The CO₂ conversion also increased from 56.11 wt.% to 60.08 wt.%. The increasing of syngas yield, CO₂ conversion and also the decreasing of CH₄ and other hydrocarbon concentration are most likely due to the CO₂/dry reforming reaction (Reaction 2.11), which is more favourable in the catalyst with high cobalt contents.

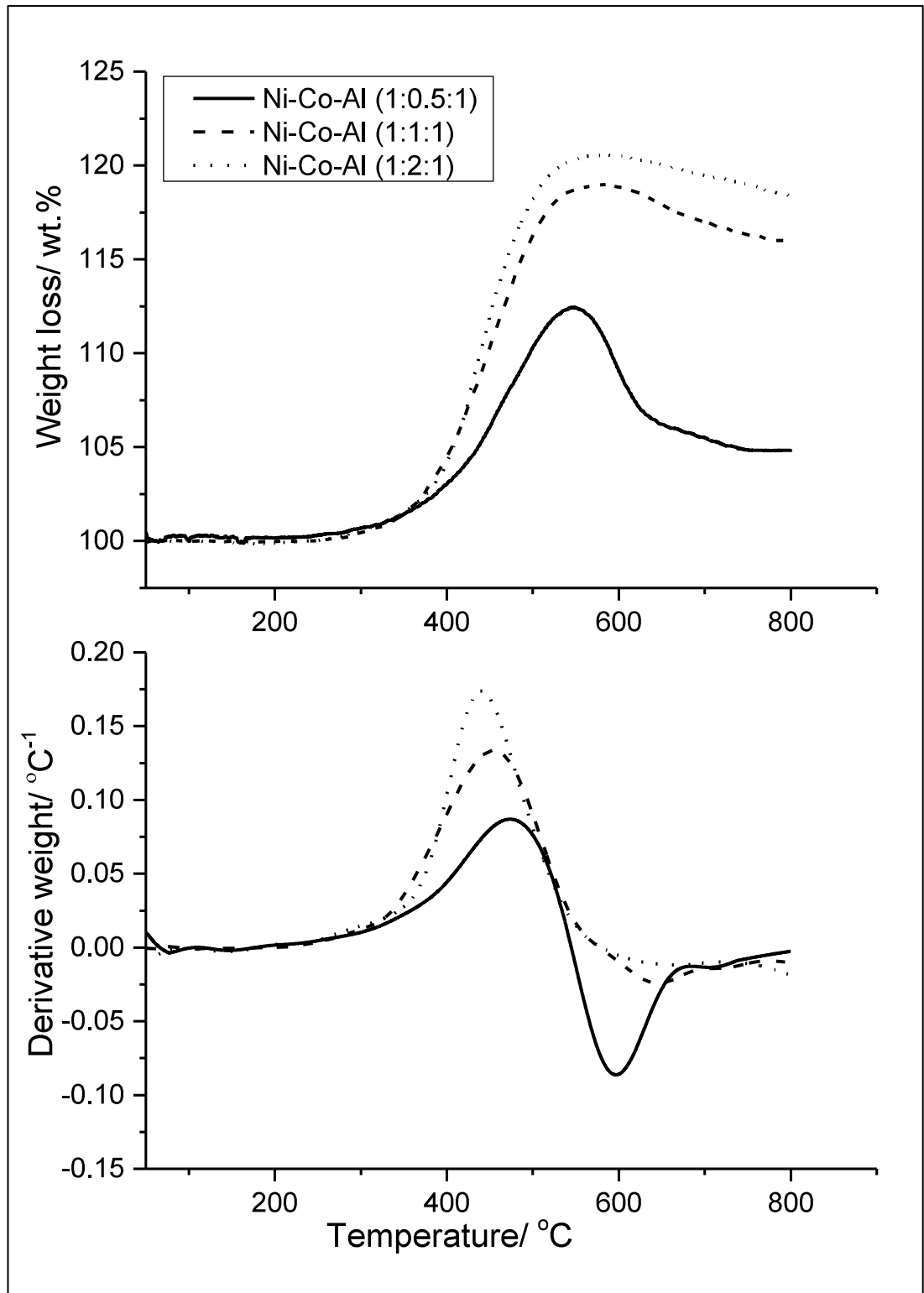


Figure 5.12 DTG-TPO thermograph of different ratio of Ni-Co/Al₂O₃ coked catalysts after pyrolysis-dry reforming of high density polyethylene

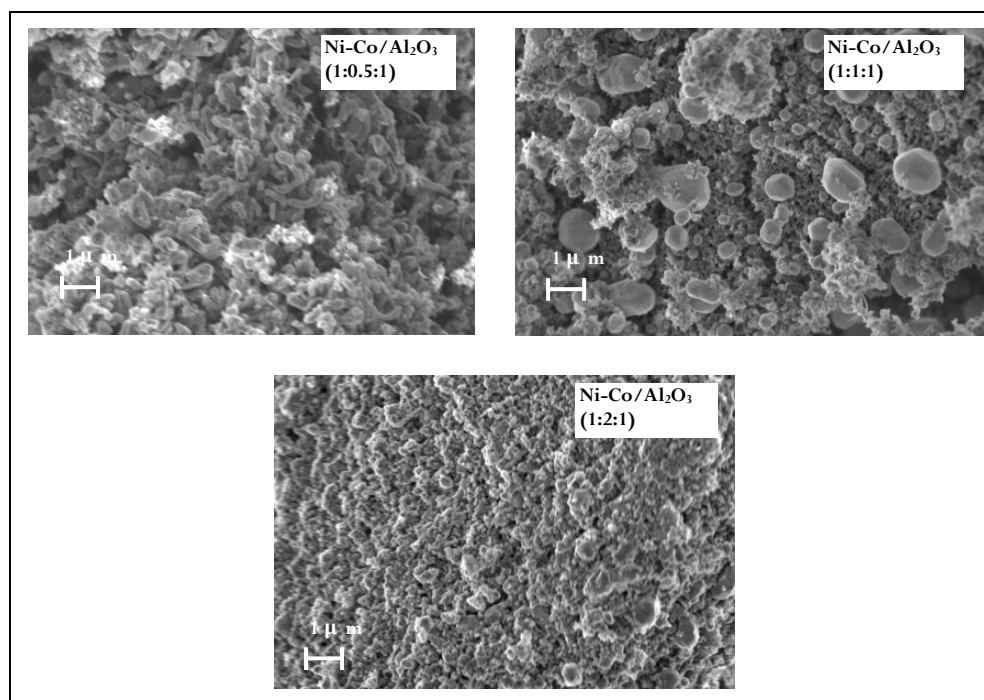


Figure 5.13 SEM results of different ratio of Ni-Co/Al₂O₃ coked catalysts from pyrolysis-gasification/reforming of HDPE, calcined at 750 °C (all SEM micrographs are at the same magnification)

5.4.5 H₂:CO molar ratio from catalytic-dry reforming of high density polyethylene

Tables 6.2 and 6.3 show the H₂:CO molar ratio of the gas produced from the CO₂ reforming of high density polyethylene in relation to the different catalysts used. The H₂:CO ratio in the absence of catalyst was high, ranging from 14.208 for the Ni/Al₂O₃ catalyst to 9.521 for the Ni-Cu/Al₂O₃ catalyst. However, when CO₂ is introduced as the reforming agent, the H₂:CO ratio was reduced to around 0.5.

There have been several reports which highlight the importance of the H₂:CO ratio in relation to the end use application of the product syngas [43-45]. For example, Song and Guo [44] describe the range of syntheses possible using syngas to produce, for example liquid fuels through Fischer Tropsch synthesis, high value chemicals (e.g. aldehydes and alcohols) through the hydroformylation reaction, production of methanol through catalytic reaction with syngas etc. The properties of the syngas, in particular the H₂:CO ratio, influence the potential end-use synthesis of the syngas, for example an ideal H₂:CO ratio for Fischer Tropsch is around 2.0, but for the hydroformylation reaction the optimum H₂:CO ratio is around 1.0 [34]. Here,

the production of a syngas with a H₂:CO ratio of <1.0 for the dry reforming of high density polyethylene is shown.

However, as discussed above for the steam, CO₂ and combined steam/CO₂ reforming of high density polyethylene in the two-stage pyrolysis-reforming reactor used here; the results showed that the hydrogen and CO concentrations in the product syngas were influenced by the relative input amounts of steam/CO₂ reforming agent. Depending on the ratio of steam/CO₂ input the syngas H₂:CO ratio could be manipulated to produce values between 1 and 2. Therefore, process conditions of the two-stage pyrolysis-reforming of plastics could be manipulated to produce a range of desired H₂:CO ratios depending on the steam and CO₂ input.

5.5 Summary

In this chapter, the influence of thermal treatment type, carbon dioxide reforming and effects of steam injection on the production of syngas, i.e. hydrogen and carbon monoxide from waste plastics have been investigated.

Based on the obtained results, it can be concluded that in the pyrolysis process, the use of carbon dioxide as carrier gas does not give a significant affect towards the syngas production. However, thermal treatment of waste high density polyethylene using a two-stage fixed bed reactor significantly improved the hydrogen production compared to the one-stage fixed bed reactor due to the thermal gasification process in the second stage of the reactor in both atmospheres.

In the two-stage fixed bed reactor system, the addition of carbon dioxide as carrier gas not only increased the hydrogen and carbon monoxide production but also reduced carbon deposition. The addition of steam resulted in a marked increase of hydrogen produced from the water gas shift reaction as expected. It is clear that the introduction of steam and carbon dioxide contributed to the improvement in the gas yields and carbon deposition. These empirical findings will serve as a base for future studies of carbon dioxide reforming of waste plastic in later chapters. Less carbon deposition is required especially when the catalyst is introduced to the system.

The addition of catalyst to the CO₂ reforming of high density polyethylene improved the production of synthesis gas (H₂ and CO). It is suggested that the catalytic CO₂/dry reforming has a significant effect on the reformation of high molecular weight of hydrocarbons to hydrogen and carbon monoxide in the catalytic dry reforming process. Carbon deposits on the catalysts were of the filamentous type and were minimised in the presence of carbon dioxide addition due to the reaction of carbon to produce carbon monoxide. Ni/Al₂O₃ catalyst with the addition of cobalt content had higher catalytic activity than Cu and Mg. No detectable carbon formation on the surface of the Ni-Co/Al₂O₃ catalyst suggested that Ni-Co/Al₂O₃ catalyst produces a very high resistance to catalyst deactivation. Adjusting the cobalt content of the catalyst facilitates high catalytic activity for reforming of high density polyethylene with CO₂, in which higher cobalt content contributes towards higher CO₂ conversion and lower coke formation.

References

1. Ramsden, E.N. A-Level Chemistry. Third Edition ed. Cheltenham: Stanley Thornes (Publishers) Ltd, 1994.
2. Beneroso, D., Bermúdez, J.M., Arenillas, A. and Menéndez, J.A. Influence of carrier gas on microwave-induced pyrolysis. *Journal of Analytical and Applied Pyrolysis*. 2015, 113, pp.153-157.
3. Chen, W.-H. and Lin, B.-J. Characteristics of products from the pyrolysis of oil palm fiber and its pellets in nitrogen and carbon dioxide atmospheres. *Energy*. 2016, 94, pp.569-578.
4. Gao, S.-p., Zhao, J.-t., Wang, Z.-q., Wang, J.-f., Fang, Y.-t. and Huang, J.-j. Effect of CO₂ on pyrolysis behaviors of lignite. *Journal of Fuel Chemistry and Technology*. 2013, 41(3), pp.257-264.
5. Farrow, T.S., Sun, C. and Snape, C.E. Impact of CO₂ on biomass pyrolysis, nitrogen partitioning, and char combustion in a drop tube furnace. *Journal of Analytical and Applied Pyrolysis*. 2015, 113, pp.323-331.
6. Zellagui, S., Schönnenbeck, C., Zouaoui-Mahzoul, N., Leysens, G., Authier, O., Thunin, E., Porcheron, L. and Brillhac, J.F. Pyrolysis of coal and woody biomass under N₂ and CO₂ atmospheres using a drop tube furnace - experimental study and kinetic modeling. *Fuel Processing Technology*. 2016, 148, pp.99-109.
7. Onwudili, J.A., Insura, N. and Williams, P.T. Composition of products from the pyrolysis of polyethylene and polystyrene in a closed batch reactor: Effects of temperature and residence time. *Journal of Analytical and Applied Pyrolysis*. 2009, 86(2), pp.293-303.
8. L.D, M., Caballero, B.M., Torres, A., Laresgoiti, M.F., M.J, C. and M.A, C. Recycling polymeric wastes by means of pyrolysis. *Journal of Chemical Technology & Biotechnology*. 2002, 77(7), pp.817-824.
9. Krevelen, D.W.V. and Nijenhuis, K.t. Thermal Decomposition. In: *Properties of Polymers*. Elsevier, 2009, pp.763-776.
10. Treacy, D. and Ross, J.R.H. The potential of the CO₂ reforming of CH₄ as a method of CO₂ mitigation. A thermodynamic study. In: *American*

- Chemical Society Energy and Fuels Symposia Spring (Anaheim), Anaheim. American Chemical Society, 2004, pp.126-127.
11. Tsang, S.C., Claridge, J.B. and Green, M.L.H. Recent advances in the conversion of methane to synthesis gas. *Catalysis Today*. 1995, 23(1), pp.3-15.
 12. Bulushev, D.D. Dry Reforming of Methane to Syn-Gas. [Online]. 2009. [Accessed 29 July 2013]. Available from: <http://www.carbolea.ul.ie/project.php?methane>
 13. Wu, C. and Williams, P.T. Pyrolysis-gasification of plastics, mixed plastics and real-world plastic waste with and without Ni-Mg-Al catalyst. *Fuel*. 2010, 89(10), pp.3022-3032.
 14. Oyama, S.T., Hacıoğlu, P., Gu, Y. and Lee, D. Dry reforming of methane has no future for hydrogen production: Comparison with steam reforming at high pressure in standard and membrane reactors. *International Journal of Hydrogen Energy*. 2012, 37(13), pp.10444-10450.
 15. Huang, C.J., Zheng, X.M., Mo, L.Y. and Fei, J.H. A novel catalyst for CO₂ reforming of CH₄. *Chinese Chemical Letters*. 2001, 12(3), pp.249-232.
 16. Edwards, J.H. and Maitra, A.M. The chemistry of methane reforming with carbon dioxide and its current and potential applications. *Fuel Processing Technology*. 1995, 42(2-3), pp.269-289.
 17. A. Shamsi. Methane Dry Reforming: Effects of Pressure and Promoters on Carbon Formation. In: American Chemical Society Energy and Fuels Symposia Fall, Washington DC. American Chemical Society, 2000, pp.690-693.
 18. Garcia, L., Benedicto, A., Romeo, E., Salvador, M.L., Arauzo, J. and Bilbao, R. Hydrogen production by steam gasification of biomass using Ni-Al coprecipitated catalysts promoted with magnesium. *Energy & Fuels*. 2002, 16(5), pp.1222-1230.
 19. Benguerba, Y., Dehimi, L., Virginie, M., Dumas, C. and Ernst, B. Modelling of methane dry reforming over Ni/Al₂O₃ catalyst in a fixed-bed catalytic reactor. *Reaction Kinetics, Mechanisms and Catalysis*. 2014, 114(1), pp.109-119.
 20. Adrados, A., de Marco, I., Caballero, B.M., Lopez, A., Laresgoiti, M.F. and Torres, A. Pyrolysis of plastic packaging waste: A comparison of plastic

residuals from material recovery facilities with simulated plastic waste. *Waste Management*. 2012, 32(5), pp.826-832.

21. Damyanova, S., Pawelec, B., Arishtirova, K. and Fierro, J.L.G. Ni-based catalysts for reforming of methane with CO₂. *International Journal of Hydrogen Energy*. 2012, 37(21), pp.15966-15975.
22. Foo, S.Y., Cheng, C.K., Nguyen, T.-H. and Adesina, A.A. Syngas production from CH₄ dry reforming over Co–Ni/Al₂O₃ catalyst: Coupled reaction-deactivation kinetic analysis and the effect of O₂ co-feeding on H₂:CO ratio. *International Journal of Hydrogen Energy*. 2012, 37(22), pp.17019-17026.
23. Wu, T., Zhang, Q., Cai, W., Zhang, P., Song, X., Sun, Z. and Gao, L. Phyllosilicate evolved hierarchical Ni- and Cu–Ni/SiO₂ nanocomposites for methane dry reforming catalysis. *Applied Catalysis A: General*. 2015, 503, pp.94-102.
24. Wang, C., Dou, B., Chen, H., Song, Y., Xu, Y., Du, X., Zhang, L., Luo, T. and Tan, C. Renewable hydrogen production from steam reforming of glycerol by Ni–Cu–Al, Ni–Cu–Mg, Ni–Mg catalysts. *International Journal of Hydrogen Energy*. 2013, 38(9), pp.3562-3571.
25. Kim, P., Kim, Y., Kang, T., Song, I.K. and Yi, J. Preparation of nickel-mesoporous materials and their application to the hydrodechlorination of chlorinated organic compounds. *Catalysis Surveys from Asia*. 2007, 11(1-2), pp.49-58.
26. Wu, C. and Williams, P.T. Investigation of Ni-Al, Ni-Mg-Al and Ni-Cu-Al catalyst for hydrogen production from pyrolysis–gasification of polypropylene. *Applied Catalysis B: Environmental*. 2009, 90(1–2), pp.147-156.
27. Wang, C., Dou, B., Chen, H., Song, Y., Xu, Y., Du, X., Luo, T. and Tan, C. Hydrogen production from steam reforming of glycerol by Ni–Mg–Al based catalysts in a fixed-bed reactor. *Chemical Engineering Journal*. 2013, 220(0), pp.133-142.
28. Cheng, C.K., Foo, S.Y. and Adesina, A.A. H₂-rich synthesis gas production over Co/Al₂O₃ catalyst via glycerol steam reforming. *Catalysis Communications*. 2010, 12(4), pp.292-298.
29. Fakeeha, A.H., Khan, W.U., Al-Fatesh, A.S., Abasaheed, A.E. and Naeem, M.A. Production of hydrogen and carbon nanofibers from methane over

- Ni–Co–Al catalysts. *International Journal of Hydrogen Energy*. 2015, 40(4), pp.1774-1781.
30. Galetti, A.E., Gomez, M.F., Arrúa, L.A. and Abello, M.C. Ni catalysts supported on modified ZnAl₂O₄ for ethanol steam reforming. *Applied Catalysis A: General*. 2010, 380(1–2), pp.40-47.
 31. Al-Fatesh, A. Suppression of carbon formation in CH₄–CO₂ reforming by addition of Sr into bimetallic Ni–Co/ γ -Al₂O₃ catalyst *Journal of King Saud University - Engineering Sciences*. 2015, 27(1), pp.101-107.
 32. Williams, P.T. and Williams, E.A. Interaction of Plastics in Mixed-Plastics Pyrolysis. *Energy & Fuels*. 1999, 13(1), pp.188-196.
 33. Yamada, H., Mori, H. and Tagawa, T. CO₂ reforming of waste plastics. *Journal of Industrial and Engineering Chemistry*. 2010, 16(1), pp.7-9.
 34. Rynkowski, J.M., Paryjczak, T. and Lenik, M. On the nature of oxidic nickel phases in NiO/ γ -Al₂O₃ catalysts. *Applied Catalysis A: General*. 1993, 106(1), pp.73-82.
 35. Wu, C. and Williams, P.T. Investigation of coke formation on Ni-Mg-Al catalyst for hydrogen production from the catalytic steam pyrolysis-gasification of polypropylene. *Applied Catalysis B: Environmental*. 2010, 96(1–2), pp.198-207.
 36. Gucci, L., Stefler, G., Geszti, O., Sajó, I., Pászti, Z., Tompos, A. and Schay, Z. Methane dry reforming with CO₂: A study on surface carbon species. *Applied Catalysis A: General*. 2010, 375(2), pp.236-246.
 37. Zhang, J., Wang, H. and Dalai, A.K. Development of stable bimetallic catalysts for carbon dioxide reforming of methane. *Journal of Catalysis*. 2007, 249(2), pp.300-310.
 38. Xu, J., Zhou, W., Li, Z., Wang, J. and Ma, J. Biogas reforming for hydrogen production over nickel and cobalt bimetallic catalysts. *International Journal of Hydrogen Energy*. 2009, 34(16), pp.6646-6654.
 39. Rahemi, N., Haghighi, M., Babaluo, A.A., Jafari, M.F. and Khorram, S. Non-thermal plasma assisted synthesis and physicochemical characterizations of Co and Cu doped Ni/Al₂O₃ nanocatalysts used for dry reforming of methane. *International Journal of Hydrogen Energy*. 2013, 38(36), pp.16048-16061.
 40. San José-Alonso, D., Illán-Gómez, M.J. and Román-Martínez, M.C. Low metal content Co and Ni alumina supported catalysts for the CO₂ reforming

of methane. *International Journal of Hydrogen Energy*. 2013, 38(5), pp.2230-2239.

41. Liu, C., Cundari, T.R. and Wilson, A.K. CO₂ Reduction on Transition Metal (Fe, Co, Ni, and Cu) Surfaces: In Comparison with Homogeneous Catalysis. *The Journal of Physical Chemistry C*. 2012, 116(9), pp.5681-5688.
42. Zhang, J., Wang, H. and Dalai, A.K. Effects of metal content on activity and stability of Ni-Co bimetallic catalysts for CO₂ reforming of CH₄. *Applied Catalysis A: General*. 2008, 339(2), pp.121-129.
43. Z. Jiang, T.X., V. L. Kuznetsov and P. P. Edwards. Turning Carbon Dioxide into Fuel. *Philosophical Transactions of The Royal Society A*. 2010, 368, pp.3343-3364.
44. Song, X. and Guo, Z. Technologies for direct production of flexible H₂/CO synthesis gas. *Energy Conversion and Management*. 2006, 47, pp.560-569.
45. Cao, Y., Gao, Z., Jin, J., Zhou, H., Cohron, M., Zhao, H., Liu, H. and Pan, W. Synthesis Gas Production with an Adjustable H₂/CO Ratio through the Coal Gasification Process: Effects of Coal Ranks And Methane Addition. *Energy & Fuels*. 2008, 22(3), pp.1720-1730.

Chapter 6

PYROLYSIS-DRY REFORMING OF VARIOUS PLASTICS FOR SYNGAS PRODUCTION

In this chapter, pyrolysis-catalytic-dry reforming of different types of waste plastics (LDPE, HDPE, PS, PET, and PP) as well as a simulated mixture of the waste plastics representative of municipal solid waste plastic has been investigated as presented in Research Objective 4. In previous Chapter, the two-stage, pyrolysis-catalytic reforming reactor system has significantly improved the production of syngas compared to one stage system. Therefore this type of reactor is chosen to implement the dry reforming reaction. The evolved gases from pyrolysis of the plastics (2 g of plastic sample) are passed to the second reactor where catalytic-dry reforming (1 g of catalyst) takes place. CO₂ input rate was 6 g h⁻¹ injected into the second furnace and N₂ was used as a carrier gas with a flow rate of and 200 ml min⁻¹ respectively. The comparison between the thermal cracking and the CO₂ dry reforming process has been studied. The effect of the Ni-Co/Al₂O₃ catalyst in relation to the CO₂ reformation of waste plastics pyrolysis gases has also been investigated. The Ni-Co/Al₂O₃ catalyst has been shown to be efficient for enhancing the syngas yields and reducing the coke formation on the catalyst surface from dry reforming of plastics as also reported in previous chapter (Chapter 5). The characteristics of the coke deposited on the catalyst are also reported.

6.1 Non-catalytic CO₂ Dry Reforming of Various Plastics

Baseline experiments were initially carried out with the HDPE, LDPE, PP, PS and PET in the absence of carbon dioxide and in the absence of the catalyst, where quartz sand was substituted for the catalyst bed in the second stage reactor. These types of plastics are the most common plastics found in municipal solid waste treatment plants and other waste streams e.g. plastics from building construction waste treatment plant and plastics from household packaging waste treatment plant. Each plastic will have different polymer structures as shown in Figure 1.7 (Chapter 2). Therefore, this study will investigate the influence of

polymer structure towards the production of syngas from the dry reforming process.

The proximate and ultimate analysis results for each individual plastic are shown in Chapter 3 (Section 3.4.1.1). Based on the result of the analysis in Table 3.10 (a), all the individual plastics; HDPE, LDPE, PP, PS and PET have no detectable of sulphur content while the raw materials from several waste treatment plants have very low sulphur content. Othman et al. also found the similar results for PE, PP and PS from electronic plastic waste, where there is no presence of sulphur content in their samples [1]. There was no oxygen detectable on the LDPE and HDPE waste plastic. It can be observed that both LDPE and HDPE were composed of almost identical hydrogen and carbon content; 18.59 wt.%, 18.86 wt.% and 83.40 wt.%, 82.25 wt.% respectively. HDPE was highest in hydrogen content while PS was highest in carbon content. PS also, on the other hand, has the lowest hydrogen content with only 12.43 wt.% was achieved. Nevertheless, the carbon content in the PET was the lowest with only 60.74 wt.%. However, PET has the highest oxygen content, 21.78 wt.% compared to others. The higher heating value (HHV) and lower heating value (LHV) are the important properties which define the quantitative energy content and determine the clean and efficient use of the waste plastic. In this investigation, the HHV and LHV of the individual plastics were in the order of: LDPE>HDPE >PS>PP>PET.

The results for the product yield and syngas yield are shown in Table 6.1. The results indicate that the highest percentage yield of gases was found in relation to the thermal processing of PET with 69.5 wt.% followed by HDPE (51.7 wt.%), LDPE (49.3 wt.%), PP (33.8 wt.%) and PS (17.2 wt.%). PET was also highest in the yield of solid residue with 19.50 wt.% while no solid residue was detected for HDPE and LDPE. PET has a chemical structure and associated thermal behaviour, which is different, compared to the polyalkene plastics, thus increasing the final amount of solid residue. Alvarez et.al [2] also reported a high solid residue in their experiments with the pyrolysis-gasification of a mixture of biomass/plastic which was attributed to the PET content of the plastics.

Table 6.1 also shows the carbonaceous coke deposited on the catalyst from non-catalytic, non-CO₂ reforming of waste plastics. The highest mass of carbonaceous coke deposited on the catalyst was found with the thermal processing of PS with 59.0 wt.% followed by PP (58.5 wt.%), LDPE (46.5 wt.%), HDPE (41.0 wt.%)

and PET (6.0 wt.%). PS was also highest in terms of liquid yield with 16 wt.% compared to other plastics, which may be due to PS which required higher reaction energy [3]. Kumagai et.al.[4] in their study on the thermal decomposition of individual and mixed plastics in an electrically heated vertical tube reactor, also found that PS was mainly decomposed into liquid at 600 °C. They also concluded that the main component of the decomposition was styrene, principally responsible for the nC₉ fraction.

Table 6.1 Two-stage pyrolysis of different plastics with no catalyst and no carbon dioxide (quartz sand in the 2nd stage at a temperature of 800 °C)

Plastic type	HDPE	LDPE	PP	PS	PET
<i>Product yield (wt. %)</i>					
Gas	51.7	49.3	33.8	17.2	69.5
Liquid	7.0	1.5	0.5	16.0	2.0
Residue	nd*	nd*	7.0	5.0	19.5
Carbon deposition	41.0	46.5	58.5	59.0	6.0
Mass balance	99.7	97.3	99.8	97.2	97.0
<i>Syngas yield (mmol_{syngas} g⁻¹_{plastic})</i>					
H ₂ + CO production	31.9	41.8	35.8	25.3	31.2
H ₂ :CO molar ratio	13.0	10.5	12.6	11.0	0.6

*nd; not detected

Table 6.2 Pyrolysis-catalysis of different plastics in the presence of carbon dioxide and no catalyst (quartz sand in the 2nd stage at a temperature of 800 °C)

Plastic type	HDPE	LDPE	PP	PS	PET
<i>Product yield (wt. %)</i>					
Gas	90.6	99.2	95.6	92.1	97.1
Liquid	2.0	0.6	0.6	1.3	2.9
Residue	0.2	0.1	1.4	0.9	4.1
Carbon deposition	2.8	3.4	4.9	8.5	0.8
Mass balance	95.6	103.3	102.5	102.8	104.9
<i>Syngas yield (mmol_{syngas} g⁻¹_{plastic})</i>					
H ₂ + CO production	105.4	117.3	94.6	91.1	39.0
H ₂ :CO molar ratio	0.5	0.5	0.5	0.4	0.2

The gases produced for the non-catalytic, none CO₂ reforming experiments showed only small amounts of carbon dioxide were produced. The carbon dioxide produced for the experiment with PET produced about 0.13g of CO₂, or 6.5 wt.% of CO₂. Therefore, the product carbon dioxide from the plastics was neglected in the CO₂ conversion calculations.

The two-stage dry reforming of HDPE, LDPE, PP, PS and PET was carried out, again in the absence of catalyst (instead, substituting quartz sand) at a carbon dioxide flow rate of 6.0 g h⁻¹. The product yield and syngas yield are shown in Table 6.2. In these dry reforming experiments, all the plastics showed a large increase in gas yield with more than 90 wt.% gas yield for each of the waste plastics. There was a corresponding marked reduction in liquid yield for all the plastics. The sand therefore shows a significant activity in relation to the interaction of the pyrolysis gases and carbon dioxide. Sand can contain trace levels of metal contaminants which may act as a catalyst for reaction. It is suggested that the presence of carbon dioxide contributes to the thermal cracking of large molecular weight hydrocarbons in the second stage reactor by introducing the dry reforming reaction (Reaction 2.11), hence increasing the amount of gases yield compared to the experiment with no carbon dioxide.

In contrast, the amount of carbon deposited on the quartz sand in the second stage reactor was reduced by more than 85% with the introduction of carbon dioxide for the dry reforming experiments for all plastics (Table 6.2) compared to the experiment with no carbon dioxide addition (Table 6.1). The reduction of carbon deposition might be caused by the Boudouard reaction (Reaction 2.10) of carbon dioxide and carbon to produce carbon monoxide in the dry reforming experiment. Figure 6.1 shows that a marked increase in carbon monoxide yield was obtained for the dry reforming of the plastics over the quartz sand. A study of CO₂-gasification in a macro-TGA by Meng et al. [5] found a large impact of mass loss on CO₂-gasification of biomass due to their high fixed carbon; they also found a slight impact on mass loss from CO₂-gasification of PET, PVC, PP and PS at temperatures above 750 °C. Chen et al. [6] also concluded that there was a high conversion efficiency of carbon dioxide and carbon in the gasification of combustible solid waste including PE and PS at a high temperature range (> 700 °C) was found in a carbon dioxide atmosphere compared to that in a nitrogen atmosphere.

The gas composition and syngas production from the two-stage dry reforming of HDPE, LDPE, PP, PS and PET with carbon dioxide in the presence of quartz sand (no catalyst) are shown in Figure 6.1 which shows the gas yields of carbon monoxide, hydrogen, methane and C₂-C₄ hydrocarbons. PET showed the highest concentration of carbon monoxide compared to other plastics in the experiment with no carbon dioxide. The gas concentration for the processing of HDPE, LDPE and PP showed comparable behaviour with quite high concentration of methane. The hydrogen concentrations were also similar for these three plastics. By comparison, there was a large increase in carbon monoxide yields for all plastics for the dry reforming experiments compared to the absence of carbon dioxide. There were only small differences in the hydrogen yields for all plastics in both conditions. It also appears that the introduction of carbon dioxide has only a small influence on the methane and C₂-C₄ hydrocarbons yields except for HDPE, which showed a reduction from 0.40 to 0.10 g_{gas} g⁻¹_{plastic}.

Figure 6.2 shows the yield of syngas (H₂ + CO) and CO₂ conversion for the thermal processing of the waste plastics under the different process conditions. The highest syngas yield was produced by LDPE at 117.3 mmol_{syngas}g⁻¹_{LDPE} for the CO₂ dry reforming experiment compared with 41.8 mmol_{syngas}g⁻¹_{LDPE} for the experiment with no carbon dioxide (Figure 6.2). LDPE also showed a large reduction of carbon deposition on the quartz sand with an ~90% reduction when carbon dioxide was introduced as the reforming gas (Comparison of Table 6.1 and Table 6.2). Carbon monoxide contributed more than 70% to the total of syngas production in the dry reforming experiment. For the CO₂ dry reforming experiments, the highest CO₂ conversion was with HDPE at 40.8%, followed by LDPE (37.9%), PS (32.1%), PP (31.9%) and PET (2.9%) (Figure 6.2).

As discussed in Chapter 5, pyrolysis of polyalkene plastics (LDPE, HDPE and PP) behave quite similarly due to their similar polyalkene chemical structure as shown in Figure 1.7 (Chapter 2). Thermal degradation of polyalkene polymers mainly produced hydrocarbon gases of the alkene group as expected; ethene, propene and butene via random scission process. The addition of the gasification stage in the 2nd furnace further gasified the pyrolysis products from the 1st furnace. Pyrolysis-gasification of polyalkene polymers produced quite similar amounts of gas yield with high concentration of hydrogen due to reformation of alkenes and alkanes from the pyrolysis stage that easily gasified in the 2nd furnace compared to aromatic compound.

The pyrolysis-gasification of PS produced the least amount of gas yield compared to other plastics. As mentioned above, thermal degradation of polystyrene requires higher reaction energy and produced highest amount of liquid (wax/oil) due to its styrene aromatic polymer structure.

The highest gas concentration was obtained from pyrolysis-gasification of PET with highest concentration of CO among other plastics. PET polymer structure as shown in Figure 1.7 (Chapter 2) contain of an aromatic ring and also O₂. High amount of CO may be formed via decarboxylation between PET and also the reaction between char and CO₂. PET also produced a high amount of residue after the experiment however the amount was reduced from only pyrolysis (Chapter 5), 23.0 wt% to 19.5 wt.% and further reduced to 4.1 wt.% in dry reforming process.

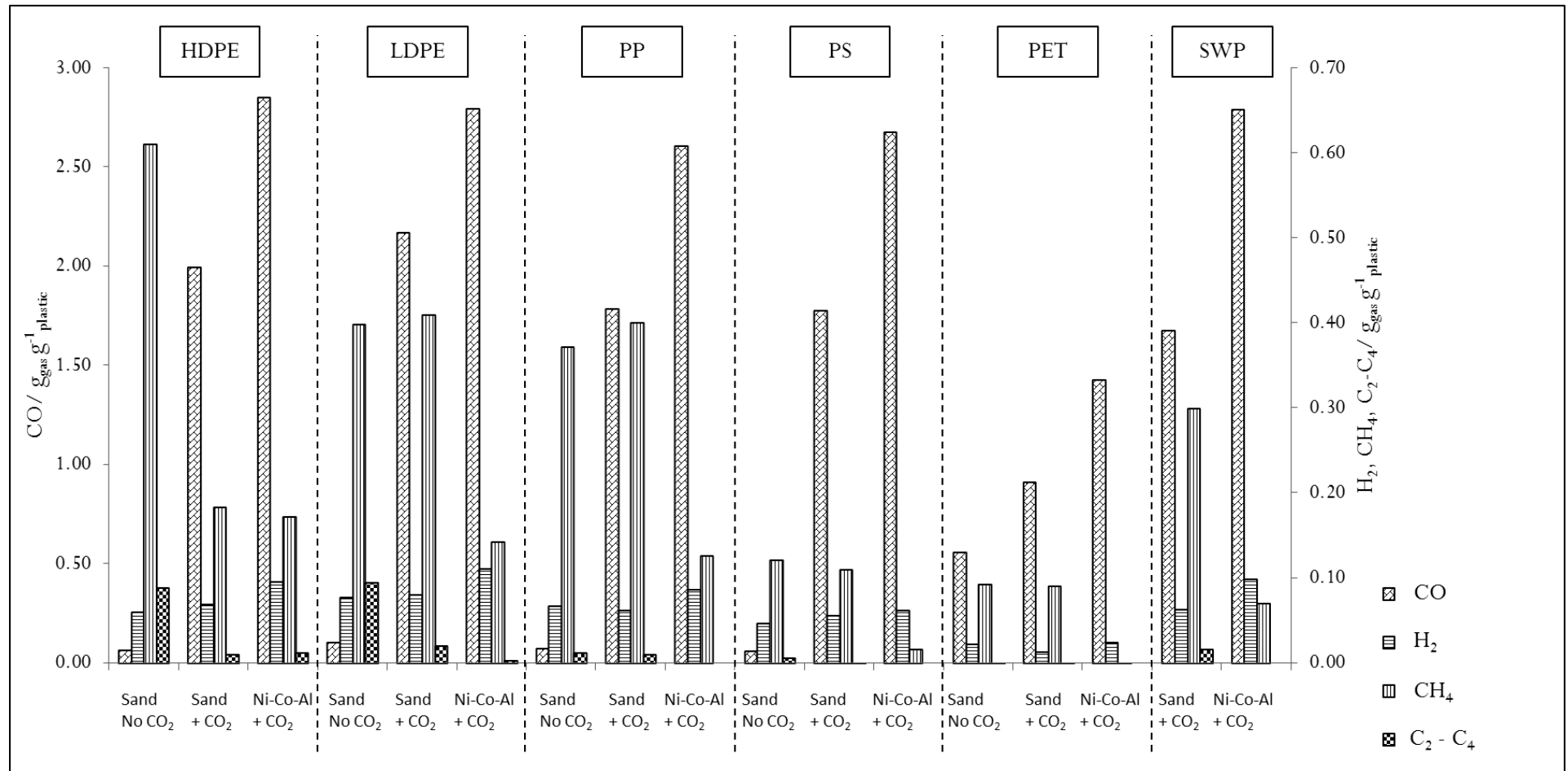


Figure 6.1 Gas compositions for the pyrolysis-dry reforming of the different plastics and the simulated mixture of plastics under various process conditions

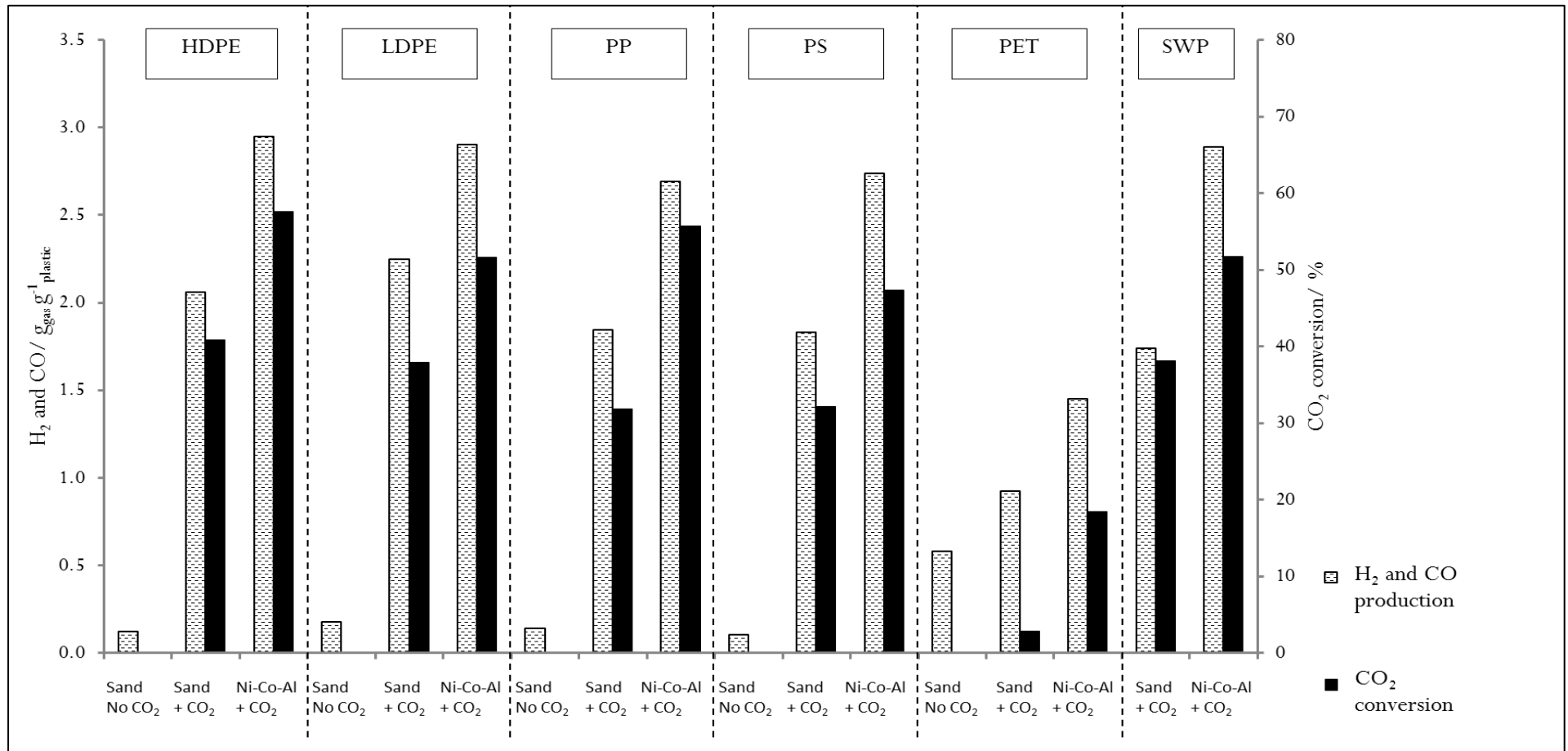


Figure 6.2 Syngas (hydrogen and carbon monoxide) production and carbon dioxide conversion from pyrolysis-dry reforming of various types of plastics

6.2 Ni-Co/Al₂O₃ Catalytic CO₂ Dry Reforming of Various Plastics

The pyrolysis-CO₂ dry reforming of the different waste plastics, (HDPE, LDPE, PP, PS and PET) was carried out with the Ni-Co/Al₂O₃ catalyst. The product yields, gas compositions and syngas production/CO₂ conversion for the catalytic-dry reforming of HDPE, LDPE, PP, PS and PET are shown in Table 6.3, Figure 6.1 and Figure 6.2.

Table 6.3 Pyrolysis-dry reforming of different plastics in the presence of Ni-Co/Al₂O₃ catalyst and carbon dioxide (catalyst temperature 800 °C and CO₂ flow rate of 6.0 gh⁻¹)

Plastic type	HDPE	LDPE	PP	PS	PET
<i>Product yield (wt. %)</i>					
Gas	94.8	98.3	90.6	97.1	94.3
Liquid	2.4	0.3	2.5	2.4	1.0
Residue	nd*	nd*	1.7	1.0	4.0
Carbon deposition	nd*	0.9	1.0	4.3	nd*
Mass balance	97.2	99.5	95.8	104.8	99.3
<i>Syngas yield (mmol_{syngas} g⁻¹ plastic)</i>					
H ₂ + CO production	149.4	154.7	136.0	126.3	63.0
H ₂ :CO molar ratio	0.5	0.6	0.5	0.3	0.2

nd; not detected

Table 6.3 shows that when the Ni-Co/Al₂O₃ catalyst was added to the 2nd stage, there appeared to be little change in the product yields; however, the composition of the gases was significantly changed (Figure 6.1). Also, the carbon deposited on the catalyst was reduced by more than 50% with the Ni-Co/Al₂O₃ catalyst addition for the dry reforming of the various waste plastics. For example, the carbon deposits on the catalyst were reduced from 3.4 to 0.9 wt.% for LDPE, 8.5 to 4.3 wt.% for PS, 4.9 to 1.0 wt.% for PP and almost no carbon was deposited on the catalyst for HDPE and PET. It is suggested that the Boudourd reaction is more active with the addition of catalyst, thus reducing the amount of carbon deposited on the catalyst.

Figure 6.1 shows the gas composition for CO₂ dry reforming of the waste plastics with the addition of Ni-Co/Al₂O₃ catalyst. A marked increase in carbon monoxide yield for all of the plastics is shown in the presence of the carbon dioxide and catalyst. This is in agreement with the dry reforming and Bourdourd reaction in which both reactions produced carbon monoxide, twice the number of moles of carbon monoxide for each reaction. This data was also supported by the major reduction of hydrocarbons concentration (methane and C₂-C₄ hydrocarbons) for the catalytic dry reforming of all of the waste plastics, which are required in the dry reforming reaction. There was only a small increase of hydrogen with the addition of catalyst for the dry reforming of the plastics.

Table 6.3 shows the yield of syngas (H₂ + CO) and the H₂:CO molar ratio for the catalytic dry reforming of the waste plastics. The addition of the Ni-Co/Al₂O₃ catalyst in the dry reforming experiments further increased the syngas yield for all plastics compared to the non-catalytic dry reforming of the plastics (Tables 6.2). The highest increase was found for HDPE with a 44% rise, from 105 to 149.4 mmol_{syngas} g⁻¹_{plastic}, followed by PP with a 41% increase, LDPE with 37%, PS with 35% and PET with a 24% rise in syngas yield (comparison of Table 6.2 and Table 6.3). The carbon dioxide conversion was also increased for all plastics in the presence of the Ni-Co/Al₂O₃ catalyst. The addition of catalyst enhanced the dry reforming reaction in the gasification reactor as well as reducing the formation of carbon on the catalyst surface compared to the non-catalytic experiment. Goula et al. [7] also reported that the presence of a catalyst in the dry reforming process enhanced syngas production.

6.3 Catalytic CO₂ Dry Reforming of Mixed Waste Plastics

Catalytic (Ni-Co/Al₂O₃ catalyst) dry reforming of a simulated mixture of the waste plastics (SWP) was carried out, blending the different waste plastics to produce a representative mixture as that found in municipal solid waste [8]. The mixture consisted of 42 wt. % LDPE, 20 wt. % HDPE, 16 wt. % PS, 12 wt. % PET, and 10 wt.% PP. In addition, a baseline experiment using quartz sand and carbon dioxide was carried out. The results are shown in Table 6.4. The experiment in the absence of carbon dioxide and catalyst/quartz sand was not carried out, since

comparison here was to show the influence of the dry reforming Ni-Co/Al₂O₃ catalyst on syngas production.

Table 6.4 Pyrolysis-CO₂ dry reforming of simulated mixture of different plastics in the presence of sand or Ni-Co/Al₂O₃ catalyst and carbon dioxide (2nd stage reactor temperature, 800 °C and CO₂ flow rate of 6.0 gh⁻¹)

Catalyst	simulated mixture of plastics	
	Sand	Ni-Co/Al ₂ O ₃
<i>Product yield (wt. %)</i>		
Gas	87.6	97.1
Liquid	1.4	0.6
Residue	1.0	0.6
Carbon deposition	5.5	1.7
Mass balance	95.5	99.9
<i>Syngas yield (mmol_{syngas} g⁻¹_{swp})</i>		
H ₂ + CO production	91.3	148.6
H ₂ :CO molar ratio	0.5	0.5

As shown in Table 6.4, the addition of the Ni-Co/Al₂O₃ catalyst decreased the amount of product liquid from 1.4 to 0.6 wt.% and catalyst carbon deposits from 5.5 to 1.7 wt.%. However, the gas yield increased from 87.6 to 97.1 wt.%. Figure 6.1 shows the composition of gases produced from the dry reforming of the simulated waste plastic mixture. Carbon monoxide contributed the highest gas yield with the quartz sand and also the Ni-Co/Al₂O₃ catalyst. The introduction of Ni-Co/Al₂O₃ catalyst reduced the methane yield from 0.15 to 0.04 g_{gas} g⁻¹_{swp}, and no C₂-C₄ hydrocarbons was detected, hence increasing the carbon monoxide from 1.7 to 2.8 g_{gas} g⁻¹_{swp} and hydrogen yield from 0.06 to 0.1 g_{gas} g⁻¹_{swp}. This suggests that the addition of the catalyst enhanced the dry reforming reaction, therefore more carbon monoxide and hydrogen was produced.

Figure 6.2 shows that the CO₂ conversion increased from 38.2% to 56.5% when the Ni-Co/Al₂O₃ catalyst was added into the CO₂ dry reforming reaction compared to quartz sand. This is also in agreement with the increase in the total syngas production from 91.3 to 148.6 mmol_{syngas} g⁻¹_{swp}. By comparison, the gas compositions from the CO₂ dry reforming of the simulated mixture of the waste plastic were similar to the gas compositions from the dry reforming of LDPE and

HDPE, suggesting the high fraction of these two plastics (42 wt.% LDPE, 20 wt.% HDPE) in the simulated mixture of waste plastics dominated the product yields and gas compositions.

6.4 Characterization of the Coked Catalyst

The carbonaceous coke deposits on the catalyst for the dry reforming experiments with the Ni-Co/Al₂O₃ catalyst were examined by SEM and TPO. Figure 6.3 shows the SEM micrographs of the reacted Ni-Co/Al₂O₃ catalyst from dry reforming of the different waste plastics and the simulated mixture of plastics. SEM observation shows that most of the carbons were amorphous in nature. Only the carbon deposited on the catalyst from dry reforming of LDPE showed any signs of the presence of filamentous carbon. The micrographs of the catalyst used for dry reforming of the different waste plastics suggest that the surface of each catalyst used developed a different surface structure depending on the type of plastic used. There was an indication that larger particles were observed for the used catalyst with PP and PS processing and LDPE produced a more amorphous structure compared with the used catalyst from SWP processing which showed smaller, more uniform particle. This may be associated with the formation of carbon on the surface or particle sintering during the catalytic dry reforming reactions [9]. The carbon formation on PS may also be due to layered carbons (reactive carbon) formation on the catalyst surface from the reformation of heavier hydrocarbon compounds from pyrolysis of PS [10].

Temperature programmed oxidation (TPO) was also carried out on the catalyst after reaction to determine the type of carbon deposited on the catalyst surface. The TGA-TPO and DTG-TPO thermograms of the coke formed on the Ni-Co/Al₂O₃ catalyst from the dry reforming of LDPE, HDPE, PS, PET, PP and the simulated waste plastic mixture (SWP) are shown in Figure 6.4. TGA-TPO observation shows an initial weight gain for all of the used catalyst, which is attributed to the oxidation of the nickel in the Ni-Co/Al₂O₃ catalyst. The DTG-TPO thermograms shows that all the catalyst have an increase in peak weight at around a temperature of 400 °C – 500 °C, attributed to the oxidation of the nickel. LDPE showed a weight loss peak around 550 °C due to the combustion of carbon on the catalyst surface during the TPO experiment, this has been confirmed by SEM analysis where filamentous type carbons were observed on the catalyst

surface. Some of the samples, e.g. PS and the SWP showed another weight loss peak at high temperature around 720 °C. Dong et al. [11] suggested that oxidation of carbon at these high temperature above 500 °C might be due to the formation of a large amount of inert carbon (such as amorphous or crystalline graphitic carbon) on the catalyst surface. Sengupta et al. [12] discussed in their TPH analysis of 15Ni/Al₂O₃, NiCo/Al₂O₃ and 15NiCo/Al₂O₃ that a high temperature peak of H₂-consumption around 820 K has been observed on these three catalysts. They concluded that these high temperature peaks were assigned to those carbon species that were inactive and may cause catalyst deactivation.

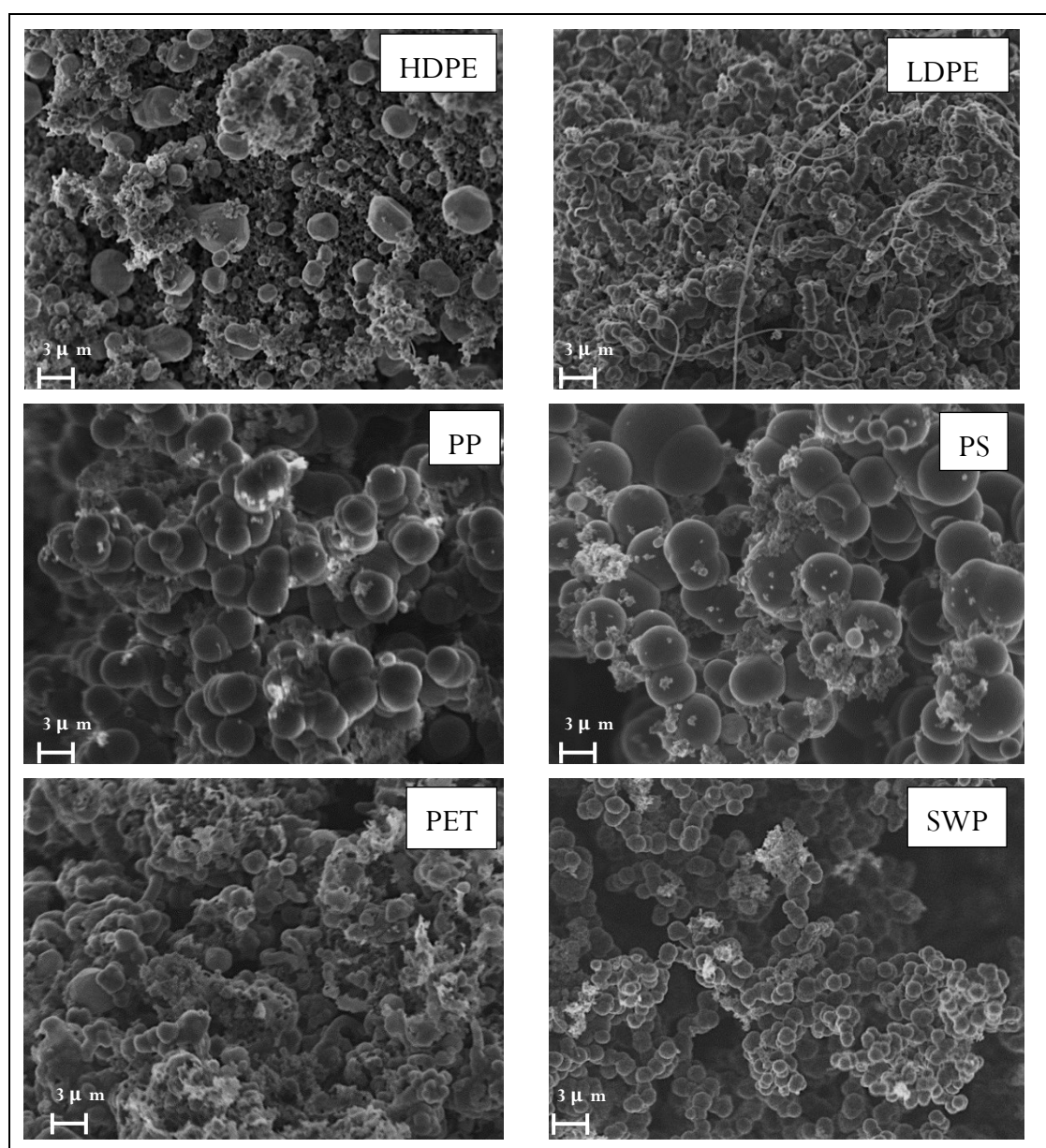
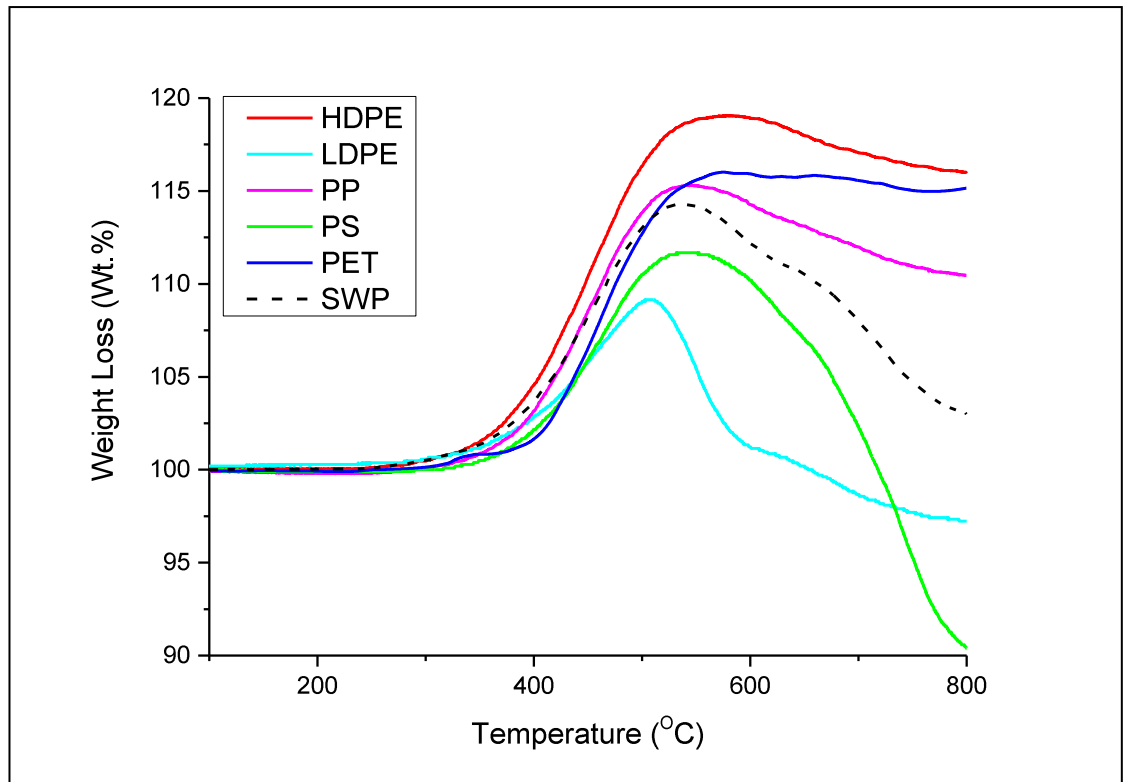
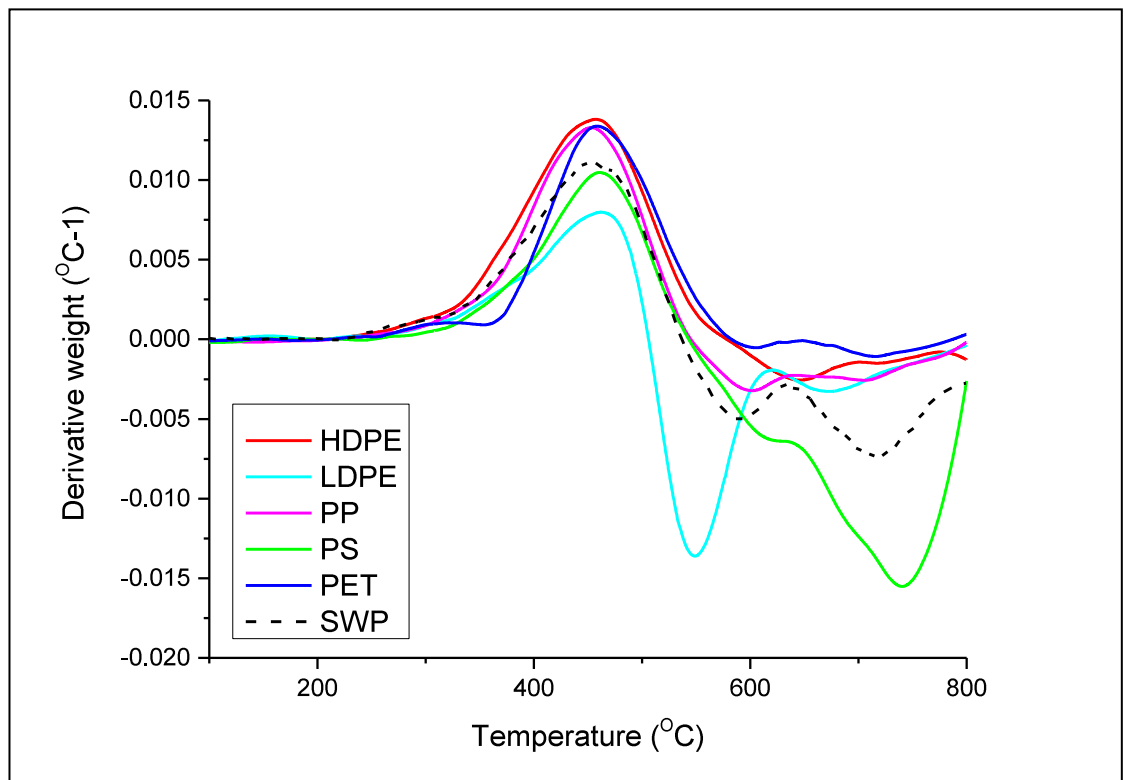


Figure 6.3 SEM tomographic images for the reacted Ni-Co/Al₂O₃ catalyst surface from catalytic-dry reforming of individual plastic (all SEM micrographs are at the same magnification)



(a)



(b)

Figure 6.4 TPO results for the reacted Ni-Co/ Al_2O_3 catalyst after catalytic-dry reforming of waste plastics; (a) TGA-TPO, (b) DTG-TPO

6.5 Summary

In this chapter, the pyrolysis-catalytic CO₂ dry reforming of various types of waste plastics (LDPE, HDPE, PS, PET, and PP) as well as a simulated mixture of waste plastics (SWP) has been investigated. The results show that the introduction of CO₂ dry reforming of the products of plastics pyrolysis in the absence of a catalyst dramatically increased the total gas production to over 90 wt.% for all of the plastics. The carbon dioxide was involved in the reforming of the product hydrocarbons formed from the pyrolysis of the plastics. The introduction of a Ni-Co/Al₂O₃ catalyst significantly improved the production of syngas comprising the hydrogen and carbon monoxide content of the product gases. The highest yield of syngas was 154.7 mmol_{syngas} g⁻¹_{plastic} produced from the pyrolysis-catalytic dry reforming of LDPE. PET produced significantly lower concentrations of syngas. The syngas yield from the processing of the simulated waste plastic mixture was 148.67 mmol_{syngas} g⁻¹_{plastic} which reflected the high content of LDPE and HDPE in the simulated waste plastic mixture.

References

1. Othman, N., Basri, N.E.A., Yunus, M.N.M. and Sidek, L.M. Determination of Physical and Chemical Characteristics of Electronic Plastic Waste (E-waste) Resin using Proximate and Ultimate Analysis Method. In: International Conference on Construction and Building Technology. 2008, pp.169-180.
2. Alvarez, J., Kumagai, S., Wu, C., Yoshioka, T., Bilbao, J., Olazar, M. and Williams, P.T. Hydrogen production from biomass and plastic mixtures by pyrolysis-gasification. International Journal of Hydrogen Energy. 2014, 39(21), pp.10883-10891.
3. Ahmed, I.I. and Gupta, A.K. Hydrogen production from polystyrene pyrolysis and gasification: Characteristics and kinetics. International Journal of Hydrogen Energy. 2009, 34(15), pp.6253-6264.
4. Kumagai, S., Hasegawa, I., Grause, G., Kameda, T. and Yoshioka, T. Thermal decomposition of individual and mixed plastics in the presence of CaO or Ca(OH)₂. Journal of Analytical and Applied Pyrolysis. 2015, 113, pp.584-590.
5. Meng, A., Chen, S., Long, Y., Zhou, H., Zhang, Y. and Li, Q. Pyrolysis and gasification of typical components in wastes with macro-TGA. Waste Management.
6. Chen, S., Meng, A., Long, Y., Zhou, H., Li, Q. and Zhang, Y. TGA pyrolysis and gasification of combustible municipal solid waste. Journal of the Energy Institute. 2015, 88(3), pp.332-343.
7. Goula, M.A., Charisiou, N.D., Papageridis, K.N., Delimitis, A., Pachatouridou, E. and Iliopoulou, E.F. Nickel on alumina catalysts for the production of hydrogen rich mixtures via the biogas dry reforming reaction: Influence of the synthesis method. International Journal of Hydrogen Energy. 2015, 40(30), pp.9183-9200.
8. Clara Delgado, Leire Barruetaña, Salas, O. and Wolf, O. Assessment of the Environmental Advantages and Drawbacks of Existing and Emerging Polymers Recovery Processes JRC37456. Brussels: European Joint Research Centre, 2007.
9. Sehested, J. Sintering of nickel steam-reforming catalysts. Journal of Catalysis. 2003, 217(2), pp.417-426.

10. Wu, C. and Williams, P.T. Pyrolysis-gasification of plastics, mixed plastics and real-world plastic waste with and without Ni-Mg-Al catalyst. *Fuel*. 2010, 89(10), pp.3022-3032.
11. Dong, L., Du, Y., Li, J., Wang, H., Yang, Y., Li, S. and Tan, Z. The effect of CH₄ decomposition temperature on the property of deposited carbon over Ni/SiO₂ catalyst. *International Journal of Hydrogen Energy*. 2015, 40(31), pp.9670-9676.
12. Sengupta, S., Ray, K. and Deo, G. Effects of modifying Ni/Al₂O₃ catalyst with cobalt on the reforming of CH₄ with CO₂ and cracking of CH₄ reactions. *International Journal of Hydrogen Energy*. 2014, 39(22), pp.11462-11472.

Chapter 7

INFLUENCE OF PROCESS PARAMETERS ON SYNGAS PRODUCTION FROM CATALYTIC-DRY REFORMING OF SIMULATED MIXED WASTE PLASTICS

In the previous chapter, syngas production from catalytic-dry reforming of each individual plastics was reported. This chapter presents work on the dry reforming of a simulated mixture of waste plastics (polyethylene/ HDPE and LDPE, polystyrene/ PS, polyethylene terephthalate/ PET and polypropylene/ PP), designated as SWP, to represent the real mixture of waste plastics in municipal solid waste, with a Ni-Co/Al₂O₃ catalyst in a two-stage, pyrolysis-catalytic CO₂ reforming fixed bed reactor as presented in Research Objective 5. The mixture proportions was based on the municipal solid waste plastics composition reported by Delgado et al. [1]; 42 wt.% of LDPE, 20 wt.% of HDPE, 16wt.% of PS, 12 wt.% of PET and 10wt.% of PP. The influences of catalyst preparation method, catalytic dry reforming temperature, CO₂ input rate and catalyst to plastic ratio on the product yields and syngas production were investigated. The chapter continues with the use of both carbon dioxide and steam in the reforming process which have been investigated with the aim of controlling the H₂/CO molar ratio as well as syngas yield as presented in Research Objective 6. The catalyst used was the Ni-Co/Al₂O₃ catalyst used before (Chapter 5), but the results were also compared with a different catalyst, Ni-Mg/Al₂O₃ that showed high catalytic activity in the steam reforming process.

7.1 Different Catalyst Preparation Methods

Two types of catalyst preparation methods were investigated, the rising-pH technique and the impregnation technique, used to prepare a 1:1:1 molar ratio of Ni:Co:Al for the Ni-Co/Al₂O₃ catalyst. The catalyst preparation methods shown to influence the catalyst activity by modifying the catalyst structure and texture, hence determine its performance in the reaction [2-4]. The catalytic dry reforming of the simulated mixture of waste plastics was carried out with 2 g of plastic, 1 g of Ni-Co/Al₂O₃ catalyst, 800 °C reforming temperature and 6.0 g h⁻¹ of CO₂ input

rate to compare the two catalyst preparation methods. The results are shown in Table 7.1, and show that the method of catalyst preparation had only a small influence on the product yield, gas composition, syngas yield or H₂:CO molar ratio. However, there were some small, but important, differences between the catalysts for example, the syngas yield (H₂ + CO) was higher with the catalyst prepared by the rising-pH technique at 148.6 mmol_{syngas} g⁻¹_{swp} compared with 127.4 mmol_{syngas} g⁻¹_{swp} for the catalyst prepared by impregnation. In addition, the CO₂ conversion was higher with the Ni-Co/Al₂O₃ catalyst prepared by the rising-pH techniques compared to the impregnation method (Table 7.1).

Table 7.1 Product yields and gas composition from the catalytic dry reforming of a simulated mixture of waste plastics (SWP) with different types of Ni-Co/Al₂O₃ catalyst preparation methods.

Catalyst preparation method	Rising – pH	Impregnation
<i>Product yield in relation to SWP+CO₂ (wt.%)</i>		
Gas	97.0	94.1
Liquid	0.6	1.0
Char	0.6	0.6
Catalyst carbon deposition	1.7	1.5
Mass balance	99.9	97.2
<i>Gas composition (g g⁻¹_{swp})</i>		
H ₂	2.79	2.41
CO	0.10	0.08
CH ₄	0.04	0.08
C ₂ -C ₄	0.0	0.0
<i>Syngas yield (mmol_{syngas} g⁻¹_{swp})</i>		
H ₂ +CO	148.6	127.4
H ₂ :CO molar ratio	0.49	0.48
CO ₂ conversion (inlet-outlet) (g g ⁻¹ _{swp})	2.07	1.87

Figure 7.1 and Figure 7.2 shows the characterization of the used Ni-Co/Al₂O₃ catalysts from catalytic dry reforming of SWP performed by TGA-TPO and SEM analysis respectively. The TGA thermographs for the catalyst prepared by the rising-pH technique, showed three peaks; around 450 °C, 570 °C and 725 °C. The mass increase starting from 300 °C and reach a peak at about 500 °C, suggests nickel oxidation. The mass loss peaks observed, at ~570 – 600 °C and ~725 °C has been attributed to oxidation of amorphous type carbon at the lower temperature and oxidation of filamentous, graphitic type carbon at the higher

temperature. This finding is also in agreement with the SEM morphologies from the surface of both Ni-Co/Al₂O₃ catalysts. As shown in Figure 7.2, the scanning electron micrographs show a smaller particle size for the rising-pH technique compared to the impregnation method of catalyst preparation. Since the catalyst prepared by the rising-pH technique produced a higher syngas (H₂ + CO) yield in terms of mmol per gram of plastic, the influence of process conditions on syngas yield was further investigated using the Ni-Co/Al₂O₃ catalyst prepared by the rising-pH technique.

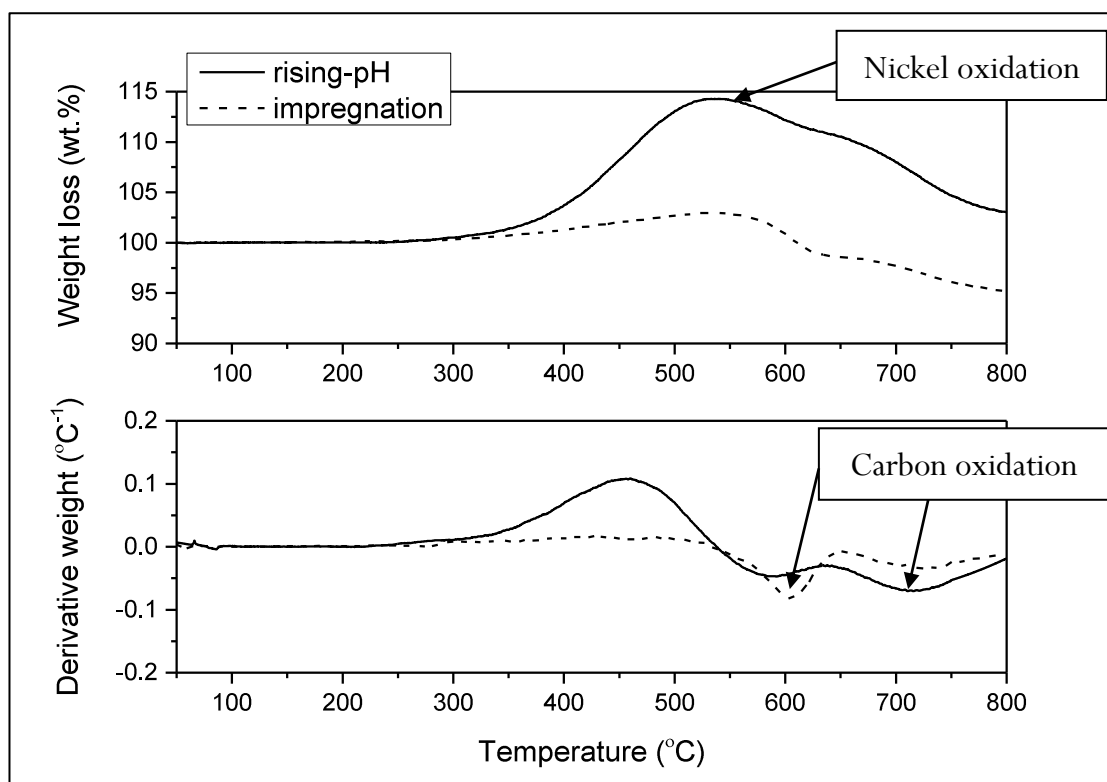


Figure 7.1 TGA and TGA-DTG thermographs of the reacted catalysts from the dry reforming of the simulated mixture of waste plastics (SWP) with catalyst prepared by the rising-pH technique and the impregnation method

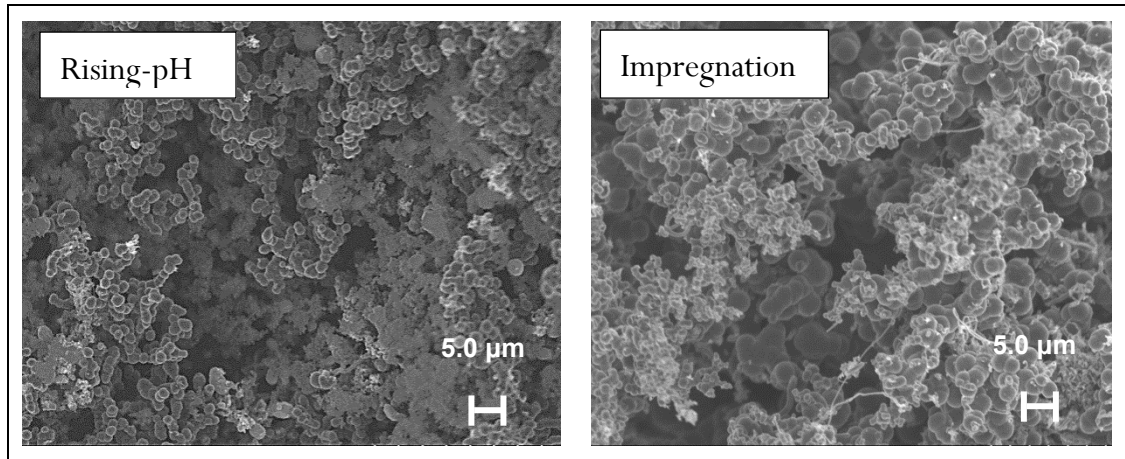


Figure 7.2 SEM micrographs of the reacted catalysts from the simulated mixture of waste plastics (SWP) with catalyst prepared by the rising-pH technique and the impregnation method

7.2 Influence of Catalyst Reforming Temperature

The investigation of the effect of catalytic reforming temperature on syngas (H_2 and CO) production was carried out at $600\text{ }^\circ\text{C}$, $700\text{ }^\circ\text{C}$, $800\text{ }^\circ\text{C}$ and $900\text{ }^\circ\text{C}$. The mass of plastic used was 2 g, with 1 g of Ni-Co/ Al_2O_3 catalyst in the reforming reactor and the CO_2 was fixed at 6.0 g h^{-1} input rate. The results are shown in Table 7.2. The total gas yield increased from 96.90 wt.% at $600\text{ }^\circ\text{C}$ to around 97 wt.% at both $700\text{ }^\circ\text{C}$ and $800\text{ }^\circ\text{C}$. The gas yields were then reduced to 93.11 wt.% at the catalytic dry reforming temperature of $900\text{ }^\circ\text{C}$. The highest carbon deposited on the Ni-Co/ Al_2O_3 catalyst surface was found at the catalytic dry reforming temperature of $900\text{ }^\circ\text{C}$ at 5.50 wt.%.

Table 7.2 Product yields, syngas yield, H₂:CO molar ratio and CO₂ conversion from the catalytic dry reforming of a simulated mixture of waste plastics (SWP) in relation to catalyst temperature

Temperature (°C)	600	700	800	900
<i>Product yield in relation to SWP+CO₂ (wt.%)</i>				
Gas	96.9	97.1	97.1	93.1
Liquid	1.0	1.1	0.6	0.6
Char	0.5	0.5	0.6	0.8
Catalyst carbon deposition	2.6	1.7	1.7	5.5
Mass balance	101.0	100.4	100.0	100.0
<i>Syngas yield (mmol_{syngas} g⁻¹_{swp})</i>				
H ₂ +CO	116.2	144.0	148.6	125.8
H ₂ :CO molar ratio	0.55	0.48	0.49	0.66
<i>CO₂ conversion (inlet-outlet) (g g⁻¹_{swp})</i>				
	1.43	2.02	2.07	1.58

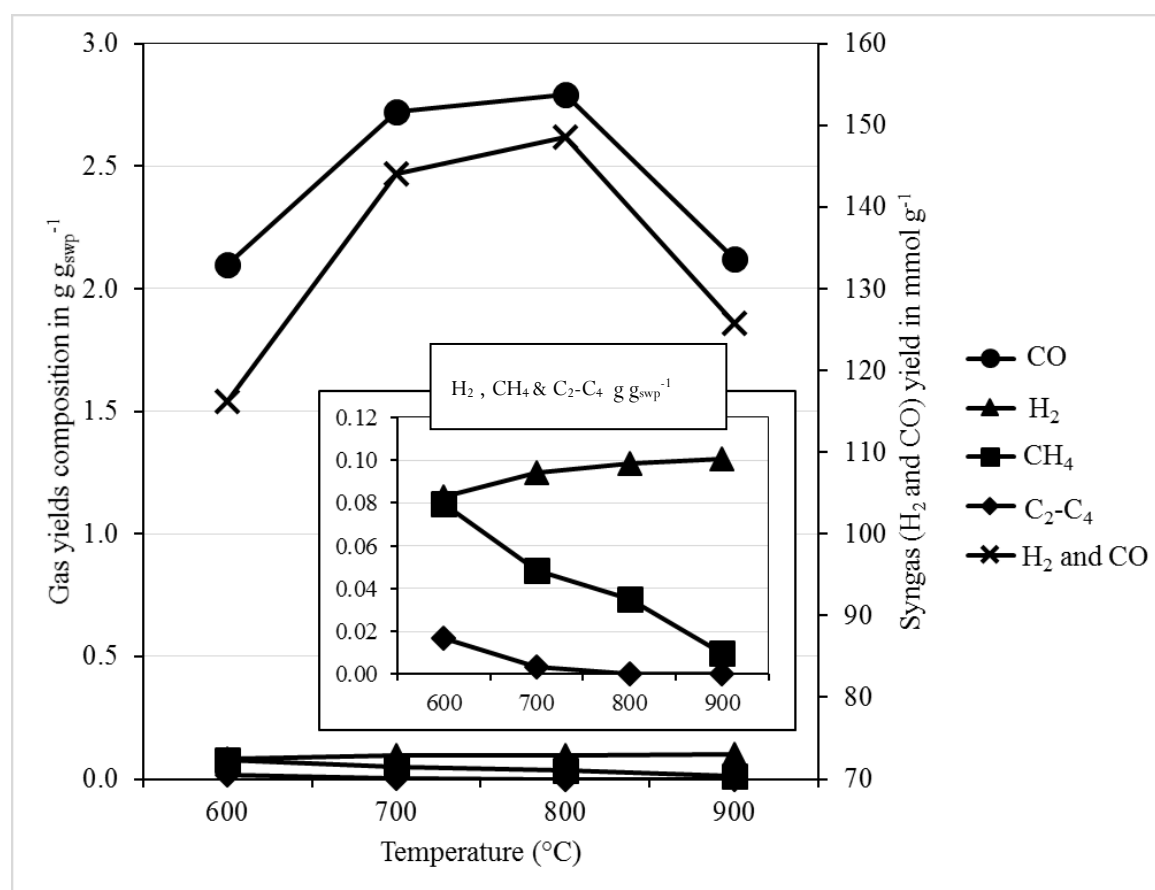


Figure 7.3 Gas compositions produced from the catalytic dry reforming of reforming of the simulated mixture of waste plastics (SWP) at different catalytic dry reforming temperatures.

The composition of product gases from the catalytic dry reforming of the mixed plastic in relation to temperature are shown in Figure 7.3. The data shows that with increased temperature, hydrocarbon gases were significantly reduced, from $0.08 \text{ g g}^{-1}_{\text{swp}}$ to $0.01 \text{ g g}^{-1}_{\text{swp}}$ for CH_4 and from $0.02 \text{ g g}^{-1}_{\text{swp}}$ to $0.0 \text{ g g}^{-1}_{\text{swp}}$ for $\text{C}_2\text{-C}_4$ hydrocarbons. In contrast, H_2 and CO yields increased as the catalyst temperature was raised from 600 to 800 °C, but thereafter declined. The production of high yields of H_2 and CO from the two-stage catalytic dry reforming of high density polyethylene with and without CO_2 has been reported to show a marked reduction in $\text{C}_1\text{-C}_4$ hydrocarbon gases [5], illustrating the dry reforming reaction of the hydrocarbon gases derived from pyrolysis of the plastic (Reaction 2.11). In addition, it has been reported that the dry reforming reaction is favourable at high temperature [6-8].

H_2 yields steadily increased from $0.08 \text{ g g}^{-1}_{\text{swp}}$ at 600 °C to $0.10 \text{ g g}^{-1}_{\text{swp}}$ at 900 °C while CO yields increased from $2.10 \text{ g g}^{-1}_{\text{swp}}$ at 600 °C to $2.79 \text{ g g}^{-1}_{\text{swp}}$ at 800 °C and decreased slightly to $2.12 \text{ g g}^{-1}_{\text{swp}}$ at 900 °C. The CO_2 conversion was closely related to syngas production, with high CO_2 conversion resulting in high syngas yields. The maximum syngas production and maximum CO_2 conversion occurred at a catalyst reforming temperature of 800 °C at $148.6 \text{ mmol}_{\text{syngas}} \text{ g}^{-1}_{\text{swp}}$ and $2.07 \text{ g g}^{-1}_{\text{swp}}$ CO_2 conversion.

The reduction in CO yield at high temperature (900 °C) may be due to reduced catalytic activity at high temperature due to sintering of the catalyst. Table 7.2 shows that catalyst activity had declined since the CO_2 conversion was reduced from $2.07 \text{ g g}^{-1}_{\text{swp}}$ at 800 °C to $1.58 \text{ g g}^{-1}_{\text{swp}}$ at 900 °C. In addition, scanning electron microscopy of the used catalyst at 900 °C also, showed an increase of the catalyst particle size, suggesting sintering had occurred.

The reduction in syngas yield at higher temperatures has also been reported by Rieks et al. [9] for methane dry reforming. But they suggested that a slight drop in the syngas yield was due to the reverse water gas shift reaction (Reaction 7.1) at temperatures above 800 °C. However, Wang et al. [10] determined the upper temperature at which the reverse water gas shift no longer occurs, which corresponded to 820 °C. This is in agreement with the results obtained in this study in which CO showed a decrease and H_2 an increase at higher temperatures above 800 °C.



At 900 °C catalyst reforming temperature, the deposited carbon on the catalyst increased to 5.5 wt.%. The formation of carbon on the catalyst surface leads towards the reduction of active sites on the catalyst surface, resulting on low activity on the performance of dry reforming reactions and thereby reduced CO₂ conversion and consequently reduced CO yield (Table 7.2 and Figure 7.3). In addition, Benguerba et al. [11] have reported that at higher temperature, the rate at which carbon gasification reactions (Reaction 2.10) occurred were not high enough to remove the deposited carbon, hence leading to higher coke formation and reduced catalyst activity. Therefore, a greater rate of the methane decomposition reaction (Reaction 2.15) compared to the carbon gasification reaction (Reaction 2.10) may also be the reason behind the carbon build-up on the catalyst surface at 900 °C. The decomposition of methane also promotes H₂ production, hence H₂ continues to increase at 900 °C. Thermodynamic calculations [12] have shown that the conversion rate of CH₄ and CO₂ are greater than those expected from the dry reforming reaction alone, demonstrating the occurrence of secondary reactions.

7.3 Influence of CO₂ Inlet Flow Rate

The CO₂ inlet flow rate of 3.0, 4.5, 6.0, 7.5 and 9.0 g h⁻¹ were investigated with 2 g of the simulated mixture of waste plastics, 1 g of the Ni-Co/Al₂O₃ catalyst and a catalytic dry reforming temperature of 800 °C. In addition, an experiment with only nitrogen was also performed as a baseline experiment. The results are shown in Table 7.3. The data shows that with the increase of CO₂ flow rate, the total gas yield increased, from 52.41 wt.% with no addition of CO₂ to 92.70 wt.% at a CO₂ flow rate of 3.0 g h⁻¹ and thereafter steadily increased to reach 99.40 wt.% at a CO₂ flow rate of 9.0 g h⁻¹. In the absence of CO₂ (N₂ carrier gas), there was a high mass of carbon deposited on the catalyst at 36.50 wt.%, however, introducing CO₂ to the catalytic dry reforming process reduced the catalyst carbon deposition to 7.3 wt.% at a CO₂ flow rate of 3.0 g h⁻¹ reducing to 1.4 wt.% at a CO₂ flow rate of 9.0 g h⁻¹.

As shown in Table 7.3 the increase of CO₂ flow rate also influenced syngas (H₂+CO) yields. The syngas yield increased from 60.68 mmol_{syngas} g⁻¹_{swp} in the

absence of CO₂ to 121.37 mmol_{syngas} g⁻¹_{swp} at a CO₂ flow rate of 3.0 g h⁻¹; increasing continually at higher CO₂ inlet flow rates to reach more 155.03 mmol_{syngas} g⁻¹_{swp} at a CO₂ flow rate of 9.0 g h⁻¹.

Figure 7.4 shows the composition of the gases produced from the catalytic dry reforming of the plastics mixture. The results show that the major increase in total gas yield (Table 7.3) when CO₂ was introduced to the process compared to the absence of CO₂ was due to the formation of CO, with a marked increase in CO yield and thereby producing a high syngas yield. However, the yield of H₂ was low in the absence of the CO₂ and was not affected by the introduction of CO₂ even at higher inlet CO₂ flow rates. This was reflected in the H₂:CO molar ratios which was high in the absence of CO₂ at 4.32, reducing to 0.81 with the introduction of CO₂ and showing decrease with increasing CO₂ flow rate.

A low yield of hydrocarbons (C₂-C₄) was produced throughout the experiments. However, Figure 7.4 also shows a dependent trend between CH₄ and H₂ yields. High concentration of H₂ gas yield correlated with low concentrations of CH₄. The highest H₂ yield was obtained at the CO₂ flow rate of 3.0 g h⁻¹ and was slightly reduced at 4.5 g h⁻¹ of CO₂ flow rate. In this study, even after increasing the CO₂/plastic ratio up to 6.0 (CO₂ flow rate of 9.0 g h⁻¹), the syngas production was still increasing, since the major contribution was from CO, where CO yield kept increasing with the increase of CO₂ flow rate.

Table 7.3 Product yields, syngas yield, H₂:CO molar ratio and CO₂ conversion from the catalytic dry reforming of a simulated mixture of waste plastics (SWP) at different inlet CO₂ flow rates

CO ₂ flow rate (g h ⁻¹)	0.0	3.0	4.5	6.0	7.5	9.0
<i>Product yield in relation to SWP+CO₂(wt.%)</i>						
Gas	52.4	92.7	96.6	97.1	98.0	99.4
Liquid	2.0	1.7	1.3	0.6	0.5	0.4
Char	3.5	1.2	0.9	0.6	0.5	0.4
Catalyst carbon deposition	36.5	7.3	2.3	1.7	1.5	1.4
Mass balance	94.4	100.9	100.9	100.0	100.4	101.5
<i>Syngas yield (mmol_{syngas} g⁻¹_{swp})</i>						
H ₂ +CO	60.7	121.4	136.8	148.6	149.0	155.0
H ₂ :CO molar ratio	4.32	0.81	0.52	0.49	0.46	0.45
<i>CO₂ conversion (inlet-outlet) (g g⁻¹_{swp})</i>						
CO ₂ conversion (inlet-outlet) (g g ⁻¹ _{swp})	N/A	1.22	1.78	2.07	2.10	2.16

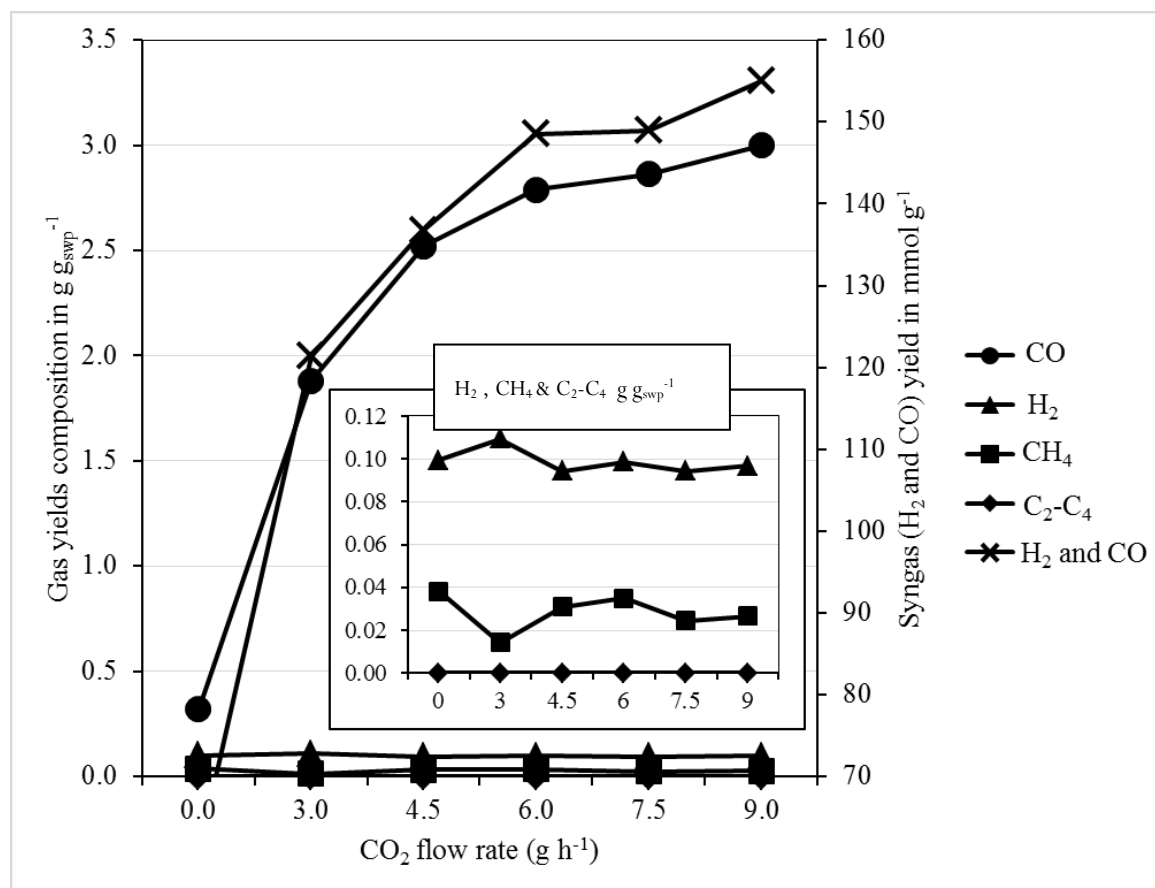


Figure 7.4 Gas compositions produced from the catalytic dry reforming of the simulated mixture of waste plastics (SWP) at different CO₂ flow rates

7.4 Influence of Catalyst to Plastic Ratio

The catalyst to plastic ratios of 0.25, 0.5, 1.0 and 1.5 were studied to evaluate their influence in relation to syngas production from the dry reforming of SWP. As a baseline experiment, substitution of sand was used instead of the Ni-Co-Al₂O₃ catalyst in the reforming reactor. The catalytic reforming temperature and CO₂ flow rate were kept at 800 °C and 6.0 g h⁻¹ respectively for the experiments. The weight of the simulated mixture of waste plastics was also fixed at 2 g. Table 7.4 shows the product yields from dry reforming of the plastics in relative to the catalyst to plastic ratio investigation. The results suggest that high carbon deposition occurred on the sand surface in the absence of catalyst, resulting in low gas production, at only 87.9 wt.%. The addition of the catalyst reduced carbon deposition from 5.5 wt.% to 1.8 wt.% at the catalyst:plastic ratio of 0.25 which steadily decreased to 1.7 wt.% at the catalyst:plastic ratio of 0.5. No obvious

carbon deposition on the used catalyst surface could be found at the catalyst:plastic ratios of 1.0 and 1.5. It has been suggested that when more catalyst is used, more pyrolysis gases could react with the catalyst, resulting in lower carbon deposition on the catalyst and higher gas production [13-14]. The highest gas yield was obtained at the catalyst:plastic ratio of 1.0, at 98.2 wt.%.

Table 7.4 also shows that the syngas yield from the different catalyst:plastic ratios for the catalytic dry reforming of the plastic mixture showing that there was a significant increase in syngas yields with the addition of catalyst, from 91.3 (sand) to 141.3 mmol g⁻¹_{swp} (catalyst addition). The syngas yield gradually increased to 148.6 mmol g⁻¹_{swp} with 1g of Ni-Co/Al₂O₃ catalyst was used, followed by a slight decrease as the catalyst:plastic ratio was increased. The gas composition derived from catalytic dry reforming of the mixed plastics are shown in Figure 7.5. The results show that there was a decrease in CH₄ and C₂-C₄ concentrations when the catalyst was introduced into the system. As a result, CO and H₂ were markedly increased, confirming that the addition of catalyst further enhanced the reforming reaction between CO₂ and hydrocarbons (Reaction 2.11). The addition of further catalyst may make it harder to drive the dry reforming reaction hence lowering CO concentration. Excess catalyst may probably enhanced side product such as water. Furthermore, from SEM analysis results (not shown here), the particle size of catalysts were increasing with the increased of catalysts:plastic ratio, showing the catalyst may already been deactivated.

Table 7.4 Product yields and gas composition from the catalytic dry reforming of a simulated mixture of waste plastics (SWP) at different catalyst:plastic ratios

Catalyst to plastic ratio (g g ⁻¹)	0.0	0.25	0.5	1.0	1.5
<i>Product yield in relation to SWP+CO₂(wt.%)</i>					
Gas	87.6	94.7	97.1	98.2	98.0
Liquid	1.4	1.0	0.6	2.4	3.9
Char	1.0	0.7	0.6	0.3	0.5
Catalyst carbon deposition	5.5	1.8	1.7	0.0	0.0
Mass balance	95.5	98.2	100.0	100.9	102.4
<i>Syngas yield (mmol_{syngas} g⁻¹_{swp})</i>					
H ₂ +CO	91.3	141.3	148.6	143.9	139.9
H ₂ :CO molar ratio	0.52	0.48	0.49	0.49	0.51
CO ₂ conversion (inlet-outlet) (g g ⁻¹ _{swp})	1.53	2.06	2.07	1.92	1.79

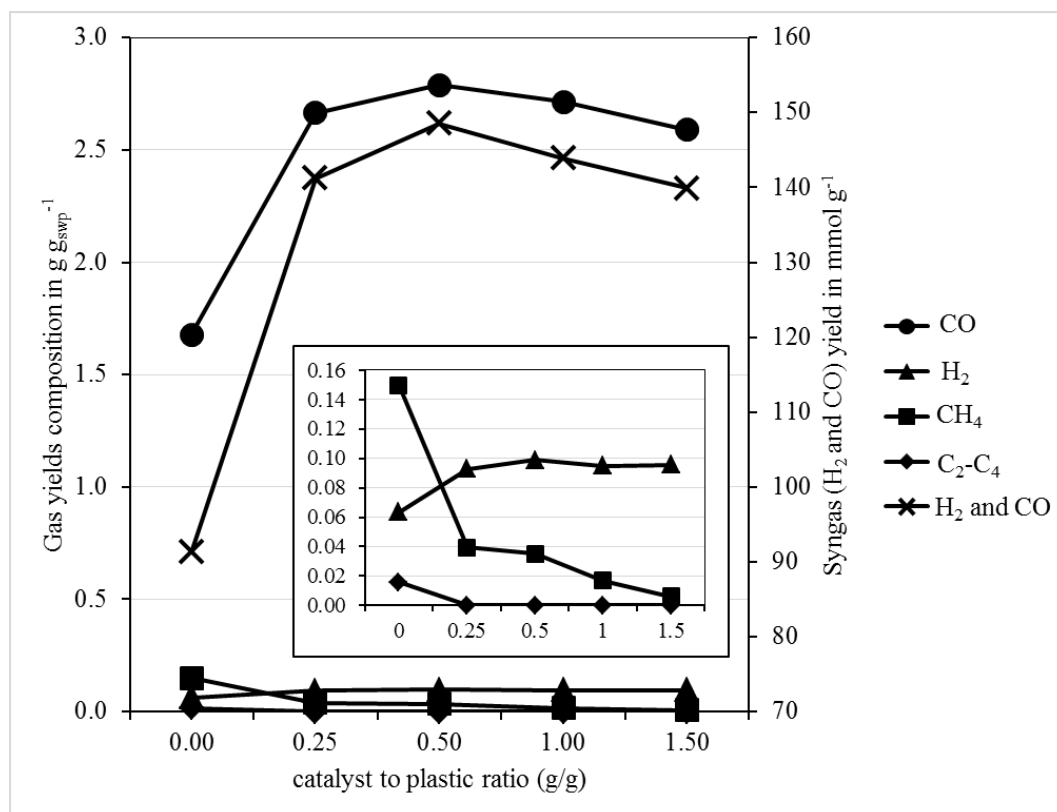


Figure 7.5 Gas compositions produced from the catalytic dry reforming of the simulated mixture of waste plastics (SWP) at different catalyst:plastic ratios

7.5 Manipulating H₂/CO ratio by the Addition of Steam

In this study, CO₂/steam ratios of 4:0, 4:0.5, 4:1, 4:1.5 and 4:2 was used for the for Ni-Co/Al₂O₃ catalyst and for the Ni-Mg/Al₂O₃ catalyst, the CO₂/steam ratios were 4:0, 4:0.5, 4:1, 4:2 and 4:3. The Ni-Mg/Al₂O₃ catalyst showed very small different with the steam/CO₂ ratio of 4:1.5 (results not shown here), hence the ratio was increased up to 4:3. The CO₂ and/or steam was fed directly into the second catalytic stage of the reactor system. Nitrogen was used as a carrier gas for the entire process at a flow rate of 200 ml min⁻¹. 2 g of plastic sample and 1 g of catalyst were used in each experiment.

Table 7.5 and Table 7.6 show the product yields from the catalytic-dry/steam reforming of the simulated mixture of LDPE, HDPE, PS, PET and PP in relation to the CO₂/steam reforming gas ratio with the Ni-Co/Al₂O₃ and Ni-Mg/Al₂O₃ catalysts respectively. For the case of Ni-Co/Al₂O₃ catalysts, as shown in

Table 7.5, the total gas yield in relation to all of the reactants (plastic, carbon dioxide and reacted water) reached the maximum point of 94.58 wt.% at the CO₂/steam ratio of 4:1.5. However, calculation of the total gas yield in relation to only the mass of plastic used in the experiments showed an increase from ~268 wt.% to 356 wt.% as the CO₂/steam ratio was increased. The reforming gases CO₂ and steam clearly contributing to the total gas product yield in addition to the hydrocarbons from the plastic pyrolysis-catalysis. The total gas yield in terms of the mass of plastic from the reforming process increased from ~268 wt.% for the CO₂/steam ratio of 4:0 to 356 wt.% at a ratio of 4:2. The residue of the simulated mixed waste plastics after the experiment in the sample holder remained unchanged, 3.0 wt.%_{plastic only}. Increasing the CO₂/steam ratio produced a large impact on the carbon deposited on the catalyst, showing a decrease from 23.50 wt.%_{plastic only} with the experiment without steam addition, to 0.50 wt.%_{plastic only} at the CO₂/steam ratio of 4:2.

Similar trends of gas and residue yields corresponding to the mass of simulated mixed waste plastics were also shown from the experiments with the Ni-Mg/Al₂O₃ as presented in Table 7.6. However, the carbon formation on the catalyst during the experiments first decreased with the increase of CO₂/steam ratio and then increased at the higher CO₂/steam ratios.

Table 7.5 Product yield distribution from catalytic-dry/steam reforming of simulated waste plastic over Ni-Co/Al₂O₃ catalyst at the gasification temperature of 800 °C

CO ₂ /steam ratio	(4:0)	(4:0.5)	(4:1)	(4:1.5)	(4:2)
<i>Product yield in relation to plastic + carbon dioxide + reacted water (wt. %)</i>					
Gas	89.32	88.66	89.76	94.58	89.76
Residue	1.00	0.96	0.86	0.82	0.76
Carbon deposition	7.83	6.85	0.29	0.14	0.13
Mass balance	98.15	96.47	90.91	95.54	90.65
<i>Product yield in relation to plastics only (wt.%)</i>					
Gas	267.95	278.39	314.16	347.58	356.35
Residue	3.00	3.00	3.00	3.00	3.00
Carbon deposition	23.50	21.50	1.00	0.50	0.50
Mass balance	295.45	302.89	318.16	351.08	359.85

Table 7.6 Product yield distribution from catalytic-dry/steam reforming of simulated waste plastic over Ni-Mg/Al₂O₃ catalyst at the gasification temperature of 800 °C

CO ₂ /steam ratio	(4:0)	(4:0.5)	(4:1)	(4:2)	(4:3)
<i>Product yield in relation to plastic + carbon dioxide + reacted water (wt. %)</i>					
Gas	87.46	90.43	95.12	96.31	100.16
Residue	1.00	0.97	0.86	0.86	0.86
Carbon deposition	8.33	6.46	1.28	1.85	4.14
Mass balance	96.79	97.86	97.26	99.02	105.16
<i>Product yield in relation to plastics only (wt.%)</i>					
Gas	262.37	279.89	333.39	337.57	351.06
Residue	3.00	3.00	3.00	3.00	3.00
Carbon deposition	25.00	20.00	4.50	6.50	14.50
Mass balance	290.37	302.89	340.89	347.07	368.56

7.5.1 Gas composition

The gases contained in the gas sample bag were analysed by gas chromatography and the results for carbon monoxide (CO), hydrogen (H₂), methane (CH₄) and C₂-C₄ hydrocarbons from the catalytic-dry/steam reforming of simulated mixed waste plastics over Ni-Co/Al₂O₃ and Ni-Mg/Al₂O₃ catalysts are shown in Figure 7.6. In general, the main gases from the catalytic-dry/steam reforming process for both catalysts were carbon monoxide and methane and lower yields of hydrogen and C₂-C₄ hydrocarbons as shown in the Figure 7.6, suggesting the reaction between pyrolytic gases and CO₂ and/or water vapour occurred in the second stage reactor. These two reactions representing the dry reforming reaction (Reaction 2.11) and the steam reforming reaction (Reaction 2.9).

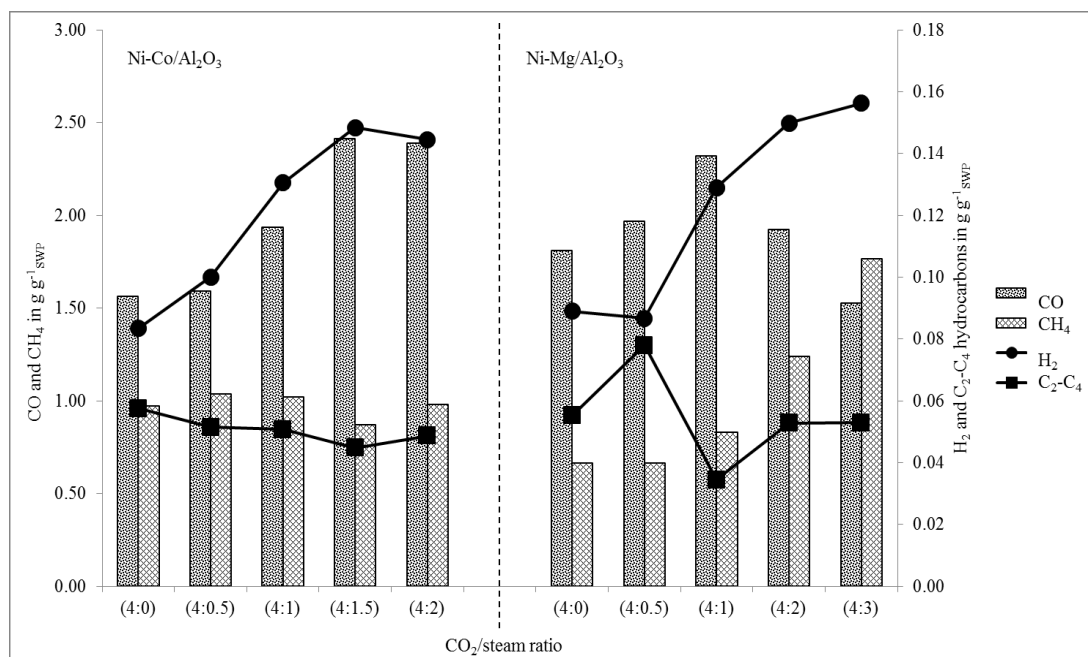


Figure 7.6 Gas composition for the catalytic-dry/steam reforming of simulated waste plastic with different CO₂/steam ratio over Ni-Co/Al₂O₃ and Ni-Mg/Al₂O₃ catalysts

The results obtained for the experiments with the Ni-Co/Al₂O₃ catalyst shown in Figure 7.6, shows a close relationship between the reactant gases produced from pyrolysis; methane and C₂-C₄ hydrocarbons, and the output gases; carbon monoxide and hydrogen. The decrease in the concentration of CH₄ and C₂-C₄ hydrocarbons corresponding to the reduction in the CO₂/steam input ratio from 4:0 to 4:1.5, resulting in an increase in the product CO and H₂. The relative increase in gas yield was more marked for CO compared to H₂, resulting in a change in the H₂/CO molar ratio. From the discussion previously, the carbon deposits on the catalyst were decreased with the increase in the CO₂/steam ratio. It is suggested that reaction occurred between carbon dioxide/steam and char/fixed carbon to produce carbon monoxide (Reaction 2.10 and Reaction 2.8).

Figure 7.6 also shows the influence of the CO₂/steam ratio for the reforming of the plastic mixture using the Ni-Mg/Al₂O₃ catalyst. In comparison with the cobalt containing Ni-Co/Al₂O₃ catalyst, the yield of CO was higher, but at higher inputs of steam, the yield of CO fell, with an improved yield of H₂. It is suggested that Ni-Mg/Al₂O₃ also promoted the water gas shift reaction (Reaction 2.8) when more steam was added to the process, hence showing reduction of carbon monoxide yield and increase of hydrogen yield.

7.5.2 Syngas production and H₂/CO molar ratio

Figure 7.7 shows the relationship between CO₂ conversion, reacted water, syngas yield and H₂/CO molar ratio from the catalytic-dry/steam reforming process of simulated mixed waste plastics over the Ni-Co/Al₂O₃ catalyst. Syngas yield reached its maximum point at the CO₂/steam ratio of 4:1.5 at 159.77 mmol g⁻¹_{SWP}. The maximum peak of CO₂ conversion_{inlet-outlet}, at 56.55 % was also found at the CO₂/steam ratio of 4:1.5. The quantity of reacted water increased with the raising of the CO₂/steam ratio to a maximum which was 0.56 g g⁻¹_{SWP} at the CO₂/steam ratio of 4:2.

However, the H₂/CO molar ratio shows a maximum at the CO₂/steam ratio of 4:1 at producing a H₂/CO molar ratio of 0.94, but decreased as the amount of steam input was increased. This might be due to the large increase in CO production compared to the H₂ yield. This also suggests that the Ni-Co/Al₂O₃ catalyst enhanced the dry reforming reaction (Reaction 2.11) as well as the Boudouard reaction (Reaction 2.10) compared to the steam reforming reaction (Reaction 2.9) hence, there was high CO yield compared to H₂ yield. Butterman et al. [15] in their study on steam gasification of biomass with the addition of CO₂, also showed that an increase of CO₂ input into the system, enhanced the production of CO with reduced H₂ yield [15].

Figure 7.8 shows the results from the catalytic-dry/steam reforming of simulated mixed waste plastics over the Ni-Mg/Al₂O₃ catalyst. A maximum peak of syngas yield at 147 mmol g⁻¹_{SWP} was obtained at the CO₂/steam ratio of 4:1. The CO₂ conversion_{inlet-outlet} and reacted water showing an opposite trend towards each other while the H₂/CO molar ratio showing a similar trend with the reacted water; increased with the increased CO₂/steam molar ratio. The drop in CO₂ reaction and the rise in steam consumption with the increase of CO₂/steam ratio, suggesting that the Ni-Mg/Al₂O₃ might promote the steam reforming reaction than the dry reforming reaction. This further confirmed that the water gas shift reaction (Reaction 2.8) occurred in the second stage reactor among the low molecular weight hydrocarbons (methane), condensable hydrocarbons (C₂-C₄) and steam/water vapour, yielding CO₂ hence, lessening CO₂ conversion_{inlet-outlet} but promoting water consumption (reacted water) starting at the CO₂/steam ratio of 4:0.5.

The results have shown that by changing the CO₂/steam input ratio, the syngas H₂/CO ratio can be manipulated between 0.74 and 0.94 for the Ni-Co/Al₂O₃ catalyst and between 0.6 and 1.4 for the Ni-Mg/Al₂O₃ catalyst. The optimum ratio of H₂/CO required for onward process utilisation depends on the application. Majewski and Wood [16] have reported that a H₂/CO ratio between 1.7 – 2.15 can be used for Fischer Tropsch processing for the production of liquid hydrocarbon fuels, depending on the type of catalyst used and the process conditions. A H₂/CO ratio between 1.5-2 can also be used for production of methanol or for dimethyl-ether synthesis. Therefore, the syngas H₂/CO ratio derived from waste plastics reported here would require supplemental hydrogen addition to raise the H₂/CO ratio for use in such applications.

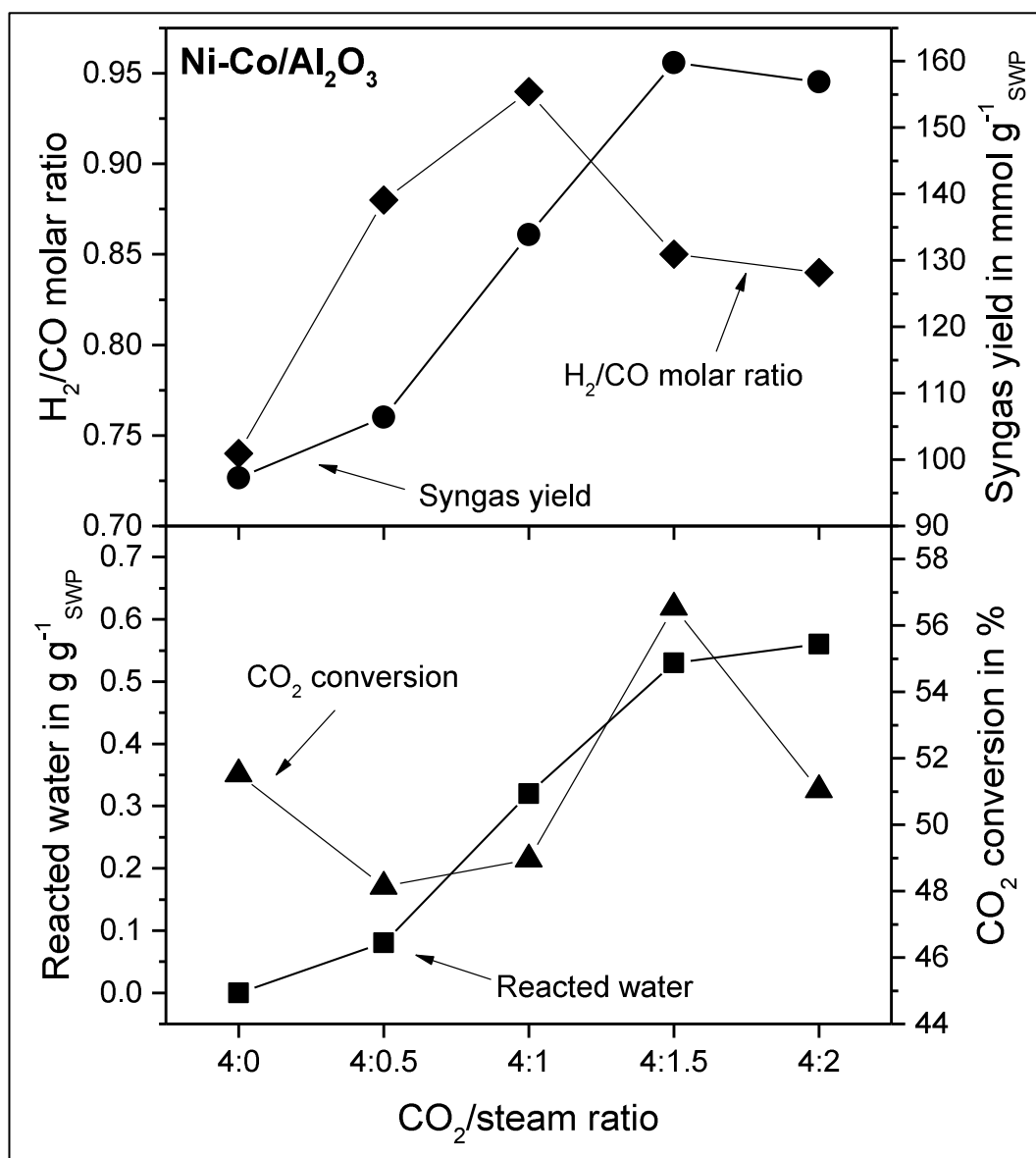


Figure 7.7 Syngas yield, H₂/CO molar ratio, reacted water and CO₂ conversion derived from dry/steam reforming process over Ni-Co/Al₂O₃ catalyst

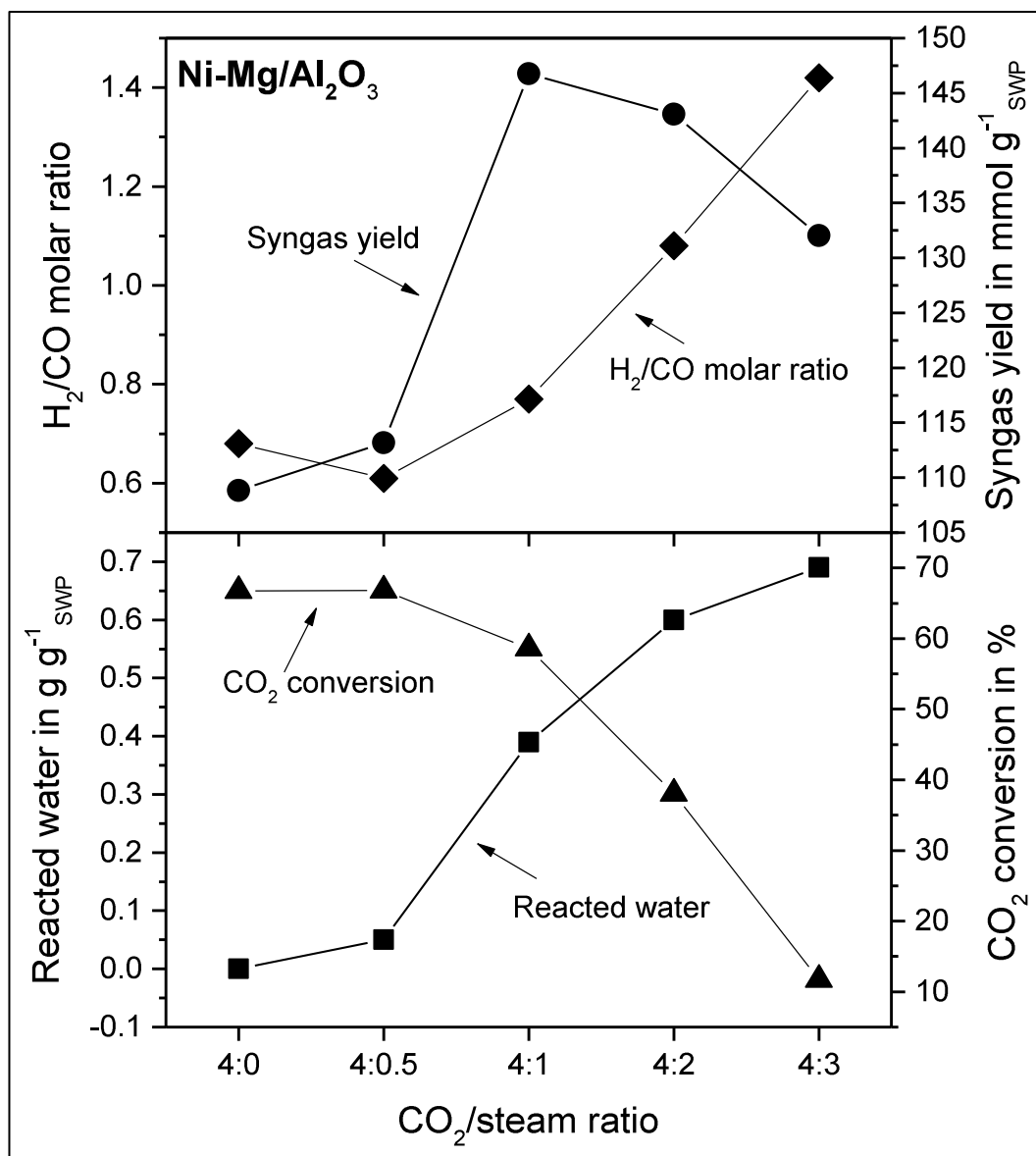


Figure 7.8 Syngas yield, H₂/CO molar ratio, reacted water and CO₂ conversion derived from dry/steam reforming process over Ni-Mg/Al₂O₃ catalyst

7.5.3 Catalyst coke formation

The reacted Ni-Co/Al₂O₃ and Ni-Mg/Al₂O₃ catalysts from the dry/steam reforming experiments of simulated mixed waste plastics with CO₂/steam feed ratio were characterized by temperature programmed oxidation (TPO) experiments using thermogravimetric analysis.

The results of TGA-TPO and DTG-TPO of both reacted catalysts are shown in Figure 7.9 and Figure 7.10 respectively. As shown in Table 7.5, the quantity of

coke deposited on the Ni-Co/ Al_2O_3 catalyst showed a significant decrease of 98 % with an increase in the CO_2 /steam ratio. This result is in agreement with the TPO experiments, where the catalysts used with higher steam inputs showed little mass loss since there were few deposits of carbon on the catalyst surface available for oxidation (combustion). Therefore it is suggested with the increase of CO_2 /steam ratio, more carbon was reacted with either carbon dioxide or steam via Reaction 2.10 and Reaction 2.7.

It should also be noted that with the reacted Ni-Co/ Al_2O_3 catalyst, there was a large increase of mass at around a temperature of 500 °C. Due to the low concentration of coke deposited on the reacted catalysts, it is suggested that the mass gain was due to oxidation of nickel and cobalt metal in the catalyst [17]. Compared to the reacted Ni-Co/ Al_2O_3 catalyst, high oxidation temperature peaks (higher than 600 °C) were also observed for reacted Ni-Mg/ Al_2O_3 catalyst as shown in Figure 7.10.

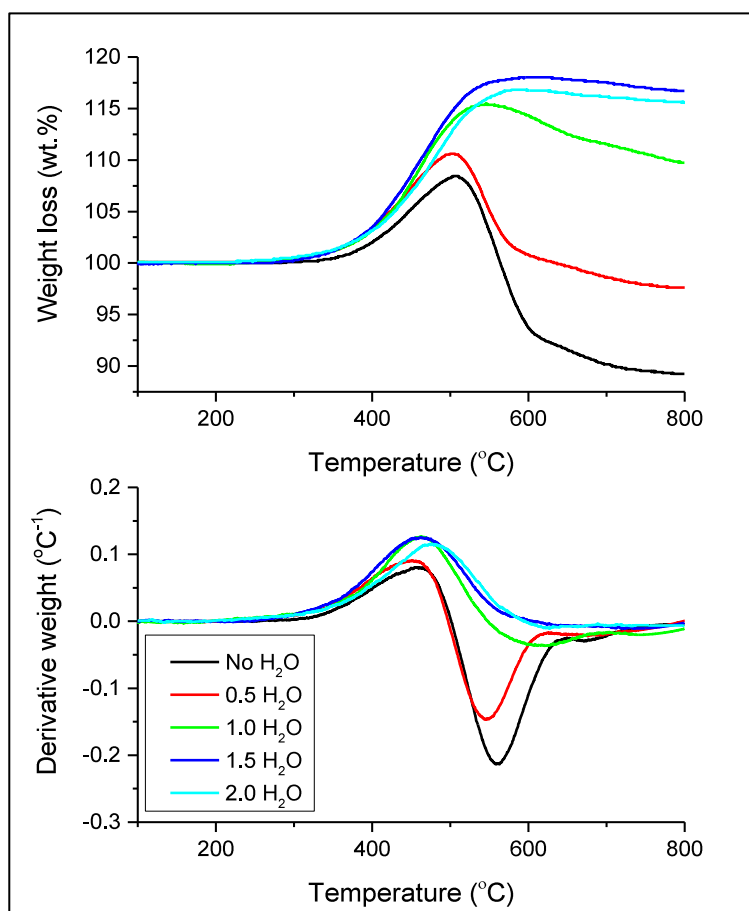


Figure 7.9 TGA-TPO and DTG-TPO analysis of different type of coked catalysts after pyrolysis-dry/steam reforming of simulated waste plastics over Ni-Co/ Al_2O_3 catalyst.

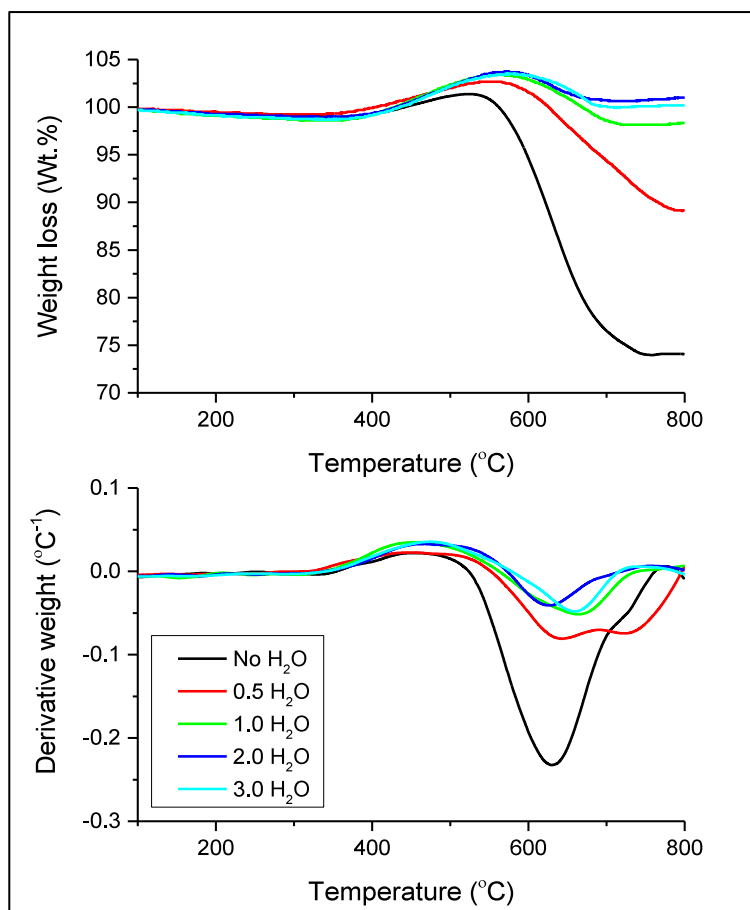


Figure 7.10 TGA-TPO and DTG-TPO analysis of different type of coked catalysts after pyrolysis-dry/steam reforming of simulated waste plastics over Ni-Mg/Al₂O₃ catalyst.

Figure 7.11 and Figure 7.12 shows the SEM micrograph of carbon formation on the reacted catalysts from the dry/steam reforming experiment of simulated waste plastic after varying the CO₂/steam feed ratio; Ni-Co/Al₂O₃ and Ni-Mg/Al₂O₃ respectively. In general, it could be seen that less sign of filamentous whisker growth were detected on the Ni-Co/Al₂O₃ compared to the Ni-Mg/Al₂O₃ reacted catalyst. This is in agreement with the DTG-TPO profile as discussed above; high oxidation temperature peak was observed from the reacted Ni-Mg/Al₂O₃ catalyst. The scanning electron microscope observation of the used catalysts confirmed that only low levels of carbon deposition occurred on the Ni-Co/Al₂O₃ catalyst compared to the Ni-Mg/Al₂O₃ reacted catalyst.

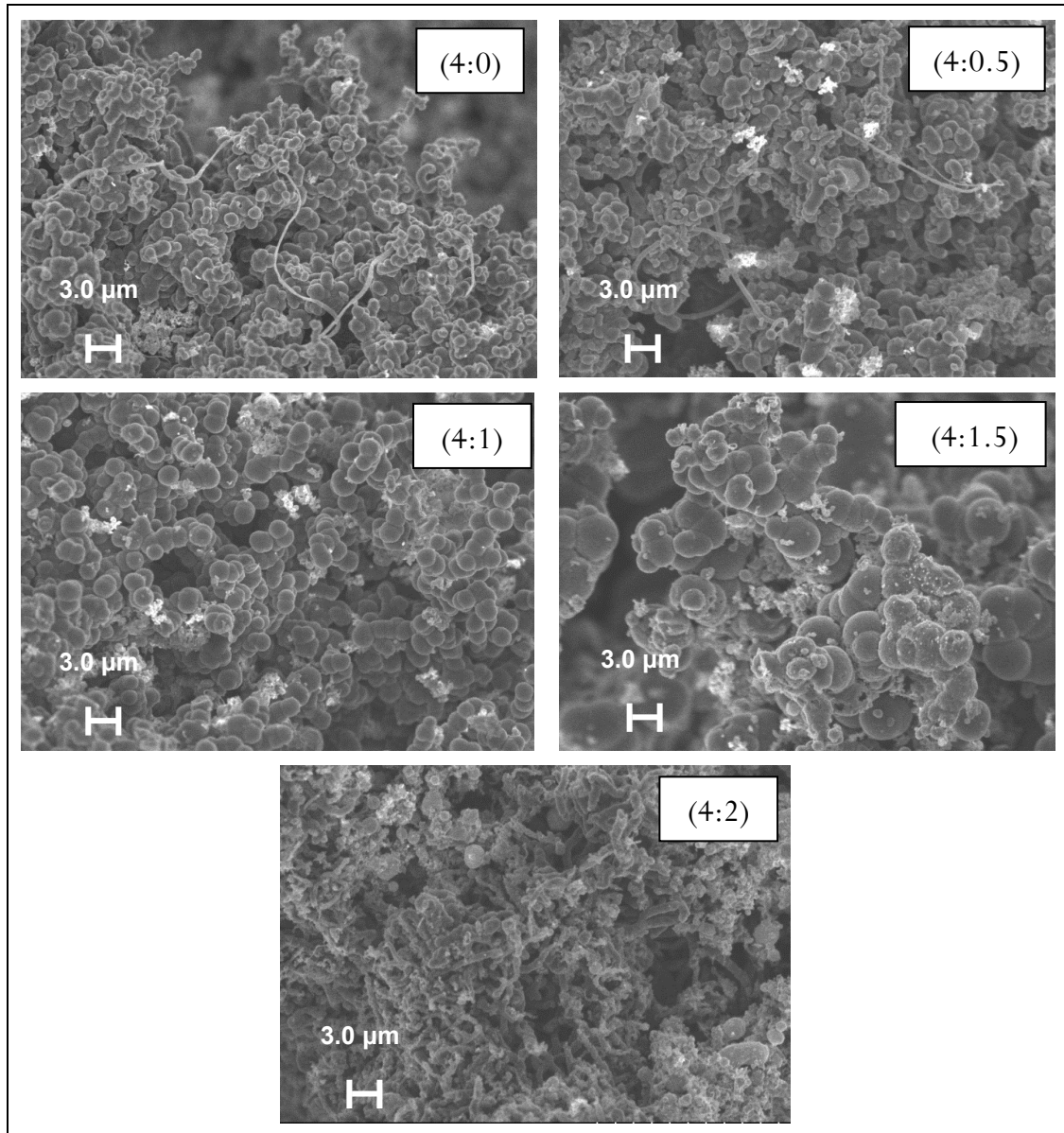


Figure 7.11 SEM results of different type of coked Ni-Co/Al₂O₃ catalysts from catalytic-dry/steam reforming of simulated waste plastic (all SEM micrographs are at the same magnification)

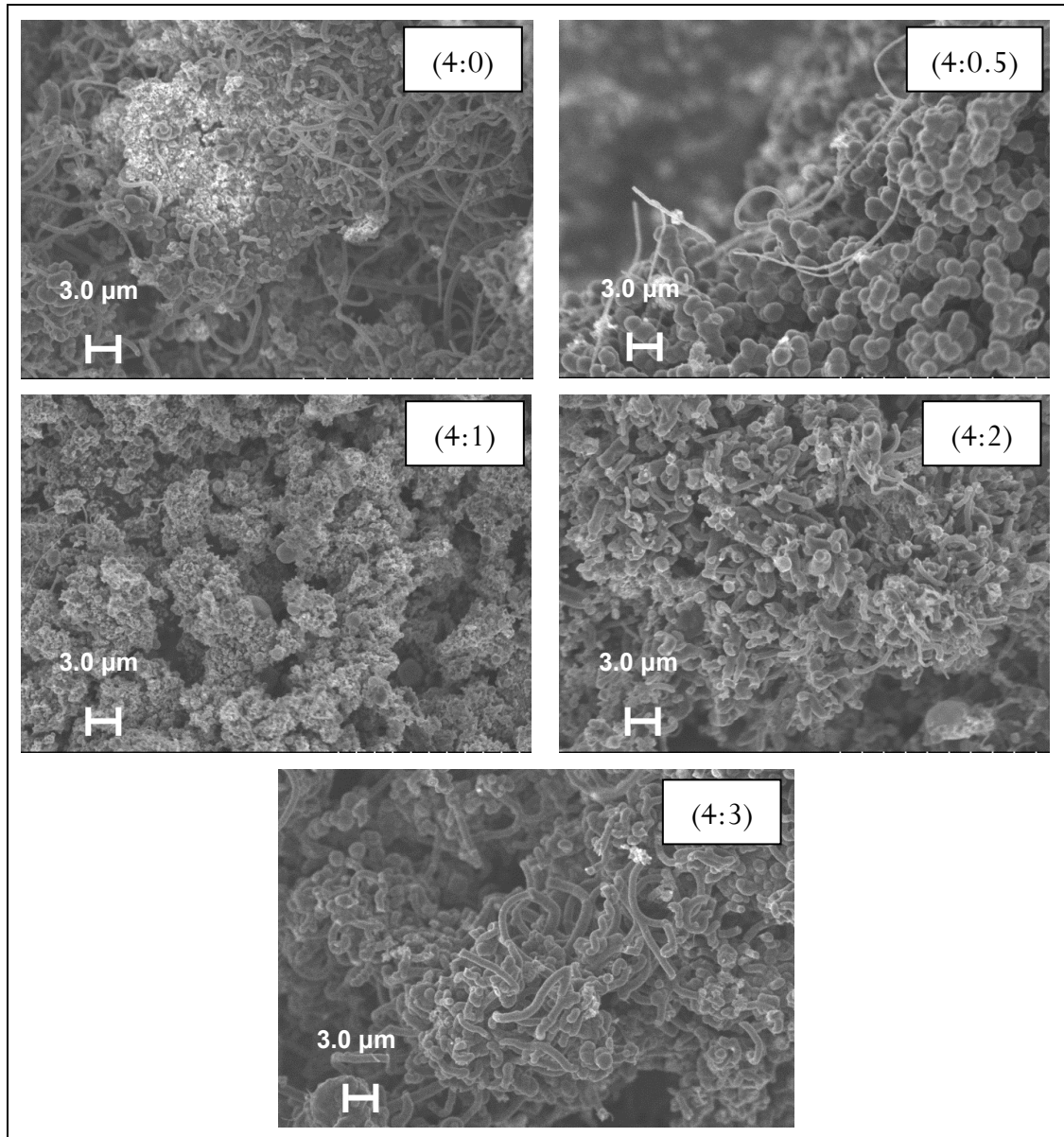


Figure 7.12 SEM results of different type of coked Ni-Mg/Al₂O₃ catalysts from catalytic-dry/steam reforming of simulated waste plastic (all SEM micrographs are at the same magnification)

7.6 Summary

This study has demonstrated that varying the experimental parameters has a significant influence on syngas production from the dry reforming of the simulated mixture of waste plastics. The catalyst preparation method also influences the properties of the catalyst and consequently the activity of the catalyst towards syngas production. The catalyst prepared using rising-pH technique reduced the

catalyst particle size resulting in higher syngas yield, when comparing with the catalyst prepared using impregnation method. The optimum syngas production was obtained at the catalyst reforming temperature of 800 °C and with the catalyst:plastic ratio of 0.5, with a yield of 148.6 mmol g⁻¹_{swp}. The increase of CO₂ flow rate, further enhanced syngas production from 60.7 mmol g⁻¹_{swp} at no CO₂ addition to 155.0 mmol g⁻¹_{swp} at 9.0 g h⁻¹ CO₂ flow rate.

Incorporating steam into the dry reforming process was investigated in order to manipulate the H₂/CO molar ratio for the end-use industrial application. The results showed that by changing the CO₂/steam feed ratio, as well as suitable catalyst selection, the syngas production and H₂/CO molar ratio could be varied. For the catalytic-dry/steam reforming of simulated mixed waste plastics over Ni-Co/Al₂O₃ catalyst, it is suggested that the optimum CO₂/steam ratio was observed at 4:1. At this ratio, the highest H₂/CO molar ratio was observed at 0.94 and an acceptable syngas yield was also obtained at 133.87 mmol_{syngas} g⁻¹_{swp}. For the reforming process over the Ni-Mg/Al₂O₃ catalyst, the optimum syngas production of 146.77 mmol_{syngas} g⁻¹_{swp} was observed at the CO₂/steam ratio of 4:1. It is also suggested that the Ni-Co/Al₂O₃ catalyst enhanced the dry reforming reaction and Bourdouard reaction hence, high CO and high syngas yield was obtained. In the case of the Ni-Mg/Al₂O₃ catalyst, the process was more favoured towards the steam reforming and water gas shift reactions hence, higher H₂ yield and higher H₂/CO molar ratios were obtained. In addition, increasing the CO₂/steam ratio with the Ni-Mg/Al₂O₃ catalyst showed an undesirable carbon build-up on the catalyst during the experiments.

References

1. Clara Delgado, Leire Barruetabeña, Salas, O. and Wolf, O. Assessment of the Environmental Advantages and Drawbacks of Existing and Emerging Polymers Recovery Processes JRC37456. Brussels: European Joint Research Centre, 2007.
2. Goula, M.A., Charisiou, N.D., Papageridis, K.N., Delimitis, A., Pachatouridou, E. and Iliopoulou, E.F. Nickel on alumina catalysts for the production of hydrogen rich mixtures via the biogas dry reforming reaction: Influence of the synthesis method. *International Journal of Hydrogen Energy*. 2015, 40(30), pp.9183-9200.
3. Li, X., Wang, S., Cai, Q., Zhu, L., Yin, Q. and Luo, Z. Effects of Preparation Method on the Performance of Ni/Al₂O₃ Catalysts for Hydrogen Production by Bio-Oil Steam Reforming. *Applied Biochemistry and Biotechnology*. 2012, 168(1), pp.10-20.
4. Rodrigues, C.P., Kraveva, E., Ehrich, H. and Noronha, F.B. Structured Reactors as an Alternative to Fixed-bed Reactors: Influence of catalyst preparation methodology on the partial oxidation of ethanol. *Catalysis Today*. 2016, 273, pp.12-24.
5. Md Saad, J., Nahil, M.A. and Williams, P.T. Influence of process conditions on syngas production from the thermal processing of waste high density polyethylene. *Journal of Analytical and Applied Pyrolysis*. 2014, (0).
6. Kang, K.-M., Kim, H.-W., Shim, I.-W. and Kwak, H.-Y. Catalytic test of supported Ni catalysts with core/shell structure for dry reforming of methane. *Fuel Processing Technology*. 2011, 92(6), pp.1236-1243.
7. Lim, Y., Lee, C.J., Jeong, Y.S., Song, I.H. and Han, C. Optimal Design and Decision for Combined Steam Reforming Process with Dry Methane Reforming to Reuse CO₂ as a Raw Material. *Industrial & Engineering Chemistry Research*. 2012, 51(13), pp.4982-4989.
8. Tsang, S.C., Claridge, J.B. and Green, M.L.H. Recent advances in the conversion of methane to synthesis gas. *Catalysis Today*. 1995, 23(1), pp.3-15.

9. Rieks, M., Bellinghausen, R., Kockmann, N. and Mleczko, L. Experimental study of methane dry reforming in an electrically heated reactor. *International Journal of Hydrogen Energy*. 2015, 40(46), pp.15940-15951.
10. Wang, S., Lu, G.Q. and Millar, G.J. Carbon Dioxide Reforming of Methane To Produce Synthesis Gas over Metal-Supported Catalysts: State of the Art. *Energy & Fuels*. 1996, 10(4), pp.896-904.
11. Benguerba, Y., Dehimi, L., Virginie, M., Dumas, C. and Ernst, B. Modelling of methane dry reforming over Ni/Al₂O₃ catalyst in a fixed-bed catalytic reactor. *Reaction Kinetics, Mechanisms and Catalysis*. 2014, 114(1), pp.109-119.
12. Serrano-Lotina, A. and Daza, L. Influence of the operating parameters over dry reforming of methane to syngas. *International Journal of Hydrogen Energy*. 2014, 39(8), pp.4089-4094.
13. Bimbela, F., Oliva, M., Ruiz, J., García, L. and Arauzo, J. Catalytic steam reforming of model compounds of biomass pyrolysis liquids in fixed bed: Acetol and n-butanol. *Journal of Analytical and Applied Pyrolysis*. 2009, 85(1–2), pp.204-213.
14. Mohanty, P., Patel, M. and Pant, K.K. Hydrogen production from steam reforming of acetic acid over Cu–Zn supported calcium aluminate. *Bioresource Technology*. 2012, 123, pp.558-565.
15. Butterman, H.C. and Castaldi, M.J. CO₂ as a Carbon Neutral Fuel Source via Enhanced Biomass Gasification. *Environmental Science & Technology*. 2009, 43(23), pp.9030-9037.
16. Majewski, A.J. and Wood, J. Tri-reforming of methane over Ni@SiO₂ catalyst. *International Journal of Hydrogen Energy*. 2014, 39(24), pp.12578-12585.
17. Tompkins, H.G. and Augis, J.A. The oxidation of cobalt in air from room temperature to 467°C. *Oxidation of Metals*. 1981, 16(5), pp.355-369.

Chapter 8

CATALYTIC-DRY REFORMING OF WASTE PLASTICS FROM DIFFERENT WASTE TREATMENT PLANTS FOR PRODUCTION OF SYNGAS

In this chapter, waste plastics derived from a range of different municipal, commercial and industrial sources have been subject to the catalytic dry reforming process. The main objective was to understand the production of syngas from different real-world plastics with their contamination, also the comparison with the simulated plastic mixtures as presented in Research Objective 7. The dry reforming of simulated waste plastic mixture (SWP) in previous chapter is also been compared in this chapter to further confirm the composition of the plastic mixture.

The plastic waste samples included; mixed plastics from household waste packaging (MP_{HP}); mixed plastics from a building construction site (MP_{BC}); mixed plastics from agriculture (MP_{AGR}); mixed plastics from electrical and electronic equipment (refrigerator and freezer (MP_F), old style television sets and monitors (MP_{CRT}) and mixture plastics (MP_{WEEE})); refuse derive fuel containing waste plastics and other waste materials (RDF). In addition, virgin high impact polystyrene (HIPS) and virgin acrylonitrile-butadiene-styrene (ABS) are also used as comparison. The SWP consisted of five components; high and low density polyethylene (20 wt.% of HDPE and 42 wt.% of LDPE), polystyrene (16 wt.% of PS), polypropylene (10 wt.% of PP) and polyethylene terephthalate (12 wt.% of PET) that are typically found in mixed waste plastic found in municipal solid waste. Both HIPS and ABS are the major components of WEEE plastics.

The catalysts used were Ni/ Al_2O_3 and Ni-Co/ Al_2O_3 catalysts prepared by the rising-PH technique. For this set of experiment, 1 g of catalyst and 2 g of plastic sample were used. The reforming gas, CO_2 was injected into the second furnace and N_2 was used as a carrier gas with a flow rate of 6 g h^{-1} and 200 ml min^{-1} respectively.

8.1 Product Yields Distribution from Dry Reforming of Waste Plastics

Prior to experiment, the ultimate and proximate analysis of each mixed plastic was analysed to determine its compositions. The results are shown in Table 3.10 (b) and Table 3.11 in Chapter 3 (Section 3.4.1.1). The proximate analysis shown in Table 3.11 summarized that all samples were high in volatile content, with the lowest volatile content observed at RDF sample; 71 wt.%. The highest ash content was observed at ABS with 7.9 wt.%, followed by PS (5.2 wt.%), RDF (4.5 wt.%), and the remaining samples with less than 4.0 wt.%. MP_F showed the highest moisture content in the sample with 20.10 wt.%.

The product yields from the catalytic-dry reforming of the different type of plastic wastes with Ni/Al₂O₃ and Ni-Co/Al₂O₃ catalyst are shown in Figure 8.1.

Figure 8.1 shows that more than 80 % of the product yield distribution from the dry reforming process with the Ni/Al₂O₃ catalyst were gases. The agricultural plastic waste, MP_{AGR} showed the highest amount of gas produced with 100.2 wt.% followed by the household plastic packaging waste, MP_{HP} with 99.9 wt.%. The simulated waste plastics, SWP produced 98.2 wt.% gas and the building construction plastic waste MP_{BC} produced 97.5 wt.% gas. The other waste plastic samples produced between 85.6-91.8 wt.% gas. Based on the proximate analysis data shown in Chapter 3, the plastic mixture wastes (MP_{HP}, MP_{BC}, MP_{AGR}) were high in volatiles, at more than 97 %, followed by plastics from WEEE (MP_{CRT}, MP_F and MP_{WEEE}). RDF contained the lowest volatile content, hence producing the lowest gas yield from the catalytic-dry reforming process. In comparison, RDF showed the highest yield of liquid with 4.2 wt.% whereas MP_F only produced 0.8 wt.%. Char yield from RDF sample was also the highest at 6.7 wt.%. The carbon deposited on the Ni/Al₂O₃ catalyst from the dry reforming of MP_{CRT} showed the highest carbon deposition with 6.3 wt.%.

The addition of Co metal in the Ni/Al₂O₃ based catalyst (Ni-Co/Al₂O₃) appeared to reduce the production of gases, with the reduction range from the smallest of 0.4 % decrease for MP_{CRT} to 88.5 wt.%, to the largest of decrease of 8.6 % for MP_{AGR} reducing the gas yield to 91.6 wt.%, except for ABS with an increase from 86 wt.% to 89 wt.%. However, the amount of liquid yield was increased for MP_{BC},

MP_{AGR} , MP_F , MP_{CRT} , RDF and HIPS but reduced for MP_{HP} , MP_{WEEE} , SWP and ABS. A similar trend of the highest char was found in the experiment with Ni-Co/ Al_2O_3 catalyst; RDF with 6.50 wt.%, although the amount were lower compared to the carbon deposition with the Ni/ Al_2O_3 catalyst. The highest carbon deposition yields was obtained from ABS with 7.60 wt.%. It should also be noted that, the amount of gases produced from the experiment are included with the unreacted carbon dioxide introduced to the system.

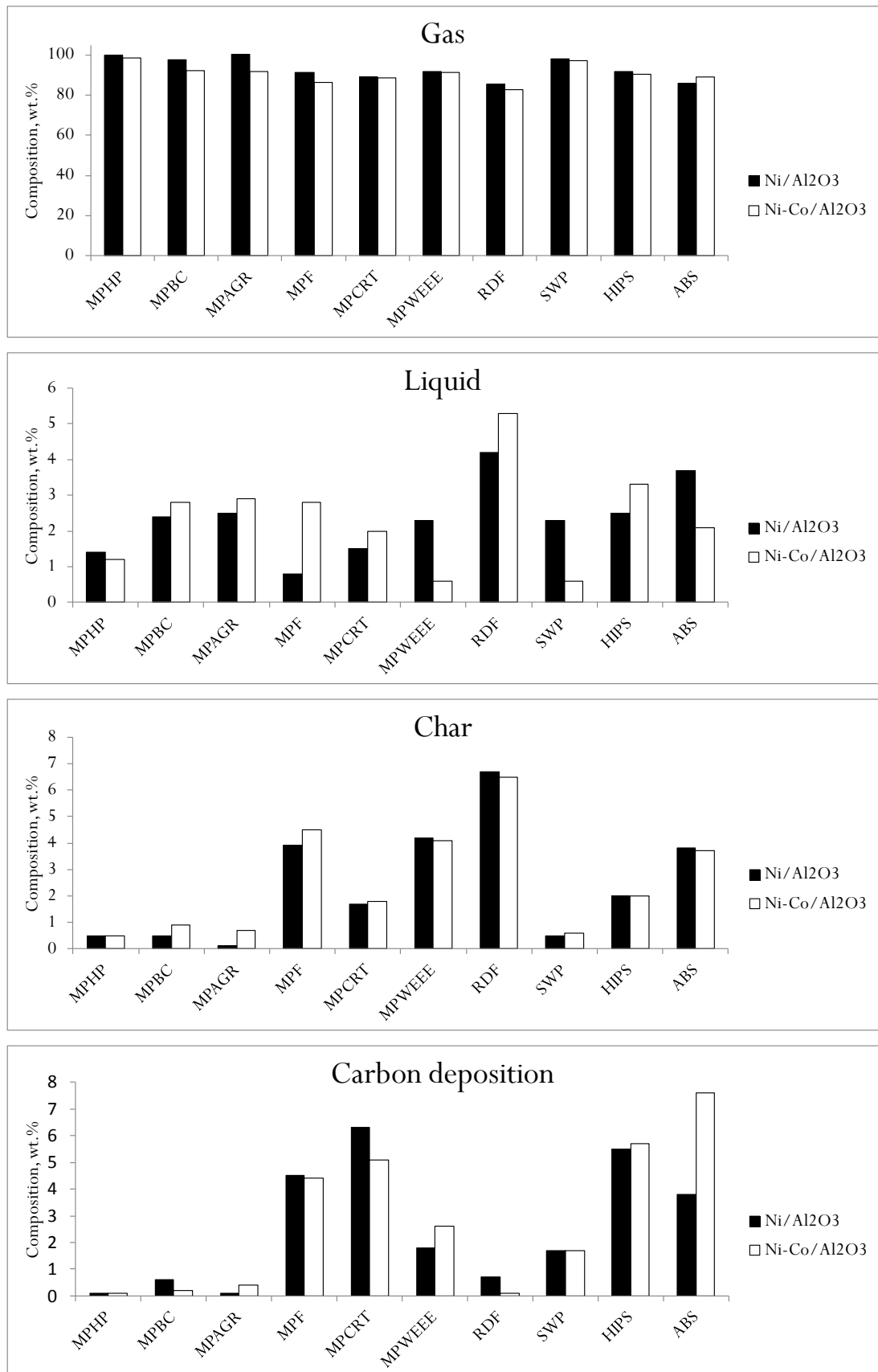


Figure 8.1 Product yields from catalytic-dry reforming of different waste samples under Ni/Al₂O₃ and Ni-Co/Al₂O₃

8.2 Gas Composition and Syngas Production from Dry Reforming of Waste Plastics

The gas compositions; carbon monoxide (CO), hydrogen (H₂), methane (CH₄) and C₂-C₄ hydrocarbons for each type of plastic waste from the catalytic-dry reforming process of the different types of waste samples with the influence of Ni/Al₂O₃ catalyst and Ni-Co/Al₂O₃ catalyst are shown in Table 8.1 and Table 8.2 respectively. For both the Ni/Al₂O₃ and Ni-Co/Al₂O₃ catalysts, the main gases produced from the catalytic-dry reforming process were carbon monoxide and smaller concentrations of hydrogen, methane and C₂-C₄ hydrocarbons, suggesting that the reformation of gaseous product with CO₂ occurred in the 2nd reactor mainly via the dry reforming reaction (Reaction 2.11).

Dry reforming of plastic wastes from different waste treatment plants over Ni/Al₂O₃ catalyst with MP_{HP}, MP_{BC} and MP_{AGR} produced the highest CO and H₂ production with a close range of between 2.7 to 2.9 g_{gas} g⁻¹_{waste} for CO and 0.09 to 0.1 g_{gas} g⁻¹_{waste} for H₂. These waste plastics contained high amounts of hydrogen and carbon as shown in Chapter 3. The RDF sample produced the lowest amount of CO and H₂ concentration with only 0.9 and 0.02 g_{gas} g⁻¹_{waste} respectively, caused by the high oxygen content of the waste sample as shown in Chapter 3, at ~50 wt.%. It is also shown from the data in Table 8.1, high CO₂ conversion resulted in high syngas yield and low CO₂ conversion resulted on low syngas yield. The syngas yield and CO₂ conversion for catalytic-dry reforming of plastic wastes from different waste treatment plants with the influence of Ni/Al₂O₃ catalyst were in the following order: MP_{AGR} > MP_{HP} > MP_{BC} > MP_{WEEE} > MP_{CRT} > MP_F > RDF.

Table 8.1 Gas compositions, syngas yield and CO₂ conversion from dry reforming of waste samples with Ni/Al₂O₃ catalyst at 800 °C gasification temperature.

Waste sample	MP _{HP}	MP _{BC}	MP _{AGR}	MP _F	MP _{CRT}	MP _{WEEE}	RDF	SWP	HIPS	ABS
<i>Gas composition (g_{gas} g⁻¹ waste)</i>										
CO	2.81	2.69	2.92	1.39	1.50	1.80	0.88	2.67	1.82	1.32
H ₂	0.09	0.10	0.10	0.05	0.05	0.04	0.02	0.09	0.05	0.04
CH ₄	0.08	0.05	0.07	0.02	0.02	0.01	0.01	0.04	0.01	0.02
C ₂ -C ₄	0.02	0.0	0.01	0.0	0.0	0.0	0.0	0.0	0.00	0.00
<i>Syngas yield (mmol_{syngas} g⁻¹ waste)</i>										
Syngas _{H₂+CO}	146.3	143.9	153.7	72.5	79.8	85.5	41.2	140.5	90.7	67.0
<i>CO₂ conversion (inlet-outlet)</i>										
CO _{2conv} (g _{co2} g ⁻¹ waste)	2.00	1.97	2.08	0.88	1.13	1.25	0.63	1.89	1.29	1.08
CO _{2conv} (%)	50.1	49.2	52.1	22.0	28.3	31.3	15.8	47.1	32.2	27.1

Table 8.2 Gas compositions, syngas yield and CO₂ conversion from dry reforming of waste samples with Ni-Co/Al₂O₃ catalyst at 800 °C gasification temperature.

Waste sample	MP _{HP}	MP _{BC}	MP _{AGR}	MP _F	MP _{CRT}	MP _{WEEE}	RDF	SWP	HIPS	ABS
<i>Gas composition (g_{gas} g⁻¹ waste)</i>										
CO	2.96	2.70	2.22	1.43	1.78	1.78	0.87	2.79	1.27	1.28
H ₂	0.10	0.09	0.09	0.04	0.06	0.05	0.02	0.10	0.05	0.04
CH ₄	0.08	0.04	0.10	0.01	0.01	0.0	0.02	0.04	0.02	0.02
C ₂ – C ₄	0.01	0.0	0.03	0.0	0.0	0.0	0.0	0.0	0.00	0.00
<i>Syngas yield (mmol_{syngas} g⁻¹ waste)</i>										
Syngas _{H₂+CO}	156.5	141.5	121.3	72.1	92.6	87.3	41.5	148.6	67.6	66.9
<i>CO₂ conversion (inlet-outlet)</i>										
CO _{2conv} (g _{co2} g ⁻¹ waste)	2.22	2.20	1.85	1.16	1.42	1.28	0.78	2.07	0.81	0.90
CO _{2conv} (%)	51.2	54.9	46.2	29.0	35.6	32.0	19.5	51.7	20.3	22.5

The influence of Co metal addition into the Ni/Al₂O₃ based catalysts produced different gas compositions for each type of waste compared to the Ni/Al₂O₃ catalyst. However, the yield of CO still dominated the gas yields from the catalytic-dry reforming process as shown in Table 8.2. In addition, the relationship between syngas yield and CO₂ conversion remained the same for the Ni-Co/Al₂O₃ catalyst, in which high CO₂ conversion resulted on high yield of syngas production. The dry reforming process over Ni-Co/Al₂O₃ catalyst has shown an improvement in syngas yield except for MP_{BC}, MP_{AGR} and MP_F. It is suggested that the addition of cobalt metal promotes either the reduction of liquid yield through the formation of light hydrocarbon gases (MP_{HP}, MP_{WEEE}, SWP and RDF) or/and reduction of carbon due to carbon gasification (MP_{CRT}, MP_{BC}, MP_F and RDF). The syngas yield and CO₂ conversion for catalytic-dry reforming of the difference types of plastic wastes with the Ni-Co/Al₂O₃ catalyst were: MP_{HP} > MP_{BC} > MP_{AGR} > MP_{CRT} > MP_{WEEE} > MP_F > RDF.

Sidik et al. [1] for the dry reforming of methane, reported that the addition of cobalt metal over Ni/MSN (mesoporous silica nanoparticle) catalyst introduced more active sites by improving the Ni dispersion and Ni particle size therefore increasing the CH₄ conversion. However, the behaviour of Ni-Co catalyst toward syngas production may vary based on the feedstock introduced. The optimization of catalyst may be implemented to improve the syngas production for example, by varying the calcination temperature, metal loading and preparation method [2, 3].

Overall, in relation to syngas production from the dry reforming of the various plastic wastes over Ni/Al₂O₃ and Ni-Co/Al₂O₃ catalysts the results can be summarized as follows; a high yield of syngas is produced from MP_{HP}, MP_{BC}, MP_{AGR} and SWP followed by mixed plastics from electrical and electronics equipment waste plants (MP_F, MP_{CRT}, MP_{WEEE}, HIPS and ABS) and with the lowest yield of syngas produced from RDF. In comparison to the use of steam in the reforming process compared to the work reported here with carbon dioxide, the syngas production from steam reforming of waste plastics shows a high concentration of hydrogen [4-6]. However, with CO₂ dry reforming, more carbon monoxide is obtained due to the promotion of steam reforming reaction that produces more hydrogen than carbon monoxide.

The results for the simulated mixture of municipal solid waste plastics (SWP) showed a syngas yield of 140.53 mmol_{syngas} g⁻¹_{waste} and 148.56 mmol_{syngas} g⁻¹_{waste} for the Ni/Al₂O₃ and Ni-Co/Al₂O₃ catalysts respectively. The gases composition and

syngas yield results were similar to the value obtained for the real-world household waste packaging plastic, suggesting that the composition of the SWP was a close approximation to real-world municipal waste plastics. In addition, the gas composition and syngas yields from dry reforming of HIPS and ABS were comparable to that produced from the waste WEEE treatment plant; MP_F , MP_{CRT} and MP_{WEEE} , suggesting that the waste collected from WEEE treatment plant contains both HIPS and ABS.

8.3 Coke Formation on the Catalyst from Dry Reforming of Wastes

Temperature programmed oxidation (TPO) experiments were carried out for the reacted Ni/Al_2O_3 and $Ni-Co/Al_2O_3$ catalysts from the dry reforming of the various waste plastics. The plotted thermographs of TGA-TPO and DTG-TPO for the reacted catalysts derived from the catalytic dry reforming of MP_{HP} , MP_{BC} , MP_{AGR} , MP_F , MP_{CRT} , MP_{WEEE} , RDF, SWP, HIPS and ABS are shown in Figure 8.2 and Figure 8.3 respectively. The TGA-TPO-weight loss thermographs as shown in Figure 8.2 indicated that the reacted Ni/Al_2O_3 and $Ni-Co/Al_2O_3$ catalysts derived from dry reforming of MP_{CRT} and MP_F produced more deposited carbon on the catalyst surface compared to the other types of wastes. From Figure 8.3, an obvious coke oxidation peak occurred at around a temperature of 650 °C to 700 °C for the reacted Ni/Al_2O_3 catalyst from dry reforming of MP_{CRT} and MP_F compared to other wastes. However, several temperature weight loss peaks related to carbon combustion occurred in the TPO experiments with the reacted $Ni-Co/Al_2O_3$ catalysts. The first temperature peak range was observed at around 550 - 600 °C (MP_{AGR} , MP_{CRT} , SWP), a second temperature peak range occurred at around 630 - 700 °C (MP_{BC} , MP_{AGR} , MP_F , MP_{CRT} , MP_{WEEE} , HIPS and ABS) and the third temperature peak occurred at around 740 - 760 °C (MP_{HP} , MP_F , MP_{CRT} , SWP, RDF). It is suggested that carbon combustion at high temperature was due to the combustion of the filamentous whisker type carbons formed on the surface of the catalyst, while low temperature carbon oxidation could be assigned to the combustion of the layered carbons which encapsulate the catalyst and which formed on the catalyst [7]. The encapsulating layered type carbons are reported to deactivate the catalyst active metal sites whereas the filamentous type carbons have less of a deactivation effect, since the formed carbons grow away from the catalyst surface [8].

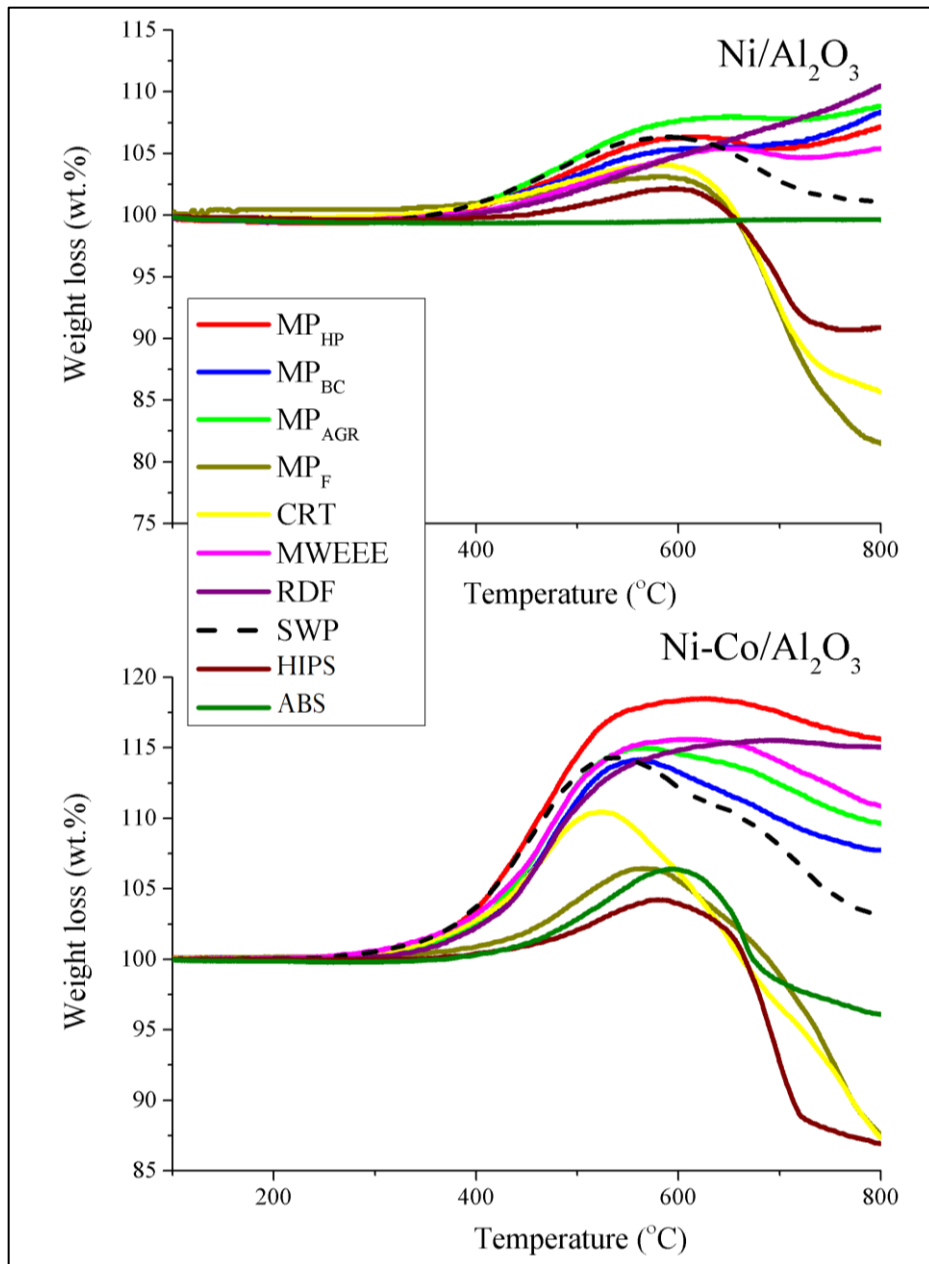


Figure 8.2 TGA-TPO weight loss thermographs of coked Ni/Al₂O₃ and Ni-Co/Al₂O₃ catalysts after dry reforming of different type of waste samples.

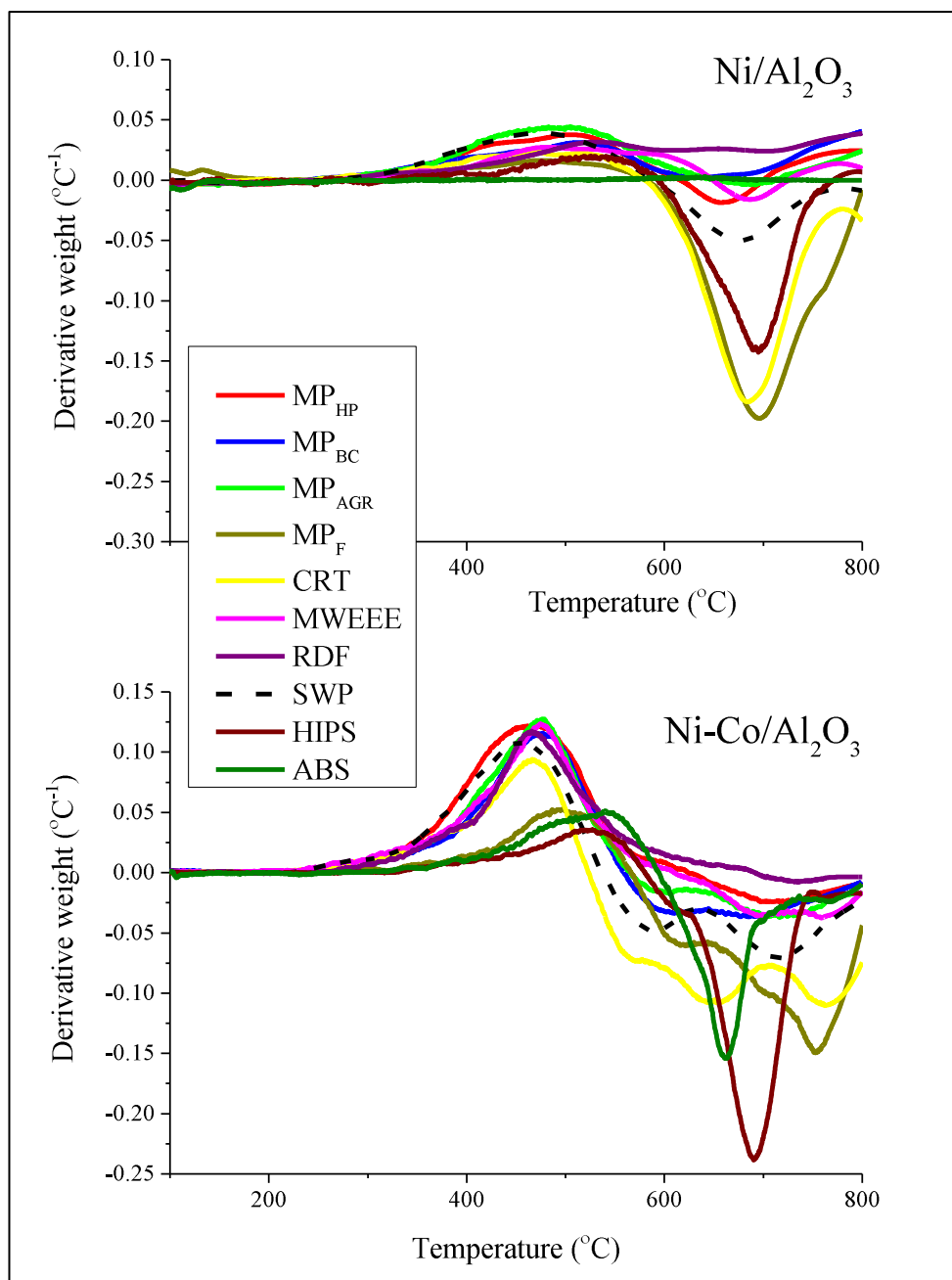


Figure 8.3 DTG-TPO thermographs of coked Ni/Al₂O₃ and Ni-Co/Al₂O₃ catalysts after dry reforming of different type of waste samples.

Figure 8.4 and Figure 8.5 show the SEM morphologies of the reacted catalysts obtained from the catalytic-dry reforming of the plastic wastes. The carbon deposit on the Ni/Al₂O₃ and Ni-Co/Al₂O₃ catalyst surface were investigated and show that for Figure 8.4, noticeable filamentous whisker carbons can be seen on the Ni/Al₂O₃ catalyst surface for the dry reforming of the MP_{BC}, MP_{AGR}, MP_{CRT} and SWP plastic wastes. Fu et al. [9] also reported a similar coke formation on the coked Ni/Al₂O₃ catalyst in their studies into the dry reforming of bio-oil model compounds, indicating the formation of graphite carbon and filamentous carbon

fibres. On the other hand, for the reacted Ni-Co/Al₂O₃ catalysts as presented in Figure 8.5, the filamentous whisker type carbons were observed on the catalyst for the MP_{BC}, MP_{AGR} and MP_{CRT} and also for RDF, while the amount was reduced for SWP.

An obvious structural change between the reacted Ni/Al₂O₃ catalyst and Ni-Co/Al₂O₃ catalysts were observed from the catalysts derived from dry reforming of the various waste plastics. Some catalysts showed an increase of the diameter of catalyst particle from the experiment with Ni/Al₂O₃ catalyst to Ni-Co/Al₂O₃ (MP_{BC}, MP_{AGR}, MPF and ABS), a growth of whisker carbons in RDF and HIPS, some showing a reduction of catalyst diameter (MP_{CRT} and MP_{WEEE}) and some catalysts showing reduction of whisker carbons (MP_{HP} and SWP). Based on the increase of carbon deposition from the dry reforming of MP_{BC}, MP_{AGR}, MP_F, HIPS and ABS with the Ni-Co/Al₂O₃ catalyst compared to the experiments with the Ni/Al₂O₃ catalyst (Figure 8.1), it can be seen that decreased syngas production was found. This may be attributed to deactivation of the catalyst caused by the formations of monoatomic carbons on the catalysts, hence blocking the access of the reactant gases into the catalysts [10, 11].

It should also be noted, that in relation to the TGA-TPO-weight loss thermographs from Figure 3, that more weight gain occurred in the TPO experiment with the reacted Ni-Co/Al₂O₃ catalyst compared to the TPO experiment with the reacted Ni/Al₂O₃ catalyst. The weight gain peak was observed starting at the temperature around 400 °C to 500 °C for both of the reacted Ni-based catalysts which was attributed to the oxidation of nickel particles. The addition of Co metal showed a further increment of the weight gain peak. Tompkins and Augis [12] reported that the oxidation of metallic Co to CoO and Co₃O₄ occurred at a temperature of 425 °C. This suggests that overlapping weight gain as determined by the TGA-TPO occurred between both nickel and cobalt particles for the reacted Ni-Co/Al₂O₃ catalyst from the dry reforming of various wastes, hence a higher weight gain peak.

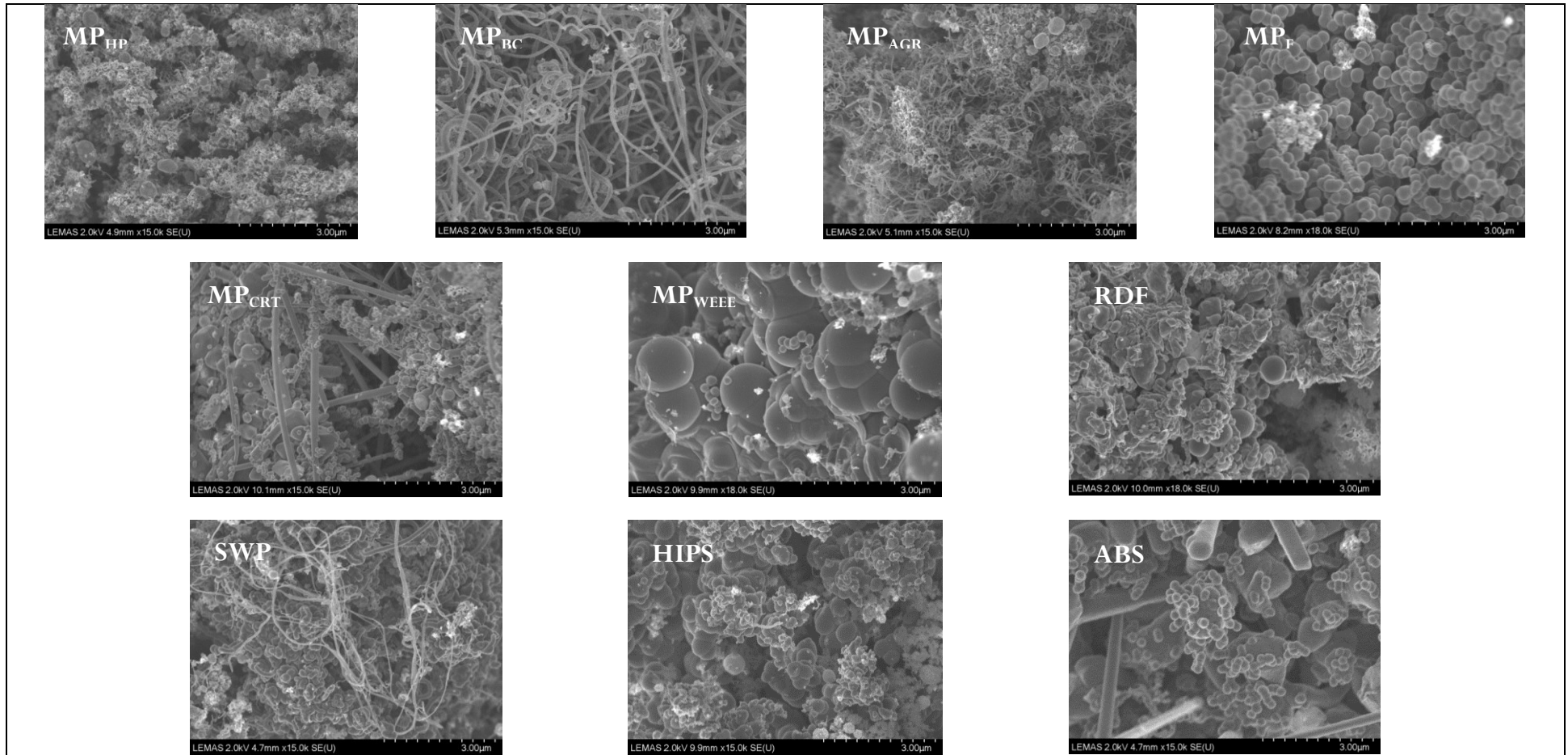


Figure 8.4 SEM morphologies of coked Ni/Al₂O₃ catalysts after dry reforming of different type of waste samples (all SEM micrographs are at the same magnification)

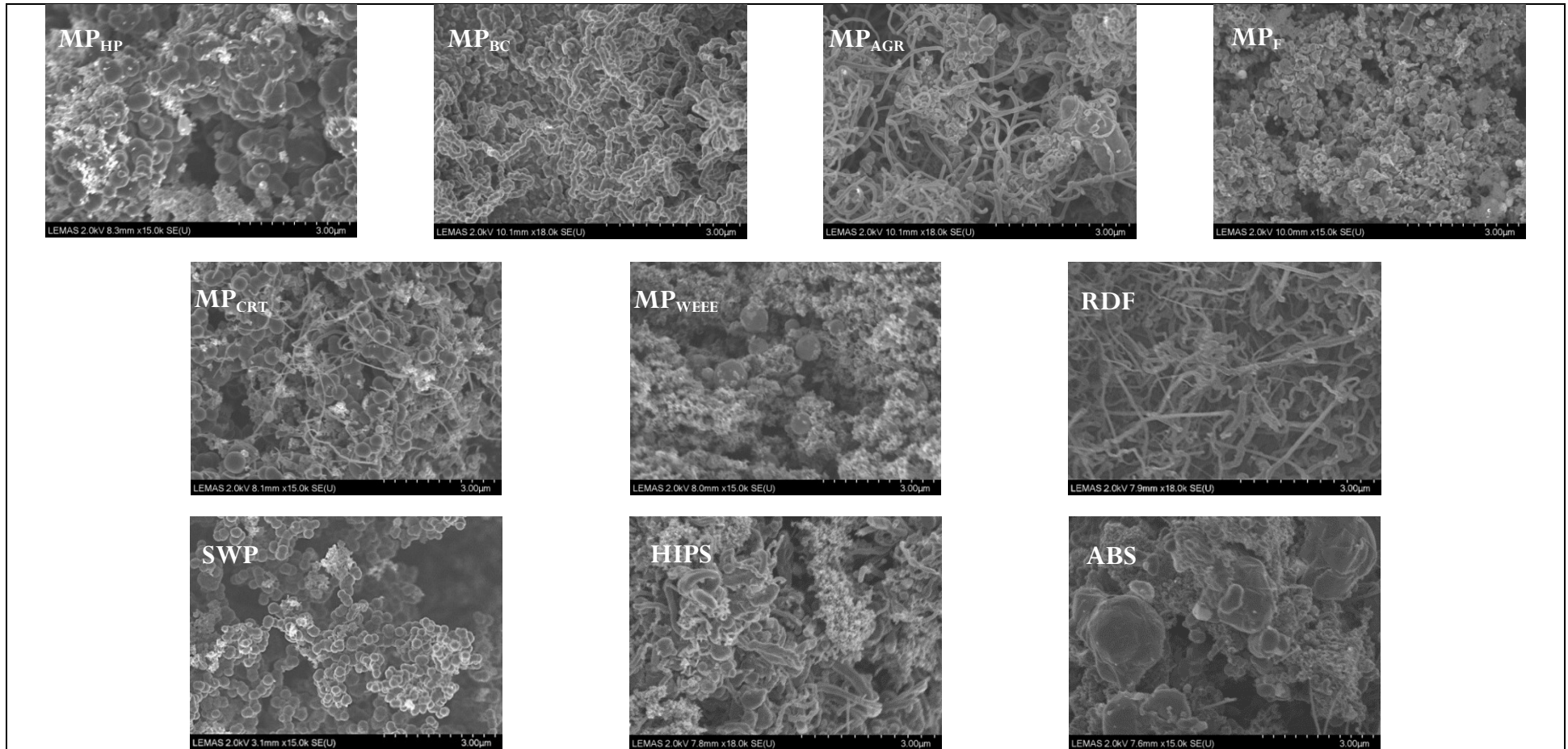


Figure 8.5 SEM morphologies of coked Ni-Co/Al₂O₃ catalysts after dry reforming of different type of waste samples (all SEM micrographs are at the same magnification)

8.4 Summary

Catalytic-dry reforming of a range of municipal, commercial and industrial waste plastics has proven successful in producing significant amounts of synthesis gases. Plastics collected from household packaging, building construction and agricultural (MP_{HP} , MP_{BC} and MP_{AGR}) showed higher yields of syngas production for both Ni/Al₂O₃ and Ni-Co/Al₂O₃, followed by plastics from electrical and electronic equipment waste plastics (MP_F , MP_{CRT} and MP_{WEEE}). On the other hand, RDF showed the least amount of syngas production and less than 1.0 g_{CO₂} g⁻¹_{waste} of CO₂ conversion compared to other plastic sample. The addition of Co metal to the Ni/Al₂O₃ catalyst showed a mixed outcome in relation to syngas production, demonstrating that different types of waste plastics might need different metal promoters to improve the production of syngas. The carbon deposits on the Ni-based catalysts have different nature of formation depending on the type of waste sample being used. In addition, the gases concentration and syngas yield obtained from catalytic-dry reforming of simulated mixture of plastics (SWP) were comparable to the value obtained from the real-world household waste packaging plastics.

References

1. Sidik, S.M., Triwahyono, S., Jalil, A.A., Majid, Z.A., Salamun, N., Talib, N.B. and Abdullah, T.A.T. CO₂ reforming of CH₄ over Ni–Co/MSN for syngas production: Role of Co as a binder and optimization using RSM. *Chemical Engineering Journal*. 2016, 295, pp.1-10.
2. Goicoechea, S., Krалеva, E., Sokolov, S., Schneider, M., Pohl, M.-M., Kockmann, N. and Ehrich, H. Support effect on structure and performance of Co and Ni catalysts for steam reforming of acetic acid. *Applied Catalysis A: General*. 2016, 514, pp.182-191.
3. Ramasamy, K.K., Gray, M., Job, H. and Wang, Y. Direct syngas hydrogenation over a Co–Ni bimetallic catalyst: Process parameter optimization. *Chemical Engineering Science*. 2015, 135, pp.266-273.
4. Ruoppolo, G., Ammendola, P., Chirone, R. and Miccio, F. H₂-rich syngas production by fluidized bed gasification of biomass and plastic fuel. *Waste Management*. 2012, 32(4), pp.724-732.
5. Acomb, J.C., Nahil, M.A. and Williams, P.T. Thermal processing of plastics from waste electrical and electronic equipment for hydrogen production. *Journal of Analytical and Applied Pyrolysis*. 2013, 103, pp.320-327.
6. Dou, B., Wang, K., Jiang, B., Song, Y., Zhang, C., Chen, H. and Xu, Y. Fluidized-bed gasification combined continuous sorption-enhanced steam reforming system to continuous hydrogen production from waste plastic. *International Journal of Hydrogen Energy*. 2016, 41(6), pp.3803-3810.
7. Wang, S. A Comprehensive Study on Carbon Dioxide Reforming of Methane over Ni/ γ -Al₂O₃ Catalysts. *Industrial & Engineering Chemistry Research*. 1999, 38(7), pp.2615-2625.
8. Wu, C. and Williams, P.T. Investigation of coke formation on Ni-Mg-Al catalyst for hydrogen production from the catalytic steam pyrolysis-gasification of polypropylene. *Applied Catalysis B: Environmental*. 2010, 96(1–2), pp.198-207.
9. Fu, M., Qi, W., Xu, Q., Zhang, S. and Yan, Y. Hydrogen production from bio-oil model compounds dry (CO₂) reforming over Ni/Al₂O₃ catalyst. *International Journal of Hydrogen Energy*. 2016, 41(3), pp.1494-1501.

10. Lee, J.-H., You, Y.-W., Ahn, H.-C., Hong, J.-S., Kim, S.-B., Chang, T.-S. and Suh, J.-K. The deactivation study of Co–Ru–Zr catalyst depending on supports in the dry reforming of carbon dioxide. *Journal of Industrial and Engineering Chemistry*. 2014, 20(1), pp.284-289.
11. Vicente, J., Montero, C., Ereña, J., Azkoiti, M.J., Bilbao, J. and Gayubo, A.G. Coke deactivation of Ni and Co catalysts in ethanol steam reforming at mild temperatures in a fluidized bed reactor. *International Journal of Hydrogen Energy*. 2014, 39(24), pp.12586-12596.
12. Tompkins, H.G. and Augis, J.A. The oxidation of cobalt in air from room temperature to 467°C. *Oxidation of Metals*. 1981, 16(5), pp.355-369.

Chapter 9

CONCLUSIONS AND SUGGESTIONS FOR FUTURE WORK

This research work was aim to investigate the dry (CO₂) reforming of plastics for synthesis gas (syngas: hydrogen and carbon monoxide) production. A preliminary study on the effect of carbon dioxide on pyrolysis of plastics was examined using a thermogravimetric analyser. The plastics decompositions and kinetic parameters were described. A two-stage reaction system was used to carry out the main experimental research programme. The performance of Ni/Al₂O₃-based catalysts were researched, focusing on the promotion of catalytic-dry reforming reactions within the reforming stage of the reaction system for synthesis gas production and reduction of catalyst coke deposition. The process parameters of catalyst reforming temperature, carbon dioxide input rate and catalyst to plastic ratio were studied. In addition, introduction of steam within the reforming stage was also investigated to control H₂/CO ratio from dry reforming of plastics. The catalytic-dry reforming process were also examined for syngas production using different types of waste plastics such as and mixed plastics from various waste treatment plants. It was found that secondary cracking of waste plastics at the gasification stage reformed better with the carbon dioxide as the reformer agent. The highest syngas production of 155.0 mmol g⁻¹_{SWP} was observed from catalytic-dry reforming of waste plastics using Ni-Co/Al₂O₃ catalyst at the gasification temperature of 800 °C, 9.0 g h⁻¹ of CO₂ flow rate and 0.5 g g⁻¹ of catalyst to plastic ratio.

9.1 General Conclusions

The following conclusions were drawn considering the order of the Research Objectives, Chapters and experimental results presented in this research work.

9.1.1 Effect of different pyrolysis atmospheres on thermogravimetric and kinetic study of various plastics

Research objective 1 was achieved in the thermogravimetric analysis and pyrolysis kinetic studies of various plastics in different pyrolysis atmospheres. The plastics degradation was investigated and reaction kinetic parameters (activation energy and pre-exponential factor) were calculated by a first order reaction model of the thermogravimetric data.

Decomposition of individual waste plastics; high and low density polyethylene (HDPE and LDPE), polypropylene (PP), polystyrene (PS) and polyethylene terephthalate (PET) from ambient temperature to 500 °C occurred at very similar temperature range with nitrogen or carbon dioxide atmospheres. Only one peak of thermal degradation was observed for all plastics in both atmospheres, but was shifted to a higher temperature in a carbon dioxide atmosphere for almost all plastics. It was found that the residual mass of each plastic was higher in a nitrogen atmosphere than in carbon dioxide. The activation energy of each individual waste plastic decreased in the following order; low density polyethylene > high density polyethylene > polystyrene > polypropylene > polyethylene terephthalate in a nitrogen atmosphere. The order with a carbon dioxide atmosphere was; high density polyethylene > low density polyethylene > polyethylene terephthalate > polypropylene > polystyrene.

Pyrolysis of the aforementioned individual waste plastics and mixed plastics; mixed plastics from waste household packaging (MP_{HP}), mixed plastics from waste building construction (MP_{BC}) and mixed plastics from waste agricultural (MP_{AGR}) over a mixture of nitrogen and carbon dioxide atmosphere from ambient temperature to 900 °C were also investigated. The N_2/CO_2 ratio of 1:0 and 7:3 were investigated based on the low amount of residual mass left after pyrolysis reaction and the low activation energy observed in the pyrolysis of high density polyethylene. No further plastic decomposition was observed for any of the plastics after 500 °C with only one degradation peak observed below 500 °C. Low density polyethylene showed the highest degradation peak temperature at around 480 °C in both N_2/CO_2 ratios, while polystyrene showed the lowest at 426 °C and 429 °C in N_2/CO_2 ratio of 1:0 and 7:3 respectively. Low activation energies were observed in almost all plastics in N_2/CO_2 ratio of 7:3, suggesting low energy required to proceed with the reactions.

9.1.2 Analysis of process conditions on synthesis gas production from pyrolysis and gasification of high density polyethylene

A range of process conditions, including the reacting atmosphere and the presence of catalyst, and their influence on the production of syngas, i.e. hydrogen and carbon monoxide, from the thermal processing of waste high density polyethylene (HDPE) has been investigated and Research Objective 2 was achieved. Pyrolysis in the presence of nitrogen and in the presence of carbon dioxide was investigated using a one-stage pyrolysis reactor. A two-stage reactor was used to investigate the pyrolysis-steam reforming and carbon dioxide/catalysis process conditions in relation to gas composition and particularly hydrogen and carbon monoxide (syngas) yield. It was found that two-stage pyrolysis at 500 °C, followed by second stage reaction at 800 °C resulted in a significant increase in hydrogen production. With the addition of carbon dioxide (dry reforming), the two stage process also increased carbon monoxide yield in addition to hydrogen. Addition of steam into the second stage reactor with the carbon dioxide (dry/steam reforming) produced a further increase in hydrogen production.

9.1.3 Characterisation and assessment of Ni/Al₂O₃ catalysts promoted with Cu, Mg and Co

A series of Ni/Al₂O₃ catalysts were prepared by a rising-pH method, with the addition of Cu, Mg and Co as metal promoters in order to improve the catalytic activity towards syngas production as acquired by Research Objective 3. The performance of the prepared Ni/Al₂O₃ catalysts was tested during the pyrolysis/dry-reforming of high density polyethylene in a two-stage fixed bed reaction system. Syngas production was favoured by carbon dioxide addition (dry reforming), with the highest production of 138.81 mmol_{syngas} g⁻¹_{HDPE}, which was about six times higher than non-catalytic, non-carbon dioxide addition.

The catalytic performances of Ni/Al₂O₃-based catalysts with different promoter metals (Cu, Mg and Co) in the dry reforming of high density polyethylene, showed that the addition of Co metal in the Ni/Al₂O₃ catalyst had an excellent anti-coking performance, with no detectable formation of coke on the catalyst surface. Moreover, the syngas production was significantly improved by the addition of Co

metal compared to other metal promoters. The CO₂ conversion for Ni-Co/Al₂O₃ catalyst was also the highest at 57.62%. Further investigation of the effect of Co metal concentration on dry reforming of high density polyethylene showed that the higher Co metal content, the higher the syngas production and CO₂ conversion.

9.1.4 Investigation of catalytic-dry reforming of various plastics for syngas production

The dry reforming of various types of waste plastics; high and low density polyethylene (HDPE and LDPE), polypropylene (PP), polystyrene (PS) and polyethylene terephthalate (PET) and a simulated mixture of the different waste plastics was investigated over a Ni-Co/Al₂O₃ catalyst using a two-stage reactor. The introduction of CO₂ without a catalyst markedly increased the dry reforming reaction and significantly improved the production of H₂/CO synthesis gas (syngas). The introduction of the Ni-Co/Al₂O₃ catalyst further significantly improved the production of syngas. Low density polyethylene produced the highest yield of syngas at 154.7 mmol_{syngas} g⁻¹ plastic from the pyrolysis-catalytic-dry reforming process. The order of syngas production for the different plastics was low density polyethylene < high density polyethylene < polypropylene < polystyrene < polyethylene terephthalate.

Different polymer structure for each type of individual plastic influenced the product yield. Polyalkene polymers such as HDPE, LDPE and PP produced high concentration of H₂, while PET produced high concentration of CO due to decarboxylation of PET that contain an aromatic ring and O₂ in its structure. On the other hand, PS produced high amount of liquid yield compared to others due to the aromatic structure of the polymer.

The syngas yield from the processing of the simulated waste plastic mixture was 148.6 mmol_{syngas} g⁻¹ plastic which reflected the high content of the linear polyalkene plastics (LDPE, HDPE and PP) in the simulated waste plastic mixture. Research Objective 4 was met with this investigation.

9.1.5 Influence of catalyst preparation methods, catalyst temperature, CO₂ input rate, catalyst:plastic ratio

Catalytic-dry (CO₂) reforming of waste plastics was carried out in a two stage, pyrolysis-catalytic reforming fixed bed reactor to optimise the production of syngas (mixture of hydrogen and carbon dioxide) as mentioned in Research Objective 5. The effects of changing the process parameters of; catalyst preparation conditions, catalyst temperature, CO₂ input rate and catalyst:plastic ratio were investigated. The plastic mixture used was a mixture of plastics simulating that found in municipal solid waste and the catalyst used was Ni-Co/Al₂O₃. The results showed that changing each of the process conditions significantly influenced syngas production.

An increase of 17 % of syngas production was achieved from the experiment with the catalyst prepared by the rising-pH technique compared to preparation via the impregnation method. Smaller catalyst particle size obtained by rising-pH technique promote higher syngas production compared to impregnation method. The optimum syngas production of 148.6 mmol_{syngas} g⁻¹_{swp} was attained at the catalytic dry reforming temperature of 800 °C and catalyst:plastic ratio of 0.5. It is suggested that dry reforming reaction required high gasification temperature due to its endothermic characteristic, hence high syngas yield with the increase of gasification temperature. The increase of CO₂ input rate promoted a higher yield of syngas, with CO yield dominating the syngas production. H₂ yield remain stable even with highest CO₂ input rate.

9.1.6 Effect of the addition of steam on catalytic-dry reforming process towards H₂:CO ratio

Two-stage pyrolysis-catalytic reforming of plastics was investigated with the aim of producing usable quality synthesis gases (syngas) comprised of H₂ and CO as required by Research Objective 6. The process consisted of pyrolysis of the plastics in the first stage and catalytic reforming with CO₂ and steam as the reforming agents in the second stage. The plastics used were a mixture of waste plastics prepared to represent those found in municipal solid waste and the catalysts studied were Ni-Co/Al₂O₃ and Ni-Mg/Al₂O₃ prepared by the rising pH technique. A range of different CO₂/steam ratios were considered; 4:0, 4:0.5, 4:1, 4:1.5 and 4:2 for

Ni-Co/Al₂O₃ catalyst and 4:0, 4:0.5, 4:1, 4:2 and 4:3 for Ni-Mg/Al₂O₃ catalyst. The results obtained demonstrated that the catalysts and the CO₂/steam ratio influence the syngas quality, as represented by the H₂/CO molar ratio value. With the Ni-Co/Al₂O₃ catalyst, the H₂/CO molar ratio was increased from 0.74 (no steam) to 0.94 (CO₂:steam ratio; 4:1) however the H₂/CO molar ratio decreased with further steam addition. Results using the Ni-Mg/Al₂O₃ catalyst showed a different trend, wherein the H₂/CO molar ratio increased with the increase of steam addition into the system. From the evaluation of the gas composition, the steam addition with the Ni-Mg/Al₂O₃ catalyst promoted hydrogen production while the Ni-Co/Al₂O₃ catalyst promoted carbon monoxide production. The addition of steam to the dry reforming of waste plastics has the potential to manipulate the H₂/CO molar ratio hence, the quality of syngas produced can be matched to the desired end-use industrial application.

9.1.7 Investigation of catalytic-dry reforming of mixed plastics from various waste treatment plants for syngas production

In order to satisfy Research Objective 7, the dry reforming of real-world waste plastic samples; mixed plastic from household packaging waste (MP_{HP}); mixed plastic from building construction waste (MP_{BC}); mixed plastics from agricultural waste (MP_{AGR}); plastics from freezer and refrigerator equipment (MP_F); plastics from waste cathode ray tube televisions and monitors (MP_{CRT}); mixed plastics from electrical and electronics equipment (MP_{WEEE}) and refuse derived fuel (RDF) were investigated using the two-stage fixed bed reactor. In addition, simulated waste plastics (SWP) which represented the composition of European waste plastics were reacted as a comparison with the waste samples. Ni/Al₂O₃ and Ni-Co/Al₂O₃ catalysts were used in order to improve the production of syngas from the dry reforming process. The results showed that the highest amount of syngas yield was obtained from the dry reforming of MP_{AGR} with the Ni/Al₂O₃ catalyst, at 153.67 mmol_{syngas} g⁻¹_{waste}. However the addition of cobalt metal promoter to the catalyst gave yields of syngas depending on the type of waste sample, with the highest yield obtained from MP_{HP}, at 156.45 mmol_{syngas} g⁻¹_{waste}. Overall, the catalytic-dry reforming of waste samples from various waste treatment plants showed great promise towards the production of synthesis gases.

9.2 Recommendations for future work

Given the various findings of the present study into syngas production from dry reforming of plastics outlined above, there are areas of the research that are needed to be further studied to provide a better understanding of the reforming mechanism of wastes, specifically plastics in carbon dioxide. The recommendations for future work in this area of research are as follows:

9.2.1 Analysis of plastic/CO₂ reaction kinetics and mechanism

The thermogravimetric analysis (TGA) of plastics in CO₂ and N₂/CO₂ mixture revealed a preliminary understanding of plastics decomposition and activation energy. Future work should consider the influence of varying pyrolysis heating rate in order to gain a clear understanding of the mechanism of waste plastics pyrolysis with the presence of CO₂. The kinetic rate expression and simulation study should also be implemented to verify the kinetic behaviour of the pyrolysis process with CO₂. The TGA tests also observed variation of residual mass changes in the pyrolysis of plastics with the N₂/CO₂ ratio of 7:3, therefore it is recommended that further studies be performed to determine the cause for the change in residual mass and identify the comparison of residue properties between N₂ and N₂/CO₂ atmospheres. The thermogravimetric analysis (TGA) coupled to a Fourier transform infrared spectrometer (FTIR) is also suggested in order to obtain further information in regard to the evolved volatile species from the pyrolysis-dry reforming of plastics. It is also recommended to conduct a further kinetic study of catalyst-dry reforming of plastics using a larger scale two-stage fixed bed reactor. Different kinetic models such as Dynamic and Friedman method may also be investigated for comparison.

9.2.2 Investigation on catalyst characterisation and activity

Ni-Co/Al₂O₃ catalysts, prepared by the co-precipitation method have demonstrated better promotion of cracking and dry reforming reactions in almost all type of plastics, resulting in high catalytic activity in regards to syngas production. Future investigations should consider the effect of varying catalyst preparation parameters such as calcination temperature, pH value, catalyst pre-treatment process and different

support. The catalyst preparation temperature is crucial in determining the catalyst particle size since the crystal growth is temperature sensitive. Also, the catalyst structure and catalyst composition might be influenced by the final pH value. The calcination temperature may also affect the catalyst properties and performance. The experiment without catalyst addition for all plastics should also be added for comparison.

Ceria or cerium oxide (Ce) as a second or third metal promoter for methane dry reforming for syngas production are of recent interest in the literature. Ce has shown good capability in regards to promoting Ni reduction and improving the dispersion of the active phase. It is recommended that applying this metal for the dry reforming process of plastics either as second or third metal promoter is carried out.

More catalyst characterisation techniques in addition to those described in this work, such as transmission electron microscopy (TEM), X-ray photoelectron spectroscopy (XPS), Raman spectroscopy and CO₂-temperature programmed desorption (CO₂-TPD) are also suggested to be applied to both fresh and reacted catalysts. These comprehensive catalyst characterizations could improve the understanding of the catalyst properties which include surface properties and carbon deposition characteristics. Furthermore, the stability of the catalysts should be conducted in long-term experiments (for more than 24 hrs) for evaluating the catalysts deactivation resistivity and suitability of the catalysts for continuous reaction in industrial-scale system.

9.2.3 Application of dry reforming process for syngas production from plastics

In order to test the performance of catalytic-dry reforming of waste plastics for industrial use, a large scale experimental setup such as a continuous fluidized bed reaction system should be considered. However, certain improvements need to be approached. For instance, the effects of plastics decomposition during the continuous feeding and the improvement on plastic feeding system should be studied. The recyclability of carbon dioxide from pyrolysis of waste mixed plastics into the system (closed-loop system) may also be investigated. It may be also useful to investigate the various markets for the subsequent use of syngas from the dry-reforming of waste plastics.